Identification of the Essential Genome of *Burkholderia cenocepacia* K56-2 to Uncover Novel Antibacterial Targets

by

April S. Gislason

A Thesis submitted to the Faculty of Graduate Studies of

The University of Manitoba

in partial fulfillment of the requirements for the degree of

Doctor of Philosophy

Department of Microbiology

University of Manitoba

Winnipeg, Manitoba, Canada

Abstract

Burkholderia cenocepacia K56-2 is a clinical isolate of the *Burkholderia cepacia* complex, a group of intrinsically antibiotic resistant opportunistic pathogens, for which few treatment options are available. The identification of essential genes is an important step for exploring new antibiotic targets. Previously, a conditional growth mutant library was created using transposon mutagenesis to insert a rhamnose-inducible promoter into the genome of *B. cenocepacia*. It was then demonstrated that conditional growth mutants under-expressing an antibiotic target were sensitized to sub-lethal concentrations of that antibiotic. This thesis describes the use of next generation sequencing to measure the enhanced sensitivity of conditional growth mutants after being grown together competitively. Evidence is provided to show that the sensitivity of a GyrB conditional growth mutant to its cognate antibiotic, novobiocin, was enhanced due to competitive growth. Screening eight antibiotics with known mechanisms of action against a pilot conditional growth mutant library revealed a previously uncharacterized two-component system involved antibiotic resistance in *B. cenocepacia*.

With the goal of exploring new *Burkholderia* antibacterial targets, the essential genome of *B. cenocepacia* K56-2 was identified by sequencing a high density transposon mutant library. Comparison of the *B. cenocepacia* K56-2 essential gene set with the essential genomes predicted for *B. thailandensis*, *B. pseudomallei*, and *B. cenocepacia* J2315 revealed strain-specific essential genes and 158 essential genes that are common to species in the *Burkholderia* genus. Three genes were identified that are essential in *Burkholderia* but not in other bacterial essential genomes identified so far, suggesting that specific cell envelope functions are critical to survival of *Burkholderia* species. To increase the diversity of the conditional growth mutant library, a method to enrich conditional growth mutants from the high density mutant library was developed and used

to isolate 830 conditional growth mutants. With the addition of these mutants, the conditional growth mutant library currently represents 23.2% of the essential operons in *B. cenocepacia* K56-2 and 36.7% of the essential genes that are common to species in the *Burkholderia* genus. In summary, this thesis has contributed to create genomic tools available for antibiotic research and has identified novel targets for fighting *Burkholderia* related infections.

Acknowledgements

First and foremost, I would like to acknowledge my PhD supervisor, Dr. Silva Cardona, who inspired me to pursue my PhD studies. Throughout my time spent in her research laboratory, both as a technician and a student, she always gave me the opportunity to explore my interests and encouraged me to challenge myself. I will be forever grateful to her for her guidance and support.

I would also like to thank my committee members, Dr. Brian Mark, Dr. Ivan Oresnik and Dr. Steve Whyard, I greatly appreciated their guidance and valuable suggestions. I would like to thank Dr. Xuan Li for his help with the statistical analysis. Thank you to Wubin Qu, Dr. Mike Domaratzki, Dr. Ruhi Bloodworth and Dr. Keith Turner for their help with bioinformatics analysis and Dr. Larry Gallagher for his help with the Tn-seq circle method. I would also like to acknowledge the support provided by Faculty of Science Graduate Scholarships and Graduate Students Association Travel Awards, during my PhD studies.

I sincerely thank all the professors, graduate students and support staff in the Department of Microbiology, including the past and present members of the Cardona lab, for creating such a welcoming and friendly environment to work in. To Dr. Deb Court and Dr. Teri de Kievit, I sincerely appreciate your kindness and encouragement during the stressful times.

I thank my wonderful lab family - Tasia Lightly, Dr. Silvina Stietz, Dr. Carrie Selin, Sol Haim, Tanya Pribytkova, Brijesh Kumar, Matthew Choy and Andrew Hogan for being so entertaining and for your friendship.

Finally, to Mom, Dad, Amber, Sean, Kristjana, Gina and Mark - thank you for your love and support, and for always believing in me.

Contributions of authors

Multiple authors contributed to the work described in Chapters 2, 3 and 4. For all the work outlined in these chapters, Dr. Silvia T. Cardona was involved in the experimental design and interpretation, as well as manuscript preparation. Dr. Xuan Li provided extensive help with the statistical analysis outlined in section 2.2.4. Wubin Qu designed the multiplex primer set outlined in 2.2.3. Matthew Choy carried out the experiments described in sections 2.2.8, 2.2.9 and 2.2.10. Dr. Silvina Stietz carried out the microscopy described in section 2.2.12. Dr. Keith Turner developed and performed the bioinformatics analysis for essential genes outlined in section 3. Dr. Ruhi Bloodworth and Dr. Mike Domaratzki wrote code and provided bioinformatic support for the analysis of the CG mutant library outlined in Chapters 3 and 4. Carmicheal Mabilangan was involved in generating and screening the conditional growth mutants described in Chapter 4.

List of copyrighted material for which permission was obtained

Chapter 1: Critical Reviews in Microbiology 2014 March; 41(4):465-72, Cardona ST, Selin C, Gislason AS. Genomic tools to profile antibiotic mode of action. Copyright © 2014 Informa Healthcare USA, Inc. http://dx.doi.org/10.3109/1040841X.2013.866073. Excerpt reproduced with permission.

MicrobiologyOpen. 2013 April; 2(2):243-258. doi: 10.1002/mbo3.71. *Burkholderia cenocepacia* conditional growth mutant library created by random promoter replacement of essential genes. (Figure 1.2) Published under the Creative Commons Attribution License, allowing reproduction with attribution.

Chapter 2: Antimicrobial Agents and Chemotherapy 2016 Dec; 27;61(1), Gislason AS, Choy M, Bloodworth RA, Qu W, Stietz MS, Li X, Zhang C, Cardona. Competitive Growth Enhances Conditional Growth Mutant Sensitivity to Antibiotics and Exposes a Two-Component System as an Emerging Antibacterial Target in *Burkholderia cenocepacia*. Copyright © 2017, American Society for Microbiology, authors retain the right to reuse the full article in his/her thesis.

Chapter 3: MBio. 2011 Jan 18;2(1):e00315-10. Gallagher LA, Shendure J, Manoil C. Genome-scale identification of resistance functions in Pseudomonas aeruginosa using Tn-seq.
Copyright © 2011 Gallagher et al. Creative Commons Attribution-Noncommercial-Share Alike 3.0 Unported License, which permits unrestricted noncommercial use, distribution, and reproduction in any medium, provided the original author and source are credited.

Table of contents

Abstract ii

Acknowledgements iv

Contributions of authors v

List of copyrighted material for which permission was obtained vi

List of tables x

List of figures xi

List of abbreviations xiii

Chapter 1: Literature review 1

1.1 The *Burkholderia cepacia* complex 2
1.1.1 Ecology 2
1.1.2 Infections with Bcc 4
1.1.3 Immunocompromised individuals 4
1.1.4 Chronic granulomatous disease 5
1.1.5 Cystic fibrosis 6

1.2 *B. cenocepacia* 8
1.2.1 B. cenocepacia genome 8
1.2.2 Genomic islands 9
1.2.3 B. cenocepacia antibiotic resistance 11
1.2.4 Modified lipopolysaccharide 11
1.2.5 Biofilms 12
1.2.6 Efflux pumps 13
1.2.7 Porins 13

1.3 Antibiotic development 14
1.3.1 In vitro assays 15
1.3.2 Whole cell screens 16

1.4 Essential genes as antibiotic targets 17
1.4.1 Essential genes 17
1.4.2 Identification of essential genes 18
1.4.3 High density transposon mutagenesis 18
1.4.4 Analysis for determining the essential genome 19
1.4.5 Whole cell chemogenetic screens 21
1.4.6 Essential genes in chemogenetic screens 23

1.5 Thesis objectives 29

Chapter 2: Competitive growth enhances conditional growth mutant sensitivity to antibiotics and exposes a two-component system as an emerging antibacterial target in *Burkholderia cenocepacia* 30

2.1 Introduction 31

2.2 Materials and methods **33**
2.2.1 Bacterial strains and growth conditions *33*
2.2.2 Growth inhibitors *38*
2.2.3 Multiplex PCR optimization, amplicon library preparation and Illumina sequencing of amplicons *38*
2.2.4 Data analysis *44*
2.2.5 Artificial depletion of CG mutants *45*
2.2.6 Competitive enhanced sensitivity assay *45*
2.2.7 Comparison of pooled and clonal growth *48*
2.2.8 Construction of the unmarked esaS deletion mutant, MKC4 (ΔesaS) *50*
2.2.9 Site directed mutagenesis to construct the esaR conditional growth mutant MKC2 (CGesaR). *54*
2.2.10 MIC ratios *54*
2.2.11 Ala-Nap uptake assay *55*
2.2.12 Microscopy analysis *55*

2.3 Results **58**
2.3.1 Quantification of CG mutant relative abundance by Illumina sequencing of multiplex-PCR amplified transposon junctions *58*
2.3.2 A competitive enhanced sensitivity assay enhanced the specific depletion of a CG mutant to its corresponding antibiotic *64*
2.3.3 The competitive enhanced sensitivity assay reveals a two-component system (TCS) involved in regulation of antibiotic resistance *68*
2.3.4 Mutational analysis of the esaSR locus suggests that esaR is an essential gene *71*
2.3.5 The esaSR locus is involved in drug efflux activity and cell membrane integrity *75*

2.4 Discussion **81**

Chapter 3: Identification and comparative analysis of the essential genome of *Burkholderia cenocepacia* K56-2 provides evidence for conservation of genus-specific essential genes **87**

3.1 Introduction **88**

3.2 Materials and methods **90**
3.2.1 Bacterial strains and growth conditions *90*
3.2.2 Production of the 1 million high-density transposon mutant library *92*
3.2.3 Molecular biology techniques *93*
3.2.4 Genomic DNA isolation *93*
3.2.5 Tn-seq circle *94*
3.2.6 Data analysis to determine gene essentiality *99*
3.2.7 Bioinformatics *100*

3.3. Results **101**
3.3.1 Production and sequencing of the HDTM library *104*
3.3.2 Analysis of possible biases in insertion site identification *108*
3.3.3 Essential gene identification *114*
3.3.4 Comparison of the essential genomes of B. cenocepacia K56-2 and J2315 *119*

3.4 Discussion **132**

Chapter 4: Enrichment of conditional growth mutants from the 1 million high density transposon mutant library **146**

4.1 Introduction **147**

4.2 Materials and methods **151**
4.2.1 Bacterial strains and growth conditions *151*
4.2.2 Enrichment of CG Mutants from the HDTM library *153*
4.2.3 Screening for the conditional growth phenotype *154*
4.2.4 Production of CG mutant subpools and the meropenem enriched CG mutant library *155*
4.2.5 Genomic DNA isolation *155*
4.2.6 Molecular biology techniques *156*
4.2.7 Tn-seq circle *157*
4.2.8 Bioinformatics *161*
4.2.9 Statistical analysis of the growth phenotype distribution obtained from the primary screen *162*

4.3 Results **164**
4.3.1 Meropenem enrichment increases the frequency of obtaining CG mutants *164*
4.3.2 CG mutant library enriched from the 1M HDTM library *167*
4.3.3 PrhaB controls essential genes in the meropenem enriched CG mutants *175*
4.3.4 Functional categories represented by the meropenem enriched CG mutant library *178*

4.4 Discussion **182**
Limitations for meropenem-enrichment of CG libraries *184*
Applications of the CG mutant library *186*

Chapter 5: Conclusions **188**
Literature cited **194**

List of tables

Table 2.1 Bacterial strains and plasmids 34

Table 2.2 List of CG transposon mutants 35

Table 2.3 Primers used to amplify CG transposon mutants 40

Table 2.4 Comparison of enhanced sensitivity of pooled and clonally grown CG mutants 67

Table 2.5 Minimum inhibitory concentrations (MICs) of selected antibiotics against *B. cenocepacia* K56-2 wild type (WT), MKC2 (CG*esaR*), MKC4 (Δe*saS*), 73-14C5 (CG transposon mutant of *esa*R), and 86-37D12 (CG transposon mutant unrelated to *esaR*) 74

Table 3.1 Bacterial strains and plasmids used in this study 91

Table 3.2 Oligonucleotides used in this study 98

Table 3.3 Summary of results from sequencing the HDTM library 104

Table 3.4 The order and orientation of the 17 contigs from the *B. cenocepacia* K56-2 assembly after alignment to B. cenocepacia J2315 replicons using progressiveMauve 120

Table 4.1 Bacterial strains and plasmids used in this study 152

Table 4.2 Oligonucleotides used in this study 160

Table 4.3 Number of putative CG mutants identified from the Bhattacharya and Modified Gregor methods. 171

Table 4.4 CG mutants isolated after enrichment of the 1M HDTM library 173

Table 4.5 Summary of meropenem enriched CG mutant library 177

List of figures

Figure 1.1 pRBrhaBoutgfp Suicide plasmid used to deliver the rhamnose-inducible promoter (*PrhaB*) by random transposon mutagenesis. 25
Figure 1.2 Conditional growth mutants show selective hypersensitivity 27
Figure 2.1 Detection of CG mutant enhanced sensitivity using Illumina MiSeq 43
Figure 2.2. Rhamnose dose response curves of pilot CG library in 7 rhamnose categories 47
Figure 2.3 Experimental design for comparing of pooled and clonal growth. 49
Figure 2.4 Colony PCR analysis of putative *esaS* and *esaSR* deletion mutants 52
Figure 2.5 Controls for the BacLight Live/Dead bacterial viability kit (Molecular Probes) 57
Figure 2.6 Optimized multiplex PCR for the pilot CG library 60
Figure 2.7 Functional categories represented by CG mutants in the original (106 mutants) and pilot CG library (25 mutants) 61
Figure 2.8 Detection of artificially depleted strains by next generation sequencing 63
Figure 2.9 Competitive ESA detects the sensitization of CGgyrB to novobiocin 65
Figure 2.10 Antibiotic profile of CG mutant 73-14C5, under-expressing EsaR 70
Figure 2.11 Depletion of EsaR and EsaS cause a growth defect and lower MIC of select antibiotics 73
Figure 2.12 Efflux activity of *B. cenocepacia* K56-2 wild type (WT), 73-14C5 (CG transposon mutant of *esaR*), MKC2 (CGesaR) and MKC4 (Δ*esaS*). 78
Figure 2.13 *B. cenocepacia* cells have a compromised membrane when depleted in EsaR 80
Figure 3.1 Enrichment of transposon-genome junctions with Tn-seq circle 102
Figure 3.2 GC content of the transposon insertion sequence is low 105
Figure 3.3 Distribution of insertion sites in the genome by GC content 106
Figure 3.4 Distribution of reads per insertion site 107
Figure 3.5 Bioinformatics pipeline to identify essential genes under control of the rhamnose inducible promoter (P*rhaB*) in the conditional growth mutant library 110

Figure 3.6 Positional effects of insertion site density and reads per insertion 111
Figure 3.7 Diagram of the 1M HDTM Taq library reads mapped to the *B. cenocepacia* K56-2 genome 112
Figure 3.8 Normalization of read counts from the 1M HDTM Taq library 113
Figure 3.9 Functional categories of the predicted essential and non-essential genes of *B. cenocepacia* K56-2 116
Figure 3.10 Functional categories of the predicted essential and non-essential 117
Figure 3.11 Comparison of the functional categories (COGs) enriched or under-represented in the essential gene sets of *B. cenocepacia* K56-2 and *E. coli* 118
Figure 3.12 Comparison of the essential genes identified in *B. cenocepacia* K56-2, *B. cenocepacia* J2315, *B. thailandensis* E264 and *B. pseudomallei* K96243 121
Figure 3.13 Insertions and corresponding reads mapping to *B. cenocepacia* K56-2 genes identified as essential in *B. cenocepacia* J2315 but not in K56-2 124
Figure 3.14 Functional categories enriched in the 158 essential genes common to *B. cenocepacia* K56-2, *B. cenocepacia* J2315, *B. thailandensis* E264 and *B. pseudomallei* K96243 128
Figure 3.15 Three cell structure biosynthesis pathways enriched in essential genes common to *B. cenocepacia* K56-2, *B. cenocepacia* J2315 (Wong et al., 2016a), *B. thailandensis* E264 (Baugh et al., 2013) and *B. pseudomallei* K96243 (Moule et al., 2014a) 129
Figure 4.1 Construction of a meropenem enriched conditional growth mutant library 166
Figure 4.2 Primary screen of 2,304 mutants for the conditional growth phenotype 168
Figure 4.3 Separation of the distribution of CG mutants from the distribution of non CG mutants 170
Figure 4.4 Distribution of the functional categories from the meropenem enriched CG mutants, non-enriched CG mutant library, and the essential and non-essential gene sets of B. cenocepacia K56-2 179
Figure 4.5 Proportion of essential operons identified in B. cenocepacia K56-2 represented by the non-enriched, and enriched CG mutants 181

List of abbreviations

ala-nap	L-alanine β-naphthylamide
BCESM	Burkholderia epidemic strain marker
bp	Base pair
CCCP	Carbonyl cyanide 3-chlorophenylhydrazone
CF	Cystic fibrosis
CFTR	Cystic fibrosis transmembrane conductance regulator gene
CG	Conditional growth
CGD	Chronic granulomatous disease
CHL	Chloramphenicol
COG	Cluster of orthologous group
COL	Colistin
DEG	Database of essential genes
DIC	Differential interference contrast
DMSO	Dimethyl sulfoxide
DNA	DNA deoxyribonucleotide
EPS	Extracellular polymeric substrate
ESA	Enhanced sensitivity assay
g	Gram
H2O2	Hydrogen peroxide
HDTM	High density transposon mutant
HITS	High density insertion sequencing
IC	Inhibitory concentration
INSeq	Insertion sequencing
IR	Inverted repeat
KAN	Kanamycin
LCB	Locally collinear blocks
LLR	Log2-likelihood ratio
m	Milli
M	Mega
MERO	Meropenem
MIC	Minimum inhibitory concentration
MOA	Mechanism of action
mRNA	Messenger RNA
n	Nano
NGS	Next generation sequencing
NOV	Novobiocin
ori	Origin of replication
PAINS	Pan-Assay interference compounds

PBS	Phosphate buffered saline
PCR	Polymerase chain reaction
P*rhaB*	Rhamnose-inducible promoter
rha	Rhamnose
RNA	Ribonucleotide
RND	Resistance nodulation cell division
sgRNAs for	Single guide rnas
siRNA	Small interfering RNA
TCS	Two component signal transduction system
TET	Tetracycline
TMP	Trimethoprim
Tn-seq	Transposon sequencing
Tnp	Transposase
TraDIS	Transposon directed insertion-site sequencing
µ	Micro

Chapter 1: Literature review

Sections 1.4.3 High density transposon mutagenesis and 1.4.5 Whole cell chemogenetic screens are reproduced from a section I wrote from Cardona ST, Selin C, Gislason AS. Genomic tools to profile antibiotic mode of action. Published in Crit Rev Microbiol. 2015;41(4):465-72. http://dx.doi.org/10.3109/1040841X.2013.866073.

Figure 1.2 has been reproduced from a paper I coauthored, published in MicrobiologyOpen, 2013: Ruhi A. M. Bloodworth, April S. Gislason and Silvia T. Cardona. (2013). *Burkholderia cenocepacia* conditional growth mutant library created by random promoter replacement of essential genes. MicrobiologyOpen. (2)- 2:243-258.
I was involved in creating the conditional growth mutant library, developing the experimental design of the enhanced sensitivity assay and performing the enhanced sensitivity experiments.

1.1 The *Burkholderia cepacia* complex

Burkholderia is a genus of Gram-negative Betaproteobacteria, first identified as the causative agent of onion rot by Walter Burkholder in 1950. Originally classified as a member of the genus *Pseudomonas*, seven strains were reclassified to the novel genus *Burkholderia* in 1992 (Yabuuchi et al., 1992). Over 100 *Burkholderia* species have been reported http://www.bacterio.net (Euzéby, 1997), most of which are not considered pathogenic to healthy humans. The strain used in this work, *Burkholderia cenocepacia,* is one of at least 20 closely related species or genomovars that form the *Burkholderia cepacia* complex (Bcc) (Mahenthiralingam et al., 2005a; Peeters et al., 2013; Smet et al., 2015; Vanlaere et al., 2008, 2009). The Bcc species identified have large multireplicon genomes, ranging from 7 – 9 Mb that usually consist of three chromosomes and a plasmid (Holden et al., 2009a; Ussery et al., 2009). The diverse metabolic capabilities encoded by the large genome allow the Bcc to occupy varied environmental niches (Mahenthiralingam et al., 2008).

1.1.1 Ecology

Bcc species can be found ubiquitously throughout the environment. Bcc can adjust to diverse ecological niches and are considered one of the most adaptable Gram-negative bacteria (Mahenthiralingam et al., 2008). Strains from the Bcc have been isolated from water, soil, rhizospheres, plants, hospitals, medical equipment, cosmetics, industrial settings and pharmaceutical products (Compant et al., 2008).

The rhizosphere of many plants are a large source of environmental *Burkholderia species* (Compant et al., 2008). In contrast to the identification of *Burkholderia* species as plant pathogens (Govan et al., 1996), many of the Bcc species have beneficial associations with plants (Parke and Gurian-Sherman, 2001). A diverse population of Bcc species have been found to be associated

with the rhizospheres of maize, pea, rice, cotton and wheat (Payne et al., 2006; Ramette et al., 2005). Bcc strains have generated much interest from the agricultural industry due to their ability to promote plant growth (Govan et al., 1996). Owing to the varied metabolic abilities encoded on their large genome, Bcc strains are able to grow on a diverse range of hydrocarbon substrates (Sangodkar et al., 1988). Bcc strains are capable of producing enzymes that degrade contaminants of ground water, including toxic chlorinated aromatic hydrocarbons (O'Sullivan and Mahenthiralingam, 2005). While the use of microorganisms for biocontrol was regulated by the Environmental Protection Agency in the United States during the 1990s, the use of microorganisms for bioremediation was not regulated. During this time, many companies marketed products for clearing drains and degreasers with proprietary formulations, suspected to contain Bcc strains (LiPuma and Mahenthiralingam, 1999). Owing to the emerging threat of the Bcc as opportunistic pathogens, this instigated outcry for new regulations from the people in the medical community (LiPuma and Mahenthiralingam, 1999).

Bcc contamination is prevalent in water supplies (Coenye and Vandamme, 2003; Koenig and Pierson, 1997) and is frequently found in cosmetics, medical equipment, pharmaceutical products (Balkhy et al., 2005; Dolan et al., 2011; Hanulik et al., 2013; Jimenez, 2001; Memish et al., 2009; Moehring et al., 2014; Pankhurst and Philpott-Howard, 1996; Shrivastava et al., 2016; Vardi et al., 2013), and, notably, biocides (Ahn et al., 2016; Baldwin et al., 2007; Kutty et al., 2007; Lee et al., 2013; Torbeck et al., 2011; Weber et al., 2007). The diverse metabolic functions and intrinsic resistance of the Bcc can be applied to alter or even metabolize antibiotics, such as penicillin (Beckman and Lessie, 1979a), and survive in disinfectants such as chlorhexidine (Heo et al., 2008) and benzalkonium chloride (Ahn et al., 2016). It is unfortunate that Bcc are ubiquitously found throughout the environment, as Bcc bacteria have emerged as opportunistic

pathogens.

1.1.2 Infections with Bcc

Bcc infection are particularly dangerous for cystic fibrosis (CF) patients and individuals with chronic granulomatous disease (CGD) (Bressler et al., 2007; Reik et al., 2005). In addition, Bcc have become more prevalent in nosocomial infections of immunocompromised individuals (Hanulik et al., 2013; Mann et al., 2010; Satpute et al., 2011). Many outbreaks have been directly linked to contamination of medical devices, disinfectants and pharmaceutical products, including inhalers (Balkhy et al., 2005; Memish et al., 2009) and nasal sprays (Cunha et al., 2007; Dolan et al., 2011), whose use provided a quick route to the respiratory tract. Since Bcc strains have not been found to colonize humans other than at the site of infection, it is assumed that in cases where no patient to patient transmission has occurred, the source of the Bcc is the environment (Mahenthiralingam et al., 2008).

1.1.3 Immunocompromised individuals

Infections with Bcc are commonly nosocomially acquired from the use of contaminated medical devices or pharmaceutical products, however, epidemic spread of *B. cenocepacia* by patient to patient transmission has also been demonstrated in non-CF patients (Siddiqui et al., 2001). The prevalence of Bcc contamination in hospital equipment and pharmaceutical products has resulted in numerous infections in patients, including bacteremia (Antony et al., 2016; Nannini et al., 2015), pneumonia (Hanulik et al., 2013; Lucero et al., 2011), septic arthritis (Miki et al., 2006; Nivedhana et al., 2016), urinary tract infections (Li et al., 2003; Souza Dias et al., 2013), and endocarditis (Falcão Pedrosa Costa et al., 2014; Williamson and McBride, 2011). Treatment

of these infections is difficult resulting in a high mortality rate because of the high intrinsic resistance of the Bcc (LiPuma et al., 2011).

1.1.4 Chronic granulomatous disease

Bcc infections cause life threatening pneumonia and septicemia in patients with CGD (Winkelstein et al., 2000). In 6% of CGD patients infected with Bcc, the infection is fatal (Marciano et al., 2015). CGD patients are susceptible to Bcc infection because mutations in genes encoding protein subunits of the NADPH oxidase complex result in an impaired oxidative burst in neutrophils and macrophages that causes defective intracellular killing of phagocytosed bacteria (Bylund et al., 2005; Porter and Goldberg, 2011; Speert et al., 1994). Bcc are the most frequently recurrent bacterial infections in CDG patients (Marciano et al., 2015). Longitudinal sampling from CGD patients with recurrent Bcc infections after antibiotic treatment suggests that the acquisition of a new strain is the cause rather than a failure to clear the initial infection (Greenberg et al., 2009). This is in contrast to lung infections in patients with cystic fibrosis whose inability to clear the infection with Bcc bacteria is thought to be the cause for reoccurrence (Chen et al., 2001). However, there is debate about whether the bacteria identified during sequential screening is indicative of the infecting strain or a representative from the microbiome (Bernhardt et al., 2003; Lipuma, 2010) and whether the sampling methods and culture-dependent techniques are adequate for interrogating the microbial community of the lower airways (Caverly et al., 2015; Dickson et al., 2013). Since Bcc species are widespread throughout the environment, continual exposure is unavoidable and recurrent infection is likely (Govan et al., 2007). Additionally, Bcc strains resistant to trimethoprim-sulfamethoxazole and ceftazidime, the two antibiotics most used to treat Bcc infections, have been isolated from CGD patients (Marciano et al., 2015), leaving few treatment options and leading to poor patient outcomes.

1.1.5 Cystic fibrosis

Cystic fibrosis (CF) is the most common inheritable disease affecting young Canadians (Ratjen and Doring, 2003). CF is an autosomal recessive disease, caused by mutations in both copies of a chloride ion transporter gene, the cystic fibrosis transmembrane conductance regulator gene (CFTR) (Kerem et al., 1989; Riordan et al., 1989; Rommens et al., 1989). Patients with CF have a decreased lifespan and are highly susceptible to respiratory infections (Gibson et al., 2003). In the lungs, mutations in CFTR results in impairment of innate antimicrobial activity (Keith et al., 2009), decreased fluidity of mucus as well as reduced depth of the surface liquid required for cilia movement (Gibson et al., 2003), resulting in impaired clearance of bacteria. In addition, release of reactive oxygen species results in airway damage in CF patients, partially due to increased inflammation caused by the release of cytokines because of delayed apoptosis of CF neutrophils (Fox et al., 2010). Patients with CF are particularly vulnerable to lung infections with Bcc (Lipuma, 2010). The outcomes CF patients infected with Bcc are unpredictable and depend on the patients' health, age, treatment history and type of mutation (Zlosnik et al., 2015). Chronic pulmonary inflammation due to infections leading to lung damage is a significant contributor of CF pathogenesis and the main cause of death (Rao and Grigg, 2006). Much progress has been made in CF therapies, however the long term effectiveness of these therapies is unknown (Bell et al., 2015) and successful treatment is dependent on which class of mutation the patient has (Amaral and Kunzelmann, 2007).

While all species of the Bcc have been shown to infect CF patients, *B. cenocepacia* poses the highest threat and, along with *B. multivorans,* is the most common species isolated from CF and non-CF patients in North America (Drevinek and Mahenthiralingam, 2010; Lipuma, 2010). CF patients infected with *B. cenocepacia* can develop "cepacia syndrome", a fatal necrotizing

pneumonia and septicemia (Isles et al., 1984). There are no indicators to predict the development of cepacia syndrome and it occurs in patients with mild disease symptoms and, reportedly, in previously healthy individuals (Pujol et al., 1992; Wong and Akerley, 2007). Colonization with *B. cenocepacia* is an indicator of poor prognosis due to the incidence of recurrent infections and the associated poor outcomes of patients, even those who receive lung transplants (Stephenson et al., 2015). This has prompted the exclusion of patients infected with *B. cenocepacia* from being considered for lung transplants (Kotloff and Thabut, 2011).

Since *B. cenocepacia* does not usually infect healthy individuals, there has been much research using *in vivo* infection models to further understand the relationship between the immune system and *B. cenocepacia*. In *in vivo* models, *B. cenocepacia* can survive within different eukaryotic cells including amoebae, epithelial cells and macrophages (Landers et al., 2000; Martin and Mohr, 2000; Saldias and Valvano, 2009). In CFTR-defective macrophages, *B. cenocepacia* evades lysosomal degradation by delaying the acidification and phago-lysosomal fusion of the *B. cenocepacia*-containing vacuoles (BcCVs). This is mediated through a type VI secretion system in viable intracellular *B. cenocepacia* cells that cause a lack of assembly of the nicotinamide adenine dinucleotide phosphate (NADPH) oxidase complex, Nox2 (Keith et al., 2009) (Aubert et al., 2015) and failure to activate Rab7 (Huynh et al., 2010; Lamothe and Valvano, 2008). Rab7 is a GTPase necessary to activate lysosome tubulation and consequent phagosome maturation (Gutierrez, 2013). The failure to form the degradative phagolysosome prevents the elimination of the bacteria (Fairn and Grinstein, 2012).

1.2 *B. cenocepacia*

The strain used in this work, *B. cenocepacia* K56-2, is a strain of Bcc genomovar III, a group of phenotypically similar isolates. Group III strains are phylogenetically divided into 4 subgroups by their r*ecA* gene (Vanlaere et al., 2009). *B. cenocepacia* strains of subgroup IIIA are epidemic strains associated with "cepacia syndrome" (Isles et al., 1984). In 1990, a subgroup IIIA strain of *B. cenocepacia* was the cause an epidemic outbreak in CF patients (Govan et al., 1993). This virulent *B. cenocepacia* strain, called the ET-12 lineage, for Edinburgh/Toronto (Sun et al., 1995) or electrophoretic type (Johnson et al., 1994), was thought to originate in Canada or the United Kingdom and was recovered from CF patients in Canada (Mahenthiralingam et al., 1996; Speert et al., 2002), the United Kingdom (Govan et al., 1993), and Europe (Vandamme et al., 2003). The severity of infections caused by patient to patient transmission of this strain instigated the implementation of strict infection controls in the CF community (Fung et al., 1998). *B. cenocepacia* K56-2, belongs to the ET12 lineage that was isolated from a patient in Canada.

1.2.1 *B. cenocepacia* genome

B. cenocepacia J2315 is the most closely related clonal strain to *B. cenocepacia* K56-2 (Mahenthiralingam et al., 2000a). K56-2 is often used in studies because it is more amenable to genetic manipulation than J2315. K56-2 is sensitive to trimethoprim, which targets dihydrofolate reductase, inhibiting the synthesis of tetrahydrofolic acid. A mutation in the *dhfrA* gene in *B. cenocepacia* J2315 causes resistance to trimethoprim. The closed genome sequence of *B. cenocepacia* J2315 has been published (Holden et al., 2009b) and has been typically used as a reference strain for *B. cenocepacia* K56-2. The 8,055,782 bp genome of *B. cenocepacia* J2315 contains 7,261 coding sequences distributed over 3 chromosomes and a plasmid, sizes 3,870,082, 3,217,062, 875,977 and 92,661 (Holden et al., 2009b). More proteins involved in core functions

are encoded on chromosome one than the smaller replicons, while higher number of proteins of unknown function and those involved in auxiliary functions are encoded on the smaller replicons (Holden et al., 2009b). The adaptability of epidemic strains of *B. cenocepacia* to the CF lung has been attributed to the plasticity of the genome mediated by the large number of genomic islands and insertion sequence (IS) families (Baldwin et al., 2004; Graindorge et al., 2012; Lessie et al., 1996). The 14 genomic islands identified in *B. cenocepacia* J2315 account for nearly 10% of the genome and *B. cenocepacia* J2315 has the highest number of IS elements of the sequenced *B. cenocepacia* strains (Graindorge et al., 2012).

The same species of bacteria can have differences in their genomic content (Turner et al., 2015). The elasticity provided by the mobile genetic elements of the *B. cenocepacia* genome is responsible for much of the divergence from other *B. cenocepacia* strains (Holden et al., 2009b). Although the strains are clonally related, from the assembly of *B. cenocepacia* K56-2, two regions corresponding to genomic islands are duplicated in *B. cenocepacia* K56-2, while they are only present in a single copies in J2325 (Bloodworth, 2013). A large duplication of 57 kb containing 57 genes encoding proteins with various functions in J2315 is not present in K56-2 (Bloodworth et al., 2013a; Holden et al., 2009b). While this region is a perfect duplication in J2315, it is notable that differences in genomic content is a common attribute of the Bcc and the genomes of even closely related strains can differ by as much as 10% (Holden et al., 2009b). The strain of *B. cenocepacia* K56-2 used in this work has been recently been sequenced and the draft genome is available (GenBank Accession LAUA00000000).

1.2.2 Genomic islands

Genomic islands were initially identified in uropathogenic *E. coli* in the 1980s as "pathogenicity islands" by Hacker et al (Hacker et al., 1990). These sequences have different GC

content and codon usage from the rest of the genome, due to recent acquisition during evolution. Genomic islands can encode genes involved in diverse functions including metabolism, symbiosis, pathogenicity, and resistance (Juhas et al., 2009). Genomic islands usually have evidence of past or current mobility and are generally unstable unless growth conditions of the bacteria select for their maintenance (Dobrindt et al., 2004). Many genomic islands contain insertion elements or transposons, indicating the insertion or removal of genes within the island (Buchrieser et al., 1998). Insertion sequences contribute to the evolution of environmental bacteria into pathogens (Juhas et al., 2009) and have been implicated in the adaptability of *B. cenocepacia* J2315 and responsible for its competence as a pathogen of CF patients (Holden et al., 2009b). *B. cenocepacia* strains are particularly susceptible to integration of foreign DNA as they do not possess a CRISPR-Cas system (Dennis, 2016; Horvath and Barrangou, 2010).

The first genomic island identified in *B. cenocepacia* contains the *Burkholderia* epidemic strain marker (BCESM). BCESM was identified by random amplified polymorphic DNA fingerprinting from virulent strains of *B. cenocepacia* genomovar III that were associated with high mortality rates in CF patients (Mahenthiralingam et al., 1997, 2001). Since BCESM was not found in all *B. cenocepacia* strains, it was proposed that it was part of an unstable region of the genome (Mahenthiralingam et al., 2000b). BCESM was found to be a part of the *cenocepacia* island (*cci*), a genomic island that encodes genes involved in pathogenicity and metabolism (Baldwin et al., 2004). The 14 genomic islands identified in *B. cenocepacia* J2315 encode genes involved in transport and metabolism, stress response, antibiotic resistance and pathogenicity (Holden et al., 2009b). Multiple genomic islands and mosaic genomic islands can be found in different locations of some genomes (Brochet et al., 2009; Clewell and Gawron-Burke, 1986; Guérillot et al., 2013). This has been seen in *Burkholderia* strains indicating a selective pressure

for conservation of these regions (Holden et al., 2009b).

1.2.3 *B. cenocepacia* antibiotic resistance

Treatment options for infections with *B. cenocepacia* are limited due to its intrinsic resistance to many antibiotics (Burns, 2007). Bcc can develop resistance to most antibiotics currently in use, particularly after chronic infections and the cycles of antibiotic treatments that occur in CF patients (Gautam et al., 2015; Govan and Deretic, 1996). Treatment regimens typically consist of trimethoprim/sulfamethoxazole, ceftazidime and meropenem along with other drugs such as penicillin, usually in conjunction or cycled (Regan and Bhatt, 2016). However, there is currently no established protocol for successful treatment of these infections (Gautam et al., 2015). Efforts have been made to define treatments that can eradicate Bcc infections or delay the onset of chronic infection (Regan and Bhatt, 2016). However, due to a lack of evidence to establish protocols for the eradication of Bcc once patients are colonized, the authors concluded that there is an urgent need for multi-center studies of novel antibiotics (Regan and Bhatt, 2016). The biggest impediment to antibiotic treatment of infections with Bcc is that they demonstrate significantly reduced drug penetration of the cell envelope (Aronoff, 1988; Burns et al., 1989; Moore and Hancock, 1986; Parr et al., 1987).

1.2.4 Modified Lipopolysaccharide

Lipopolysaccharide (LPS) is an endotoxin with a tripartite structure consisting of lipid A, a core oligosaccharide and O-antigen, in the outer leaflet of the outer membrane in Gram-negative bacteria (Whitfield and Trent, 2014). For infections with Gram-negative bacteria, the polymixin antibiotic colistin, is currently the most effective treatment, and is often used as a last resort (Falagas et al., 2005a). Polymixins are amphiphilic cyclic polycationic peptide antibiotics that have

an affinity for the negatively charged outer membranes of Gram-negative bacteria (Katsu, 1991). Polymixins increase the permeability of cells by disrupting the cell envelope (Vaara, 1992). Unfortunately, Bcc are intrinsically resistant to antimicrobial peptides like polymyxin due to a modified lipopolysaccharide (Cox and Wilkinson, 1991; Moore and Hancock, 1986). The LPS of Bcc bacteria is distinct because the core oligosaccharide contains fewer phosphate and 3-deoxy-D-manno-oct-2-ulosonic acid (KDO) than other Gram-negative bacteria (Manniello et al., 1979). The Lipid A of Bcc also contains a phosphodiester-linked 4-amino-4-deoxyarabinose (Ara4N) moieties (Isshiki et al., 1998). Overall these modifications result in a reduction in negative charge of the outer membrane causing the reduced affinity of cationic peptides like polymixin (Cox and Wilkinson, 1991).

1.2.5 Biofilms

Biofilms are surface attached or free aggregates of bacteria within a matrix of extracellular polymeric substrate (EPS) produced by the bacterial cells (Flemming et al., 2016). EPS can protect against antibiotic diffusion by adsorbing or reacting with the antibiotic, resulting in a higher tolerance of the bacteria within biofilms (Daddi Oubekka et al., 2012). The presence of other strains and extracellular DNA within the matrix of the biofilm provides an opportunity to exchange antibiotic resistance genes by horizontal gene transfer (Madsen et al., 2012). Bacteria in biofilms exist mostly as sessile cells in stationary phase which are less susceptible to antibiotic treatment (Amato et al., 2014). *B. cenocepacia* forms biofilms *in vitro* (Conway et al., 2002; Huber et al., 2001; Riedel et al., 2001) where they have been shown to become more resistant to ceftazidime and ciprofloxacin than planktonic cells (Desai et al., 1998). While recent evidence suggests that *B. cenocepacia* does not exist as a biofilm in the CF lung (Schwab et al., 2014), Bcc biofilms in hospitals and on equipment have been suspected as the cause of epidemic outbreaks (Dolan et al.,

2011; Heo et al., 2008; Lucero et al., 2011).

1.2.6 Efflux pumps

Depending on the substrate affinity, efflux pumps can provide resistance to a broad range of antibiotics. Early evidence suggested the involvement of efflux in the resistance of *B. cenocepacia* to fluoroquinilones, chloramphenicol, trimethoprim, and ciprofloxacin (Burns et al., 1996; Hancock, 1998; Zhang et al., 2001). Nair et al. showed that the activity of an efflux pump from the resistance nodulation cell division (RND) family, CeoAB-OpcM, was inducible with salicylate and chloramphenicol (Nair et al., 2004). Six families of efflux pumps have been identified in the genome of *B. cenocepacia* J2315 (Holden et al., 2009b). Of these, efflux pumps of the RND family are the best characterized. Of the sixteen efflux pumps of the RND family that have been identified in *B. cenocepacia* J2315 (Holden et al., 2009b), six, RND1, RND3, RND4, RND8, RND9, and RND10, have been shown to be involved in antibiotic resistance (Bazzini et al., 2011; Buroni et al., 2009, 2014; Coenye et al., 2011; Nair et al., 2004; Scoffone et al., 2015). Mutations in the regulator of RND3 is responsible for efflux pump mediated antibiotic resistance of clinical strains of the Bcc (Tseng et al., 2014). Mutational analysis has revealed that RND3 and RND4 contribute the most to the intrinsic resistance of planktonic cells, while RND3, RND8, and RND9 are involved in resistance to tobramycin in sessile cells (Buroni et al., 2014).

1.2.7 Porins

The permeability of the envelope of bacterial cells, providing a selective barrier to protect against harmful compounds while letting nutrients into the cell, is mediated through the activity of porins (Koebnik et al., 2000). Porins are water-filled pores that span the outer membrane allowing the uptake of hydrophilic compounds less than a specific size (Nakae, 1976). While large

antibiotics enter the cell by slow diffusion through the outer membrane, most hydrophilic and amphiphilic antibiotics get across the outer membrane through porins (Nikaido, 2003; Pagès et al., 2008). In *E.coli*, the permeability of the membrane is mostly dependent on the general OmpC/OmpF porins, with a size exclusion limit of 600 Da (Zgurskaya et al., 2015). A homolog of the *E. coli* OmpF general porin, Omp38/OpcP, has been identified in two other *Burkholderia* strains, *B. thailandensis* and *B. pseudomallei* (Siritapetawee et al., 2004a). Whether this porin functions similarly to OmpF is unclear. One study on the Omp38/OpcP porin from *B. thailandensis* and *B. pseudomallei* found that it functions similarly to the *E. coli* OmpF (Siritapetawee et al., 2004b) while another study found that it is less permeable than OmpF (Suginta et al., 2011). However, the reduced permeability of antibiotics in Bcc species has previously been attributed to the small channel size of porins in comparison with *E. coli* porins (Parr et al., 1987).

1.3 Antibiotic development

In recent decades there has been a shortage of the production of new antibiotics (Payne et al., 2007). This is a substantial problem, since the emergence of antimicrobial resistant bacteria, like the Bcc, pose a significant threat to public health (Forum, 2014; Organization, 2014).

A lack of the production of new antibiotics against new targets can be attributed to the underrepresentation of compounds with novel scaffolds used in screens by pharmaceutical companies, as well as the lack of new targets being investigated (Boucher et al., 2009). Since the 1960's the focus of the pharmaceutical industry has been on medicinal chemistry to alter existing antibiotic scaffolds to combat resistance development. The benefits from these modifications are relatively short lived (Brown and Wright, 2016). The lack of screening for new antibiotics is driven by the fact that these screens are not economic, requiring a large investment of time and money

with low chance of seeing returns. While this risk reduction is fiscally reasonable, antibiotics with new chemical scaffolds and novel targets are needed (Walsh and Wencewicz, 2014). Since the first genome was sequenced, an effort to screen for new antibiotics was undertaken by the pharmaceutical industry. A literature review by P.F. Chan and colleagues (Chan et al., 2004) showed that from 1995 to 2004, a time predicted to reflect a genomics-based industry approach, 34 companies performed 127 antibacterial screens on more than 70 different bacterial targets, garnering no new antibiotic drugs. In addition, Payne et al. described the lack of success of finding lead compounds from over 100 chemogenetic screens of at Galaxo-Smith Kline (Payne et al., 2007). Conventionally, pharmaceutical companies limited the lead compounds to those that have broad spectrum activity. However, the benefits of using narrow-spectrum antibiotics are now being considered, which would open up a collection of compounds with antibiotic activity to investigate (Maxson and Mitchell, 2016).

1.3.1 *In vitro* assays

Biochemical screens on isolated targets have been unsuccessful at identifying lead compounds (Payne et al., 2007; Projan and Youngman, 2002). The failure of these screens to produce viable drugs prompted questions about the use of *in vitro* screening of targets instead of whole-cell assays, as well as the use of chemical libraries biased for compounds against eukaryotic targets (Lewis, 2013; Payne et al., 2007). Many compounds with *in vitro* inhibition are not active against whole cells or the compounds do not inhibit the anticipated target once in the context of the whole cell (Baell and Holloway, 2010). Currently, the main challenge for developing new antibiotics against Gram-negative bacteria is not only finding antibiotics with a new chemical scaffold that binds to a specific target, but that is capable of entering the cell (Silver, 2011).

In order to increase the chance of identifying compounds that are able to penetrate the cell envelope, there has recently been a shift from the convention of enriching libraries for compounds that follow the Lipinski rules (Lewis, 2013; Lipinski, 2000). The Lipinski rules are good at predicting oral availability, however, these compounds are inherently poor at penetrating the outer membrane of Gram-negative bacteria (Lipinski, 2000). This, combined with the vast library of small compounds available to screen against bacteria, shows promise for identifying antibiotic leads. Although it is predicted that 10 million compounds have already been screened against prokaryotes, (ZINC database) (Irwin and Shoichet, 2005), there still a large theoretical chemical space of small molecules yet to be interrogated for antibiotic properties (Bohacek et al., 1996).

1.3.2 Whole cell screens

The majority of current antibiotics were originally identified because of their capability to inhibit bacterial growth (Breithaupt, 1999). More recently, the first new anti-tubercular drug approved by the FDA since the 1970's, Bedaquiline, for treatment of multi-drug resistant tuberculosis, was identified from a high throughput whole cell screen (Andries et al., 2005; Matteelli et al., 2010). The advantage of whole cell screens is the ability to identify compounds that can penetrate the cell membrane and have growth inhibitory effects. However, the disadvantage is that the MOA of the compound is unknown, which can lead to investing time and money into investigating the MOA of compounds that act through non-specific MOAs (Burdine and Kodadek, 2004). Many previous failed compounds from whole cell screens were due to the identification of hit compounds that act through non-specific mechanisms of actions (Lewis, 2013; Payne et al., 2007). A huge investment of time and money has been wasted investigating these compounds. However, since the identification of the common attributes associated with these

nuisance compounds or Pan-Assay InterfereNce compoundS (PAINS), chemical libraries are being pre-filtered to exclude these types of molecules (Baell and Walters, 2014).

1.4 Essential genes as antibiotic targets

1.4.1 Essential genes

Essential genes are the genes required for growth or survival of a cell. However, this is contextual based on the selective pressures of the environment, within the context of the expression of other genes within the cell, or even the definition of a live cell (D'Elia et al., 2009; Gerdes et al., 2006). While the essential genome has been defined as the genes required "to sustain a functioning cellular life form under the most favorable conditions imaginable" (Koonin, 2000), a practical and standard definition is genes that are required for growth in rich media are considered essential (Reich, 2000).

The identification of essential genes is a key step to studying their function (D'Elia et al., 2009). In this work, the main reason for studying essential genes is to identify targets for novel antibiotics. Currently, the most successful antibiotics target a few processes that are essential for growth: protein synthesis, DNA replication and cell wall synthesis. Therefore, it is likely that previously unexplored essential gene products will provide suitable targets for novel antibiotics (Murima et al., 2013). Since resistance mechanisms that have evolved to counter the activity of antibiotics can be applied to new antibiotics that target the same functions, there is motivation to consider alternative essential cellular processes as targets for the development of antibacterial classes. The conventional methods used to identify essential genes are systematic gene-by-gene inactivation (Baba et al., 2006; Kobayashi et al., 2003), based on bioinformatics analysis (Juhas et al., 2012a) or transposon mutagenesis (Hutchison et al., 1999; Jacobs et al., 2003).

1.4.2 Identification of essential genes

Once the first sequenced genomes of *Haemophilus influenza* (Fleischmann et al., 1995) and *Mycoplasma genitalium* (Fraser et al., 1995) became available, comparative genomics was used in an attempt to determine the minimal core genome, resulting in the identification of 256 essential genes (Mushegian and Koonin, 1996). However, as more genomes of prokaryotes were sequenced and compared, the number of shared genes drastically decreased, resulting in a core genome predictions consisting of very few genes (Brown et al., 2001; Charlebois and Doolittle, 2004; Harris et al., 2003; Koonin, 2003). Restricting the comparison to genomes of phylogenetically related organisms is better for making predictions as they have higher sequence homologies (Juhas et al., 2011). By comparing 51 genomes of *Burkholderiales* species, Juhas *et al*. identified 610 orthologous groups shared between the genomes which correspond to 645 genes in *B. cenocepacia* J2315. However, the issue with identifying conserved genes as essential is that the genetic conservation of genes does not necessarily correlate with essentiality (Fang et al., 2005). Fang et al. differentiates these genes as "persistent nonessential genes" and experimentally essential genes (Fang et al., 2005).

1.4.3 High density transposon mutagenesis

The essential genomes of model bacteria have been determined by the ability to recover mutants after concerted disruption of nonessential genes (Baba et al., 2006; Gerdes et al., 2003; Kobayashi et al., 2003; Mori, Isono, Horiuchi, & Miki, 2000). A more feasible approach is to use random transposon mutagenesis.

The breakthrough of next generation sequencing (NGS) is the ability to produce an enormous number of DNA sequences at a low cost in the form of millions of short reads per instrument run (Metzker, 2010; Shendure and Ji, 2008). In 2009, four methods were published by independent research groups, Tn-seq (Opijnen et al., 2009), TraDIS (Langridge et al., 2009), INSeq (Goodman et al., 2009) and HITS (Gawronski et al., 2009), designed to simultaneously sequence insertion junctions of high-density transposon mutant (HDTM) libraries composed of pools of hundreds of thousands of transposon mutant clones. Since then, these methods have been widely used for determining genes required for the fitness of multiple microorganisms in various *in vitro* and *in vivo* conditions. To sequence HDTM libraries, genomic DNA is randomly sheared or cleaved by specific enzymes, oligonucleotide adapters are added to the fragments and then the transposon-containing fragments are sequenced directly or PCR amplified and sequenced. Mapping the distribution of transposon insertion sites across the entire microbial genome can identify genes that lack insertions, while genes containing insertions can be considered to be nonessential in the experimental conditions where the transposon mutants were selected (Langridge et al., 2009). HDTM libraries are valuable for essential gene set mapping, as multiple lethal insertions can be located throughout a single gene, tracking the effect of gene disruption at different positions. This avoids false negatives, like insertions located near the 5′- or 3′-end termini of an essential gene that result in a viable mutant if the truncated protein is functional (Hutchison et al., 1999).

1.4.4 Analysis for determining the essential genome

After the reads are mapped to the reference genome, different methods for determining the essential gene set can be used. Many of these methods determine the likelihood that a gene is essential by considering only the number of insertions per gene (Christen et al., 2011a; Moule et

al., 2014a). In the TraDIS (Transposon directed insertion-site sequencing) method, the number of insertion sites per gene are tallied and divided by the gene length, generating an "insertion index" for each gene (Langridge et al., 2009). The insertion indexes for each gene generally produce a bimodal distribution (Barquist et al., 2013). To determine the essential genes, distributions are fitted to the two modes corresponding to the essential gene and nonessential gene sets and a log2-likelihood ratio (LLR) is then calculated for each gene. A LLR of greater than 2 means that that gene is 4 times more likely to fit in the non-essential mode, while a LLR less than -2 is four times more likely to be in the essential mode.

More recently, methods have been developed to account for the relative abundance of each insertion mutant in the library (Lee et al., 2015; Robinson et al., 2010; Turner et al., 2015). Lee et al. used a method that calculates both the insertions per kb and the reads per kb, which are then divided by the corresponding gene lengths. After calculating the distributions for the insertions and reads per genes, essential genes are classified for genes with a zero value and P value of less than 0.001. Turner et al. developed an approach that uses an RNA-seq data analysis pipeline (Anders et al., 2013) to test the significance of gene essentiality by accounting for the abundance of each transposon mutant in the library and the probability that a gene would be considered essential by chance (Turner et al., 2015). To determine the essential gene set, the reads for each insertion site are randomly mapped throughout the genome in a Monte Carlo simulation to create an expected pseudodata set. The real and pseudodata sets are then compared to determine the genes that are significantly depleted in the real data set. Genes are defined as essential if they are significantly depleted by a negative binomial test and if the probability that it belongs to the reduced mode of a bimodal Gaussian mixture model was less than 0.01 (Turner et al., 2015).

1.4.5 Whole cell chemogenetic screens

Large collections of mutants created by random or systematic mutagenesis offer the attractive approach of providing insight into nonessential gene function. By investigating mutant fitness in different conditions, a direct link between genotype and phenotype can be created. Thus, a quantitative analysis of mutant growth within the mutant population across conditions is necessary. Foundational work in prokaryotes by Badarinarayana et al. (Badarinarayana et al., 2001) showed that the fitness contribution of *E. coli* genes under specific growth conditions could be evaluated using the analysis of the transposon mutant library composition before and after exposure to those conditions. NGS technology has showed promise for enhancing the power of transposon mutant libraries in fitness studies.

Pioneering work in chemical genomics with a barcoded yeast library demonstrated that the cost of massive assays can be reduced by highly multiplexed sequencing (Smith et al., 2009, 2010). Once a HDTM library is constructed, a fitness analysis can be performed by tracking the fate of individual transposon mutants in pools grown under selective conditions. This can be achieved by extracting the genomic DNA of the sample, sequencing the insertion sites and calculating enrichment or depletion ratios of each mutant in the pool, before and after a certain selective pressure, such as antibiotic treatment, is applied (Gawronski et al., 2009; Langridge et al., 2009; Opijnen and Camilli, 2010). Importantly, the differential enrichment or depletion ratio of a transposon mutant can link the transposon-tagged gene to the tested antibiotic, providing insights into the genes that may enhance or reduce the antibiotic effect.

An adapted Tn-seq method, Tn-seq circle (Gallagher et al., 2011a) was used to study the intrinsic resistance of *Pseudomonas aeruginosa* to tobramycin. NGS was performed on an outgrowth pool of 100,000 transposon insertion mutants, grown in the presence or absence of a

subinhibitory concentration of tobramycin. Mutants lost or underrepresented in the tobramycin selective condition, compared to the control condition, indicated that the mutated gene is involved in tobramycin resistance. Overall, this screen identified 117 genes involved in tobramycin resistance, including 13 new genes revealing previously unknown tobramycin-resistance functions. The data sets generated by Tn-seq and related methods, TraDIS (Langridge et al., 2009), INSeq (Goodman et al., 2009) and HITS (Gawronski et al., 2009), can be used to create networks in order to analyze genetic interactions. Recently, van Opijnen & Camilli (Opijnen and Camilli, 2012) analyzed combined data obtained from *in vitro* and *in vivo* studies of *Streptococcus pneumoniae* transposon insertion libraries to create a genotype–phenotype interaction map. By comparing overlapping virulence phenotypes *in vivo* to *in vitro* conditions, they were able to identify selective pressures present in the host model. This study revealed over 1800 genetic interactions, including niche-specific virulence pathways, representing putative targets for antibiotic development. These Tn-seq approaches represent model assays for analyzing pathways and processes related to antibiotic profiling. While there is no doubt that high density transposon mutant libraries are powerful tools, their limitation is that only non-essential genes are interrogated since disruption of an essential gene renders the bacteria nonviable. Generation of spontaneous resistant mutants in response to incubation with successive increasing doses of antibiotics has successfully identified targets of antibiotics. However, this method may identify multidrug resistance mechanisms related to off-target processes such as the overexpression of efflux pumps (Scoffone et al., 2015).

1.4.6 Essential genes in chemogenetic screens

In innovative work using a heterozygote *Saccharomyces cerevisiae* strains, Shoemaker and Giaever analyzed drug sensitivities of individual haploinsufficient strains from an array simultaneously (Giaever et al., 1999; Shoemaker et al., 1996). The only way to employ a similar method to study essential genes in bacteria is by using conditional mutagenesis. In order to obtain viable cells, the essential gene is expressed in a permissive condition, but can be titrated in non-permissive conditions to create a sensitized strain (Cardona et al., 2015a). Diminished expression of an essential protein generates a growth defect in the mutant. The expression of the essential gene can be controlled by the use of antisense RNA (Forsyth et al., 2002a), CRISPR interference (Larson et al., 2013a) or promoter replacement (Judson and Mekalanos, 2000a).

Whole cell chemogenetic screens using a library of 245 siRNA essential gene mutants of *Staphylococcus aureus* have identified the mechanisms of action (MOAs) of antibiotics with novel scaffolds, plantensimycin, platencin and kibdelomycin (Phillips et al., 2011; Singh et al., 2006; Wang et al., 2007). While this is encouraging, the phenotype of antisense RNA strains is not always reliable or specific since antisense RNA can inhibit mRNA with similar sequences, confounding hit identification (Jackson et al., 2003; Ji et al., 2001).

CRISPR interference is a form of adaptive immunity used by bacteria where small RNAs target foreign nucleic acids (Marraffini and Sontheimer, 2010). CRISPR interference can be used to conditionally express essential genes by inducible expression of single guide RNAs (sgRNA) that inhibit transcription by base-pairing to the targeted sequence of DNA (Qi et al., 2013). CRISPR interference identifies essential operons as genes both downstream and upstream of the target DNA have decreased expression (Peters et al., 2016a). Using this method Peters et al. identified the target of a novel compound with an unknown mechanism of action (Peters et al.,

2016a). A drawback of this method is that the sequence of the targeted essential gene is required to design the sgRNAs for CRISPR interference so it is not conducive to screens using non-model organisms whose essential genome is unknown.

Conditional mutagenesis by replacing an essential genes promoter with an inducible promoter can be achieved by targeted insertion (Carroll et al., 2005; Ehrt et al., 2005a) or by inserting the promoter randomly using a transposon (Bloodworth et al., 2013a; Judson and Mekalanos, 2000b).

With the goal of identifying the essential genome of *B. cenocepacia* K56-2, we previously used transposon mutagenesis to insert a rhamnose-inducible promoter, P*rhaB*, into the genome. This was accomplished by introducing a suicide plasmid pRBrhaBoutgfp into *B. cenocepacia* K56-2 by triparental mating. The suicide plasmid contains the miniTn5 transposon sequence derived derivative of the Tn5 transposon (Berg et al., 1975) originally discovered as imparting kanamycin and neomycin resistance in *Klebsiella*. In pRBrhaBoutgfp, P*rhaB* and a trimethoprim resistance cassette are flanked by 19 base pair inverted repeat sequences. The associated transposase of the Tn5 is located externally from the inverted repeats of the transposon, and is thus capable of creating a stable insertion (Figure 1.1). After the transposon inserts in the genome the outward facing P*rhaB* controls the expression of genes within the same transcriptional unit, downstream of the insertion. After screening 200,000 transposon mutants for a conditional growth (CG) phenotype in response to rhamnose, approximately 106 CG mutants from 50 unique operons were obtained (Bloodworth et al., 2013a).

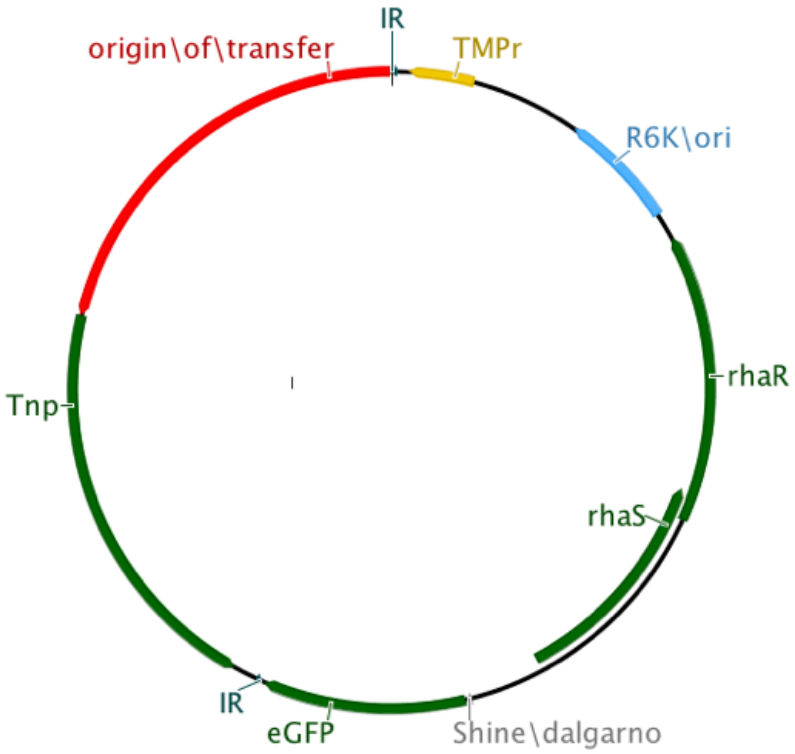

Figure 1.1 pRB*rhaB*out*gfp* Suicide plasmid used to deliver the rhamnose-inducible promoter (P*rhaB*) by random transposon mutagenesis.

Tnp, transposase; IR, inverted repeat. P*rhaB* is located upstream of eGFP. See text for details.

Using selected strains from the library of CG mutants, we demonstrated that limiting the amount of rhamnose available to induce expression, cause the CG mutants become sensitized to antibiotics that target the essential gene product that is underexpressed (Bloodworth et al., 2013a). We established our ability to detect target-drug matches using a *gyrB* mutant that is hypersensitive to its cognate antibiotic, novobiocin in an enhance sensitivity assay (ESA) (Bloodworth et al., 2013a). During the creation of the conditional growth mutant library, two independent *gyrB* insertion mutants were found (Bloodworth et al., 2013). The *gyrB* mutant can be induced to underexpress the target for the antibiotic novobiocin which binds the GyrB subunit of DNA gyrase, blocking ATP hydrolysis and preventing the introduction of negative supercoils into the DNA, causing a severe growth defect (Lewis et al., 1996). When the *gyrB* mutant's growth is inhibited to 30 to 60% of wildtype growth by titrating the amount of rhamnose available to induce expression of the *gyrB* gene and incubated in the presence of sublethal concentrations of novobiocin, a greater than 10-fold reduction is seen when the percent of optimal growth in rhamnose without antibiotic is compared to the percent of optimal growth in the presence of antibiotic. The pilot ESA also showed that other CG mutants did not have an enhanced sensitivity to a sublethal concentration of novobiocin (1 μg/ml), and further that none of the CG mutants showed enhanced sensitivity to a sublethal concentration of chloramphenicol (2 μg/ml), which inhibits protein synthesis by binding the 50S ribosomal subunit (Wilson, 2011), when the CG mutants were grown to 30-60% of wildtype growth (Figure 1.2). This pilot ESA proves that the manipulation of the copy number of an essential gene product via Pr*haB* combined with exposure to sublethal concentrations of an antibiotic targeting that gene, can cause sensitization of a CG mutant.

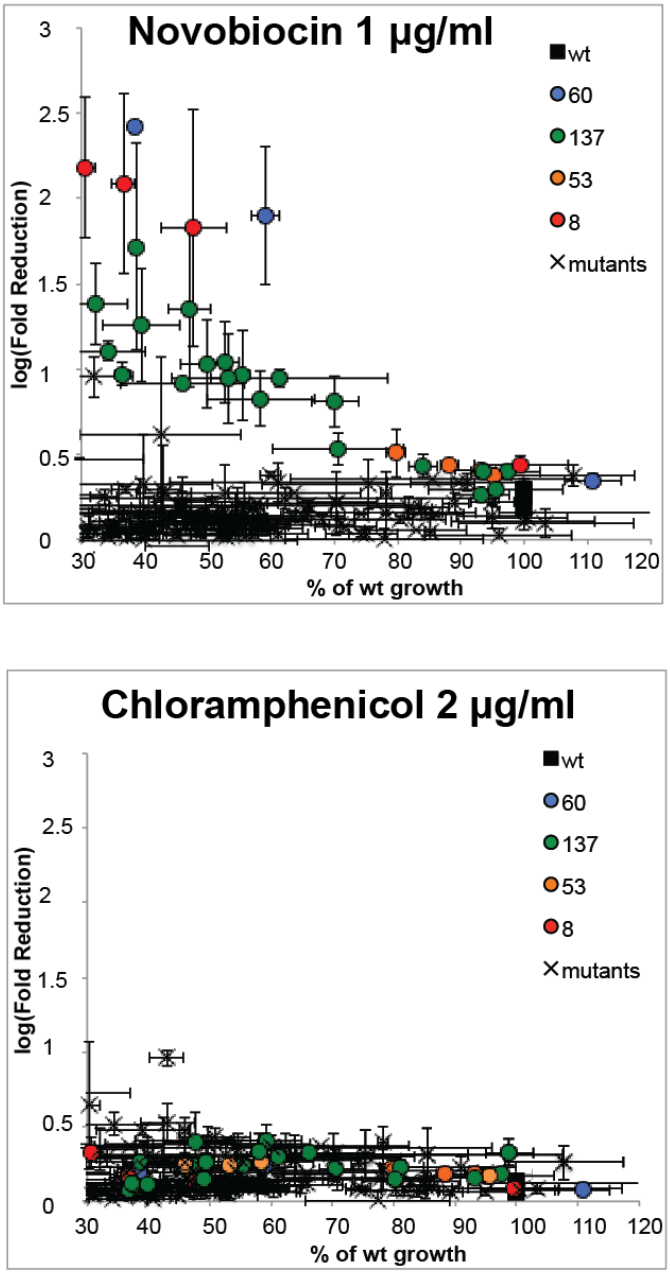

Figure 1.2 Conditional growth mutants show selective hypersensitivity.

Mutants were grown in rhamnose concentration gradients estimated to produce more than 30% of wild type growth and challenged with either novobiocin or chloramphenicol at the IC_{30} of the wild type. Circles represent CG mutants of the direct target of novobiocin, *gyrB*. Green crosses represent a CG mutant of the electron transfer flavoprotein gene (*etfA)*. Black crosses correspond to non-sensitive mutants. Mutants of *gyrB* show hypersensitivity to novobiocin when grown in rhamnose concentrations producing 30 to 60% of wild type growth but not when grown in rhamnose concentrations producing 80 to 100% of wild type growth. A CG mutant of *etfA* shows

intermediate hypersensitivity. None of the mutants showed hypersensitivity to chloramphenicol. Error bars represent 1 standard deviation calculated from 2 biological replicates.

1.5 Thesis objectives

The hypothesis of this thesis is that chemogenomic exploration of *B. cenocepacia* essential genes will result in the identification of new antibiotic targets. The pilot ESA proved that the manipulation of the copy number of an essential gene product via Pr*haB* combined with exposure to sublethal concentrations of an antibiotic targeting that gene product, causes sensitization of the CG mutant. However, the limitations of this assay were: 1) A low frequency of isolating CG mutants: In order to obtain the library of 106 CG mutants, 200,000 transposon mutants were screened for defective growth phenotype in the absence of the inducer, rhamnose; a hit frequency of 1 CG mutant isolated for every 1500 screened (Bloodworth et al., 2013a). 2) For the ESA, the CG mutants were grown clonally in liquid medium and their growth was measured by optical density, which is not conducive to a high throughput of a chemogenomic screen without the use of advanced robotic equipment. The objectives of this work are as follows:

1. To provide proof of principle that next generation sequencing could be used to detect the CG mutants when competitively grown together in a pool.

2. To create and sequence a HDTM library to determine the essential genome of *B. cencepacia* K56-2.

3. To enrich the HDTM library for CG mutants to add to the existing CG mutant library.

Chapter 2: Competitive growth enhances conditional growth mutant sensitivity to antibiotics and exposes a two-component system as an emerging antibacterial target in *Burkholderia cenocepacia*

Reproduced from: Antimicrobial Agents and Chemotherapy, 2016: Gislason AS, Choy M, Bloodworth RA, Qu W, Stietz MS, Li X, Zhang C, Cardona ST. Competitive Growth Enhances Conditional Growth Mutant Sensitivity to Antibiotics and Exposes a Two-Component System as an Emerging Antibacterial Target in *Burkholderia cenocepacia*. Antimicrob Agents Chemother. 2016 Dec 27;61(1).

April Gislason designed the experiments and performed the enhanced sensitivity assays and efflux activity assays; Ruhi Bloodworth wrote the bioinformatics scripts; Matthew Choy performed the MIC ratio and made the mutation insertion and deletion experiments; Silvina Stietz performed the microscropy; Wubin Qu designed the multiplex primer set; and Xuan Li was involved with the statistical analysis.

2.1 Introduction

The increasing occurrence of multidrug resistant infections has become a global concern (Bush et al., 2011). Moreover, there is a high demand to develop new therapeutics against multidrug resistant Gram-negative bacteria as they are predicted to be the biggest threats (Boucher et al., 2009). One example is *Burkholderia cenocepacia*, which belongs to the *Burkholderia* cepacia complex (Bcc), opportunistic pathogens that cause lung infections in immunocompromised and cystic fibrosis (CF) patients (Mahenthiralingam et al., 2005b). *B. cenocepacia* is inherently multidrug resistant owing to an impermeable outer membrane (Burns, 2007), diverse metabolic (Beckman and Lessie, 1979b) and efflux capabilities (Guglierame et al., 2006), and is capable of developing additional resistance to all classes of antibiotics *in vivo*, prohibiting effective antibiotic treatment . Despite the severity of Bcc infections and the high antibiotic resistance of Bcc (Zhou et al., 2011) isolates, there are very few efforts to develop alternative drugs for treatment. Furthermore, there is very little understanding of how antibiotic resistance is regulated and can be targeted to increase the usefulness of current antibiotics to treat Bcc infections.

Identifying novel antibacterial targets and targets for antibiotic adjuvant therapy are important steps of the antibacterial drug discovery pipeline (Brown and Wright, 2005; Burdine and Kodadek, 2004) . Chemogenetic approaches (Giaever et al., 1999; Shoemaker et al., 1996), where underexpression of single essential gene products sensitize strains to specific inhibitors of those products, are useful to identify targets and processes affected by small molecules of unknown mechanisms of action (MOAs) (Azad and Wright, 2012; Cardona et al., 2015b). Generating mutant profiles for antibiotics becomes more informative as the diversity of the mutant library increases. To modulate essential gene expression antisense RNA induction (Forsyth et al., 2002a; Wang et

al., 2006) or systematic replacement of essential gene promoters with inducible systems(Carroll et al., 2005; Ehrt et al., 2005b; Judson and Mekalanos, 2000b; Wang et al., 2011) have been employed. Recently, CRISPR interference (Larson et al., 2013a) was used to generate the first bacterial comprehensive essential gene-knockdown library (Peters et al., 2016b). However, these methodologies are not without challenges, as they employ bacterial mutants grown clonally. Bacterial growth is measured by optical density (in liquid medium) or colony size (on solid medium). Hundreds of microtiter plates, robotic equipment and specific standardization methods are required to minimize the systematic variation and batch effects across plates (Blomberg, 2011). Using an Illumina next generation sequencing platform (Bentley et al., 2008), a method to profile a library of loss-of-function yeast strains in response to small molecules was developed (Smith et al., 2009). This is in contrast with approaches to determine the targets of antibiotics (Xu et al., 2010a), which have not yet taken advantage of the sensitivity, dynamic range (Smith et al., 2009), and throughput of detection by next generation sequencing.

We previously developed a library of 106 *B. cenocepacia* K56-2 conditional growth (CG) mutants (Bloodworth et al., 2013a), expressing suboptimal levels of essential genes from a rhamnose-inducible promoter (Cardona et al., 2006a). Here, we developed a method for tracking the relative abundance of pooled conditional growth mutants after exposure to several antibiotics by Illumina sequencing of the transposon insertion tags, after amplification by multiplex-PCR. Despite our method limiting the number of mutants that could be included in the assay, antibiotic profiling revealed a CG mutant of an uncharacterized two-component signal transduction system (TCS) that was hypersensitive to several antibiotics. Genetic analysis, efflux activity assays and microscopy provided further evidence that this TCS is involved in controlling multidrug efflux

and cell membrane integrity, respectively, exposing a novel target for antibiotic drug therapy in Bcc.

2.2 Materials and Methods

2.2.1 Bacterial strains and growth conditions

Fifty-six strains (see Table 2.1 and Table 2.2) from a library of *B. cenocepacia* K56-2 CG mutants (Bloodworth et al., 2013a; Cardona et al., 2006a) were used. All strains were cultured in Luria Bertani (LB) media (Difco) (Becton, Dickenson and Company, Sparks, MD, USA) supplemented as required with 100 μg/ml trimethoprim (TMP) and different inducing concentrations of rhamnose with shaking at 37˚C. Standardized glycerol stocks of *B. cenocepacia* K56-2 (wild type) or equally pooled CG mutants within the same rhamnose category were prepared as previously described (Bloodworth et al., 2013a) (Bloodworth, Gislason, & Cardona, 2013c) (26). For growth in 96-well plates, glycerol stocks were thawed, inoculated at a final optical density (OD_{600nm}) of 0.001 in a total volume of 200 μL, and incubated at 37°C with shaking at 220 rpm for 22 h. Growth (OD_{600nm}) was measured using a BioTek Synergy 2 plate reader (BioTek Instruments, Inc. Winooski, VT, USA).

Table 2.1 Bacterial strains and plasmids

Strains	**Features**	**Source**
B. cenocepacia K56-2	Cystic fibrosis clinical isolate	(Mahenthiralingam et al. 2000)
B. cenocepacia MKC2	Site-directed CG mutant. P*rha*B promoter replacement of *esaR*	This study
B. cenocepacia MKC4	Δ*esaS*	This study
E. coli SY327	*araD*, Δ(lac *pro*) *argE* (*Am*) *recA*56 *rif*^{r} *nalA* *λpir*	(Miller and Mekalanos 1988)
Plasmids		
pRK2013	ori$_{colE1}$, RK2 derivative, Kan$^+$ mob$^+$ tra$^+$	(Figurski and Helinski 1979)
pSC201	Ori$_{R6K}$, *rhaR, rhaS,* P*rha*B *dhfr*	(Ortega et al. 2007)
pMC2	pSC201 derivative, Ori$_{R6K}$, *rhaR, rhaS,* P*rha*B, *dhfr*	This study
pGPI-SceI	ori$_{R6K}$, Tmp^R, mob$^+$, carries I-SceI cut site	(Flannagan et al 2008)
pMC4	pGPI-SceI containing upstream and downstream region of *esaS*	This study
pMC5	pGPI-SceI containing upstream and downstream region of *esaSR*	This study
pDAI-SceI	ori$_{pBBR1}$, Tet^R, mob$^+$, P$_{dhfr}$, I-SceI gene	(Flannagan et al 2008)

Table 2.2. List of CG transposon mutants

Strain name[1,2]	Locus of insertion site[3]	Genes controlled	Function
4-7D1	BCAL1506	*infB, rbfA, truB*	Translation
4-22D3	BCAL3142	*pyrR, pyrB, pyrX, plsC*	DNA replication, recombination, and repair, Nucleotide transport and metabolism, Lipid metabolism
8-15C6	BCAL0691	Unknown	Cell envelope biogenesis, outer membrane
16-2C5	BCAL2676	*pepA*	Amino acid transport and metabolism, DNA replication, recombination, and repair
28-9C11*	BCAL1299	Unknown	Unknown
28-10H8*	BCAL1515	*sucB, odhL*	Energy production and conversion
28-13B11*	BCAL1003	*lepB2*	Transport
29-15E2*	BCAL1291	hypothetical protein	Unknown
29-3B1	BCAL0330	Unknown	Stringent response
30-4C6*	BCAL0029	*atpB, atpE, atpF, atpH, atpA, atpG, atpD, atpC*	Energy production and conversion
31-7D3	BCAL1941	*dnaB*	DNA replication, recombination, and repair
31-17A3*	BCAL3471	*mraZ, mraW, ftsL, ftsI, murE, murF, mraY, murD, ftsW, murG, murC, ddl ftsQ, ftsA, ftsZ, lpxC*	Cell envelope biogenesis, outer membrane, Cell division and chromosome partitioning, posttranslational modification
32-30H3	BCAL0879	*aspS, ntpA*	Translation, DNA replication, recombination, and repair, lipid metabolism
32-32F10	BCAL2068	Unknown	Unknown
34-16F6	BCAL2388	*purD, hemF, cafA*	Nucleotide transport and metabolism, coenzyme metabolism, translation cell division and chromosome partitioning
34-17G4	BCAL3433	*ffh*	Intracellular trafficking and secretion
34-24C5	BCAL0653	hypothetical protein	Unknown
46-32G1*	BCAL2736	Unknown	Energy production and conversion
48-31G4	BCAL2408	Unknown	Cell envelope biogenesis, outer membrane

Table 2.2 List of CG transposon mutants continued

Strain name[1,2]	Locus of insertion site[3]	Genes controlled	Function
48-43H3*	BCAM0916	*dnaG*	DNA replication, recombination, and repair, transcription
51-6G10	BCAL3035	*trxB*	Posttranslational modification
51-13E10*	BCAM0911	*Dxs*	Lipid metabolism
53-15F3	BCAL3468	*murE, murF, mraY, murD, ftsW, murG, murC, ddl, ftsQ, ftsA ftsZ, lpxC*	Cell envelope biogenesis, outer membrane, cell division and chromosome partitioning posttranslational modification
57-31D10	BCAM0967	*sdhA, sdhB*	Energy production and conversion
58-14E1*	BCAL0421	*gyrB*	DNA replication, recombination, and repair
58-18F5*	BCAL2199	*iscS, hscB, hscA, fdx*	Amino acid transport and metabolism, energy production and conversion, posttranslational modification
58-21H7*	BCAM0972	*gltA*	Energy production and conversion
64-10H7*	BCAL3335	*fis, purH, ruvC, ruvA, ruvB*	Nucleotide transport and metabolism, DNA replication, recombination, and repair
67-4B6	BCAL1255	*rnhA, dnaQ*	DNA replication, recombination, and repair
67-4F2	BCAL0895	*pdxA, ksgA*	Coenzyme metabolism, translation, translation
67-5H10*	BCAL2343	*nuoC, nuoD, nuoF, nuoH, nuoJ, nuoK, nuoL, nuoM, nuoN*	Energy production and conversion, DNA replication, recombination, and repair
67-10H9*	BCAL0035	*atpD, atpC*	Energy production and conversion
67-17C2	BCAL0425	Unknown	Intracellular trafficking and secretion
69-18F6	BCAL0804	*lolB*	Cell envelope biogenesis, outer membrane
69-21A5*	BCAL3306	*secD, secF*	Intracellular trafficking and secretion
70-1E1	BCAL2959	*ubiG*	Coenzyme metabolism
70-13E1	BCAL0991	*fabH2, fabD2, fabG2, acp2*	Lipid metabolism
72-10F11*	BCAL3266	*panB*	Coenzyme metabolism
73-14C5*	BCAL0471	Unknown	Signal transduction
76-5B4	BCAL3351	Unknown	Unknown
77-4D9	BCAL3013	*gmk, rpoZ, spoT*	Nucleotide transport and metabolism, transcription
77-16C10	BCAL2934	*etfA*	Energy production and conversion

Table 2.2 List of CG transposon mutants continued

Strain name[1,2]	Locus of insertion site[3]	Genes controlled	Function
78-16D7*	BCAL3053	*ribH, nusB*	Coenzyme metabolism, transcription
79-12B10	BCAL3111	*waaA*	Cell envelope biogenesis, outer membrane
81-26F1	BCAL0272	Unknown	Unknown
82-25B9	BCAL0875	*ubiB*	Unknown
83-9H10*	BCAL3419	*accB, accC, prmA, tpx*	Lipid metabolism, translation, posttranslational modification, carbohydrate transport and metabolism, cell envelope biogenesis, outer membrane
84-37D12*	BCAL2838	*purC, purE, purK*	Nucleotide transport and metabolism
86-3D16*	BCAM1908	Unknown	Unknown
87-8E1	BCAM0909	Unknown	Unknown
94-10O20*	BCAL2153	Unknown	Unknown
96-1K12*	BCAM1881	Unknown	Unknown
99-8N4	BCAL3274	Unknown	Translation
rhaboutgfp1*	BCAL2770	Unknown	Phospholipid metabolism
rhaboutgfp5	BCAL1262	*carB, greA*	Amino acid transport and metabolism, transcription
rhaboutgfp10	BCAL0040	*hemE*	Coenzyme metabolism

*Pilot CG library
[1] (Bloodworth et al., 2013a)
[2] (Cardona et al., 2006a)
[3] (Winsor et al., 2008)

2.2.2 Growth inhibitors

All chemicals were purchased from Sigma Aldrich (St. Louis, MO) unless otherwise indicated. Novobiocin (NOV), chloramphenicol (CHL), tetracycline (TET), kanamycin (KAN), colistin (COL), carbonyl cyanide 3-chlorophenylhydrazone (CCCP), hydrogen peroxide (H2O2), and dimethyl sulfoxide (DMSO), were supplemented at concentrations that inhibit wild type growth 10 and 30%, referred herein as IC_{10} and IC_{30}, respectively. To calculate the IC_{10} and IC_{30}, standardized glycerol stocks of *B. cenocepacia* K56-2 were inoculated in 96-well plates with and without a 2-fold dilution series of each antibiotic. After incubation, growth was measured by OD_{600nm} and the inhibitory concentrations predicted by nonlinear regression analysis from fitting the $\log_{10}$ (inhibitor) OD_{600nm} readings to the Hill equation using GraphPad prism (GraphPad Software Inc., La Jolla, CA).

2.2.3 Multiplex PCR optimization, amplicon library preparation and Illumina sequencing of amplicons

A multiplex primer set was designed (Shen et al., 2010), consisting of a common transposon-specific forward primer and genome-specific reverse primers (see Table 2.3), to amplify the transposon-genome interface of each conditional growth (CG) mutant (see Table 2.2) in a multiplex PCR (Figure 2.1). The starting template concentration and number of cycles that produced exponential amplification of amplicon pool was determined by qPCR using IQ SYBRgreen Supermix (Bio-Rad) in a Bio-Rad IQ5 thermocycler (Bio-Rad, Hercules, CA, USA). Since the qPCR shows the average amplification of all the amplicons, next generation sequencing was used to determine the amplification reproducibility of the individual CG mutants. Each 100 µl multiplex PCR used 20 ng of genomic DNA template, IQ Supermix (Bio-Rad, Hercules, CA,

USA) and individual primer concentrations adjusted to achieve reproducible amplification of each CG mutant. Reactions were done in an Eppendorf Mastercycler ep gradient S thermal cycler (Eppendorf Canada Ltd., Mississauga, ON, Canada) using 5 minutes denaturation at 95˚C, 27 cycles of denaturation at 95˚C for 30 seconds, annealing at 67˚C for 30 seconds, extension at 72˚C for 30 seconds, followed by a final extension at 72˚C for 10 minutes. Amplicons created in the multiplex PCR containing the transposon-genome interface were size selected using Agencourt AMPure XP beads (Beckman Coulter, Brea, CA, USA) and used as the template for the indexing PCR. To identify amplicons created using different primer concentrations, indexing primers containing 5' adapters with the index sequences and Illumina MiSeq-specific adapter sequences (Nextera Index Kit; Illumina Inc., San Diego, CA), were added to the amplicons using PCR conditions recommended by the manufacturer. Amplicons were sequenced on an Illumina MiSeq (Illumina Inc., San Diego, CA) platform at the Children's Hospital Research Institute of Manitoba (Winnipeg, Canada) using either a micro or standard flow cell, following the manufacturer's instructions.

Table 2.3 Primers used to amplify CG transposon mutants

Primer	Sequence**	Concentration (μM)
4-7D1RP	GTCTCGTGGGCTCGGAGATGTGTATAAGAGACAGgttcctcgacatactcgccgacttc	0.025
4-22D3RP	GTCTCGTGGGCTCGGAGATGTGTATAAGAGACAGactcatgcgtgccctgcttc	0.025
8-15C6RP	GTCTCGTGGGCTCGGAGATGTGTATAAGAGACAGttcgaaagtggcggacatgatgaag	0.025
16-2C5RP	GTCTCGTGGGCTCGGAGATGTGTATAAGAGACAGgtcaccgcatcgttataggctttct	0.025
28-9C11RP*	GTCTCGTGGGCTCGGAGATGTGTATAAGAGACAGtccagcttcaaaatacaccgttccg	0.025
28-10H8RP*	GTCTCGTGGGCTCGGAGATGTGTATAAGAGACAGaccttgtcggtctcgagttcgatc	0.025
28-13B11RP*	GTCTCGTGGGCTCGGAGATGTGTATAAGAGACAGacctgcttcatgcgtttcttacctt	0.025
29-15E2RP*	GTCTCGTGGGCTCGGAGATGTGTATAAGAGACAGgcgcaatgacatcctcgctaaattg	0.025
29-3B1RP	GTCTCGTGGGCTCGGAGATGTGTATAAGAGACAGtccgtcttgtcttcgaatttggcaa	0.025
30-4C6RP*	GTCTCGTGGGCTCGGAGATGTGTATAAGAGACAGttgtcgaaaatcgttttgcccgttc	0.025
31-7D3RP	GTCTCGTGGGCTCGGAGATGTGTATAAGAGACAGcacgcacgatttccgcatagc	0.025
31-17A3RP*	GTCTCGTGGGCTCGGAGATGTGTATAAGAGACAGcgagatcgacgtccatcgcattg	0.025
32-30H3RP	GTCTCGTGGGCTCGGAGATGTGTATAAGAGACAGcgcagtattcagtacgcatcgacat	0.025
32-32F10RP	GTCTCGTGGGCTCGGAGATGTGTATAAGAGACAGgggtgtcgtgacgggtttgatc	0.025
34-16F6RP	GTCTCGTGGGCTCGGAGATGTGTATAAGAGACAGgacgtgatgtcgacgttcttcagac	0.025
34-17G4RP	GTCTCGTGGGCTCGGAGATGTGTATAAGAGACAGgatcacggcggtcagttccttc	0.025
34-24C5RP	GTCTCGTGGGCTCGGAGATGTGTATAAGAGACAGgactttcaggaacgcggccatctg	0.025
46-32G1RP*	GTCTCGTGGGCTCGGAGATGTGTATAAGAGACAGtacatgttctcgatcagcacttcgc	0.025
48-31G4RP	GTCTCGTGGGCTCGGAGATGTGTATAAGAGACAGgatccggttcgagacatactgaagc	0.025
48-43H3RP*	GTCTCGTGGGCTCGGAGATGTGTATAAGAGACAGgtgatagaactgcttggtcggactg	0.025
51-6G10RP	GTCTCGTGGGCTCGGAGATGTGTATAAGAGACAGcgaagacgatttcggtgttgaagcg	0.025
51-13E10RP*	GTCTCGTGGGCTCGGAGATGTGTATAAGAGACAGgtcaggatcttgtgcgggtaggtc	0.025
53-15F3RP	GTCTCGTGGGCTCGGAGATGTGTATAAGAGACAGcacgacgtcttgccgttcgtac	0.025
57-31D10RP	GTCTCGTGGGCTCGGAGATGTGTATAAGAGACAGcagaaatggtggaagaaggccca	0.025

Table 2.3 Primers used to amplify CG transposon mutants continued

58-14E1RP*	GTCTCGTGGGCTCGGAGATGTGTATAAGAGACAGgtcatcttcacgtcggtcggaatc	0.025
58-18F5RP*	GTCTCGTGGGCTCGGAGATGTGTATAAGAGACAGgaccgcgatgatgatgtcggcaac	0.025
58-21H7RP*	GTCTCGTGGGCTCGGAGATGTGTATAAGAGACAGgtcgatgtacgtgatcgccgaatta	0.025
64-10H7RP*	GTCTCGTGGGCTCGGAGATGTGTATAAGAGACAGgtgtaatcggccacttcggtcac	0.025
67-4B6RP	GTCTCGTGGGCTCGGAGATGTGTATAAGAGACAGgtgacccagcctttcttcttccac	0.025
67-4F2RP	GTCTCGTGGGCTCGGAGATGTGTATAAGAGACAGgttgttcatcgcacgctcgaattc	0.025
67-5H10RP*	GTCTCGTGGGCTCGGAGATGTGTATAAGAGACAGcagttgttcgtgaccgacagcag	0.025
67-10H9RP*	GTCTCGTGGGCTCGGAGATGTGTATAAGAGACAGcagcacgttggtgttcagaccac	0.00425
67-17C2RP	GTCTCGTGGGCTCGGAGATGTGTATAAGAGACAGgtacacgtcggtcgagaacttcac	0.025
69-18F6RP	GTCTCGTGGGCTCGGAGATGTGTATAAGAGACAGgtcgaagttgccgtacacgttctg	0.025
69-21A5RP*	GTCTCGTGGGCTCGGAGATGTGTATAAGAGACAGgacttctgcagcaggtccttgac	0.025
70-1E1RP	GTCTCGTGGGCTCGGAGATGTGTATAAGAGACAGgatcgcctcgtaatcgaccgaaatg	0.025
70-13E1RP	GTCTCGTGGGCTCGGAGATGTGTATAAGAGACAGgaagtcgcgacgatgatcaggtc	0.025
72-10F11RP*	GTCTCGTGGGCTCGGAGATGTGTATAAGAGACAGctcgcccttgacgaagaattccttg	0.025
73-14C5RP*	GTCTCGTGGGCTCGGAGATGTGTATAAGAGACAGggacatcatgatcacgggcatcg	0.025
76-5B4RP	GTCTCGTGGGCTCGGAGATGTGTATAAGAGACAGgttgtcggtcaggtacagcgtcatc	0.025
77-4D9RP	GTCTCGTGGGCTCGGAGATGTGTATAAGAGACAGgtaacgttcgacagcagcatcgtc	0.025
77-16C10RP	GTCTCGTGGGCTCGGAGATGTGTATAAGAGACAGgagtagtccttcgcgatgttcagc	0.025
78-16D7RP*	GTCTCGTGGGCTCGGAGATGTGTATAAGAGACAGgatacgagcagcacgtcttcacc	0.025
79-12B10RP	GTCTCGTGGGCTCGGAGATGTGTATAAGAGACAGgatttcgtcacgtgcagcaggttc	0.025
81-26F1RP	GTCTCGTGGGCTCGGAGATGTGTATAAGAGACAGaaaacaaaaggcgatgaccgggaag	0.025
82-25B9RP	GTCTCGTGGGCTCGGAGATGTGTATAAGAGACAGgttctcgtcgagccagtattcgg	0.025
83-9H10RP*	GTCTCGTGGGCTCGGAGATGTGTATAAGAGACAGtgaatctagatcgcgaaatcagccg	0.025
84-37D12RP*	GTCTCGTGGGCTCGGAGATGTGTATAAGAGACAGccttcacctgctcgacttcgtc	0.025
86-3D16RP*	GTCTCGTGGGCTCGGAGATGTGTATAAGAGACAGgcttcgacaggcaatccccatattt	0.00425
87-8E1RP	GTCTCGTGGGCTCGGAGATGTGTATAAGAGACAGaccgcatccattgttcgaatgtcat	0.025

Table 2.3 Primers used to amplify CG transposon mutants continued

94-10O20RP*	GTCTCGTGGGCTCGGAGATGTGTATAAGAGACAGcttgatcttgtcgaccacgtcctg	0.025
96-1K12RP*	GTCTCGTGGGCTCGGAGATGTGTATAAGAGACAGtggcattgagaaggtccgtaaatgg	0.025
99-8N4RP	GTCTCGTGGGCTCGGAGATGTGTATAAGAGACAGgatagccgttcgacgtgagcagatg	0.025
rhaboutgfp1RP*	GTCTCGTGGGCTCGGAGATGTGTATAAGAGACAGatccagcccttgaacgcgtc	0.025
rhaboutgfp5RP	GTCTCGTGGGCTCGGAGATGTGTATAAGAGACAGcttccaccgagaaaccgatgaacagg	0.025
rhaboutgfp10RP	GTCTCGTGGGCTCGGAGATGTGTATAAGAGACAGgggaatcgtcagaatgtccgagaac	0.025
Tn-specificFP*	TCGTCGGCAGCGTCAGATGTGTATAAGAGACAGNNNNagctgtacaagtaaggcctaggtgg	1.4[a],0.625[b]

*pilot CG library
**upper case letters: adapter sequence; lower case letters: genome-specific sequence
[a]concentration used in multiplex PCR with 56 reverse primer set
[b]concentration used in multiplex PCR with 25 reverse primer set

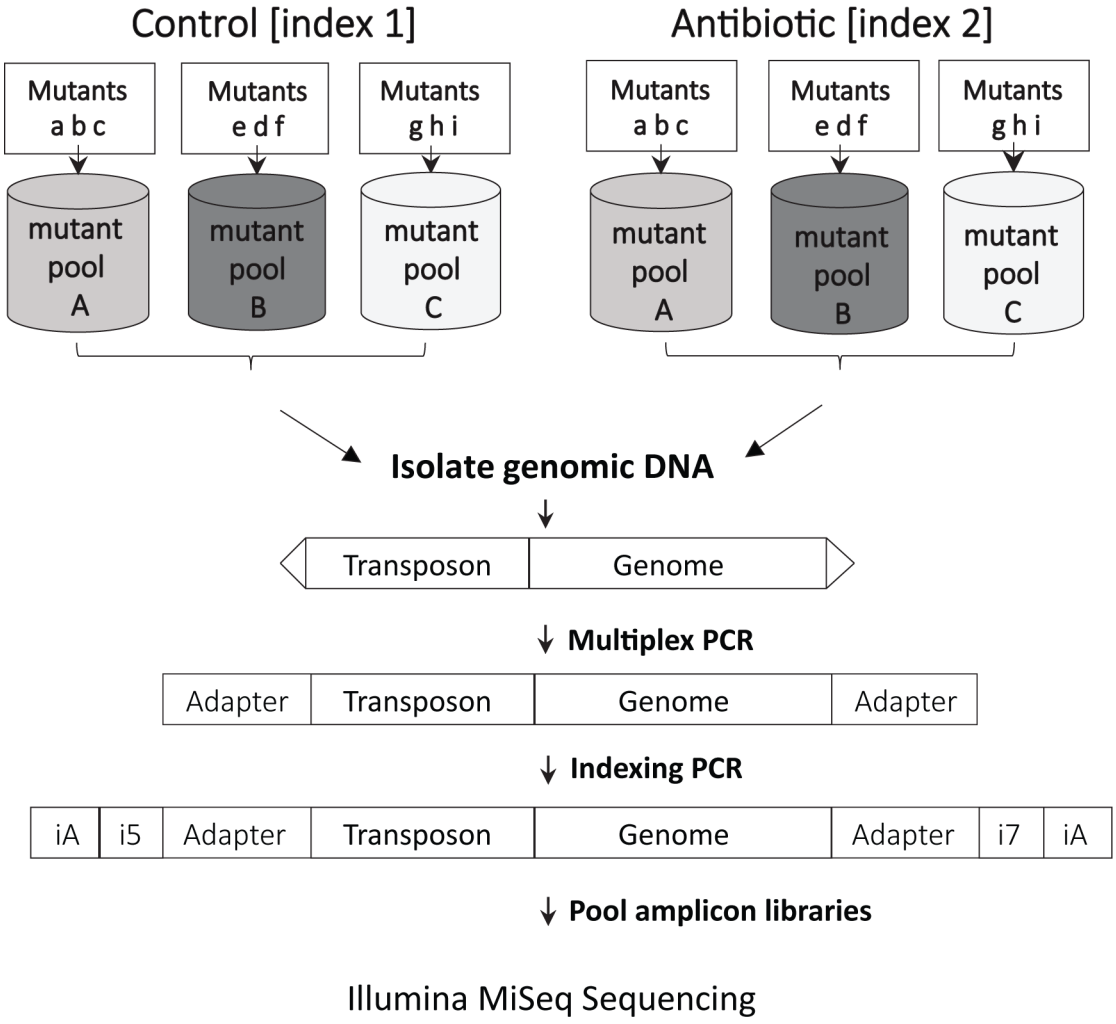

Figure 2.1. Detection of CG mutant enhanced sensitivity using Illumina MiSeq.

Mutants with similar rhamnose sensitivities (Mutants a, b, c; e, d, f; and g, h, i) are pooled together in equal amounts (Pools A, B and C) and incubated with and without antibiotic. CG mutant pools are combined, genomic DNA extracted and the transposon-genome interface amplified by multiplex PCR using a common transposon-specific forward primer and a genome-specific reverse primer, both of which contain 5' adapter sequences (Adapter). The index PCR adds indexes to the amplicons using primers complementary to the adapter sequences and containing 5' indexes (i5 and i7), and Illumina MiSeq-specific adapter sequences iA. The amplicons are then sequenced in one run of a MiSeq and the reads, separated by treatment, containing transposon insertion sites are assigned to their corresponding CG mutant. The relative abundance (RA) of reads corresponding to each CG mutant within the total reads per index is calculated and CG mutant depletion in response to an antibiotic is expressed as the ratios between control RA and antibiotic RA.

2.2.4 Data analysis

We previously determined the location of the insertion sites of the CG mutants by sequencing the transposon-genome interface of each CG mutant and aligning the resulting read against the genome of *B. cenocepacia* J2315 (Bloodworth et al., 2013a). This information was used to create a file containing the genomic portions of the amplicon sequences for each CG mutant. Demultiplexed fastq files obtained from sequencing were converted to fasta using prinseq-lite version 0.20.3 (Schmieder and Edwards, 2011). The sequences in the forward read fasta files were filtered to include only the reads containing the transposon sequence and aligned to the amplicon sequences of the CG mutants using a standalone version of BLASTn from NCBI (Altschul et al., 1990). The amplicon count from BLASTn was converted to tabular format using the command line outfmt 6. For determining amplicon read counts, sequences with more than 90% identity, at least 45 base alignment to an amplicon in the blast library and a transposon score greater than 39 were included in the analysis. The analysis to identify mutants with enhanced sensitivity was based on a previously developed method (Donald et al., 2009a) with the following modifications: For the antibiotic and no antibiotic (control) treatments, reads corresponding to a CG mutant were normalized as the relative abundance (RA) of the total reads per index (treatment). CG mutant depletion ratios in response to an antibiotic ($DR_{antibiotic}$) were calculated as a $\log_{10}$ of the mean $RA_{control}$ divided by the $RA_{antibiotic}$. To determine significance of depletion, Z-scores were calculated using error models ($DR_{control}$) generated for each mutant from replicate controls:

$$Z = \frac{DR_{antibiotic} - MeanDR_{control}}{Median\ (|DR_{antibiotic} - MeanDR_{control}|)}$$

CG mutants with $\log_2$ depletion ratios and Z scores greater than 2, were deemed significantly depleted in a given condition.

2.2.5 Artificial depletion of CG mutants

Pools of CG mutants were created from the pilot CG library by growing the selected strains clonally then combining them together in specific ratios based on their OD_{600nm}. CG mutants were combined together in equal amounts (pool A) and four depletion pools were generated from the same clonally grown strains with selected mutants depleted by 10-fold or 100-fold (pools B, C, D and E), in comparison with the equally pooled library. The transposon-genome interface of the CG mutants in each pool was then amplified by two-step PCR and sequenced in parallel on the Illumina MiSeq. Depletion of each CG mutant was assessed by comparing the percent abundance of each mutant in the depleted pool to the percent abundance of CG mutants pooled together in equal amounts.

2.2.6 Competitive enhanced sensitivity assay

Each CG mutant of the pilot CG library was categorized into rhamnose categories based on similar growth phenotype in response to rhamnose, as described previously (Bloodworth et al., 2013a). CG mutants that reached 30-60% of wild type growth at a given rhamnose concentration were combined together for growth in pools (Figure 2.2). For the assay, standardized glycerol stocks containing equally pooled CG mutants were thawed and inoculated at a final OD_{600nm} of 0.001 in 96-well plates with the chosen rhamnose concentrations and antibiotics. After incubation for 22 hours with shaking at 220 rpm, equal volumes of mutant pools exposed to the same treatment were combined together and the genomic DNA of each library extracted. Amplicon libraries of the CG mutant transposon-genome interfaces were prepared by two-step PCR. First, adaptors were added by a multiplex PCR that uses a common transposon-specific forward primer and a genome-specific reverse primer, both of which contain 5' adapter sequences. Then, an index PCR added

indexes to the amplicons using primers complementary to the adapter sequences and containing 5' indexes and Illumina MiSeq-specific adapter sequences. Each unique index identified the treatment each library was exposed to (control or antibiotic). Amplicon libraries were sequenced in parallel on the Illumina MiSeq as described above.

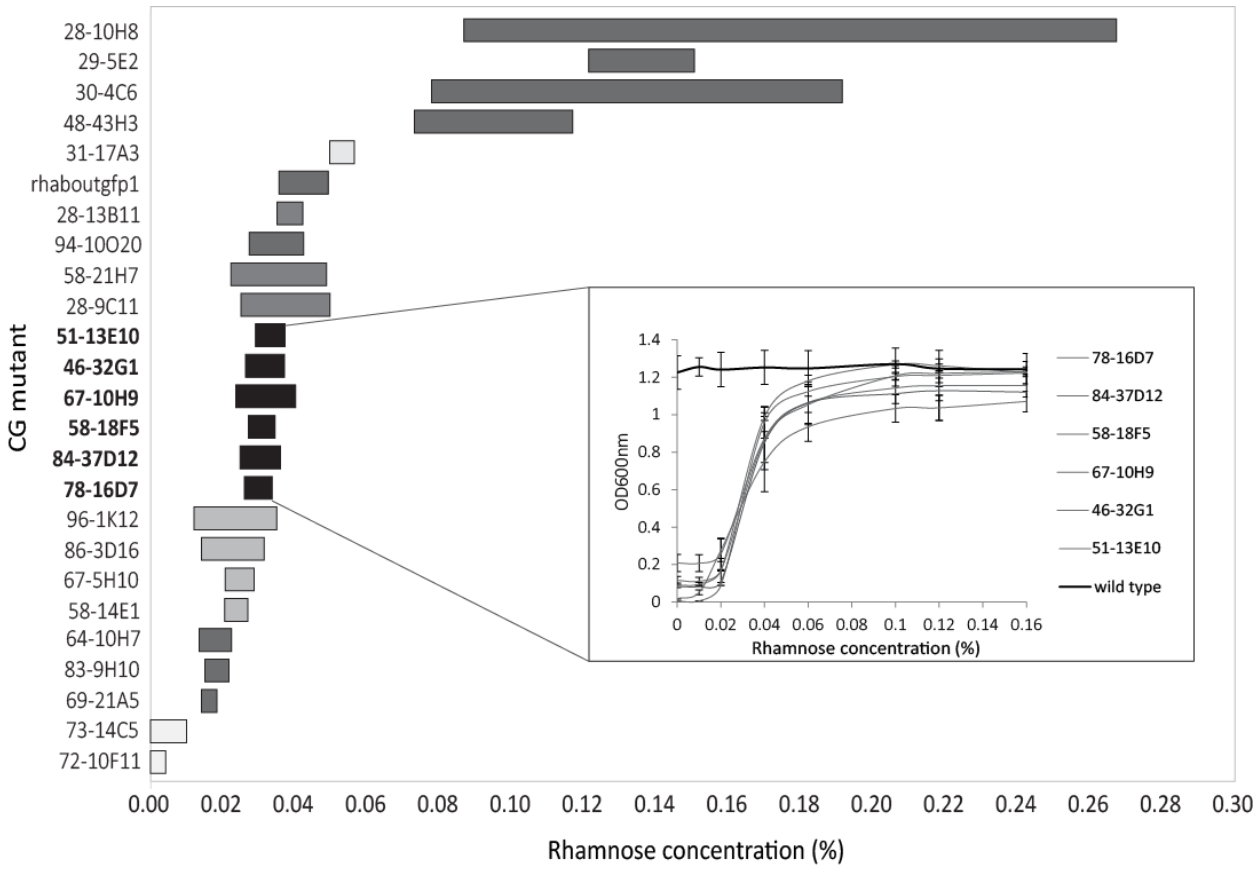

Figure 2.2 Rhamnose dose response curves of pilot CG library in 7 rhamnose categories.

CG mutants with the similar rhamnose dose response curves categorized into groups (shaded bars). The left and right boundaries represent the concentration of rhamnose required for 30% and 60% of wild type growth, respectively. Inset: Rhamnose dose response curves were determined for each CG mutant by measuring their growth in various concentrations of rhamnose, the OD_{600nm} readings were fitted to the Hill equation using GraphPad prism (GraphPad Software Inc., La Jolla, CA). Gray lines represent CG mutants assigned to each group, the black line represents *B. cenocepacia* K56-2 wild type growth. Error bars represent the standard deviation of two biological replicates.

2.2.7 Comparison of pooled and clonal growth

Standardized glycerol stocks of equally pooled or individual CG mutants (58-14E1, 67-5H10, 86-3D16, 96-1K12) from the same rhamnose group (Figures 2.2 and 2.3), were inoculated at a final OD_{600nm} of 0.001 and grown clonally or in a pool in the presence or absence of novobiocin and chloramphenicol at their IC_{10}. After incubation, genomic DNA of the co-cultured CG mutants was isolated directly, while the OD_{600nm} of the clonally grown strains was measured, then equal volumes of each strain was pooled together before extracting the genomic DNA. Indexed amplicon libraries were produced from each condition and sequenced on the Illumina MiSeq. To compare the relative abundance of each mutant between treatment conditions, amplicon reads were normalized by dividing the number of reads from each CG mutant amplicon by the total reads for one condition. Fold depletion was determined by dividing the normalized reads for each CG mutant from the no antibiotic condition by the normalized reads from each CG mutant in the antibiotic condition. As a control, the depletion ratio of pooled growth and clonal growth was compared for each CG mutant in the no antibiotic condition by dividing normalized reads for each CG mutant grown in a pool by the normalized reads from each CG mutant grown clonally.

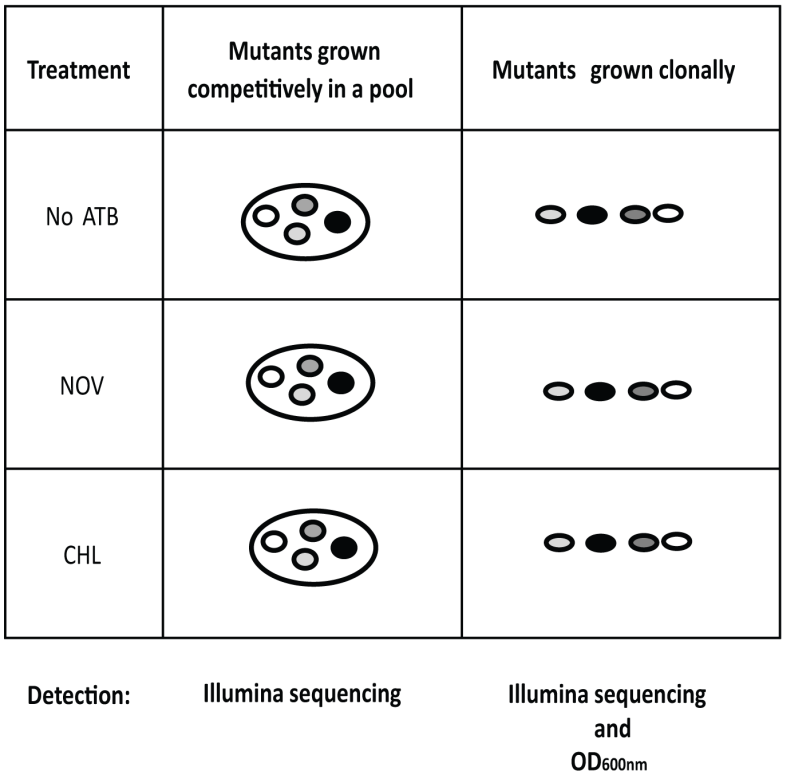

Figure 2.3 Experimental design for comparing of pooled and clonal growth.

Four strains were grown clonally and in a pool with no antibiotic (No ATB), novobiocin IC_{10} (NOV), and chloramphenicol IC_{10} (CHL). The fold depletion of 58-14E1 (CGgyrB) in response to novobiocin when grown competitively with 3 strains, 67-5H10, 86-3D16, 96-1K12, was quantified by Illumina sequencing and compared to the fold depletion of clonally grown 58-14E1 (CGgyrB). The effect of quantifying mutant growth by Illumina sequencing was assessed by comparing the fold depletion of strains measured by turbidity (OD_{600nm}) and Illumina sequencing.

2.2.8 Construction of the unmarked *esaS* deletion mutant, MKC4 (Δ*esaS*)

An unmarked deletion of *esaS* (BURCENK56V_RS04770) in *B. cenocepacia* K56-2 was produced as described in Flannagan *et al.* 2008 (Flannagan et al., 2008). Primers 666 5'-(AGATAATCTAGAGACTTCGAGCTGAATCCGA) and 665 (5'-ATATGGATCCGTTCGGTCACCGTGAAG) were used to amplify a 450 bp fragment upstream of *esaS*. Primers 664 5'- (ATATGGATCCCAAAGGCAGCGTAAATGGCA), and 663 5'-(AATTATCCCGGGGCTTGAGCTTGCGATACAG) were used to amplify a 450 bp region downstream of *esaS*. These amplicons were digested with BamHI (New England Biolabs Inc., Ipswich, MA, USA) and ligated with T4 DNA Ligase (New England Biolabs Inc., Ipswich, MA, USA). The resulting DNA fragment was digested with XbaI and XmaI (New England Biolabs Inc., Ipswich, MA, USA) and ligated into the XbaI and XmaI-digested pGPI-SceI, to create plasmid pMC4. To attempt deletion of the *esaSR* locus, a 925 bp DNA fragment consisting of 450 bp regions upstream and downstream of *esaSR* was synthesized from Blue Heron Biotech, digested with XbaI and XmaI and ligated into the XbaI and XmaI-digested pGPI-SceI, to create plasmid pMC5. pMC4 and pMC5 were conjugated into *B. cenocepacia* K56-2 and merodiploids were selected on LB agar plates supplemented with 100 μg/ml trimethoprim (TMP) and 50 μg/ml gentamicin. To initiate the second recombination event, the pDAI-SceI, which carries the yeast homing endonuclease I-SceI coding gene, was introduced by triparental mating into TMP resistant clones. Tetracycline resistant clones were screened for the loss of TMP resistance and the recovered TMP susceptible clones were screened by colony PCR to isolate deletion mutants. To identify the deletions of *esaS* and *esaSR,* primers 615 (5'-AATTAACATATGGTGATCGTCTCGACCGTCG) and 616 (5'-ATATAATCTAGAGATGTAGATGATCCCGCCCG) were used, which amplify 270 bp

corresponding to the 5'end of *esaS*; as well as primers 666 and 663, which amplify *esaS* with flanking 500bp segments upstream and downstream of the gene (Figure 2.4). Confirmed deletion mutants were passaged in LB broth over a period of nine days to cure colonies of pDAI-SceI, selection was done with replica plating on LB agar plates and LB agar plates supplemented with 100 μg/ml tetracycline.

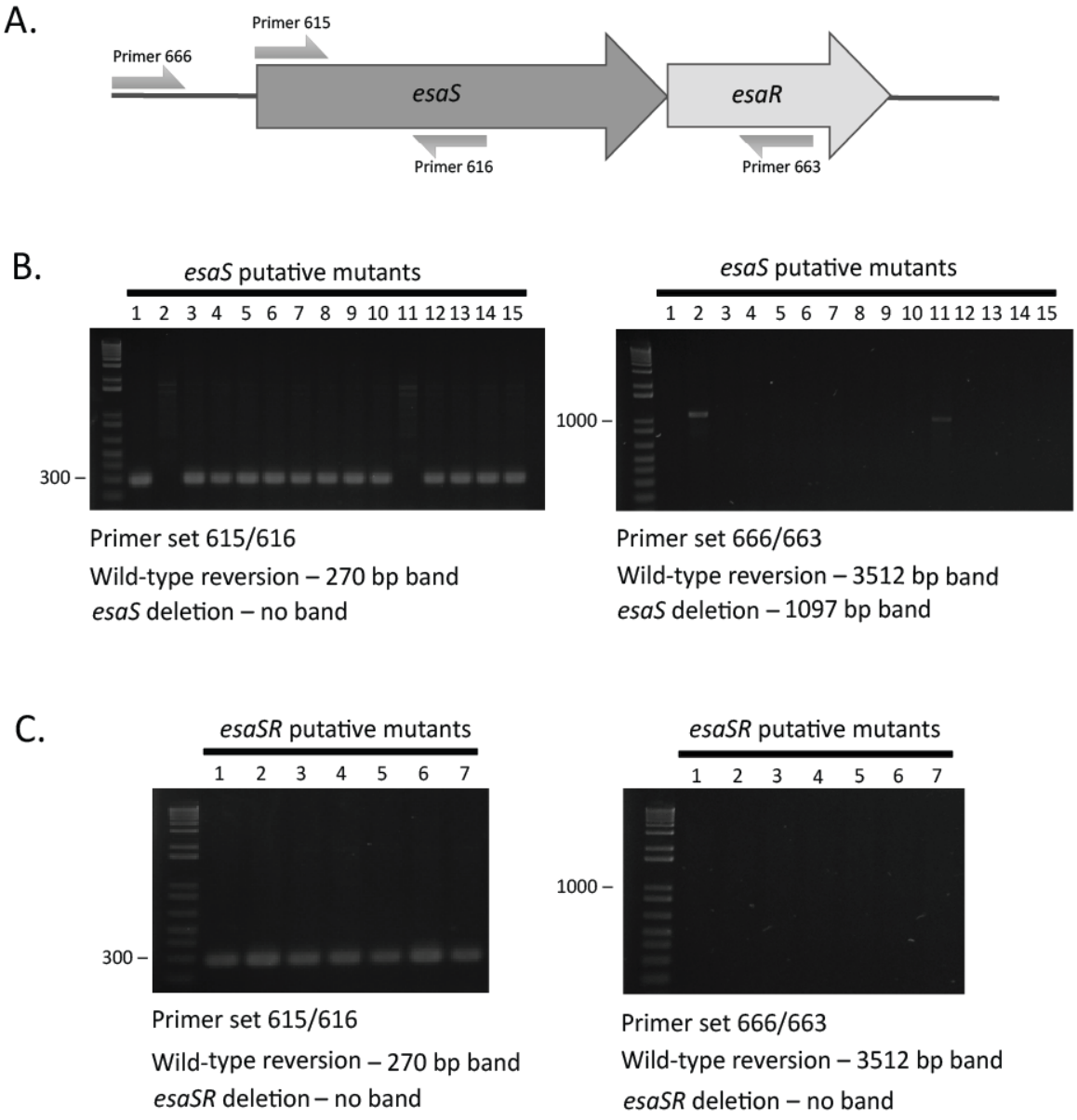

Figure 2.4 Colony PCR analysis of putative *esaS* and *esaSR* deletion mutants.
A) Schematic diagram of *esaSR* and flanking regions with primer binding sites used for colony PCR screen. B) Agarose gel electrophoresis of colony PCR amplicons corresponding to *esaS* putative deletion mutants. Left gel shows primer set 615/616 PCR amplification. Colonies 2 and 11 show absence of the 270-bp band, suggesting successful deletion of *esaS*, whereas all other colonies show the 270-bp band, indicating wild-type genotype reversion. Right gel shows primer set 666/663 PCR amplification of region upstream and downstream of *esaS*. Colonies 2 and 11 show the 1100-bp band confirming the deletion of *esaR*. Amplification of the wild type reversion band (3512 bp) was unsuccessful in the colony PCR reaction, probably due to length and high CG content of the region.
C) Agarose gel electrophoresis of colony PCR amplicons corresponding to *esaSR* putative deletion mutants. Left gel shows primer set 615/616 PCR amplification. All colonies screened show the

270-bp band, indicating wild-type genotype reversion. Right gel shows primer set 666/663 PCR amplification of region upstream and downstream of *esaS*. Amplification of the wild type reversion band (3512 bp) was unsuccessful in the colony PCR reaction, probably due to length and high CG content of the region.

2.2.9 Site directed mutagenesis to construct the *esaR* conditional growth mutant MKC2 (CG*esaR*).

The 5'end (170 bp) of *esaR* was amplified via PCR using HotStar HiFidelity polymerase (Qiagen, Hilden, Germany) with primers 633 (5'-AATTAACATATGATGGCAACCATCCTGGTG) and 634 (5'-ATATAATCTAGACATTCCTTGAGCAGCGTGAC), digested with NdeI and XbaI (New England Biolabs Inc., Ipswich, MA, USA), and cloned into pSC201, immediately downstream of the rhamnose-inducible promoter. The resulting mutagenesis plasmid pMC2, was introduced into *B. cenocepacia* K56-2 by triparental mating (Craig et al., 1989) (Craig, Coote, Parton, Freer, & Gilmour, 1989) (32). Exconjugants were selected on LB agar plates supplemented with 0.2% rhamnose, 100 μg/ml trimethoprim and 50 μg/ml gentamicin. Insertional mutants were confirmed by PCR using primer 645 (5' –GCCCATTTTCCTGTCAGTAACGAGA) and primer 652 (5'-GCATCCAGATATCGAGCAGCA), which anneal with pSC201 and a region downstream of the 170bp 5' end fragment of *esaR*, respectively.

2.2.10 MIC ratios

Minimal inhibitory concentration (MIC) assays were performed in *B. cenocepacia* K56-2 (wild type), 73-14C5 (CG transposon mutant of *esaR*), MKC2 (CG*esaR*), MKC4 (Δ*esaS*) and 84-37D12 (CG transposon mutant unrelated to *esaR*) in a final volume of 200 μl. Standardized glycerol stocks were diluted to a final OD_{600nm} of 0.001 in LB broth and added to 96-well plates containing two-fold serial dilutions of the antibiotic to be tested. When required, rhamnose was added at a final concentration of 0.16% (w/v). The highest concentrations of antibiotics tested were: novobiocin at 64 μg/ml, ciprofloxacin at 64 μg/ml, chloramphenicol at 64 μg/ml, tetracycline at 64 μg/ml, DMSO at 25% (v/v), kanamycin at 8 mg/ml, hydrogen peroxide at 3 mM, and

meropenem at 64 μg/ml. Plates were incubated for 22 h at 37 °C without shaking. The MIC ratios were calculated for each strain as the MIC of the wild type divided by the MIC of the mutant, grown without rhamnose.

2.2.11 Ala-Nap uptake assay

Efflux activity was determined by measuring the amount of cleavage of P(Ala-Nap) to fluorescent β-naphthylamine by bacterial cells as previously described (Lomovskaya et al., 2001; Rajendran et al., 2010). Bacteria were grown overnight in LB or LB with 0.2% (w/v) rhamnose where indicated. Cultures were washed and resuspended in buffer solution [K_2HPO_4 (50 mM), $MgSO_4$ (1 mM), and glucose (0.4%)] at pH 7.0. To initiate the reaction, 100 μl cell suspensions at an OD_{600nm} of 1.0 were treated with Ala-Nap at a final concentration of 128 μg/ml in black 96-well flat-bottom plates (Corning Inc., Kennebunk, ME, USA). Fluorescence was measured every 45 seconds for 1 h on a BioTek Synergy 2 plate reader (BioTek Instruments Inc., Winooski, VT, USA) with excitation of 360 nm and emission of 460 nm. To induce efflux, cultures at an OD_{600nm} of 1 were incubated in LB with 5 μg/ml chloramphenicol for 3 hours with shaking at 37˚C. Cells were then washed and the OD_{600nm} was adjusted to 1 before performing the Ala-Nap uptake assay. For treatment with CCCP to inhibit active efflux, ten minutes into the assay, CCCP was added at a final concentration of 10 μM.

2.2.12 Microscopy analysis

Bacterial strains were inoculated into 5 mL of LB+ 0.2% rhamnose to a final OD_{600nm} of 0.001, and incubated at 37°C, shaking at 220rpm for 16-17 h. 15 μL of each strain was then subcultured into 5mL of LB or LB+0.2% rha, and incubated at 37°C with shaking at 220 rpm. After 24 h of incubation, cultures were diluted 1 in 20 with PBS to prepare for staining using

SYTO9 dye and propidium iodide (PI) from the *Bac*Light Live/Dead Bacterial Viability Kit (Molecular Probes). Controls were setup using wild type *B. cenocepacia* K56-2, added at a final 1/10 dilution to 4 mL phosphate buffered saline (PBS) or 4 mL 70% isopropanol, as the live and dead controls, respectively (See Figure 2.5). Control tubes were incubated at room temperature for one hour, with quick vortexing every 15 min. Diluted bacterial samples were stained with 3 uL SYTO9 dye and PI staining solution for 15 min. 10 μL of samples and controls were spotted onto 1% agarose-coated microscope slides and covered with cover slips. Slides were imaged using an AxioCamMR attached to an Axio Imager Z1 (Carl Zeiss) at 1000x magnification using differential interference contrast (DIC), rhodamine, and GFP fluorescence filters. To determine the proportion of cells with a compromised membrane, 100 fluorescent cells from each biological replicate were counted and the average percent of red cells and the standard deviation reported.

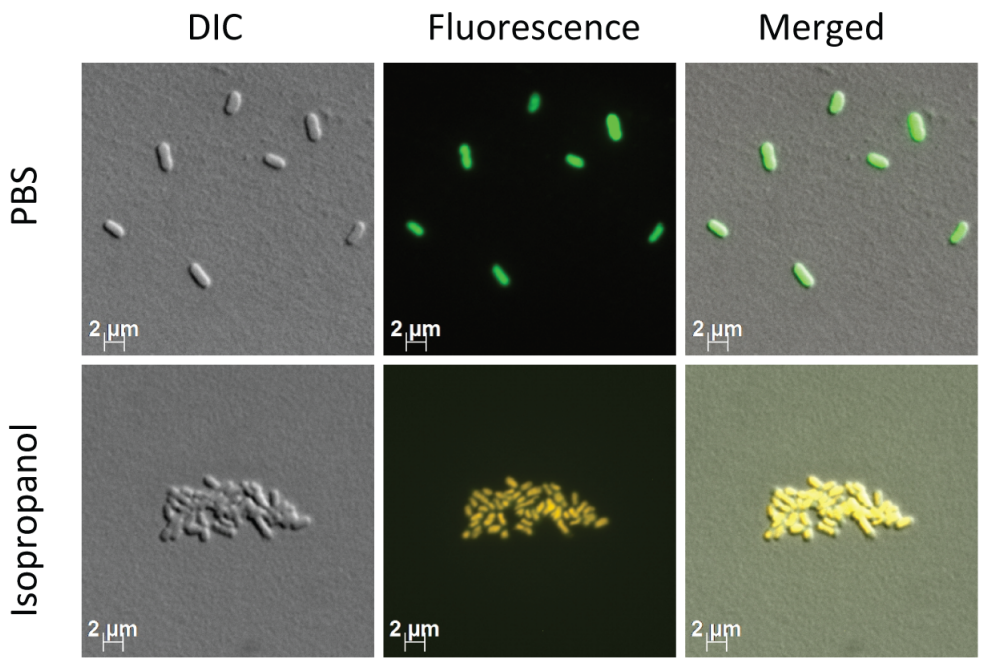

Figure 2.5 Controls for the BacLight Live/Dead bacterial viability kit (Molecular Probes) Wild type *B. cenocepacia* K56-2 was diluted 1/10 to at a final volume of 4mL PBS or 4mL 70% isopropanol, as the live and dead controls, respectively. DIC, differential interference contrast (right column); Fluorescence, obtained using rhodamine and GFP fluorescence filters (middle column); Merge, DIC and fluorescence overlay (right column).

2.3 Results

2.3.1 Quantification of CG mutant relative abundance by Illumina sequencing of multiplex-PCR amplified transposon junctions

Our original CG mutant library consisted of 106 mutants where the rhamnose-inducible promoter controls the expression of essential genes in 50 unique operons (Bloodworth et al., 2013a). Taking advantage of this transposon mutant library, we developed a method to detect the enhanced sensitivity of CG mutants when they are grown competitively in the presence of an antibiotic (Figure 2.1). The strategy involved pooled growth experiments where CG mutants with similar rhamnose dose-response curves (Figure 2.2) were exposed to several antibiotics. CG mutant pools that received the same treatment were combined, the genomic DNA was extracted and the transposon-genome interface was amplified by multiplex PCR. The amplicons were then Illumina sequenced and the relative abundance (RA) of each CG mutant was calculated for each treatment.

In order to avoid a possible misidentification of CG mutants due to the presence of close transposon insertions, we selected 56 CG mutants from the original CG mutant library (Bloodworth et al., 2013a), which had insertion sites located at least 10 Kb apart from each other in the genome. To determine the amplification reproducibility of the transposon-genome junction of the individual CG mutants, the genomic DNA of equally pooled CG mutants was extracted, used as the template in the multiplex PCR, and the resulting amplicons sequenced on an Illumina MiSeq. Initially, two CG mutant amplicons (67-10H9 and 86-3D16) accounted for 30% of the total reads, 12 had read counts that varied between replicates and 19 were not detected. To increase sequencing depth and improve the amplification of the variably amplified and undetected amplicons, the primer concentrations for 67-10H9 and 86-3D16 were decreased to reduce the

over-represented amplicons (Table 2.3). Adjusting the primer concentrations increased the sequencing depth of the other amplicons in the library (data not shown) while maintaining the reproducible detection of 25 CG mutants (Figure 2.6). However, detection and reproducibility was not improved for the variably amplified and undetected CG mutants. A pilot CG library, comprised of the 25 CG mutants that had reproducible amplification in the multiplex PCR, was then used to profile antibiotics. Despite its small size, the pilot CG library contains representatives of 25 unique essential operons covering the main essential functional categories identified in the original CG mutant library (Bloodworth et al., 2013a) (Figure 2.7).

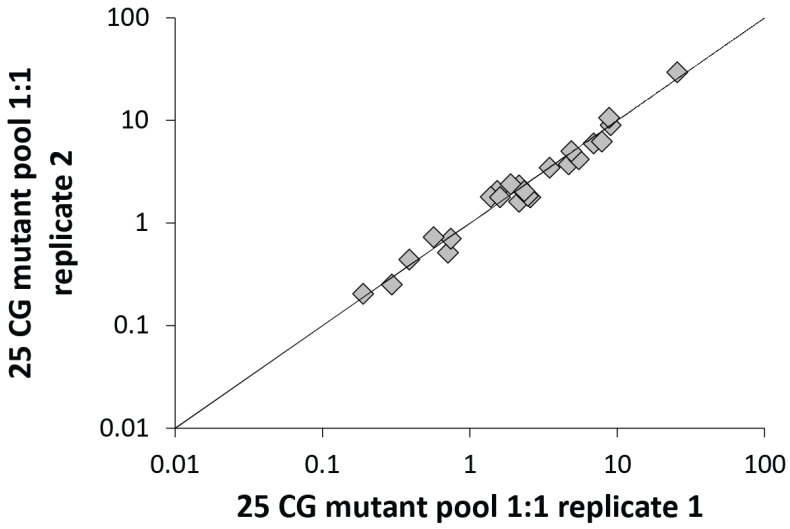

Figure 2.6 Optimized multiplex PCR for the pilot CG library.
Comparison of replicate multiplex PCRs using a template of 25 CG mutants that were grown clonally then pooled together in equal amounts by cell density (OD_{600nm}). The percent abundance of reads of the CG mutant library from one technical replicate (x-axis) is plotted against those from a second technical replicate (y-axis). Gray line represents theoretical 1:1 ratio.

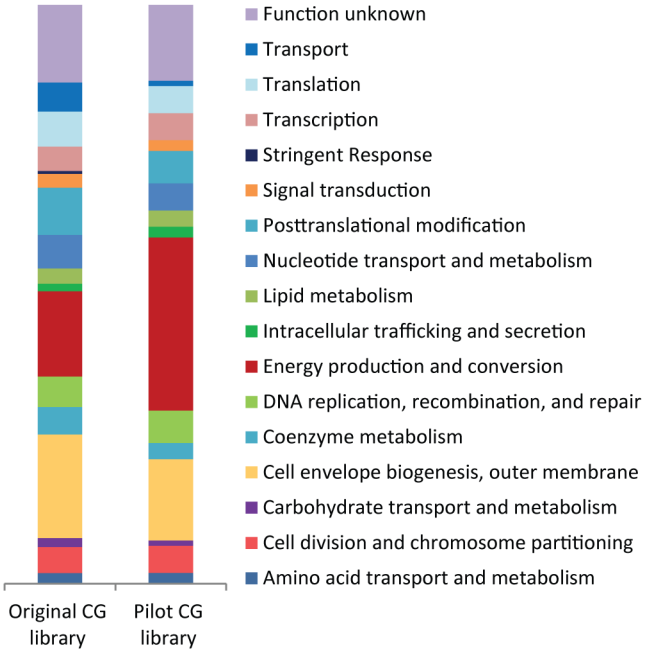

Figure 2.7 Functional categories represented by CG mutants in the original (106 mutants) and pilot CG library (25 mutants).

Sixteen out of the 17 functional categories, determined by the GO (Gene Ontology) and COG (Cluster of Orthologous Genes) annotations, identified in original mutant library (26) are represented in the pilot CG library. The proportion of each category is based on the function of annotated genes in the *B. cenocepacia* J2315 genome that are predicted to be in an operon downstream of the transposon insertion site.

To demonstrate that we could detect CG mutant depletion by multiplexed Illumina sequencing, the ratios of the CG mutants were artificially adjusted to mimic antibiotic-driven mutant depletion. Five CG mutant pools were generated, pool A contained all mutants in the pilot CG library combined together in equal amounts (based on OD_{600nm}) and pools B-D contained the majority of mutants pooled together in equal amounts with 2 to 8 CG mutants depleted by 10-fold or 100-fold in each pool, with respect to pool A. The observed depletion of CG mutants was representative of the initial concentrations (10-fold or 100-fold) of each mutant within the pools. The percent abundance of each CG mutant in the pools from duplicate multiplex PCRs was consistent showing that each CG mutant was reproducibly amplified and detected (Figure 2.8). Therefore, sequencing amplicons from the multiplex PCR accurately measures CG mutant depletion in the pilot CG library.

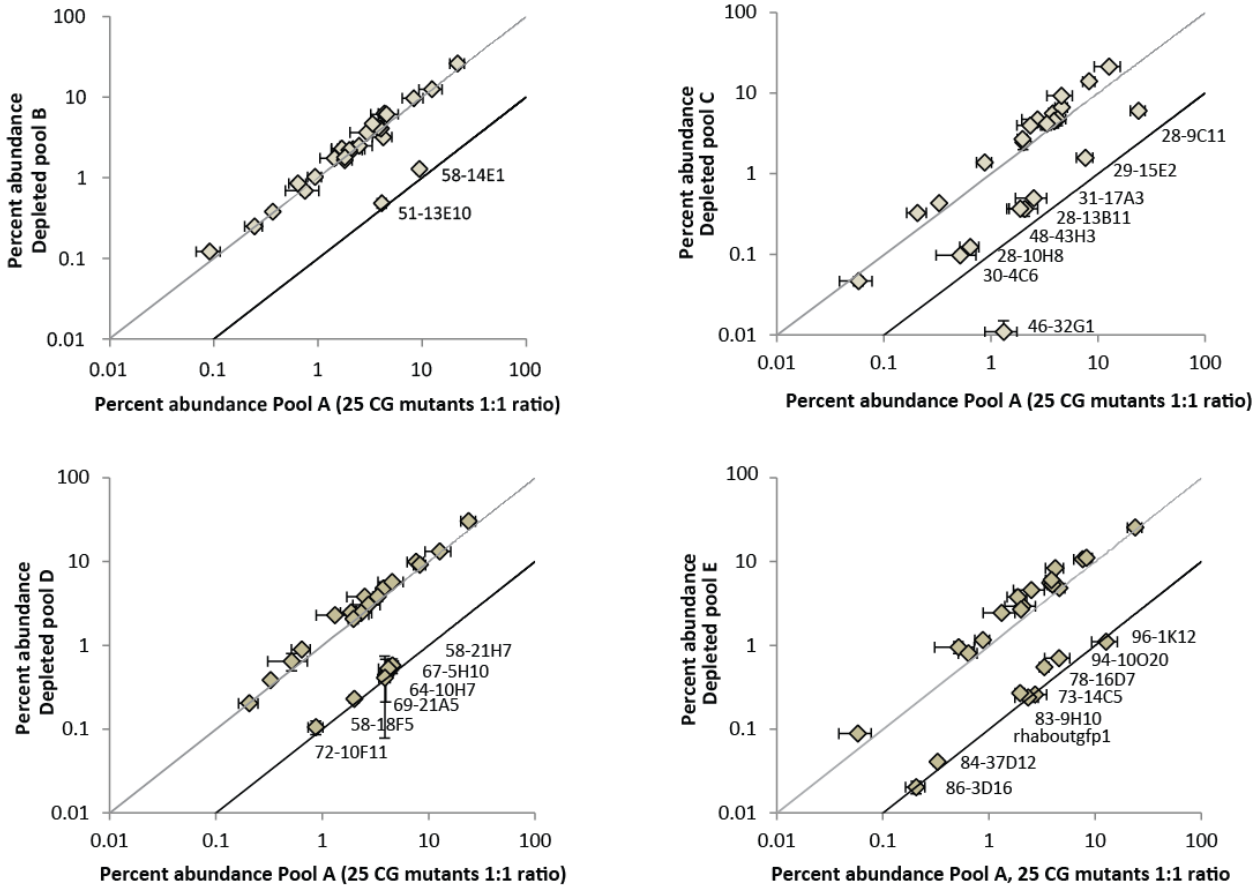

Figure 2.8 Detection of artificially depleted strains by next generation sequencing.

To mimic CG mutants with specific enhanced sensitivity, CG mutants from the pilot CG library were grown clonally, pooled together in equal amounts or depleted by cell density (OD_{600nm}) with respect to the equally pooled mutants: Pool A, 25 CG mutants pooled together equally; Pool B: 58-14E1 and 51-13E10 10-fold depleted; Pool C: 28-9C11, 28-10H8, 28-13B11, 29-15E2, 30-4C6 and 31-17A3 depleted 10-fold, 46-32G1 depleted 100-fold; Pool D: 58-18F5, 58-21H7, 64-10H7, 67-5H10, 69-21A5 and 72-10F11 depleted 10-fold; Pool D: rhaboutgfp1, 73-14C5, 78-16D7, 83-9H10, 84-37D12, 86-3D16, 94-10O20, and 96-1K12. The percent abundances of CG mutants from the four depleted pools B, C, D and E (y-axis) is compared to the percent abundance of the CG mutants pooled together in equal amounts (x-axis). The diagonal lines represent theoretical no depletion (gray) and 10-fold depletion (black). Error bars represent the standard deviation of two replicate multiplex PCRs.

2.3.2 A competitive enhanced sensitivity assay enhanced the specific depletion of a CG mutant to its corresponding antibiotic

To sensitize CG mutants to antibiotics, we used rhamnose concentrations that allow 30 to 60% wild type growth, as previously determined (Bloodworth et al., 2013a). Pools of mutants with similar response to rhamnose were made and grown in the presence or absence of antibiotics. Cultures exposed to the same treatment were combined by volume, the genomic DNA extracted and used as template in a two-step PCR where a unique index identified the treatment. The CG mutant 58-14E1, named herein CG*gyrB*, was included in the pilot CG library. This mutant strain was sensitized to produce suboptimal levels of the DNA gyrase subunit GyrB, which is the target of novobiocin (Lewis et al., 1996). A bioactive target-match was evident in the competitive ESA where exposure to sublethal concentrations of novobiocin caused more than 10-fold depletion of the sensitized CG*gyrB* (Figure 2.9). CG*gyrB* also showed enhanced sensitivity to tetracycline IC_{10} and IC_{30}, with $\log_2$ depletion ratios at or slightly above the cut-off level of significance, respectively and Z scores higher than 2 for both conditions (Figure 2.9, right panel). The $\log_2$ depletion ratio of CG*gyrB* in response to colistin IC_{30} was slightly below 2, while the Z score was above the cut-off level of significance. However, CG*gyrB* was not hypersensitive to colistin IC_{10} as the $\log_2$ depletion ratio and Z score were lower than 2. Similarly, CG*gyrB* did not show enhanced sensitivity to the other antibiotics tested (Figure 2.9, right panel) and with the exception of mutant 73-14C5 (see below), the other CG mutants were not sensitive to novobiocin (Figure 2.9, left panel). Together, the assay was able to detect specific sensitivity of CG*gyrB* to its corresponding antibiotic.

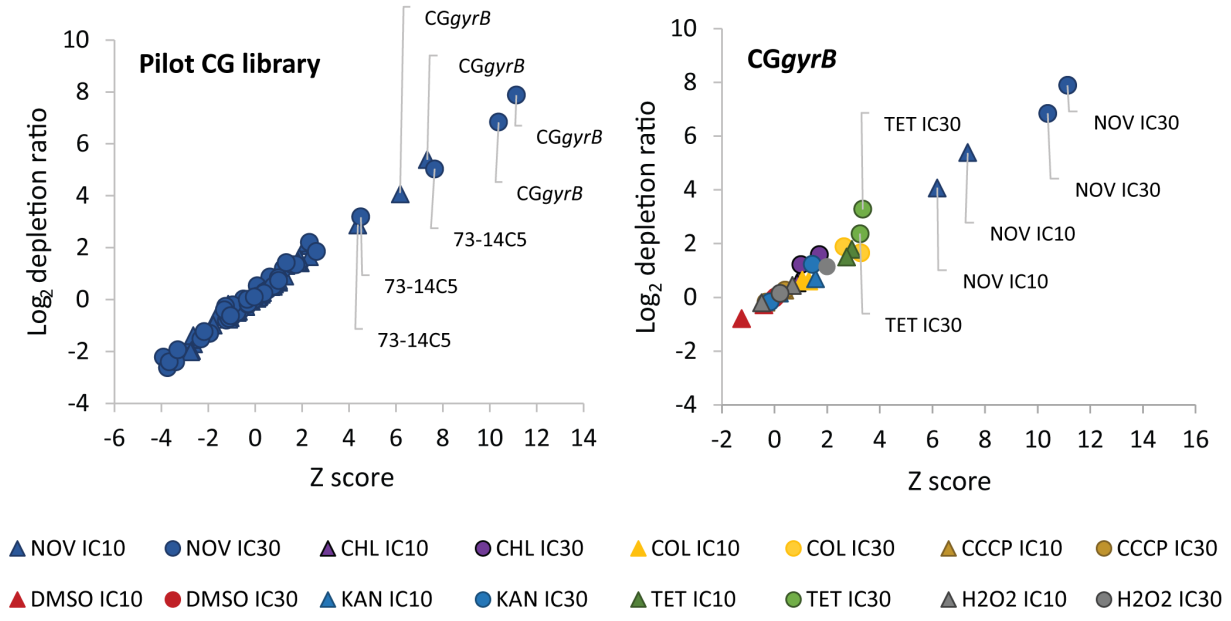

Figure 2.9 Competitive ESA detects the sensitization of CG*gyrB* to novobiocin.

Log_2 depletion ratios and Z scores from two independent experiments are overlaid. NOV, novobiocin; DMSO, dimethyl sulfoxide; KAN, kanamycin; COL, colistin; TET, tetracycline; CHL, chloramphenicol; H2O2, hydrogen peroxide; CCCP, carbonyl cyanide 3-chlorophenylhydrazone; IC10 and IC30, concentration of antibiotic inhibiting 10% or 30% of wild type growth, respectively. Left panel: CG mutant enhanced sensitivity in response to novobiocin. CG mutants showing enhanced sensitivity to novobiocin are labeled. Right panel: Antibiotic profile of the GyrB-depleted CG*gyrB* mutant. Antibiotics causing enhanced sensitivity are labeled.

Estimating bacterial growth by turbidimetry or colony size is limited by the detection range of the spectrophotometer or the resolution of the visualization tool used, respectively. Tracking bacterial growth by Illumina sequencing should observe a greater detection range limited only by the depth of coverage. In addition, Illumina sequencing allows mutant detection during competitive growth. To investigate the contribution of competitive growth to the specific enhanced sensitivity of the CG*gyrB* when exposed to novobiocin, CG*gyrB* was grown in a pool at one rhamnose concentration with 3 other CG mutants, and their relative abundance compared when they were grown competitively in a pool or grown clonally by Illumina sequencing. The depletion of CG*gyrB* in response to novobiocin was greater than 17 fold when grown in co-culture with 3 other CG mutants, and 2-fold when grown clonally (Table 2.4). Competitive growth did increase the sensitization of CG*gyrB* to when exposed to an IC_{10} of novobiocin, but not to an IC_{10} of chloramphenicol. The fold depletion of clonally grown strains measured by Illumina sequencing was consistent with that calculated by measuring the OD_{600nm} (Table 2.4). The observed low sensitivity of the clonal enhanced sensitivity assay was expected as novobiocin was used at the very low concentration of IC_{10}. However, this slight inhibitory concentration was sufficient to cause a severe depletion of the CG*gyrB* mutant growing within the pool. These results demonstrate that competitive growth can enhance the specific sensitivity of a CG mutant against its cognate antibiotic.

Table 2.4 Comparison of enhanced sensitivity of pooled and clonally grown CG mutants.

	Fold depletion (SD)[a]			
	CG*gyrB*	67-5H10	86-3D16	96-1K12
NOV pool, NGS	17.16 (2.81)	1.36 (0.39)	1.09 (0.13)	0.64 (0.02)
NOV clonal, NGS	2.37 (0.30)	1.11 (0.20)	1.13 (0.08)	0.80 (0.05)
NOV clonal, OD_{600nm}	2.60 (0.09)	1.19 (0.05)	1.13 (0.12)	0.87 (0.06)
CHL pool, NGS	1.17 (0.11)	1.03 (0.23)	0.75 (0.12)	0.92 (0.04)
CHL clonal, NGS	0.88 (0.05)	1.09 (0.18)	1.16 (0.16)	1.03 (0.04)
CHL clonal, OD_{600nm}	1.16 (0.12)	1.45 (0.03)	1.30 (0.10)	1.22 (0.04)
no ATB pool/no ATB clonal, NGS	1.07 (0.35)	0.99 (0.38)	1.27 (0.07)	0.93 (0.01)

[a]Mean (standard deviation) of two independent experiments

NOV, novobiocin; CHL, chloramphenicol; ATB, antibiotic; NGS, next generation sequencing

2.3.3 The competitive enhanced sensitivity assay reveals a two-component system (TCS) involved in regulation of antibiotic resistance

The transposon insertion of mutant 73-14C5 is located 58 bp upstream of the 3' end of the BURCENK56V_RS04770 locus, which seems to form an operon with the downstream gene BURCENK56V_RS04765. While it is not clear whether the transposon insertion in mutant 73-14C5 functionally disrupted RS04770, it placed the rhamnose-inducible promoter to control RS04765. In the *B. cenocepacia* K56-2 draft genome (Varga et al., 2013) RS04770 and RS04765 are preliminarily annotated as a histidine kinase coding gene and a XRE family transcriptional regulator gene, respectively, suggesting that they form a two-component system (TCS). These genes are homologs of BCAL0471 and BCAL0472, respectively, in the *B. cenocepacia* J2315 complete genome (Holden et al., 2009a). From profiling the pilot CG library with several growth inhibitors, we found that the CG mutant 73-14C5 had significant depletion ratios in response to novobiocin (Figure 2.9A and Figure 2.10A), chloramphenicol, tetracycline, kanamycin, and CCCP (Figure 2.10A). CG mutant 73-14C5 was not sensitive to hydrogen peroxide, colistin, or DMSO. The enhanced sensitivity of 73-14C5 in response to antibiotics tested in the competitive ESA, as well as ciprofloxacin and meropenem, was confirmed by growing the strains clonally and calculating the depletion ratio based on the OD_{600nm} of the cultures. In agreement with the results from the competitive ESA, mutant 73-14C5 showed a similar antibiotic profile and also demonstrated enhanced sensitivity to ciprofloxacin and meropenem (Figure 2.10B). The CG mutants 79-30H5 and 81-36C9 (Bloodworth et al., 2013a), which contain the transposon insertion in the same location and were independently obtained, showed similar profile (data not shown). Taken together these results show that this TCS is involved in antibiotic resistance to different classes of antibiotics including inhibitors of cell wall synthesis (meropenem), DNA replication

(novobiocin and ciprofloxacin), and protein synthesis (tetracycline, kanamycin and chloramphenicol). The RS04770 and RS04765 genes were designated *esaS* and *esaR*, respectively, for *E*nhanced *S*ensitivity to *A*ntibiotics *S*ensor and *R*esponse regulator.

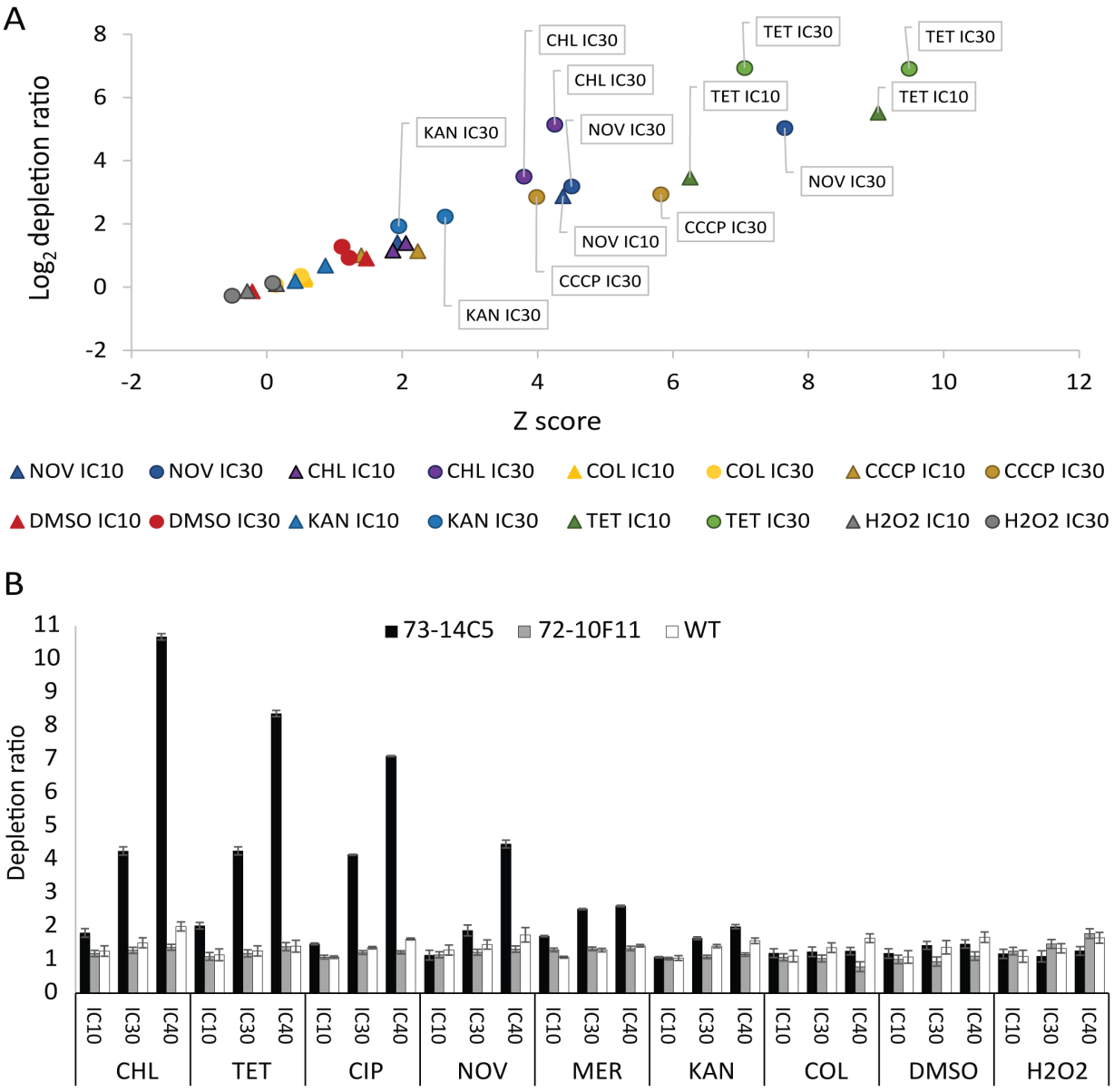

Figure 2.10. Antibiotic profile of CG mutant 73-14C5, under-expressing EsaR.

NOV, novobiocin; CIP, ciprofloxacin; DMSO, dimethyl sulfoxide; KAN, kanamycin; COL, colistin; MER, meropenem; TET, tetracycline; CHL, chloramphenicol; H2O2, hydrogen peroxide; CCCP, carbonyl cyanide 3-chlorophenylhydrazone; IC10, IC30, IC40: concentration of antibiotic inhibiting wild type growth by 10%, 30% or 40%, respectively. A) Antibiotic profile for CG mutant 73-14C5 from the competitive ESA. Log_2 depletion ratios and Z scores for each antibiotic treatment from two independent experiments are overlaid. Antibiotics causing hypersensitivity are labeled. B) Enhanced sensitivity measured by OD_{600nm}. Depletion ratio of 73-14C5, 72-10F11 (the CG mutant co-cultured with 73-14C5 in the competitive ESA), and *B. cenocepacia* K56-2 wild type strain (WT) in response to antibiotics. Depletion ratio was calculated by dividing the OD_{600nm} of the no antibiotic control by the OD_{600nm} of the antibiotic condition. Error bars represent the standard deviation from three independent experiments.

2.3.4 Mutational analysis of the *esaSR* locus suggests that *esaR* is an essential gene

The transposon insertion site within the 3'end of *esaS* and upstream of *esaR* in 73-14C5 suggested that the CG phenotype was due to downregulation of *esaR* in the absence of rhamnose. In the majority of our CG mutant library, downregulation of essential genes by the rhamnose-inducible promoter results in the absence of growth (Bloodworth et al., 2013a). Instead, 73-14C5 displayed 50% of wild type growth in the absence of rhamnose (Fig. 2.11A), suggesting that downregulation of *esaR* expression caused a fitness defect but that the gene was not essential. Alternatively, low protein turnover or leaky levels of expression from the rhamnose-inducible promoter even in the absence of rhamnose may provide cellular levels of an essential protein that are compatible with viability and a low growth phenotype (Ortega et al., 2007a). To further explore the essentiality of the *esaSR* locus we set out to perform gene deletion experiments. We first attempted deletion of the complete *esaSR* locus with a mutagenesis system that uses the homing endonuclease I-SceI (Flannagan et al., 2008). First, we delivered a suicide plasmid carrying a trimethoprim (TMP) resistance cassette, the flanking regions of *esaSR* and the I-SceI recognition site to *B. cenocepacia* K56-2, resulting in TMP resistant transformants, arising from the plasmid-targeted insertion into the chromosome via a first event of homologous recombination. Next, we introduced the plasmid pDAI-SceI that constitutively expresses the I-SceI nuclease and contains a tetracycline (TET) resistance cassette. I-SceI causes a double strand break into the inserted plasmid sequence, which stimulates intramolecular recombination. The resolution of this cointegrate can either restore to a wild type configuration or cause a gene deletion, depending on the site of the crossover. This second event of recombination can be selected by screening colonies for TMP susceptibility, which correspond to the loss of the antibiotic resistance marker. Typically, 50% of the TMP sensitive screened colonies harbor the deletion genotype, which can be then confirmed

by colony PCR using appropriate primers. We reasoned that if *esaR* was essential, resolution of the cointegrate would result in 100% wild type configurations. Two consecutive attempts to delete the *esaSR* resulted in 100% wild type configurations. We then attempted to delete the *esaSR* locus for a third time while simultaneously attempting to delete only *esaS*. After the first event of recombination and for each deletion experiment, twenty-four TMP resistant colonies harbouring pDAI-SceI, were grown in the absence of TMP and screened for the loss of the TMP resistance phenotype. Fifteen and seven colonies were found to be TMP susceptible for the *esaS* and the *esaSR* loci deletion attempts, respectively. From those, two colonies were found to have a deletion of the *esaS* gene (Figure 2.4). In contrast, all colonies corresponding to the *esaSR* deletion attempt had reverted to the wild type configuration. The success in obtaining an unmarked deletion of the histidine kinase gene at locus *esaS* but not of the TCS locus, *esaSR,* confirms that *esaS* is dispensable and strongly suggests that *esaR* is essential for growth. The *esaS* gene deletion mutant (Δ*esaS*) was named MKC4 and selected for further phenotypic analysis. To investigate the phenotype caused by depletion of *esaR*, we placed the rhamnose-inducible promoter upstream of *esaR* by site directed mutagenesis, leaving intact the *esaS* locus. This new CG mutant was called MKC2 (CG*esaR*). In the absence of rhamnose, MKC2 showed a more severe growth defect than 73-14C5, while MKC4 observed moderate growth defect, intermediate between 73-14C5 and the wild type (Figure 2.11A).

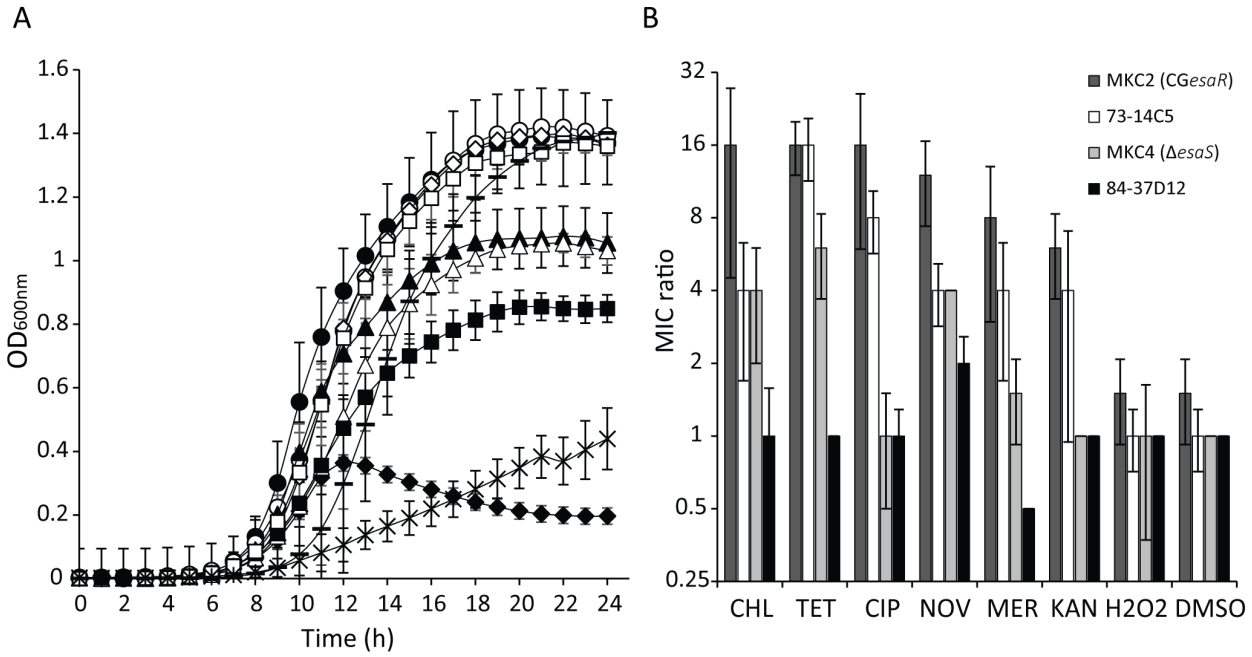

Figure 2.11 Depletion of EsaR and EsaS cause a growth defect and lower MIC of select antibiotics.

A) Growth curves of strains grown in LB in the presence and absence of rhamnose (rha). *B. cenocepacia* K56-2 wild type, rha, ○; no rha, ●; 73-14C5 (CG transposon mutant of *esaR*), rha, □; no rha, ■; MKC2 (CG*esaR*), rha, ◊; no rha, ♦; MKC4 (Δ*esaS*), rha, ✕; no rha, ▲; and 84-37D12, rha ▬, no rha, X. Error bars represent the standard deviation of at least two independent experiments. B) Minimum inhibitory concentration (MIC) ratios of MKC2 (CG*esaR*), MKC4 (Δ*esaS*), 73-14C5 (CG transposon mutant of *esaR*) and 84-37D12 (CG transposon mutant unrelated to *esaR*), in response to CHL, chloramphenicol; TET, tetracycline; CIP, ciprofloxacin; NOV, novobiocin; KAN, kanamycin; MER, meropenem; DMSO, dimethyl sulfoxide; and H2O2, hydrogen peroxide. MIC ratio is calculated as the MIC of the wild type divided by the MIC of the mutant in the absence of rhamnose. MICs used for the MIC ratio calculation are listed in Table 2.5. The median MIC ratios and standard deviation of at least three independent experiments are shown.

Table 2.5. Minimum inhibitory concentrations (MICs) of selected antibiotics against *B. cenocepacia* K56-2 wild type (WT), MKC2 (CG*esaR*), MKC4 (Δ*esaS*), 73-14C5 (CG transposon mutant of *esaR*), and 86-37D12 (CG transposon mutant unrelated to *esaR*).

	MIC*							
	WT	MKC4 (Δ*esaS*)	MKC2 (CG*esaR*)		73-14C5		84-37D12	
	no rha	no rha	no rha	rha	no rha	rha	no rha	rha
CHL (μg/ml)	16	4	1	16	4	16	16	32
TET (μg/ml)	8	1.5	0.75	4	0.5	8	8	8
CIP (μg/ml)	2	2	0.125	3	0.25	2	2	2
NOV (μg/ml)	8	2	1	12	4	2	8	8
MER (μg/ml)	32	24	4	48	8	8	64	64
KAN (μg/ml)	1000	1000	187.5	1000	250	1000	1000	1000
H_2O_2 (mM)	0.1875	0.234375	0.140625	0.28125	0.1875	0.1875	0.1875	0.1875
DMSO (%, v/v)	12.5	12.5	9.375	12.5	12.5	12.5	12.5	12.5

*Median MIC from three independent experiments.

2.3.5 The *esaSR* locus is involved in drug efflux activity and cell membrane integrity

To confirm that the *esaSR* locus was related to antibiotic resistance in *B. cenocepacia,* we determined antibiotic minimum inhibitory concentrations (MICs) against *B. cenocepacia* K56-2 wild type, MKC2 (CG*esaR*), MKC4 (Δ*esaS*) and 73-14C5 (Table 2.5). Since MKC2 (CG*esaR*) has a pronounced growth defect, a CG mutant, 83-37D12, that has a similar growth defect as MKC2 (CG*esaR*) in the absence of rhamnose was included in the assay (Figure 2.11) (Bloodworth et al., 2013a). In 84-37D12, the rhamnose-inducible promoter is controlling the expression of four genes, BURCENK562V_RS02270, BURCENK562V_RS02265, BURCENK562V_RS02260 and BURCENK562V_RS02255, that are predicted to be in an operon (Mao et al., 2014a) and involved in purine metabolism (Winsor et al., 2008). The MIC ratios, calculated as the fold change in the MIC of the wild type with respect to each mutant grown without rhamnose (Figure 2.11B), were in agreement with the antibiotic sensitivity profile of 73-14C5 in the ESA (Figure 2.10). Both mutants in which the rhamnose-inducible promoter controls the expression of *esaR*, showed at least a 4-fold decrease in the MIC of chloramphenicol, tetracycline, ciprofloxacin, novobiocin, and meropenem, in the absence of rhamnose. The mutant unrelated to MKC2, but possessing a similar growth defect, 84-37D12, did not show the same level of sensitivity as the *esaR*-depleted strains. This result, in concordance with the antibiotic sensitivity of the EsaR-depleted mutant, 73-14C5, which does not have a severe growth defect, indicates that the increased MIC ratio of MKC2 (CG*esaR*) to antibiotics is not an effect of the lack of growth. MKC4 (Δ*esaS*) showed at least a 4-fold MIC ratio to chloramphenicol, tetracycline and novobiocin, but not to the other antibiotics tested. None of the *esa* mutants showed this increased level of sensitivity to DMSO or hydrogen peroxide when compared to the wild type (Figure 2.11B, Table 2.5). Since the *esaR* and *esaS* mutants were sensitive to different classes of antibiotics, we investigated whether mutation at these

loci causes a lack of efflux, resulting in the increased sensitivity to antibiotics. Efflux activity was assessed by measuring the fluorescence from β-naphthylamine, which is the cleavage product produced immediately upon the uptake of Ala-Nap into the cell (Lomovskaya et al., 2001). As Ala-Nap is known to be a substrate of the MexAB-OprM efflux pump of *Pseudomonas aeruginosa* and AcrAB-TolC pump of *Escherichia coli,* an increase in fluorescence indicates inhibition of efflux activity (Lomovskaya et al., 2001). Mutants 73-14C5 and MKC2 (CG*esaR*) had an approximate 8- and 3-fold increase in fluorescence, respectively, compared to the wild type at the 1-hour time point of the assay (Figure 2.12A). This increase in fluorescence over time was observed for 73-14C5 and MKC2 (CG*esaR*) when grown overnight without rhamnose. When grown in the presence of rhamnose to induce expression of *esaR*, the fluorescence produced by 73-14C5 and MKC2 (CG*esaR*) was as low as that of the K56-2 wild type, indicating a role of EsaR in activating efflux or maintaining the integrity of the membrane (Figure 2.12A). The effect of deleting *esaS* was not as strong, as MKC4 (Δ*esaS*) observed only 1.5-fold increase in fluorescence compared to the wild type.

In an effort to induce efflux prior to the Ala-Nap uptake assay, we pre-treated the cells with chloramphenicol for three hours in the absence of rhamnose. Similar to the results of Figure 2.12A, untreated 73-14C5 and MKC2 (CG*esaR*), but not MKC4 (Δ*esaS*), observed an increase in fluorescence relative to that of wild type cells (Figure 2.12B) and the difference was statistically significant (WT vs. 73-14C5, $p < 0.01$; WT vs. MKC2, $p < 0.05$). Chloramphenicol caused a decrease in the fluorescence of the wild type cells compared to the non-antibiotic control (WT no CHL vs. WT + CHL, $p < 0.001$) suggesting that chloramphenicol induced efflux. In agreement with a role of *esaS* in chloramphenicol-mediated induction of efflux, MKC4 (Δ*esaS*) did not show any decrease in fluorescence in the presence of chloramphenicol. On the contrary fluorescence

increased nearly 2-fold compared to the non-chloramphenicol condition ($p < 0.05$) (Figure 2.12B). There were no significant differences between untreated and chloramphenicol-treated cells when they were depleted of *esaR* (73-14C5 and MKC2). Treatment of wild type cells with the proton gradient-uncoupling agent carbonyl cyanide *m*-chlorophenylhydrazone (CCCP) significantly inhibited efflux in wild type cells (WT vs. WT CCCP $p < 0.01$) and Δ*esaS* (MKC4 vs. MKC4 + CCCP $p < 0.01$), but did not result in a significant increase in fluorescence in the EsaR-depleted mutants.

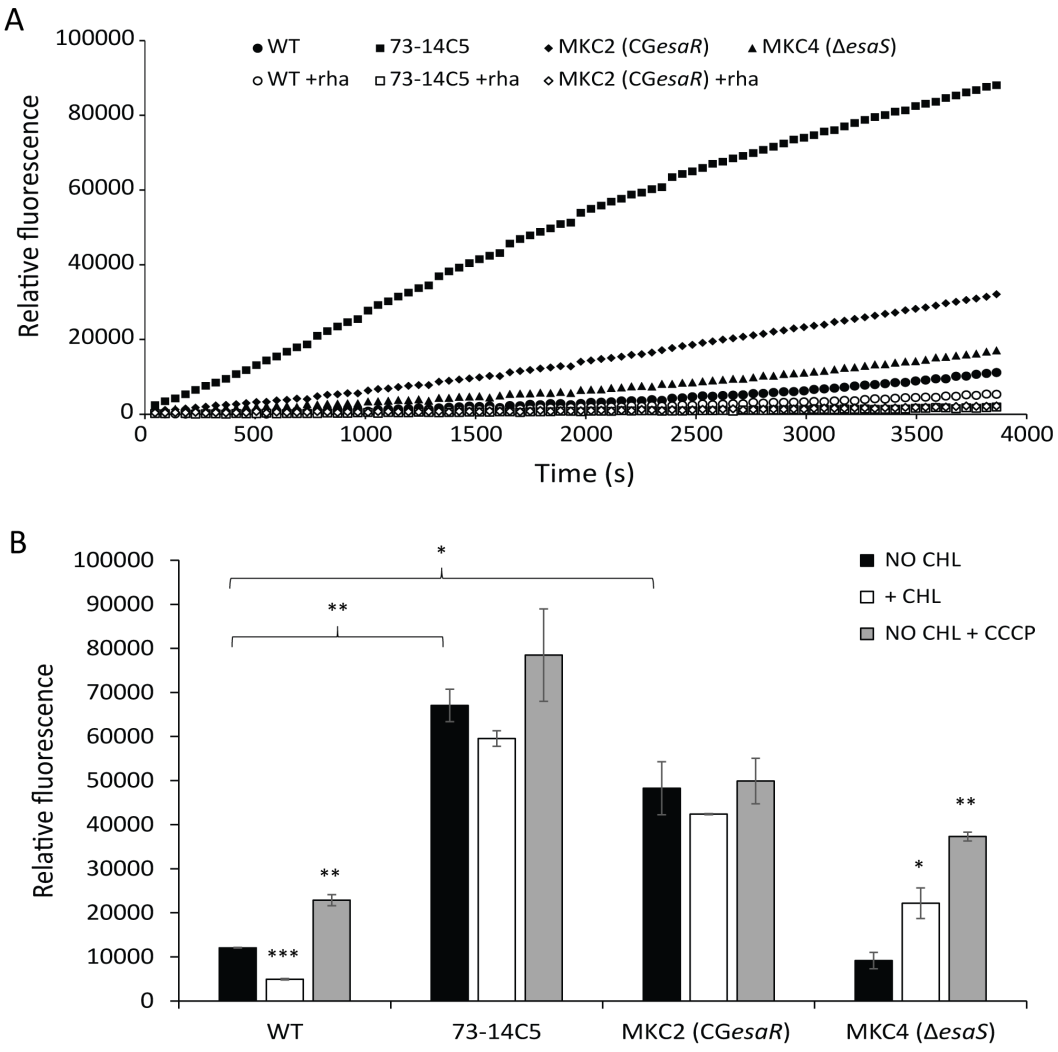

Figure 2.12. Efflux activity of *B. cenocepacia* K56-2 wild type (WT), 73-14C5 (CG transposon mutant of *esaR*), MKC2 (CG*esaR*) and MKC4 (Δ*esaS*). Efflux activity was assessed by measuring the relative fluorescence produced by cultures treated with Ala-Nap. The rate of uptake of non-fluorescent Ala-Nap and immediate cleavage to fluorescent β-naphthylamine is indicative of the efflux activity of the cell. A) The relative fluorescence of cultures over time when grown overnight in the presence (white symbols) and absence of rhamnose (black symbols). Results shown are representative of three independent experiments. B) The relative fluorescence of chloramphenicol-treated and untreated cultures at the 1 h time point of the Ala-Nap assay. Cultures grown overnight without rhamnose were adjusted to an OD_{600nm} of 1.0 and incubated in the absence (black bars) or in the presence (white bars) of chloramphenicol (CHL) for 3 hours prior to the Ala-Nap assay. Ten minutes into the assay, 10 μM CCCP was added to cells to disrupt efflux (gray bars). Error bars represent the standard deviation of two biological replicates. A t test was performed with GraphPad software to determine significant differences. *, $p < 0.05$; **, $p < 0.01$; ***, $p < 0.001$.

DIC microscopy imaging was used to further characterize the phenotype of EsaS and EsaR-depleted cells. After 24 h of growth in the presence of rhamnose, MKC2 (CG*esaR*) and 84-37D12 showed rod-shaped morphology, similar to the wild type phenotype (Figure 2.13). All of the EsaR-depleted MKC2 (CG*esaR*) cells examined were small, spherical cells while MKC4 (Δ*esaS*) and 84-37D12 cells had rod shapes more similar to the wild type when grown for 24 h without rhamnose (Figure 2.13). In the Ala-Nap assay, the strong fluorescent signal and lack of chloramphenicol-induced efflux in MKC2 (CG*esaR*) and 73-14C5 raised the question of whether efflux is solely responsible for the increased uptake of Ala-Nap, or if the lack of EsaR also compromises the cell membrane. To explore the membrane integrity of *esaR*-depleted cells, we examined microscopy images of cells stained with the fluorophores SYTO9 and propidium iodide (PI). SYTO9 is a green fluorescent nucleic acid stain capable of passing through intact membranes while PI is a hydrophobic red fluorescent nucleic acid stain that only stains cells with compromised membranes. PI staining was observed in 50% of the EsaR-depleted MKC2 (CG*esaR*) cells, indicating that EsaR-depleted cells have a compromised membrane (Figure 2.13). The other strains examined had intact cell membranes as less than 4% of WT, MKC4 (Δ*esaS*), and 84-37D12 cells were stained with PI (Figure 2.13). Together with the increased MIC ratios of 73-14C5, MKC2 (CG*esaR*) and MKC4 (Δ*esaS*) combined with the increased Ala-Nap uptake in *esaR*-depleted cells and *esaS*-depleted cells treated with chloramphenicol, our results strongly suggest that the *B. cenocepacia* two-component system *esaSR* regulates resistance to antibiotics by maintaining cell envelope integrity and through efflux activity.

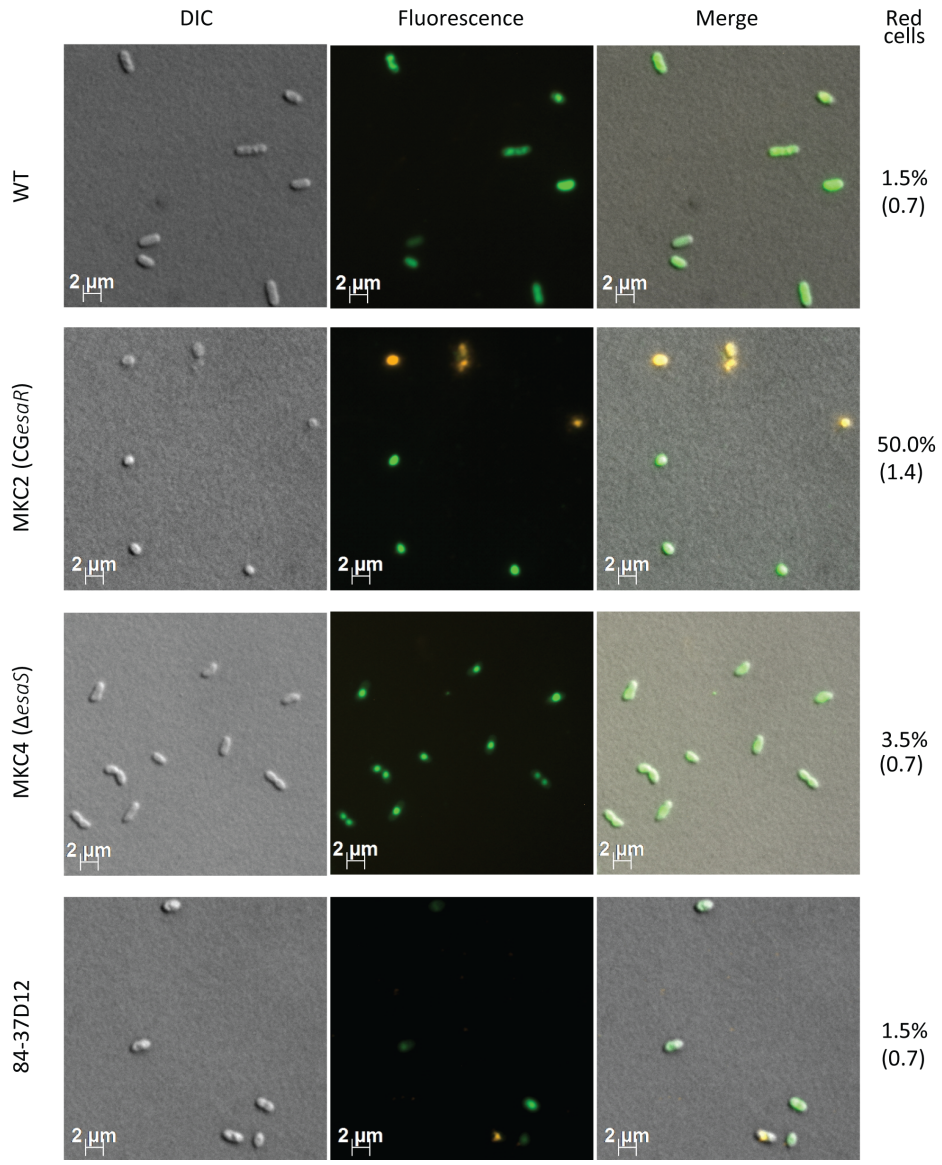

Figure 2.13. *B. cenocepacia* cells have a compromised membrane when depleted in EsaR. Cultures of wild type (WT), MKC2 (CG*esaR*), MKC4 (Δ*esaS*) and 84-37D12 (CG mutant unrelated to *esaR*), incubated for 24 h in the absence of rhamnose, were stained with STYO9 and propidium iodide (PI) from the *Bac*Light Live/Dead bacterial viability kit (Molecular Probes) and visualized by fluorescence microscopy. Fluorescent green bacteria indicate intact membranes, while fluorescent red stained cells represent bacteria with compromised membranes. The average percent of fluorescent red cells and standard deviation (in brackets) from two independent experiments is reported.

2.4 Discussion

In this work, we identified and characterized a two component system as a promising antibiotic target for Bcc infections. We used a pilot CG library under-expressing essential genes, grown competitively in a pool and quantified their relative abundance quantified using next generation sequencing. The pilot CG library included a *gyrB* CG mutant (CG*gyrB*) previously shown to have enhanced sensitivity in the presence of sublethal concentrations of novobiocin, when measured by OD_{600nm} (Bloodworth et al., 2013a). Growing CG mutants together in the competitive ESA magnified the level of enhanced sensitivity of CG*gyrB* to novobiocin (Table 2.4). We consider pooled growth to be advantageous over clonal growth, as it reduces the amount of reagents required, notably the amount of compound needed, and does not require specialized robotic equipment or imaging software. Tracking the relative abundance of competitively grown mutants by Illumina sequencing increases the dynamic range of sensitization detection than when measuring mutant growth by OD_{600nm}. In any assay, expanding the signal window allows for more accurate discrimination of signal over noise. The ability to generate a strong signal using a low dose of compound is significant as using higher doses of compound can have an obscuring effect as it increases the signal of not only the strain under-expressing the target, but all the strains due to non-specific toxicity. The increased hypersensitivity from competitive growth that we observed coupled with the nearly unlimited dynamic range of detection of Illumina sequencing, shows promise for this method to generate detailed mutant profiles. The identification of both strongly and moderately sensitized mutants creates profiles for novel compounds that can inform genes capable of buffering compound activity and in turn facilitate rational drug design and point to potential combination therapies. Another reason for generating comprehensive mutant profiles to

determine MOA is that while depletion of the antimicrobial target is likely to have the strongest signal, this is not always the case. An example to the contrary is aminoglycosides, where the mutant profiles represent that mechanism of killing is similar to membrane disrupting antibiotics (Donald et al., 2009b), and does not reflect its target, the ribosome (Davis, 1987). In addition to novobiocin, CG*gyrB* showed marginal enhanced sensitivity to tetracycline IC_{10} and IC_{30} and colistin IC_{30}, which highlights the complexity of sensitization profiles for compounds, even when the compounds are associated with a single target. A likely explanation is that the hypersensitivity of non-target CG mutants to a compound may be observed where there is an associated cellular process involved. Donald *et al.* (Donald et al., 2009b) reported that a GyrB-depleted strain of *Staphylococcus aureus* showed enhanced sensitivity to daunorubicin, a tetracycline-like compound. While inhibition of DNA gyrase activity interferes with DNA replication (Gellert et al., 1976a, 1976b), daunorubicin intercalates within DNA and causes DNA fragmentation and single strand breaks (Aubel-Sadron and Londos-Gagliardi, 1984). Therefore, inhibition of DNA replication may sensitize *S. aureus* against daunorubicin. Underexpression of *gyrB* sensitizes *B. cenocepacia* (this study) and *S. aureus* to tetracycline (Donald et al., 2009b). Despite the ribosome being the primary target of tetracycline (Buck and Cooperman, 1990), tetracycline can also can bind and introduce damage to DNA, which is enhanced by the formation of metal complexes (Khan and Musarrat, 2003; Khan et al., 2003). GyrB-depletion also sensitized *B. cenocepacia* to colistin although this effect was only observed with colistin at the IC_{30}. Colistin is a polypeptide antibiotic of the polymixin family, which targets the cell membrane through initial interaction with the lipopolysaccharide portion of the outer membrane (Falagas et al., 2005b). While the reasons for the marginal enhanced sensitivity of colistin against the *B. cenocepacia* CG*gyrB* mutant are not known, a likely explanation is that both inhibition of DNA replication by *gyrB* depletion and the

action of colistin increase the production of reactive oxygen species (ROS), contributing to the sensitization mechanism. Although there are no data available for novobiocin or colistin-mediated ROS production, the fluoroquinolone moxifloxacin, at a concentration that inhibits the DNA gyrase, induced the production of hydroxyl radical (Ferrandiz et al., 2015). Similarly, Polymixin B was shown to kill *Acinetobacter baumanni* by hydroxyl radical production (Sampson et al., 2012). In addition to identifying the drug binding targets, the increased signal in the competitive enhanced sensitivity assay facilitates the identification of subtle interactions of affected pathways by generating an intricate CG mutant profile for each antibiotic, to determine the MOA of novel antibiotics. These detailed mutant profiles can provide a tool to direct chemical engineering during compound optimization.

While we were able to reliably quantify the relative abundance of the CG mutants in the pilot CG library, using a single multiplex PCR restricted the number of strains we were able to screen, which is a limitation of this assay. No correlation was found between amplicon size, thermodynamic properties of the primers or amplicons and relative detection or amplification variability of the CG mutants (data not shown). However, it is possible to include more CG mutants using a manifold of individually optimized multiplex PCRs, as done previously (Donald et al., 2009a). Creating amplicons by other methods, such as the Tn-seq circle (Gallagher et al., 2011b), or using barcoded transposons as in RB-TnSeq (Wetmore et al., 2015) or TagModules (Oh et al., 2010), which do not require the use of multiplex PCR primers, would be more amenable to the addition of new strains in the ESA since they do not require previous knowledge of transposon insertion sites or optimization of multiplex PCRs. This would be advantageous since profiling more strains through the ESA will increase the likelihood of matching novel growth inhibitors to their targets.

Profiling the sensitivity of the CG mutants to several antibiotics uncovered a CG mutant of a TCS, which was hypersensitive to several classes of antibiotics. This putative TCS (named *esaSR* for *E*nhanced *S*ensitivity to *A*ntibiotics *S*ensor kinase and *R*esponse regulator) is encoded by BURCENK56V_RS04770 and BURCENK56V_RS04765, which likely form an operon. The *B. cenocepacia* K56-2 *esaSR* genes are homologous to the BCAL0471-BCAL0472, which have also been annotated as forming a putative TCS in the *B. cenocepacia* J2315 genome (Winsor et al., 2008). Remarkably, the BCAL0471-BCAL0472 locus is just one of more than forty TCSs that remain uncharacterized in *B. cenocepacia* genomes. TCSs are used by bacteria to sense environmental stimuli through a membrane bound histidine kinase which activates a cytoplasmic response regulator that in turn mediates changes in gene expression (Stock et al., 2000). Many TCSs have been implicated in the regulation of antibiotic resistance (Comenge et al., 2003; Muller et al., 2011; Stephenson and Hoch, 2002) through the overexpression of efflux pumps (Baranova and Nikaido, 2002; Deng et al., 2013; Hirakawa et al., 2003; Marchand et al., 2004; Nishino and Yamaguchi, 2002; White et al., 1997) or maintaining cell membrane integrity (Gunn and Miller, 1996; Ji et al., 2016; Svensson et al., 2009; Vogt and Raivio, 2012). Outer membrane permeability and efflux activity are synergistic processes that are often associated (Delcour, 2009). Reactive oxygen and nitrogen species are known to induce expression of efflux pumps through activation of TCSs (Fetar et al., 2011; Fraud and Poole, 2011; Hwang et al., 2012) and outer membrane permeability can be regulated in response to oxidative stress (Heijden et al., 2016). It is notable that the sensor histidine kinase (BURCENK56V_RS04770) contains a PAS domain, which is used to sense the redox state of the cell in many prokaryotes (Taylor and Zhulin, 1999).

Genetic analysis of the *esaSR* locus strongly suggests that *esaR* is an essential gene. Gene essentiality is challenging to demonstrate experimentally. Systems where a gene is deleted in the

presence of a second copy expressed from a plasmid are available for some bacteria (Cardona and Valvano, 2005a). In those cases, plasmid maintenance in the absence of selection is deemed as a confirmation of gene essentiality (Pickering and Oresnik, 2010). The limited availability of genetic tools for *B. cenocepacia* precluded us from using this approach. However, we demonstrated that although the first event of homologous recombination directed to mutagenize *esaR* was achieved, resolution of the cointegrate in the merodiploids always rendered excision of the integrated plasmid with reversion to the wild type conformation. In contrast, parallel experiments aimed at deleting *esaS* resulted in *esaS* deletion mutants. This observation strongly suggests that while *esaS* is dispensable, *esaR* is not. In support of this, a recent high density transposon mutagenesis study in *B. cenocepacia* J2315 did not identify any mutants with insertions in the homolog of *esaR*, BCAL0472, indicating that it is essential, while mutants with insertions that disrupted *esaS* were recovered (Wong et al., 2016b). A few essential TCSs have been described with a regulatory role in cell wall homeostasis (Ji et al., 2016; Svensson et al., 2015). The *S. aureus* WalKR system is remarkable in that temperature-sensitive mutants are also hypersusceptible to antibiotics (Martin et al., 1999). It is possible then, that the essentiality of the *B. cenocepacia esaR* is related to a similar role, controlling cell envelope processes. We have demonstrated that depletion of *esaS* or *esaR* also results in an increase of fluorescence during the Ala-Nap uptake assay, which suggests reduced efflux of the Ala-Nap reagent. However, to expose the involvement of *esaS* in activating efflux, previous treatment with chloramphenicol was necessary (Figure 2.12B). Instead, depletion of EsaR increases Ala-Nap uptake regardless of previous induction with chloramphenicol, indicating that *esaS* and *esaR* can regulate different processes, efflux and membrane integrity. The lack of increased Ala-Nap uptake by both the CCCP treated MKC2 (CG*esaR*) and 73-14C5 suggests that depletion of *esaR* causes either a comprehensive shutdown of efflux or an increase

in the permeability of the membrane. The fact that 73-14C5 was hypersensitive to CCCP supports the latter explanation since a cell with an unstable membrane would be more susceptible to disruption of the proton motive force. Results from the Ala-Nap uptake assay are consistent with the microscopy images showing that MKC2 (CG*esaR*) has a compromised membrane, where the lack of PI staining in MKC4 (Δ*esaS*) indicates an intact membrane. Importantly, while the differential staining of STYO9 and PI is conventionally used to assess cell viability, cells stained with PI may be viable (Shi et al., 2007).

It is tempting to speculate that EsaS-dependent phosphorylated EsaR activates efflux pump genes but unphosphorylated EsaR is capable of regulating cell envelope processes. Therefore, while *esaS* seems to regulate antibiotic-induced efflux it remains to be demonstrated to what extent the role of *esaR* is related to regulation of efflux pumps, cell envelope homeostasis, or a contribution of both mechanisms.

Much interest has been focused on TCSs as valuable drug targets due to the fact that TCSs are not present in humans and targeting them could reduce virulence (Gotoh et al., 2010; Worthington et al., 2013) and antibiotic resistance (Worthington et al., 2013). Inhibitors of a TCS involved in antibiotic resistance could provide effective therapies for treating multidrug resistant infections, in combination with antibiotics. A TCS that mediates antibiotic resistance to different antibiotics represents a lucrative target in *B. cenocepacia* for combatting antibiotic resistance since inhibitors of this TCS could render the strain susceptible to antibiotics currently in use.

Chapter 3: Identification and comparative analysis of the essential genome of *Burkholderia cenocepacia* K56-2 provides evidence for conservation of genus-specific essential genes

3.1 Introduction

Determining the essential genomes of bacterial pathogens has helped to identify fundamental processes that can be exploited as novel targets of antibacterial therapies (Fields et al., 2016). The identification of essential genes is challenging due to the lethal phenotype that mutagenesis of essential genes cause. Yet, the identification of essential genes in laboratory conditions has been achieved by recovering mutants growing in rich, undefined medium after concerted disruption of nonessential genes (Baba et al., 2006; Gerdes et al., 2003; Kobayashi et al., 2003; Mori et al., 2000). Since then, next generation sequencing has facilitated the use of saturated transposon mutagenesis to identify the essential genomes of many bacteria. To identify essential genes from a high-density transposon mutant (HDTM) library, the genomic DNA from the library is isolated and the transposon-genome junctions are selectively amplified by PCR and then sequenced. Transposon insertion sites are then identified by mapping the reads to the genome. Identification of transposon insertion sites in HDTM libraries has resulted in the successful for the identification the essential genomes of many different bacteria (Christen et al., 2011b; Langridge et al., 2009; Turner et al., 2015; Weerdenburg et al., 2015; Yang et al., 2014). Different methods for creating, sequencing and analyzing HDTM libraries have been developed including HITS (Gawronski et al., 2009), IN-seq (Goodman et al., 2009), TraDIS (Langridge et al., 2009) Tn-seq, and Tn-seq circle (Gallagher et al., 2011c). The statistical frameworks that can been applied for accurate essential gene identification are also diverse (Christen et al., 2011a; Moule et al., 2014a; Wong et al., 2016a). By considering the abundance of each clone in the library, degree of the essentiality of a gene can be identified. In this work, we used a recently developed data analysis pipeline that compares the abundance of each transposon mutant in the library with the variance

of neutral dataset generated by Monte Carlo simulations to determine the probability that a gene is essential (Turner et al., 2015).

Identifying the essential genomes of species belonging to the *Burkholderia* genus is important as this genus includes the *B. pseudomallei* group and the *Burkholderia cepacia* complex, two groups of opportunistic human pathogens, characterized by their intrinsic antibiotic resistance (Eberl and Vandamme, 2016). Members of the *B. pseudomallei* group include *B. pseudomallei*, *B. mallei* and *B. thailandensis. B. pseudomallei* is the most virulent *Burkholderia* species and is the causative agent of meliodosis (Wiersinga et al., 2006). Members of the *B. cepacia* complex are well known for causing severe lung infections in cystic fibrosis (CF) patients (Aris et al., 2001; Mahenthiralingam et al., 2005b; Saiman et al., 2014; Schaffer, 2015). *B. cenocepacia* K56-2 is a *B. cepacia* complex strain of the epidemic ET12 (Darling et al., 1998; LiPuma et al., 2001). K56-2 was isolated from a cystic fibrosis patient in Canada and is clonally related to the European strain J2315. K56-2 is more virulent than J2315 in zebra fish and *C. elegans* host models (Cardona et al., 2005; Vergunst et al., 2010) and has been used extensively in studies because it is less antibiotic resistant and more amenable to genetic manipulation. The genome of J2315 has been sequenced, revealing 3 chromosomes and a plasmid, for which closed sequences are available (Holden et al., 2009b). However, there is only a draft genome available for K56-2.

The essential genomes of three species of *Burkholderia, B. pseudomallei* K96243 (Moule et al., 2014a), *B. thailandensis* E264 (Baugh et al., 2013) and *B. cenocepacia* J2315 (Wong et al., 2016a) have been identified but no comparisons have been performed to identify common essential genes. In this work, we used the using the Tn-seq circle method (Gallagher et al., 2011a) and the data analysis pipeline developed by Turner et al (Turner et al., 2015) to identify the essential genome of *B. cenocepacia* K56-2. With the goal of identifying putative antibacterial targets

common to the *B. pseudomallei* and *B. cepacia* complex lineages, we identified 158 essential genes that are common to the four *Burkholderia* essential genomes. A porins, a lysophospholipid transporter, and a protein involved in polymixin resistance are essential in the *Burkholderia* species analyzed but not in any other bacterial essential genome described so far. Our work underscores particular aspects of the cell envelope as uniquely essential biological functions in *Burkholderia*.

3.2 Materials and Methods

3.2.1 Bacterial strains and growth conditions

The bacterial strains and plasmids used in this study are listed in Table 3.1. *B. cenocepacia* K56-2, a clonal strain of J2315 isolated from a cystic fibrosis patient (Darling et al. 1998), was the strain used in this study. All bacteria grown in this study were grown in Luria-Bertani (LB) media (BD, Franklin Lakes, NJ) at 37°C with shaking at 220 rpm in a New Brunswick Scientific E24 shaking incubator (Edison, NJ) for broth cultures unless otherwise indicated. *E. coli* strains were grown in 40 μg/mL of kanamycin (Kan40) or 50 μg/mL of trimethoprim (TMP50) when appropriate. *B. cenocepacia* transposon mutants were selected for in 100μg/mL of TMP (TMP100), 50 μg/mL of gentamicin (Gm50), and 0.2% rhamnose (0.2% rha). Additionally, the transposon mutants were grown in TMP100 with or without 0.2% rha when appropriate. Growth was estimated by measuring OD_{600nm} using a Biotek Synergy 2 plate reader (Winooski, VT). All chemicals were purchased from Sigma Chemical Co. (St. Louis, MO) unless otherwise indicated.

Table 3.1 Bacterial strains and plasmids used in this study

	Features[a]	Source
Strains		
Burkholderia cenocepacia K56-2	ET12 lineage, CF isolate	Darling et al. (1998)
Escherichia coli SY327	*araD* Δ(*lac pro*) *argE* (Am) *recA56* Rif^r *nalA λ pir*	Miller and Mekalanos (1988)
E. coli MM290	F$^-$, φ 80 lacZΔM15 *endA1 recA1 hsdR17* ($r_H^- m_K^+$) *supE*44 *thi*-1 Δ*gyrA96* (*ΔlacZYA-arg*F) U169 *relA*1	Bloodworth et al. (2013)
Plasmids		
pRK2013	ori_{colE1}, RK2 derivative, Km^r *mob*$^+$ *tra*$^+$	Figurski and Helinski (1979)
pRBrhaBoutgfp	pSCrhaBoutgfp derivative (Cardona et al. 2006), ori_{R6K}, *rhaR rhaS PrhaB* e-*gfp*	Bloodworth et al. (2013)

[a]CF = cystic fibrosis, Km = kanamycin, Rif = rifampicin

3.2.2 Production of the 1 million high-density transposon mutant library

Triparental matings were carried out to conjugate pRBrhaBoutgfp into wild type *B. cenocepacia* K56-2 using an *E. coli* SY327 donor strain (Miller and Mekalanos, 1988) and an *E. coli* MM290 helper strain carrying the pRK2013 plasmid (Figurski and Helinski, 1979). *E. coli* SY327 and MM290 were plated in LB agar supplemented with TMP50 or Kan40 respectively. *B. cenocepacia* K56-2 was grown in LB broth. All three strains were grown for 16-18 h at 37°C. Afterwards, *B. cenocepacia* K56-2 was subcultured in 5 mL of LB broth at 37°C until an OD_{600nm} of 0.3-0.6 was reached. The *E. coli* SY327 and MM290 colonies were collected and resuspended in 5 mL LB in separate snap cap tubes. From each of the *E. coli* SY327 and MM290 suspensions, volumes equivalent to 1.5 mL with an OD_{600nm} of 0.3 were mixed with *B. cenocepacia* suspension equivalent to 0.5 mL with an OD_{600nm} of 1.0. The mixture was vortexed then centrifuged for 1 min at 6,000 rpm. After the pellet was resuspended, approximately seventy 20-25 μL aliquots of the triparental mating were spotted on LB agar plates containing 0.2% rhamnose, allowed to dry and then incubated at 37°C for 2 h. Bacteria from the triparental mating spots were combined and resuspended in 6-7 mL of LB broth. Aliquots of 500 μl of bacteria were plated onto 8-10 Q-trays containing LB agar with 0.2% rhamnose, TMP 100 μg/ml and Gm50 μg/ml and incubated for 48 h. After incubation, pools of approximately 20,000 bacterial cells were collected into 5 mls of LB with 20% glycerol (v/v) and stored at -80°C in 400 μl aliquots. Nine triparental mating experiments were performed to produce an HDTM library of approximately 1,000,000 mutants. To create the sequencing-ready HDTM library, glycerol stocks from each triparental mating were pooled together such that there was equal representation of each transposon mutant.

3.2.3 Molecular biology techniques

The DNA concentration of the samples was measured using the Qubit dsDNA BR Assay kit (Invitrogen, Carlsbad, CA). 1-2 µL of DNA was added to Qubit dsDNA BR working solution such that the total volume was 200 µL. The mixture was vortexed for 2-3 sec, ensuring that no bubbles formed. The mixture was then incubated for 2-5 min at room temperature prior to the measurement of DNA concentration with a Qubit 2.0 fluorometer (Invitrogen).

DNA purification of amplicons was carried out using the Agencourt AMPure XP system (Beckman Coulter, Brea, CA). Room temperature AMPure XP beads were mixed with DNA samples in low DNA-binding microcentrifuge tubes (Eppendorf, Hamburg, Germany), after which the mixtures were incubated for 5 min at room temperature. The tubes were then placed next to the magnets on the magnet rack to sit until all the beads were pulled towards the magnet. The supernatant was then removed, after which the beads were washed twice with 1 mL of 80% ethanol while the tubes were still on the rack. After the supernatant was removed, the beads were allowed to air dry for 5 min on the magnet to allow evaporation of excess ethanol. The tubes were removed from the magnets, and DNA was eluted with EB buffer (QIAgen, Hilden, Germany) The DNA samples were quantified after purification.

3.2.4 Genomic DNA isolation

0.5-1 mL cell suspensions were washed twice, first in 500 µL 0.85% saline followed by 500 µL TES (10 mM Tris, 30 mM EDTA, 150 mM NaCl in milliQ H2O). Afterwards, the pellet was resuspended in 250 µL T10E25 (25 mM Tris, 62.5 mM EDTA in milliQ H2O). 50 µL of 2 mg/mL lysozyme solution and 1 µL of 100 mg/mL RNase (QIAgen) were added, then incubated for 15 min at 37°C. 60 µL of sarcosyl-protease solution (19.5 mM Tris, 0.974 mM EDTA, 100

mg/mL sarcosyl, 5 g/mL protease K in milliQ H_2O) was added, followed by incubation for 16-18 h at 37°C. After incubation, the suspension was mixed with 361 µL P:C:I (50% buffer-saturated phenol, 48% chloroform, 2% isoamyl alcohol, Invtrogen), then gently inverted for 10 min until the mixture was homogenous. The suspension was transferred to a 1.5 mL phase-lock gel tube (Five Prime, San Francisco, CA) and centrifuged for 5 min at 13,000 rpm. Afterwards, the upper aqueous phase was transferred to a low DNA-binding microcentrifuge tube. To precipitate the DNA, 0.10 volumes of 10mM sodium acetate was added, followed by 0.54 volumes of isopropanol. The suspension was allowed to sit at room temperature for at least 30 min then centrifuged for 30 min in a table top centrifuge at 13,000 rpm at 4°C. After removal of the supernatant, 1 mL of ice-cold 70% ethanol was added. The suspension was centrifuged for 10 min at 13,000 rpm at 4°C. After removal of the ethanol, the DNA pellet was allowed to air dry for five minutes to allow evaporation of excess ethanol. The DNA was resuspended in TE (Tris, EDTA) buffer and stored at 4°C. More TE buffer was added as necessary until the DNA was fully solubilized. Agarose gel electrophoresis was carried out to assess the quality of the DNA before quantifying by Qubit.

3.2.5 Tn-seq Circle

The Tn-seq circle method (Gallagher et al., 2011c) was used to enrich for the transposon-genome junction from the genomic DNA of transposon mutant libraries for subsequent sequencing to identify the transposon insertion sites. The oligonucleotides used are listed in Table 3.2. 130 µL of approximately 38 ng/µL of genomic DNA was fragmented to an average size of 300 bp via ultrasonication using a Covaris S220 (duty factor of 10%, a peak incident power of 140, 200 cycles per burst, and a treatment time of 4 cycles at 20 sec each). The 130 µL aliquots of fragmented DNA were transferred to new low DNA-binding PCR tubes (Eppendorf) and end repaired using a

NEBNext End Repair kit (NEB). In each tube, 15.5 µL of 10x NEBNext buffer, 1.75 µL nuclease-free H_2O (Ambion, Austin, TX), and 7.75 µL enzyme were mixed for a total volume of 153 µL. The reaction mix was incubated for 30 min at 20°C in an Eppendorf Mastercycler ep gradient S thermal cycler. Afterwards, the end-repaired DNA samples were purified using 1:1.8 sample:AMPure XP beads, eluted in a final volume of 50 µL EB buffer (Qiagen) and quantified by Qubit.

A-tailing was carried out on the purified end-repaired DNA in 50 µL reaction mixtures composed of 25 µL end-repaired DNA, nuclease-free H_2O, 5 µL QIAgen 10x buffer, 10 µL (1 mM) dATP, and 0.2 µL of Taq (QIAgen). The reaction mixtures were incubated for 20 min at 72°C in the thermal cycler. Afterwards, the A-tailed DNA samples were purified using 1:1.8 sample:AMPure XP beads, eluted in 30 µL EB buffer and quantified by Qubit. Adapters were prepared by annealing the single stranded oligos 683 and 684 (Table 3.2). The annealing reaction consisted of 90 µL of each oligo at 100 µM in 10 mM Tris, 20 µL NaCl (100 mM), and 10 mM EDTA as follows: 2 min for 97°C, 72 cycles of 1 min at 97°C (-1°C per cycle), followed by 5 min at 25°C. The adapters were then stored at -20°C. Oligomers 683 and 684 were ligated to the purified A-tailed DNA using a Quick Ligation kit (NEB). The molar quantity of the DNA was first calculated to determine the appropriate volumes for the reaction mixture. Using approximately 3 µg of DNA, the ligation was carried out in 80 µL reactions composed of A-tailed DNA, 20x molar excess of adapter relative to the A-tailed DNA, 40 µL of 2x Quick Ligation Buffer, 0.3 µL nuclease-free H_2O, and 2.96 µL Quick Ligase. Reaction mixtures were incubated for exactly 15 min at room temperature. Adapters were removed by mixing the reaction mixture with an equal volume of AMPure XP beads (1:1). The DNA was quantified by Qubit. Size-selected DNA with ligated adaptors were then digested with PacI (NEB) in 50 µL reaction mixtures containing DNA,

nuclease-free H_2O, 5 µL Cutsmart buffer, and 1µL PacI for 16-18 h at 37°C. Size selection for 200-400 bp fragments was repeated, followed by DNA quantification.

Circularization of the digested DNA was carried out in 30 µL reaction mixtures in 0.2 mL thin-walled PCR tubes (Axygen) containing 1-4 pmol DNA, 10x molar excess of collector probe (682), 3 µL of 10x Ampligase buffer, 0.5 µL Ampligase, and nuclease-free H_2O. Two controls, no Ampligase and no probe were prepared simultaneously. The reaction mixtures were cycled as follows: 30 sec at 95°C, 25 cycles of 30 sec at 95°C and 3min at 67°C, followed by 3 min at 72°C, 2 min at 95°C, and holding at 4°C. Afterwards, 2 µL of exonuclease mixture composed of 0.50 µL Exonuclease I (NEB, 20 U/µL), 0.75 µL Lambda Exonuclease (NEB, 5 U/µL), and 0.75 µL T7 Gene 6 Exonuclease (USB, 50 U/µL (Cleveland, OH)) was added to the Ampligase reaction mixtures. The reaction mixtures were incubated for 16 h at 37°C followed by 20 min at 85°C in the thermal cycler. The DNA was then purified and quantified.

Prior to PCR amplification, the optimal number of cycles was first tested via real-time PCR using a Bio-Rad CFX Connect thermocycler (Mississauga, ON). The enrichment of the transposon-genome junctions was confirmed by comparing the amplification of the HDTM library with K56-2 wild type prepared simulateously via real-time PCR using a Bio-Rad CFX Connect thermocycler (Mississauga, ON). 10 µL reaction mixtures composed of template DNA, nuclease-free H_2O, 0.2 µM of each primer, 690 and 681 (Table 3.2), and 5 µL iTaq SYBRgreen Supermix (Bio-Rad) were cycled as follows: 3 min at 95°C, 35 cycles of 30 sec at 95°C, 30 sec at 63.5°C, and 30 sec at 72°C. For amplicons created using KAPA polymerase (Kapa Biosystems, Wilmington, MA), 10 µL reaction mixtures composed of template DNA, nuclease-free H2O, 0.2 µM of each primer, 690 and 681 (Table 3.2), 0.1 µL of SYBRgreen (Life technologies) 100x in DMSO, and 5 µL KAPA HiFi polymerase ready mix (Kapa Biosystems) were cycled as follows:

3 min at 95°C, 35 cycles of 20 sec at 95°C, 15 sec at 72°C, and 30 sec at 72°C. The optimal number of cycles was determined as at least 25% of maximum fluorescence, but still exponential amplification of the DNA. The optimal number of cycles was 20-25 cycles. The PCR was repeated using new reaction mixtures prepared as before. The reaction was carried out until the determined optimal number of cycles was reached. The PCR products were purified using 1:0.8 sample:AMPure XP beads, resuspended in EB buffer and quantified using a qubit. The removal of primers containing the MiSeq adapter sequences from the amplicons was verified by running the sample on a bioanalyzer. The purified samples were sequenced using the Illumina MiSeq standard kit v2 with 150 bp single reads at the Children's Hospital Research Institute of Manitoba (Winnipeg, Canada) following the manufacturer's instructions. The Illumina sequencing reads were deposited in the NCBI Sequence Read Archive (SRA) repository, accession number SRP112587, https://www.ncbi.nlm.nih.gov/sra/?term=SRP112587.

Table 3.2. Oligonucleotides used in this study

Name	Sequence (5' - 3')[a]	Purpose
683	CCGTAGTGAGTTCTTCGTCCGAGCCACTCGGAGATGTGTATAAGAGACAGT	Top strand adaptor (has 3' T overhang) for Tn-seq circle
684	CTGTCTCTTATACACATCTCCGAGTGGCTCGGACGAAGAACTCACTACGG	Bottom strand adaptor for Tn-seq circle
682	CACAAGTGCGGCCGCACTAGTCTAGATTTAAATTACCGTAGTGAGTTCTTCGTCCGAGCCAC	Oligo probe for Tn-seq circle
690	AATGATACGGCGACCACCGAGATCTACACTAGATCGCTCGTCGGCAGCGTCAGATGTGTATAAGAGACAGNNNNAATCTAGACTAGTGCGGCC	Illumina Index N501 Tn-seq circle forward primer
681	CAAGCAGAAGACGGCATACGAGATTCGCCTTAGTCTCGTGGGCTCGGAGATGTGTATAAGAGACAG	Nextera Index N701 Tn-seq circle reverse primer

[a]N is any nucleotide.

3.2.6 Data analysis to determine gene essentiality

Gene essentiality was determined using modified versions of the custom scripts developed by Turner *et al*. (Turner et al., 2015). From the *B. cenocepacia* K56-2 gene feature format (gff) file, the 10% from the 3' and 10% from 5' end was trimmed off of each feature using the Perl script, GFFTrim.pl, so that insertions that are not likely to disrupt function are not included in the analysis. TnSeq2.sh (https://github.com/khturner/Tn-seq/tree/master/TnSeq2.sh) was used to identify reads containing the transposon sequence, remove the transposon tag and then map the remaining genomic sequences of the reads to the 17 contigs of the K56-2 draft genome (Genbank accession LAUA00000000) using Bowtie2 (Langmead and Salzberg, 2012). To avoid considering insertion sites that are over represented due to amplification bias, reads were discarded from the 100 most abundant insertion sites. To account for mutant abundances associated with position-dependent insertion bias, PCR and sequencing bias, we normalized the read data across the position of each contig, then based on GC content of the region of insertion using the "lm" function in R. The gff file containing the truncated gene features for *B. cenocepacia* K56-2 was then used to calculate the normalized number of reads per truncated gene as well as the number of insertion sites per gene. A Monte Carlo simulation then was run where insertion sites were moved randomly across the genome to generate an "expected" pseudodata set. This simulation was repeated 2000 times. The Monte Carlo simulations provided an estimate of the variance that would be expected if there were no essential genes. Since it is possible to have a gene with no insertions when comparing the real and pseudo data sets, to avoid dividing by zero, one was added to the read count for each gene.

The R package EdgeR (Robinson et al., 2010) was used to compare the variance of the pseudo data set with the mean read count per gene of the real data. To determine the differences of mutant abundance between the real and pseudo data sets, EdgeR uses a negative binomial test. Since multiple comparisons increase the rate of identifying false positives (Noble, 2009), to control the false discovery rate (FDR), the Benjamini-Hochberg method was used, which computes an upper bound for the expected FDR and adjusts the *p* value accordingly to correct for multiple testing (Benjamini and Hochberg, 1995). The R mclust package (Fraley and Raftery, 1999, 2002) was used to perform bimodal clustering of genes to either a "reduced" or "unchanged" mode, by fitting a parameterized bimodal Gaussian mixture model to the log2-transformed fold change mutant abundance. A gene was classified as essential if it was significantly depleted in the real data compared to the pseudo data ($p < 0.05$, negative binomial test), and clustered in the "reduced" mode ($p < 0.05$, maximum likelihood estimation).

3.2.7 Bioinformatics

The protein sequences from the 508 predicted essential genes of *B. cenocepacia* K56-2 were searched against all the bacterial essential genes in the database of essential genes (DEG 10, version 14.7, updated Oct. 24, 2016) (Luo et al., 2014a) using BLASTP with the default parameters provided in DEG and an E-value cutoff of 10^{-10}. *B. cenocepacia* K56-2 homologs in *B. cenocepacia* J2315, (Wong et al., 2016a) *B. thailandensis* E264 (Baugh et al., 2013), and *B. pseudomallei* K96243 (Moule et al., 2014a) were identified as the best hit from performing BLASTP using Geneious software with an E-value cutoff of 10^{-10}, minimum 30% sequence identity and 45% coverage. Operon predictions and clusters of orthologous category (COG) (Tatusov et al., 2000) were assigned to genes of *B. cenocepacia* K56-2 from the corresponding

homologous gene in *B. cenocepacia* J2315 listed in the Database of Prokaryotic Operons (Mao et al., 2014b).

3.3 Results

3.3.1 Production and sequencing of the HDTM library

With the goal of identifying the essential genome of *B. cenocepacia* K56-2, we used high density transposon mutagenesis (HDTM) followed by Illumina sequencing of the transposon insertion sites. We first introduced the suicide plasmid pRBrhaBoutgfp into *B. cenocepacia* K56-2 by triparental mating and generated a HDTM library of 1 million mutants. The transposon mutants were selected in the presence of rhamnose to allow the growth of mutants where the rhamnose-inducible promoter is controlling the expression of an essential gene. In this way, insertions in non-essential genes that may be lethal due to polar effects on downstream essential genes are avoided. To enrich for the transposon-genome junctions and identify the location of the insertion sites, we used the Tn-seq circle method (Gallagher et al., 2011c) (Figure 3.1).

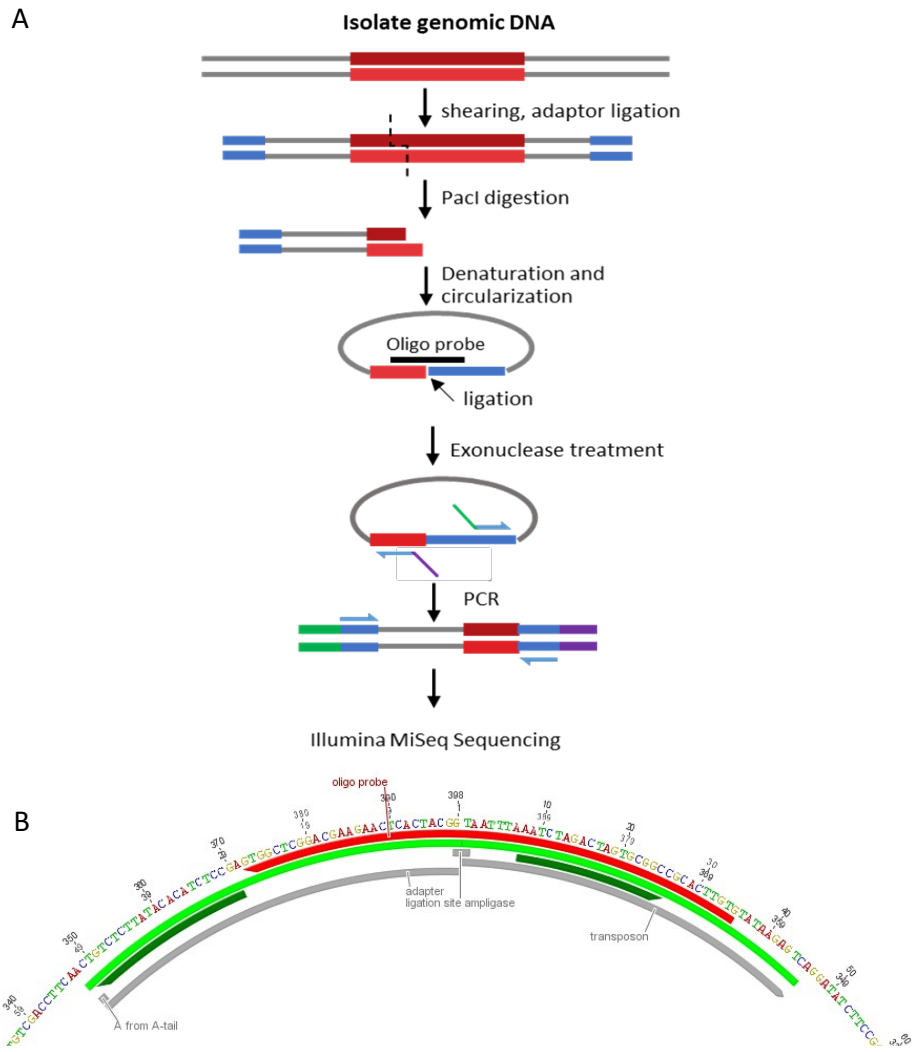

Figure 3.1 Enrichment of transposon-genome junctions with Tn-seq circle.
A. Outline of the steps in Tn-seq circle modified from Gallagher et al. (Gallagher et al., 2011a). Adapters were ligated to genomic DNA that was sheared to an average size of 300 bp. Following PacI digestion, the DNA was denatured and annealed to an oligo probe. Only fragments containing the transposon and adapter sequences are circularized using the oligo probe. Exonuclease treatment degrades all linear DNA fragments, leaving behind fragments with the transposon-genome junction to be amplified by PCR prior to sequencing with Illumina MiSeq. Reproduced with modification from MBio. 2011 Jan 18;2(1):e00315-10. Gallagher LA, Shendure J, Manoil C. Genome-scale identification of resistance functions in Pseudomonas aeruginosa using Tn-seq. Copyright © 2011 Gallagher et al. Creative Commons Attribution-Noncommercial-Share Alike 3.0 Unported License. B. Example of circularization of a transposon mutant. Non-genomic sequences (transposon and adapter, (annealed 683 and 684, Table 3.2) are indicated by the light green bar; transposon sequence, adapter sequence, and ligation site are indicated; oligo probe binding site, 682 (Table 2), red bar; primer binding sites, 690 and 681 (Table 3.2), dark green bars.

As *Burkholderia* species have large multireplicon genomes with 67% GC content (Mahenthiralingam and Vandamme, 2005), we first considered using a Hi-fidelity KAPA polymerase (KAPA bioscience) to PCR amplify the transposon insertions. The KAPA polymerase has been successfully used to increase the proportion of reads from transposon junctions in GC rich regions in *B. thailandensis* (Gallagher et al., 2013) and has minimal amplification bias (Quail et al., 2011). However, an analysis of the Tn5 transposon sequence used revealed a low GC content (Figure 3.2). The lower GC content of the transposon sequence may imply that PCR amplification of the transposon junctions may not be favored by the KAPA DNA polymerase. To test the ability of the KAPA DNA polymerase to PCR amplify the transposon junctions, the sequences of the 1M HDTM library performed after PCR amplification with the KAPA DNA polymerase were compared with those obtained with the iTaq DNA polymerases, which is not indicated for amplification of high CG content regions. Sequencing the 1M HDTM library after PCR-amplification with the KAPA polymerase resulted in 89,983 unique insertion sites with an average of 1 insert every 87 bases and a read GC content of 61% (Table 3). Instead, PCR amplification with the iTaq DNA polymerase revealed 293,569 unique insertion sites, with an average of 1 insert every 27 bases and a read GC content of 59.7% (Table 3). While the reads in the 1M HDTM KAPA library had less A/T bias than in the 1M HDTM Taq library, it had a lower proportion of insertion sites mapping to GC rich regions compared to the 1M HDTM Taq library (Figure 3.3). In addition, the total reads from PCR amplification of the 1M HDTM library with the iTaq DNA polymerase were more evenly distributed over the insertion sites, whereas the 1M HDTM KAPA library had many insertions with low numbers of reads and a large proportion of reads mapping to a small number of insertion site (Figure 3.4). Since the 1M HDTM Taq library had the most insertions sites and even distribution of reads per site, it was used for the essential gene analysis.

Table 3.3 Summary of results from sequencing the HDTM library

HDTM library preparation	Total reads	No. of reads containing the transposon sequence and mapping to the genome	GC content of reads	No. of unique insertion sites	Frequency of Tn insertion
KAPA	20,459,975	4,370,457 (21%)	61.0%	89,983	1/87 bp
iTaq	15,132,067	6,936,891 (46%)	59.7%	293,568	1/27 bp

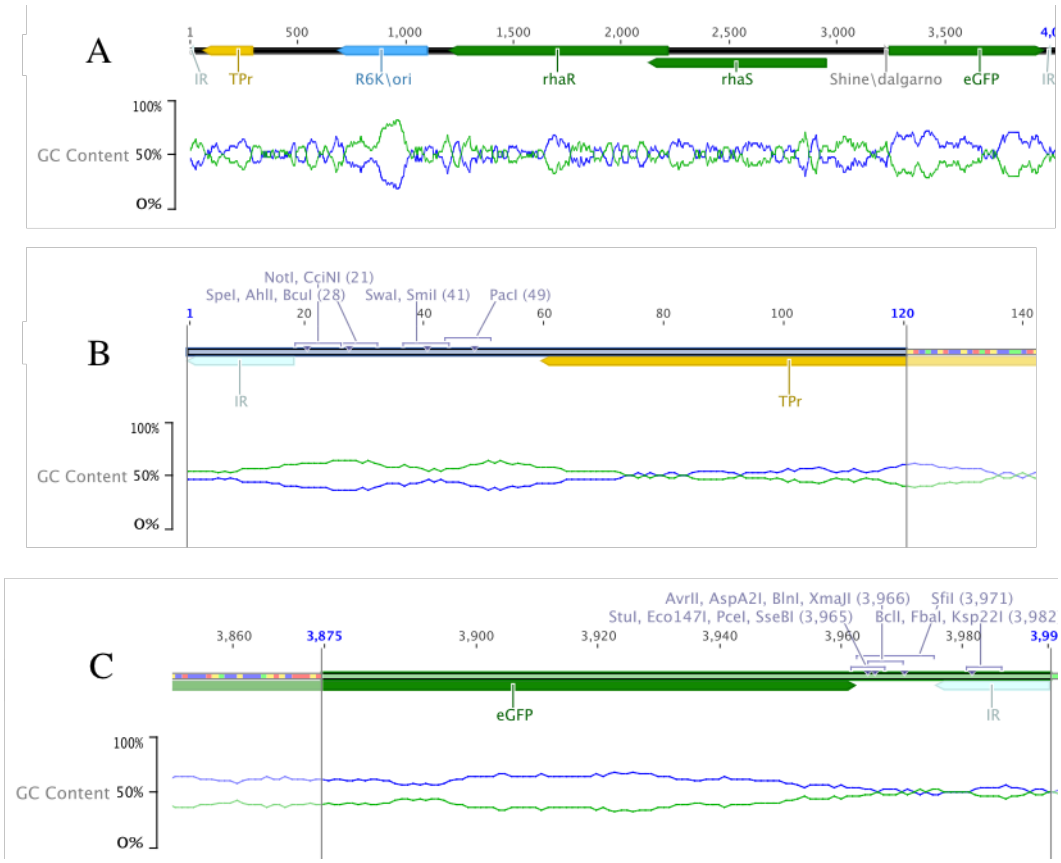

Figure 3.2 The GC content of the transposon insertion sequence is low

A) The sequence of the transposon inserted into the genome, containing 51.3% GC content overall. B) The 5' end of the transposon insertion sequence containing the pacI site. C) The 3' end of the transposon insertion sequence containing the eGFP coding sequence located just downstream of P*rhaB*. GC(blue)/AT(green) content is indicated below each sequence. Sites of commercially available restriction enzymes that cut once within the insertion sequence are indicated.

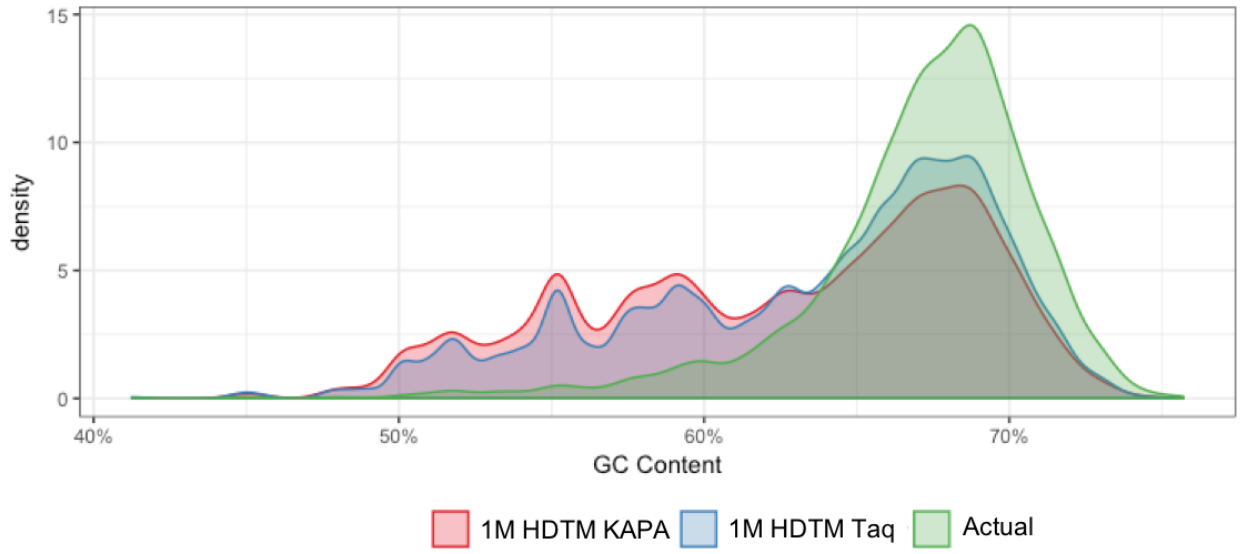

Figure 3.3 Distribution of insertion sites in the genome by GC content

A higher proportion of insertion sites in GC-rich regions were identified in the 1M HDTM Taq library, compared to the 1M HDTM KAPA library. Density of insertions sites (Y-axis) in the genome by GC content (number of insertion sites within a sliding window of 1 KB) scaled to a maximum value of 15; X-axis, GC content. Insertion site density of 1M HDTM KAPA library (pink) 1M HDTM Taq library (blue), actual GC content of the genome (green).

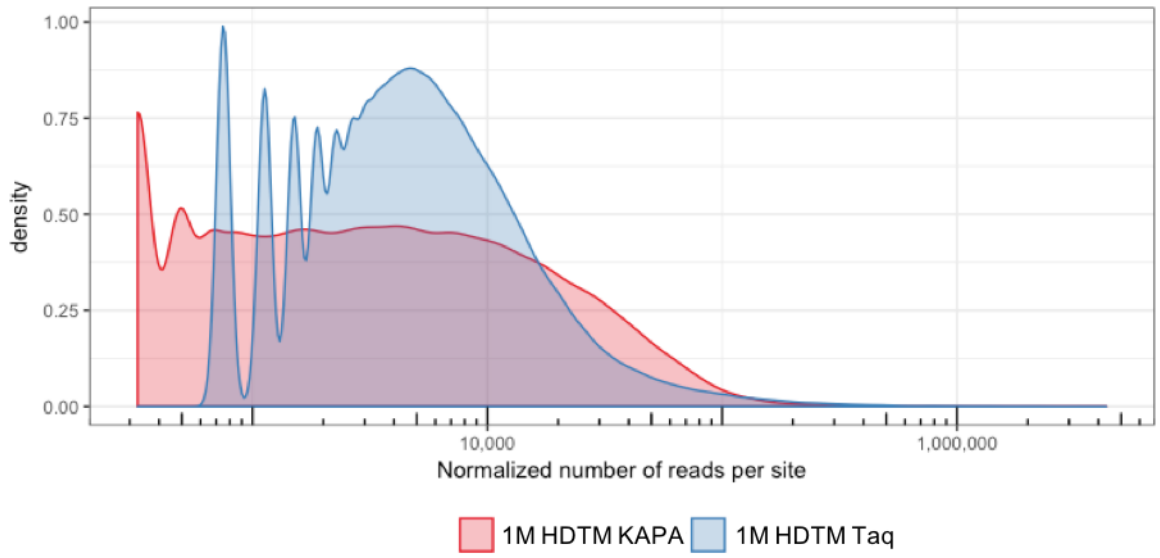

Figure 3.4. Distribution of reads per insertion site
The frequency of reads per insertion site is shown for the HDTM libraries. The 1M HDTM KAPA library has a more skewed distribution of reads per site than the 1M HDTM Taq library. 1M HDTM KAPA, pink; 1M HDTM Taq, blue; Y-axis, density of insertions sites scaled to a maximum value of 1; X-axis, normalized number of reads per insertion site ($1x10^4$ x number of reads per insertion site divided by the mean number of total reads).

3.3.2 Analysis of possible biases in insertion site identification

The first step in Tn-seq data analysis is to map the reads against the genome of the microorganism under investigation (Figure 3.5). As a complete genome of *B. cenocepacia* K56-2 is not available, we sequenced the *B. cenocepacia* K56-2 genome using PacBio and assembled it *de novo* into 17 contigs. We then mapped the Tn-seq reads against the 17 contigs and removed the 100 highest-read sites. After removing these reads, it was evident that there were positional effects on the insertion density and read counts (Figure 3.6). One possibility was that these highly-represented regions marked the proximity to the origin of replication for each of the chromosomes. Due to the merodiploid state created at the beginning of chromosome replication (Lemon and Grossman, 1998), reads mapping to loci closer to the origin of replication typically have a greater number of insertions. Reads corresponding to these insertion sites can be normalized by nucleotide position in a closed genome using LOESS to prevent interference in gene essentiality analysis (Gallagher et al., 2011a; Turner et al., 2015; Zomer et al., 2012). To identify if the insertion bias corresponded to the putative origins of replication for the replicons of the *B. cenocepacia* K56-2 genome, the contigs were aligned to the closed genome of *B. cenocepacia* J2315, using a progressive Mauve algorithm (Darling et al., 2010). The GC skew (Grigoriev, 1998) for each assembled replicon of *B. cenocepacia* K56-2 suggests that the ordering of contigs is correct, since the leading strand is richer in guanine than the lagging strand in the three chromosomes (Figure 3.7). Based on the origins of replication identified for each replicon in *B. cenocepacia* J2315 (Du et al., 2016) combined with the analysis of the GC skew of the *B. cenocepacia* K56-2 replicons, the origins of replication of *B. cenocepacia* K56-2 replicons were predicted and then compared with the regions with insertion/read count bias. We observed that the regions with high read counts

did not correspond to regions close to the origins of replication and were located intermittently throughout each chromosome (Figure 3.7). The regions with high coverage were not a bias of the Tn-seq circle transposon enrichment as sequencing the whole genome of *B. cenocepacia* K56-2 on the Illumina MiSeq platform reproduced the same trend (Figure 3.7). These regions corresponded to zones of unusually high coverage previously observed during the *B. cenocepacia* K56-2 *de novo* assembly of the PacBio reads (Bloodworth, 2013), likely caused by inappropriately collapsed repeats. Further analysis showed that 17 of the 20 remaining insertion sites with high read counts are in regions predicted to be genomic islands by Islandviewer3 (Dhillon et al., 2015) (Figure 3.7). Moreover, the reads were not evenly scaled across the contigs and the variations in insertion density were strongly correlated with the GC content (Figure 3.7). To account for these biases, we created a model of read depth as a function of the position along each contig and GC content. We then corrected the read count based on the model prediction to normalize the reads by contig and GC content, prior to the essentiality analysis, which minimized the effects of position and GC content on read density (Figure 3.8).

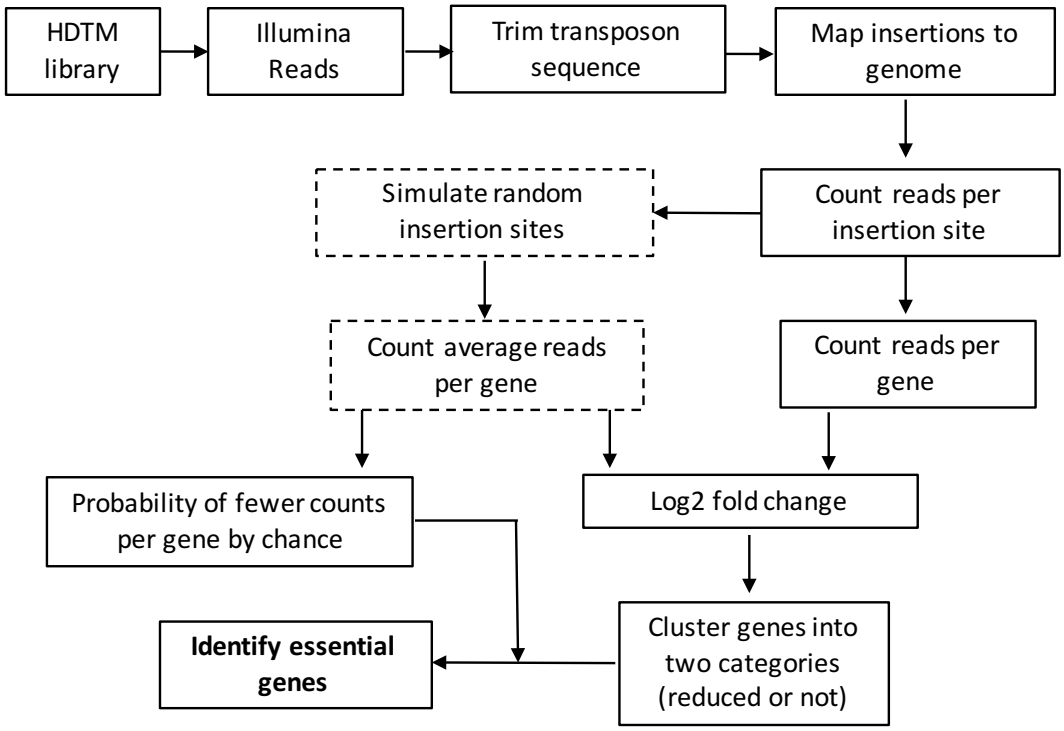

Figure 3.5. Bioinformatics pipeline to identify essential genes under control of the rhamnose inducible promoter (P*rhaB*) in the conditional growth mutant library.
For the HDTM libraries, reads not containing a transposon sequence are discarded and the sequence is trimmed from the remaining reads. The trimmed reads are mapped against the reference genome using bowtie2 (Langmead et al., 2009) and the position of each insertion and the number of reads mapping to it are collected. To identify essential genes using the HDTM library, the read counts are normalized to remove noise and position dependent differences. Then, simulations are run randomly moving the insertions throughout the genome as if there were no essential genes. For the experimental data and each simulated run, the number of insertion reads per annotated gene is collected, where insertions into the first 20% of the 5' end and last 10% of the 3' end of a gene are not considered disruptive. The log2 fold-change (experimental/mean simulated reads per gene) is calculated, as well as the probability of seeing fewer than the experimentally observed number of reads solely by chance.

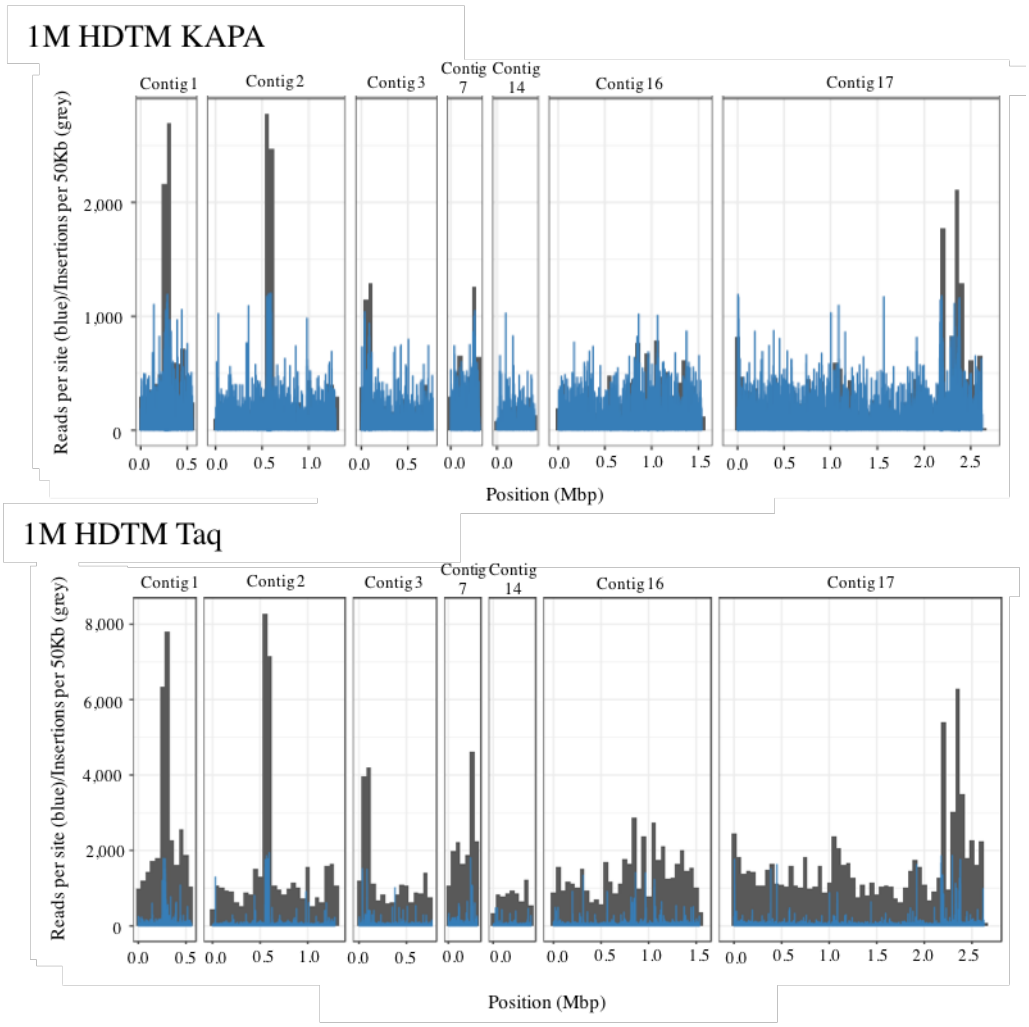

Figure 3.6. Positional effects of insertion site density and reads per insertion.

The number of insertion sites (grey bars) mapping to the 7 largest contigs in a sliding window of 50Kb is indicated after the removal of the 100 insertion sites with the highest read counts (Y-axis). The read count per insertion site for each library is overlaid (y-axis, blue bars). X-axis, basepair position in each contig, 1M HDTM KAPA library (top), 1M HDTM Taq library (bottom).

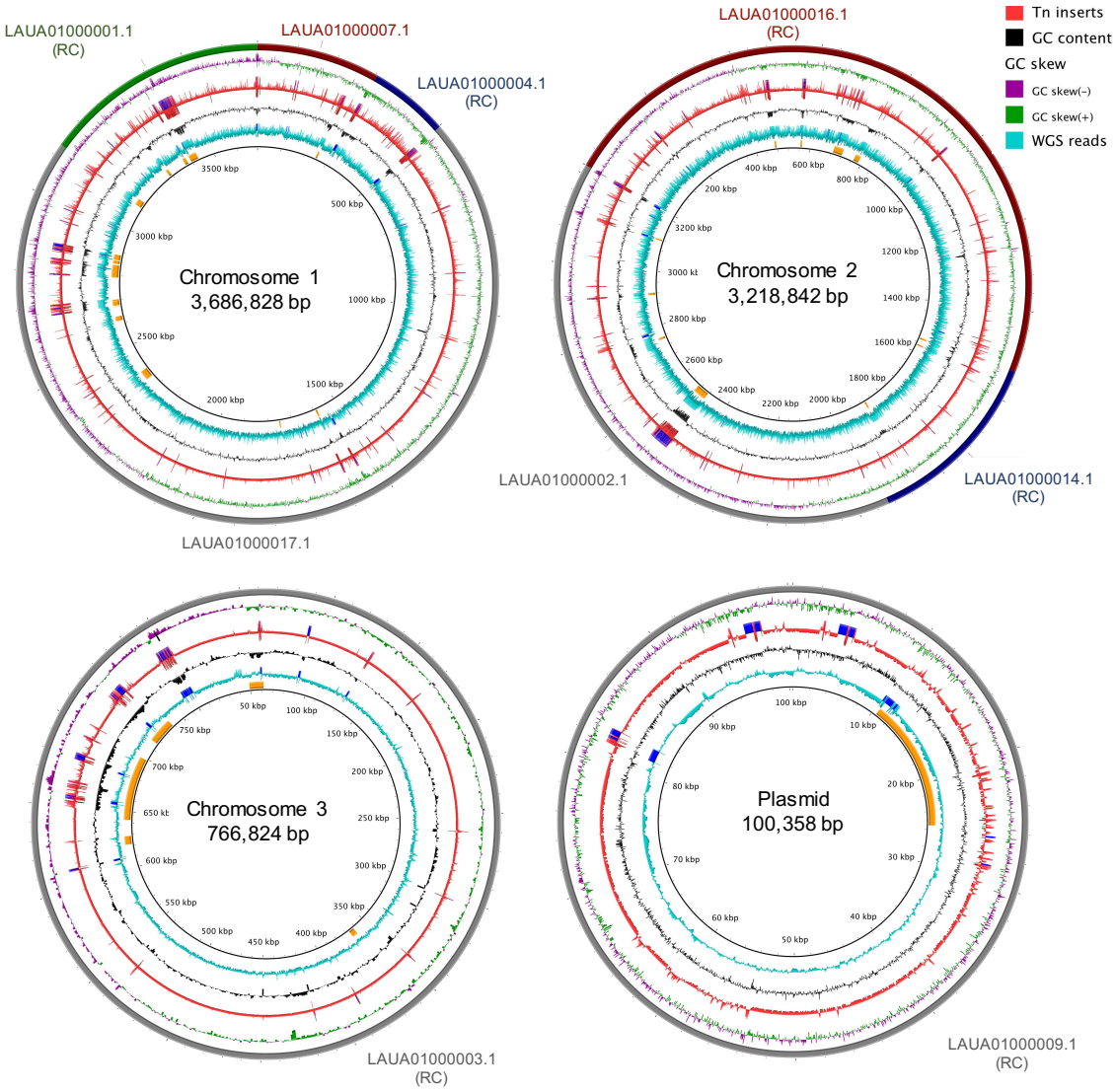

Figure 3.7 Diagram of the 1M HDTM Taq library reads mapped to the *B. cenocepacia* K56-2 genome.

From the outer most ring inwards: Ring 1: Contigs from the *B. cenocepacia* K56-2 assembly aligned to *B. cenocepacia* J2315 replicons using progressiveMauve, RC: Reverse complemented. (Darling et al., 2010). Ring 2: GC skew, positive (green), negative (purple). Ring 3: Alignment of reads from sequencing the 1M HDTM Taq library (Tn inserts, red). Ring 4: GC content (black). Ring 5: Alignment of reads from the whole genome sequencing of K56-2 prepared with the Nextera XT kit (WGS reads, turquoise). Rings 3 and 5: Genome regions with read coverage more than one standard deviation from the mean read coverage are indicated by blue regions. The innermost ring is the bp maker, with the genomic islands indicated by yellow arcs. Replicons are not to scale. Figure created using BLAST Ring Image Generator (BRIG 0.95) (Alikhan, Petty, Ben Zakour, & Beatson, 2011).

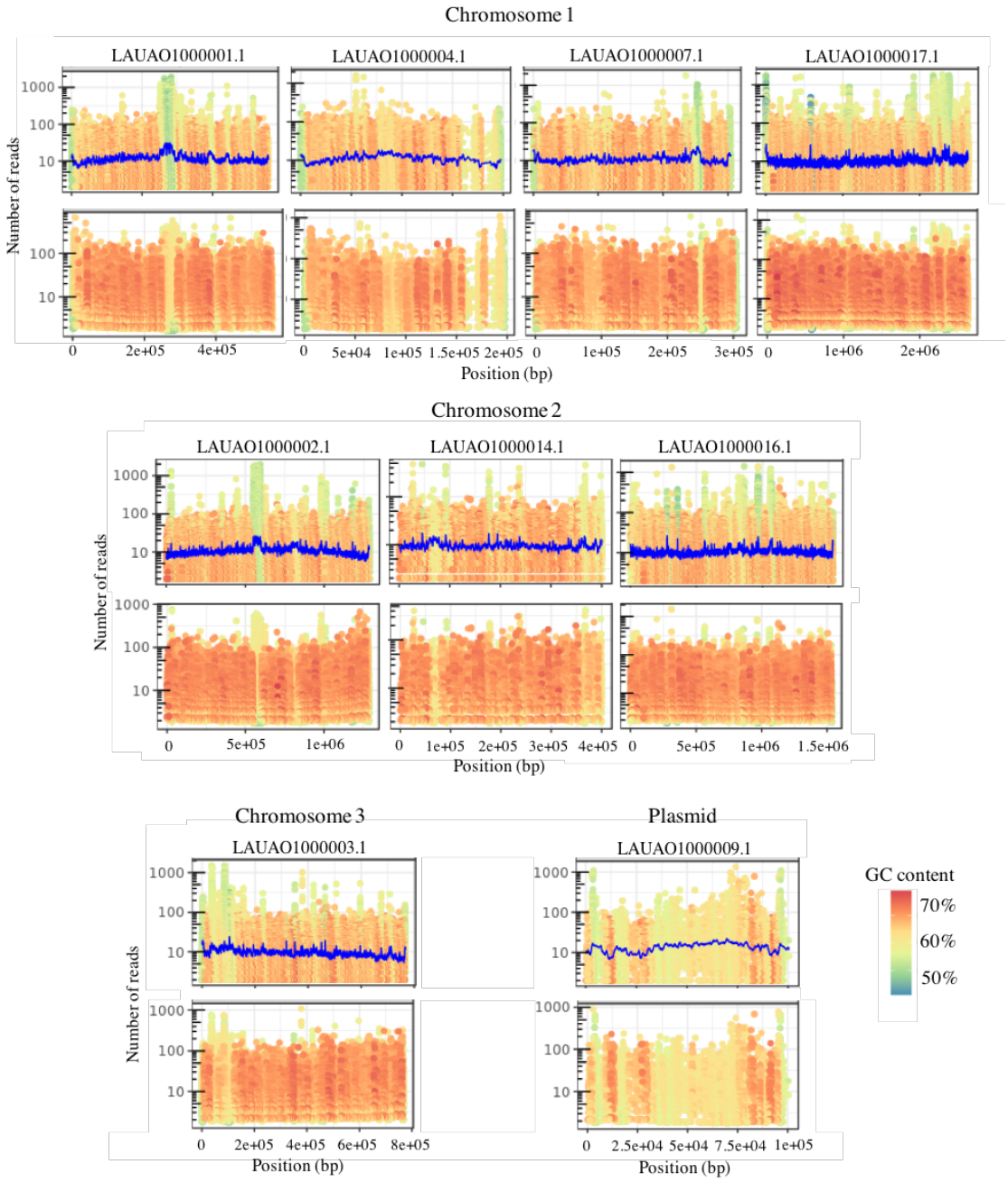

Figure 3.8 Normalization of read counts from the 1M HDTM Taq library
Read counts mapping to each contig, arranged by replicon, and colour coded based on GC content (legend). Y-axis, number of reads, X-axis, base position in contig (bp). Top panels: Observed read counts for the contigs from each chromosome. The blue line represents the number of reads predicted from the model (read depth as a function of GC content and position along each contig). Bottom panels: Normalized read count after correction using the model prediction.

3.3.3 Essential gene identification

After normalizing the reads by contig and GC content, pseudocounts were generated by 2000 simulations of randomly rearranging the read counts for each insertion site around the genome (Figure 3.5). We then compared the mean read count from the actual data to the variance of the pseudocounts using the R package, EdgeR (Robinson et al., 2010). Essential genes were identified based on whether the mean read counts for a gene were statistically different than would be expected if the gene were not essential. Using this analysis, we identified 508 essential genes in *B. cenocepacia* K56-2. Included in our predicted essential gene set are genes that have been previously experimentally identified as essential in *B. cenocepacia*, where mutation causes a lethal phenotype: *dxs* (BCAM0911), *hemE* (BCAL0040), *infB* (BCAL1507), *gyrB* (BCAL0421), *ubiB* (BCAL0876), *valS* (BCAL1448), BCAL3369, and *murJ* (BCAL2764) (Cardona et al., 2006b; Juhas et al., 2012b; Mohamed and Valvano, 2014; Ortega et al., 2007a). In addition, we identified essential genes previously characterized by our laboratory. These genes encode EtfAB, an essential electron transfer flavoprotein (Bloodworth et al., 2015) and EsaR, an essential response regulator involved in cell envelope integrity (Gislason et al., 2016).

To identify which functional categories are represented in the essential genome of *B. cenocepacia* K56-2 we classified the essential and non-essential genes according to the cluster of orthologous group (COG) categories (Tatusov et al., 2000) previously identified for the K56-2 homologs in J2315, listed in the Database of prOkaryotic OpeRons (DOOR) (Mao et al., 2014b). The enrichment of functions encoded by the predicted essential gene set for *B. cenocepacia* K56-2 with respect to non-essential genes in the genome was assessed and then compared with conserved essential functions that have been identified in other bacteria. The essential gene set of

B. cenocepacia K56-2 was enriched for genes involved in cell division, cell wall functions, protein synthesis, replication, and coenzyme metabolism (Figure 3.9). Genes related to translation/ribosomal structure/biogenesis were the most highly enriched category in *B. cenocepacia* K56-2 (Figure 3.9). The enrichment pattern observed was similar to that of *E. coli* (Baba et al., 2006) with the exceptions of three categories i) energy production and conversion, ii) replication, recombination and repair, and iii) cell motility (Figure 3.10), possibly due to species-specific differences. In contrast to *E. coli*, both the predicted essential gene sets of K56-2 and J2315, are significantly over-represented in genes involved in replication, recombination and repair and under-represented in genes involved in cell motility (Figure 3.10 and Figure 3.11, left panel).

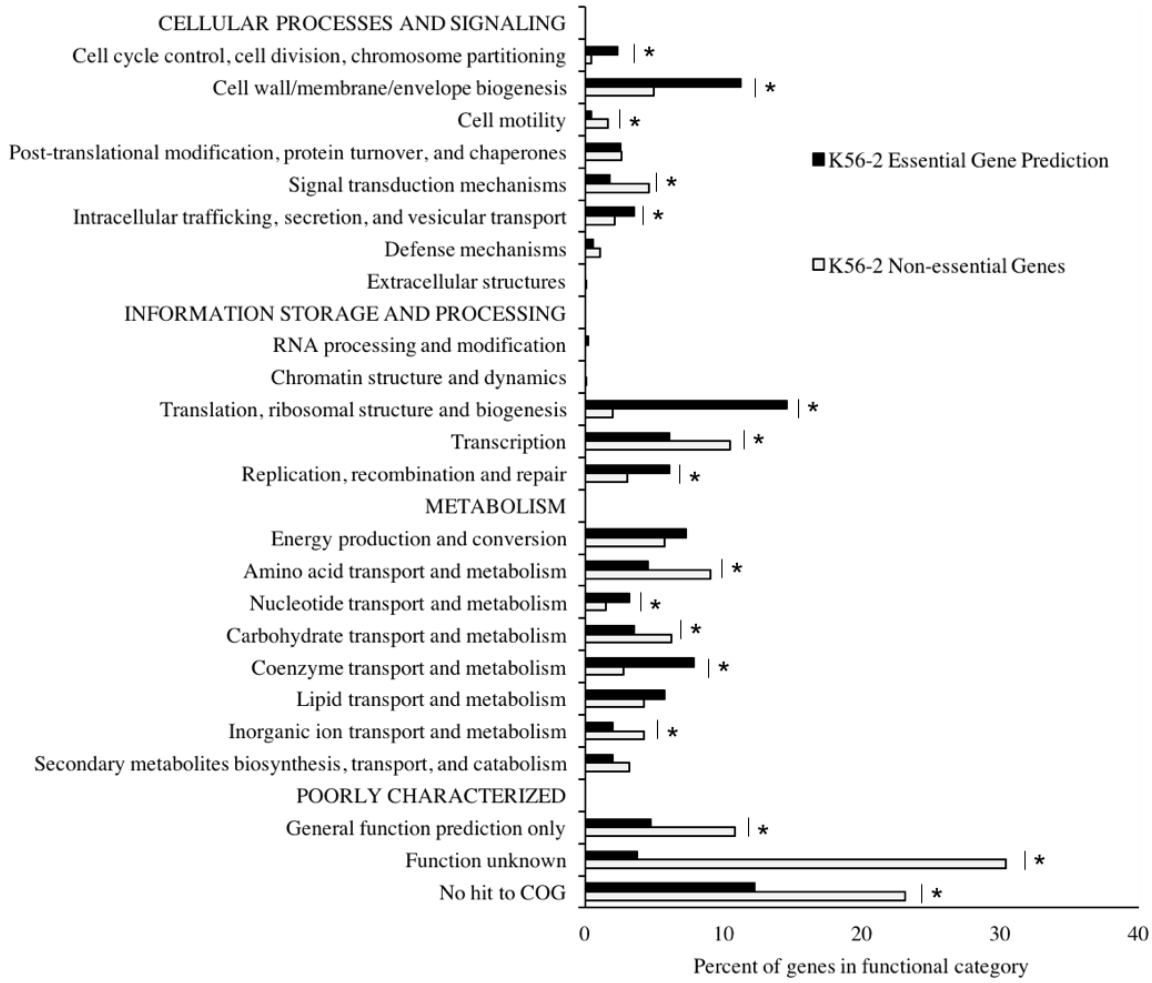

Figure 3.9 Functional categories of the predicted essential and non-essential genes of *B. cenocepacia* K56-2

Functional categories are based on the clusters of orthologous groups (COG) (Tatusov, Galperin, Natale, & Koonin, 2000), which were assigned to genes of *B. cenocepacia* K56-2 from the corresponding homologous gene in *B. cenocepacia* J2315. Functional categories significantly enriched or underrepresented in the essential gene seta re indicated with an asterisk (p-value <0.05, Fisher exact test).

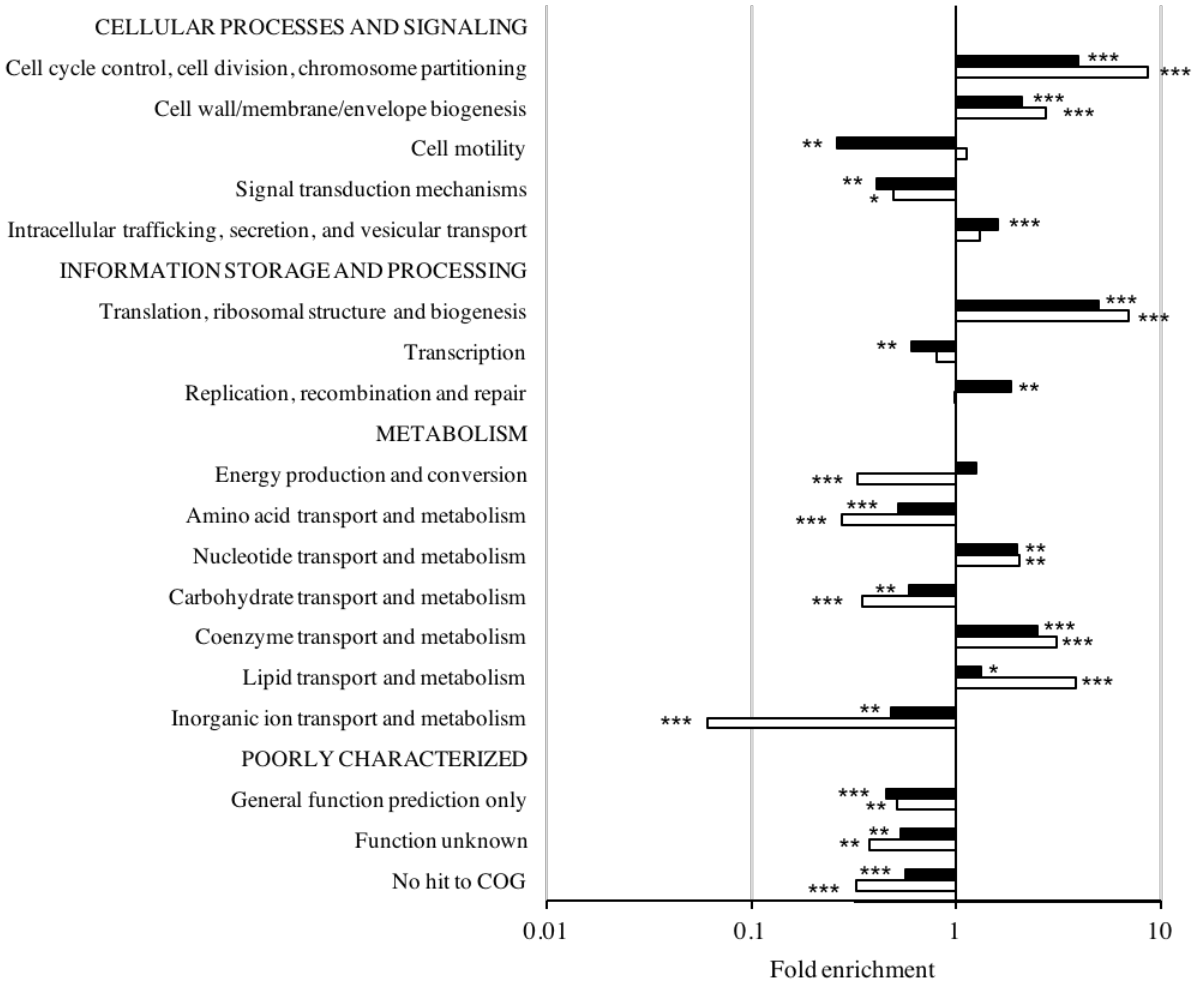

Figure 3.10 Comparison of the functional categories (COGs) enriched or under-represented in the essential gene sets of *B. cenocepacia* K56-2 and *E. coli* (Baba et al., 2006).
Enrichment and depletion of essential genes in COG categories compared to the representation of each genome were determined by Fisher's exact test, *, p-value <0.1 **, p-value <0.05 ***, p-value <0.001. *B. cenocepacia* K56-2 (black bars) and *E. coli* (white bars).

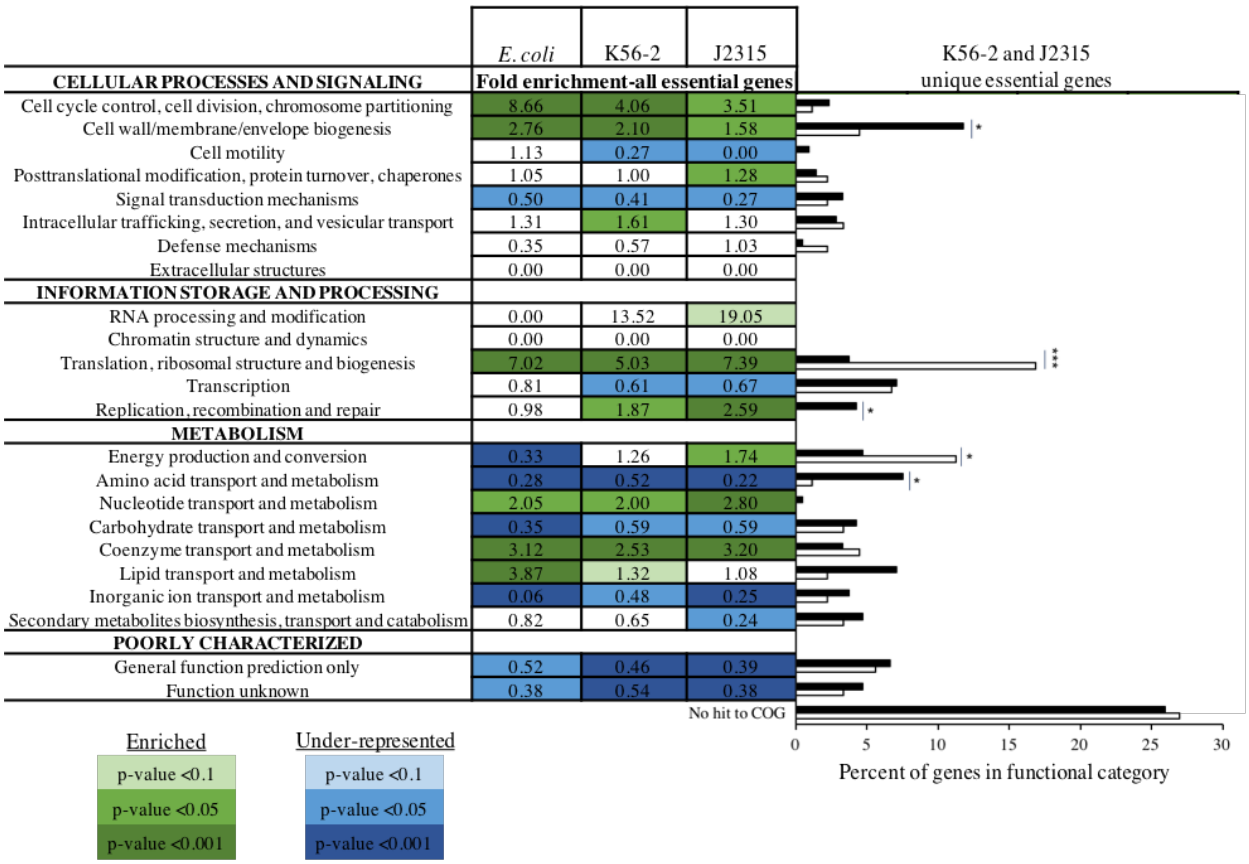

Figure 3.11 Comparison of the functional categories (COGs) enriched or under-represented in the essential gene sets of *B. cenocepacia* K56-2, *B. cenocepacia* J2315 and *E. coli* (Baba et al., 2006).

Left panel: Fold enrichment of COG functional categories for the *B. cenocepacia* K56-2, *B. cenocepacia* J2315 and *E. coli* essential genes compared to the all genes in each respective genome (Fisher's exact test). Functional categories enriched (green) or under-represented (blue) in the essential gene sets are colour coded coded by p-value (legend). Right panel: Percent of uniquely essential genes in *B. cenocepacia* K56-2 (black bars) and *B. cenocepacia* J2315 (white bars) in each COG category. Functional categories significantly different between the two unique essential gene sets are indicated (Fisher's exact test). *, p-value <0.05; ***, p-value<0.001.

3.3.4 Comparison of the essential genomes of *B. cenocepacia* K56-2 and J2315

As a recent study reported the candidate essential genome of *B. cenocepacia* J2315 (Wong et al., 2016a), we predicted that the identified gene set for K56-2 in our study would overlap substantially with the one reported by Wong et al., given that K56-2 and J2315 belong to the same ET12 epidemic lineage. The candidate essential gene set of J2315 consists of 383 genes (Wong et al., 2016b). Two hundred and ninety-six of the 508 *B. cenocepacia* K56-2 genes predicted to be essential have homologs with 294 candidate essential genes in *B. cenocepacia* J2315 (Wong et al., 2016a) (Figure 3.12). While the number of essential genes predicted for K56-2 is in line with that published for *B. pseudomallei*, the essential genome of *B. cenocepacia* K56-2 includes more than 200 genes than the candidate essential gene set of *B. cenocepacia* J2315. In *B. cenocepacia* K56-2, 491 of the predicted essential genes correspond to 358 predicted essential operons, 204 of which were also identified as essential in J2315 (Wong et al., 2016a). Eighty-nine and 212 genes were uniquely essential to J2315 and K56-2, respectively. This finding was surprising as *B. cenocepacia* K56-2 and J2315 belong to the same epidemic ET12 lineage. We then examined the essential genes unique to each strain. We first compared the functional categories (COGs) represented by each unique set of essential genes. Although essential genes in energy production and conversion are more significantly enriched in J2315 (1.74-fold, p-value<0.05), it is consistent with K56-2 essential genes (1.26-fold, p-value 0.103). The majority of the genes in functional categories were not significantly different (p-value >0.05, Fisher's exact test) between the two clones (Figure 3.11, right panel).

However, some functional categories were differentially enriched between the two unique essential gene sets. The 212 genes unique to K56-2 were significantly over-represented (p-value

<0.05) in the cell wall/membrane/envelope biogenesis, replication/recombination/repair, and amino acid transport/metabolism categories while the essential genes unique to J2315 were significantly enriched in translation/ribosomal structure/biogenesis and energy production /conversion categories (p-value <0.001) (Figure 3.11, right panel). Since our essentiality analysis used the read count per gene, which reflects the abundance of transposon mutants in the library, the genes identified as essential in K56-2, but not J2315, may represent genes that are not absolutely essential, but important for growth. To determine if the 212 essential genes identified as uniquely in K56-2 could result in a growth defect if disrupted, we compared these essential genes with the candidate essential gene sets Wong *et al*. identified after passage of a J2315 transposon mutant library through LB or M9 (Wong et al., 2016a). From this analysis, we identified 37 homologs in J2315 that are essential for growth in LB and 50 that are essential for growth in M9, indicating that in addition to finding essential genes, we could be identifying genes that elicit a growth defect when disrupted. However, 9 and 22 of the J2315 genes required for growth in M9 and LB, respectively, have homologs that were identified as essential in *B. pseudomallei* or *B. thailandensis* as well, and my truly be essential in K56-2. Overall, for the genes identified as essential in K56-2, but not J2315, 55 have homologs identified as essential homologs in either *B. pseudomallei* or *B. thailandensis*. Of the 157 K56-2 essential genes that did not have essential homologs in *B. cenocepacia* J2315, *B. thailandensis* E264 or *B. pseudomallei* K96243, 70 have homologs in the Database of Essential Genes (DEG) and 47 are annotated as hypothetical proteins that could represent essential genes specific to *B. cenocepacia* K56-2.

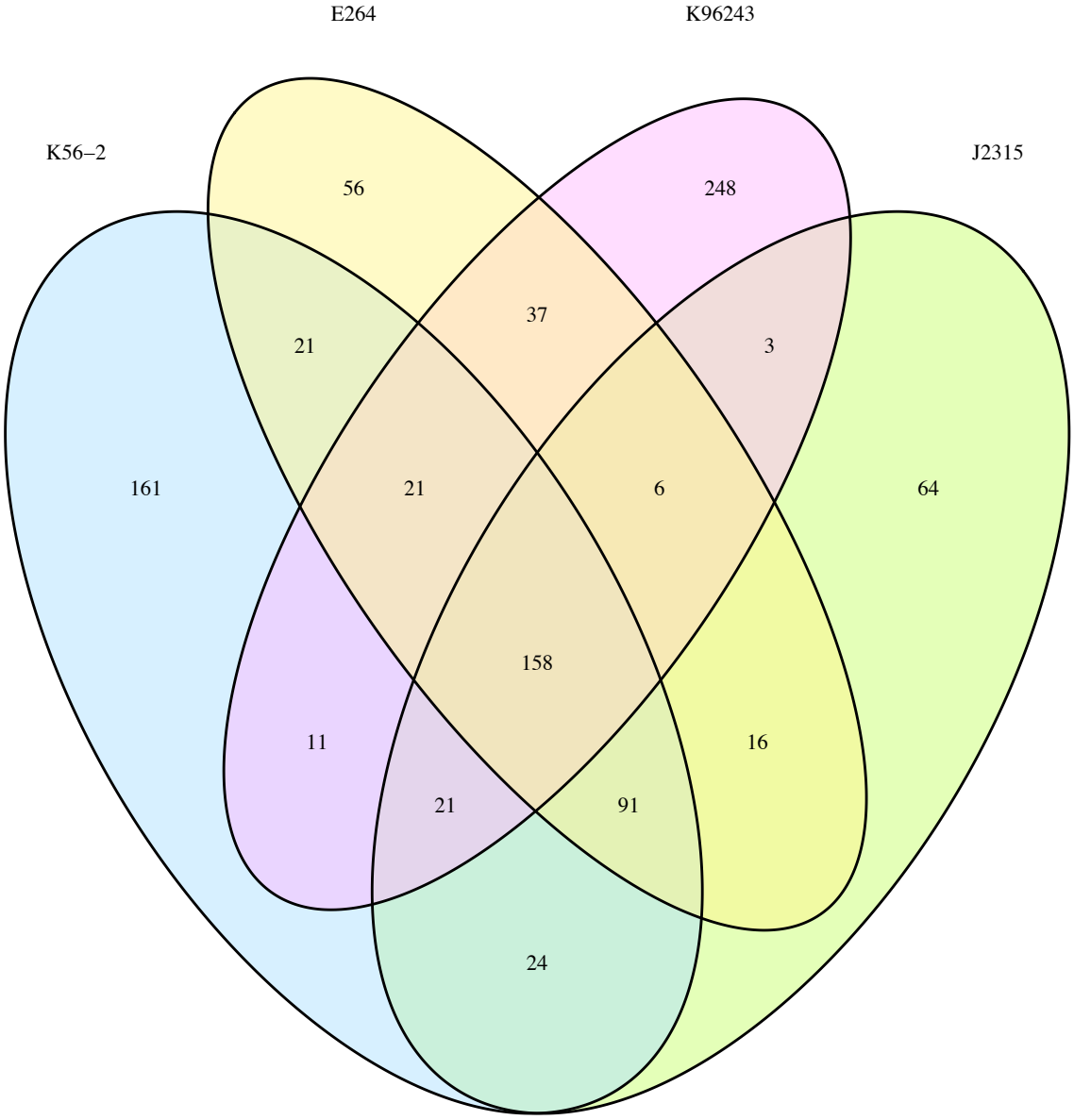

Figure 3.12 Comparison of the essential genes identified in *B. cenocepacia* K56-2, *B. cenocepacia* J2315, *B. thailandensis* E264 and *B. pseudomallei* K96243

The common and unique essential genes between *B. cenocepacia* K56-2, *B. cenocepacia* J2315 (Wong et al., 2016a), *B. thailandensis* E264 (Baugh et al., 2013) and *B. pseudomallei* K96243 (Moule et al., 2014a). Homologs were identified as the best hit from performing BLASTp using Geneious software with an E-value cutoff of 10^{-10}, minimum 30% sequence identity and 45% coverage.

Of the 89 genes that are uniquely essential in J2315, 59 do not have essential homologs in either *B. thailandensis* or *B. pseudomallei,* 38 of which do not have homologs in the DEG and 8 do not have homologs in K56-2. For the remaining 81 J2315-specific essential genes that have homologs identified as non-essential in K56-2, we confirmed that 49 contain high numbers of reads corresponding to multiple insertions throughout the gene and do not appear be essential in K56-2 (See BCAL0301-BCAL0303, Figure 3.13A). However, 14 genes had significantly less reads (EdgeR P-value <0.05, negative binomial test) that could not be classified as essential with a high level of certainty (P-value >0.05, maximum likelihood estimation) and could be important for growth or essential in K56-2, as in J2315. From the remaining 32 genes, although reads mapped to insertions within the internal 10-90% of a gene, 10 have the rhamnose inducible promoter oriented to express the gene downstream of the insertion (See BCAL3163, Figure 3.13B) and one gene had a similar insertion pattern, but also had an insertion where P*rha* is oriented in the opposite direction of the orf (See BCAL2054, Figure 3.13C). BCAL2054 encodes a putative HEAT-like repeat protein involved in energy production and conversion. The insertions within BCAL2054 may not be disruptive, since it contains multiple phycobilisome (PBS) lyase HEAT-like repeat domains (IPR004155) (Winsor et al., 2008), which may still be able to form a functional protein. Similarly, 21 genes contain insertions that only disrupt within the last 35% of the 3' end of the orf (See BCAL0115, Figure 3.13D), suggesting that only insertions into the 5' end disrupt an essential function of these genes. It is possible that this trend is also true for genes in the operon BCAL2340-BCAL2329, which was identified as essential in both K56-2 and J2315 (Figure 3.13E). However, 3 genes, BCAL2332, BCAL2334 and BCAL2337, within this operon were identified as essential in J2315 only (See Figure 3.13E). BCAL2332 encodes an NADH dehydrogenase subunit M and had no insertions in the 5' end of the gene in the K56-2 HDTM Taq library. However, BCAL2332

contained inserts disrupting the proton conducting membrane transporter domain (PF00361), which is likely essential for function. Alternatively, BCAL2334 and BCAL2337 had inserts that may not cause a functional disruption of the genes. BCAL2334 had inserts disrupting the middle of the gene with P*rha* in the same orientation as the orf, and inserts within the last 32% of the 3'end, while BCAL2337 had insertions disrupting the last 13% of the 3'end and 33% from the 5' end with P*rha* in the correct orientation for expressing the rest of the gene (Figure 3.13E).

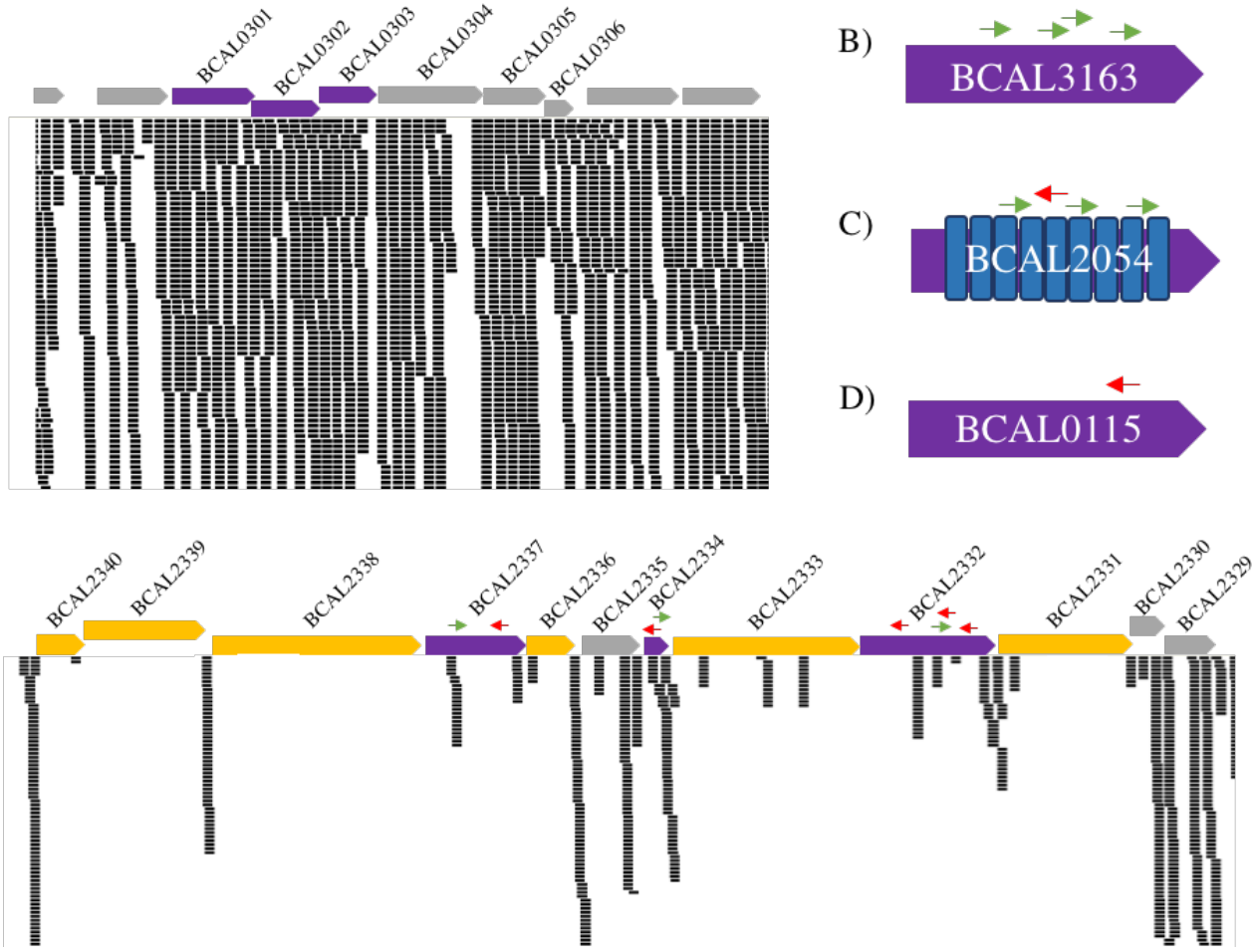

Figure 3.13 Insertions and corresponding reads mapping to *B. cenocepacia* K56-2 genes identified as essential in *B. cenocepacia* J2315 but not in K56-2

Arrows represent the orientation of the P*rhaB* promoter (green, same direction as the orf; red opposite direction to the orf). A) Operon BCAL0301-BCAL0306 involved in secondary metabolites biosynthesis, transport, and catabolism. BCAL0301, BCAL0302, and BCAL0303 (purple) were identified as essential in J2315, but had numerous insertions in K56-2. B) BCAL3163 encodes a putative nucleotidyltransferase, reads mapped to 4 insertions in K56-2, all with P*rhaB* oriented in the same direction as the orf. C) BCAL2054 encodes a putative putative HEAT-like repeat protein involved in energy production and conversion that contains multiple phycobilisome (PBS) lyase HEAT-like repeat domains (IPR004155). D) Example of possible essential gene containing an insertion that disrupts within the last 35% of the 3' end of the orf. BCAL0115 encodes a 30S ribosomal protein S21. Only one transposon mutant was recovered containing the insertion disrupting the last 22% of the 3' end of the orf. E) Operon BCAL2340-BCAL2329: 3 genes were not identified in either K56-2 and J2315 (gray), 6 were identified as essential in both K56-2 and J2315, while 3 were identified as essential in J2315 only (purple). BCAL2332 has inserts disrupting the proton conducting membrane transporter domain (PF00361). BCAL2334 has one insert disrupting the middle of the orf with P*rhaB* in the same orientation as the orf, and one insert disrupting the last 32% of the 3'end with P*rhaB* in the opposite orientation

of the gene. BCAL2337 has one insert disrupting 13% of the 3'end with P*rhaB* in the opposite orientation of the gene inserts disrupting 33% from the 5' end with P*rhaB* in the correct orientation for gene expression.

3.3.5 Comparing four essential genomes of *Burkholderia*

The availability of four *Burkholderia* essential genomes, *Burkholderia cenocepacia* K56-2 (this study), *B. cenocepacia* J2315 (Wong et al., 2016a), *B. thailandensis* E264 (Baugh et al., 2013) and *B. pseudomallei* K96243 (Moule et al., 2014a), representing the two groups of human pathogens allowed us to investigate conservation of essential genes with the goal of identifying common putative targets for antibacterial development. To find essential genes conserved across the four *Burkholderia* genomes, we compared the K56-2 essential gene homologs with the other *Burkholderia* essential genes sets. The essential gene sets of *B. cenocepacia* J2315, *B. thailandensis* E264 and *B. pseudomallei* K96243 are predicted to contain 383, 406 and 505 genes, respectively. We found 158 genes that were commonly essential to the four *Burkholderia* strains (Figure 3.12). The most significantly enriched essential functions (p-value <0.001) of the 158 common essential genes set were translation, ribosomal structure and biogenesis, nucleotide transport and metabolism was the and cell wall/membrane/envelope biogenesis, in all four strains (Figure 3.14). In order to identify pathways enriched in essential genes common to the four *Burkholderia* strains, the 158 essential genes were mapped to the J2315 pathway and a perturbation score (PPS) was computed using BioCyc (Caspi et al., 2016). The pathways of J2315 were scored to measure the extent of the enrichment of the 158 essential genes in a pathway by combining the essentiality of all reactions in the pathway. From essential genes identified as common to the four *Burkholderia* strains, we found that three pathways, involved in the maintenance of the cell envelope, were enriched in essential genes: lipid IV_A biosynthesis, peptidoglycan biosynthesis and polymixin resistance (Figure 3.15). While peptidoglycan and lipid A biosynthesis are essential in many Gram-negative bacteria (Onishi et al., 1996; Tomasz, 1979), resistance to polymixin is

usually induced upon exposure to cationic antimicrobial peptides, not constitutively expressed as in intrinsically resistant *Burkholderia* (Loutet and Valvano, 2011).

	B. cenocepacia K56-2	*B. cenocepacia* J2315	*B. pseudomallei* K96243	*B. thailandensis* E264
CELLULAR PROCESSES AND SIGNALING	**Fold enrichment**			
Cell cycle control, cell division, chromosome partitioning	4.35	4.86	4.42	4.25
Cell wall/membrane/envelope biogenesis	2.49	2.23	2.34	2.31
Cell motility	0.00	0.00	0.00	0.00
Posttranslational modification, protein turnover, chaperones	0.74	0.77	0.67	0.63
Signal transduction mechanisms	0.29	0.32	0.31	0.32
Intracellular trafficking, secretion, and vesicular transport	1.73	1.35	1.25	1.21
Defense mechanisms	0.61	0.62	0.61	0.55
Extracellular structures	0.00	0.00	0.00	0.00
INFORMATION STORAGE AND PROCESSING				
RNA processing and modification	0.00	0.00	0.00	0.00
Chromatin structure and dynamics	0.00	0.00	0.00	0.00
Translation, ribosomal structure and biogenesis	6.33	6.26	5.73	5.52
Transcription	0.44	0.64	0.60	0.59
Replication, recombination and repair	2.13	3.14	2.68	2.35
METABOLISM				
Energy production and conversion	1.97	2.05	2.15	2.07
Amino acid transport and metabolism	0.29	0.26	0.32	0.32
Nucleotide transport and metabolism	6.04	6.79	5.99	5.89
Carbohydrate transport and metabolism	0.53	0.59	0.62	0.61
Coenzyme transport and metabolism	2.64	2.73	2.48	2.36
Lipid transport and metabolism	1.32	1.39	1.39	1.41
Inorganic ion transport and metabolism	0.16	0.15	0.15	0.15
Secondary metabolites biosynthesis, transport and catabolism	0.00	0.00	0.00	0.00
POORLY CHARACTERIZED				
General function prediction only	0.37	0.38	0.42	0.43
Function unknown	0.27	0.23	0.24	0.24

Enriched	Under-represented
p-value <0.1	p-value <0.1
p-value <0.05	p-value <0.05
p-value <0.001	p-value <0.001

Figure 3.14 Functional categories enriched in the 158 essential genes common to *B. cenocepacia* K56-2, *B. cenocepacia* J2315, *B. thailandensis* E264 and *B. pseudomallei* K96243. Fold enrichment of COG functional categories for the 158 essential gene set common to *B. cenocepacia* K56-2, *B. cenocepacia* J2315, *B. pseudomallei* and *B. thailandensis* compared to the all genes in each respective genome (Fisher's exact test). Functional categories enriched (green) or under-represented (blue) in the essential gene sets are colour coded coded by p-value (legend).

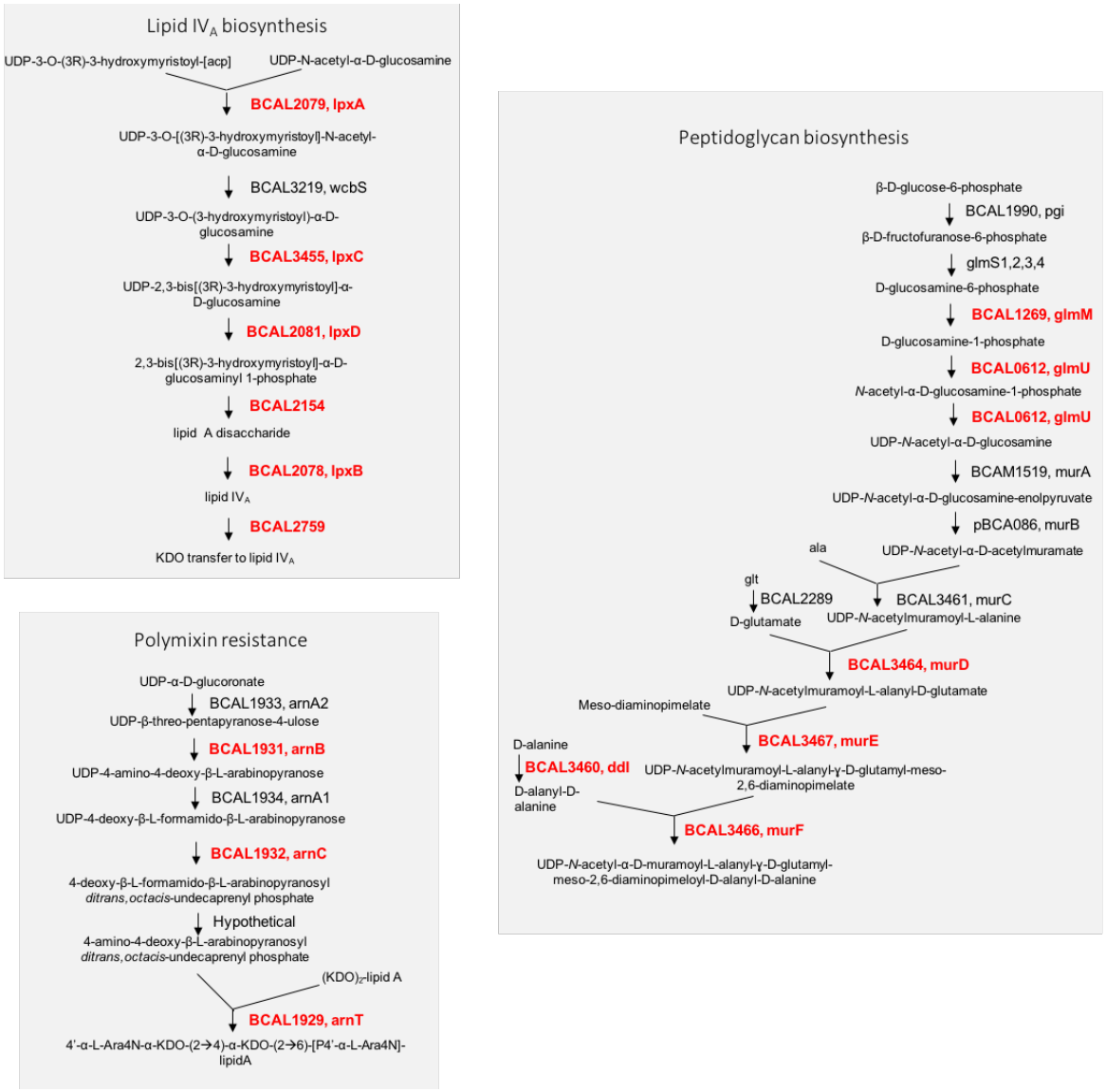

Figure 3.15 Three cell structure biosynthesis pathways enriched in essential genes common to *B. cenocepacia* K56-2, *B. cenocepacia* J2315 (Wong et al., 2016a), *B. thailandensis* E264 (Baugh et al., 2013) and *B. pseudomallei* K96243 (Moule et al., 2014a).
Pathways enriched in essential genes were determined using the pathway perturbation score (PPS) computed by BioCyc (Caspi et al., 2016). Essential genes, red; Non-essential genes, black.

We also identified a gene encoding an ortholog of the *Burkholderia* general porin Omp38 (OpcP), as essential in K56-2 (WQ49_RS05300), J2315 (BCAM1931) and *B. thailandensis* E264 (BTH_II1520) (Winsor et al., 2008). Omp38 (OpcP) is a homologue of OmpF in *E. coli* (Siritapetawee et al., 2004b, 2004a). In *E. coli*, OmpF is a major general porin, but it is not essential for growth (Baba et al., 2006). While the ortholog of Omp38 (OpcP) in *B. pseudomallei*, BPSS0879, (reciprocal best hit, BLASTP), was not identified as essential by Moule et al., four putative porins were (Moule et al., 2014a). The porins predicted to be essential in *B. pseudomallei* have sequence similarity to Omp38 (OpcP): BPSL1655 (41% identity, 95% coverage), BPSL1674 (40% identity, 94% coverage), BPSL1728 (43% identity, 95% coverage), and BPSS0252 (34% identity, 100% coverage), and could possibly perform an analogous function to Omp (OpcP). Notably, the essentiality of the Omp38 (OpcP) homolog appears to be unique to *Burkholderia* as *opcP* had no hits to essential genes in the DEG outside of the *Burkholderia* (BLASTP, expect value cutoff 10^{-5}).

We next asked whether there might be essential genes that are common to the four *Burkholderia* genomes, but non-essential in other bacteria investigated so far. The amino acid sequences of the 158 common essential genes in *B. cenocepacia*, *B. thailandensis and B. pseudomallei* were then searched against all the strains in the database of essential genes (DEG), excluding *Burkholderia* (Luo et al., 2014b). This analysis identified two genes involved in membrane integrity that are uniquely essential in the four *Burkholderia* genomes (BLASTP, expect value cutoff 10^{-5}). These genes are annotated as a polysaccharide deacetylase and a lysophospholipid transporter, LplT, encoded at the loci WQ49_RS30025 and WQ49_RS29130, respectively in *Burkholderia* K56-2. Both proteins are required for maintaining the integrity of cell envelope in Gram-negative bacteria (Harvat et al., 2005; Ortega et al., 2007b).

The putative polysaccharide deacetylase encoded at WQ49_RS30025 is an ortholog of the protein encoded at BCAL1935 in *B. cenocepacia* J2313 (reciprocal best hit, BLASTP), BTH_I2189 in *B. thailandensis* and BPSL1468 in *B. pseudomallei* (Winsor et al., 2008). This protein is a member of the putative aminoarabinose (Ara4N) biosynthesis gene cluster in *B. cenocepacia* J2315 and has been previously identified as essential in *B. cenocepacia* K56-2 (Ortega et al., 2007b). The Ara4N biosynthesis gene cluster replaces LPS phosphate groups with 4-amino-4-deoxy-l-arabinose (L-Ara4N), reducing the negative charge of the outer membrane, decreasing the affinity of cationic antimicrobial peptides, which disrupt the cell membrane through initially binding negatively charged phosphates in LPS (Raetz et al., 2007). Production of L-Ara4N has been demonstrated to be non-essential for growth in other Gram-negative bacteria and synthesis is usually initiated in response to the presence of outer membrane stressors, such as acid and antimicrobial peptides (Moskowitz et al., 2004; Raetz et al., 2007; Wang and Quinn, 2010; Zhou et al., 2001). However, in the four *Burkholderia* genomes analyzed L-Ara4N synthesis may be constitutive, suggesting that addition of L-Ara4N to LPS is necessary for outer membrane integrity.

The second gene that is uniquely essential in *Burkholderia* is WQ49_RS29130, which encodes a lysophospholipid transporter, LplT. LplT is an ortholog of the protein encoded by BCAL2111 in *B. cenocepacia* J2313 (reciprocal best hit, blastp), BTH_I2006 in *B. thailandensis* and BPSL2180 in *B pseudomallei* (Winsor et al., 2008) and functions to transfer lysophospholipids across the inner membrane (Harvat et al., 2005). Bacterial membranes are mainly composed of diacylphospholipids that constitute the integrity of the membrane. Bacteria maintain the stability of their outer membranes by recycling the diacylphospholipids and modifying their fatty acid chains (Zhang and Rock, 2008). Phospholipases produced by host cells and competing bacterial

strains disrupt the membrane by deacylating diacylphospholipids causing an accumulation of lysophospholipids (Elsbach and Weiss, 1993; Russell et al., 2013; Wright et al., 1990). These lysophopholipids act as detergents, increasing membrane permeability and curvature resulting in disruption of the cell (Fuller and Rand, 2001; Koller and Lohner, 2014). In order to repair the membrane, the inner membrane-bound transporter, LplT, belonging to the major facilitator superfamily, transports lysophospholipids into the cell where they can be re-acylated by an acyltransferase/acyl-acyl carrier protein synthetase (Aas) (Harvat et al., 2005). While LplT is required for membrane phospholipid repair, it is not essential for growth in *E.coli* (Baba et al., 2006; Lin et al., 2016). Knowledge about the biological relevance of the LplT-Aas system is limited, and the reason why LplT is essential for growth in vitro in *Burkholderia* is unknown.

3.4 Discussion

One million mutants were collected and analyzed to determine the essential gene set of *B. cenocepacia* K56-2. As the identification of essential genes is based on the relative abundance of reads for each gene in the genome, it is important not to include reads that are present as a result of experimental bias due to amplification of insertion, as these reads are not indicative of the abundance of transposon mutants in the library. A lack of coverage of a region due to bias or a redundant mutant library can lead to the false identification of a region as essential. The essential analysis used in this work was modified from Turner et al. (Turner et al., 2015) to account for the multireplicon genome of *B. cenocepacia* K56-2 as well as the experimental bias.

Reads from the HDTM library had low GC content compared the GC content of the genome. Previous work by Gallagher et al. demonstrated that the A/T bias of the reads was drastically improved by preparing the sequencing ready library using KAPA (Gallagher et al., 2013), which is more efficient at amplifying sequences with high GC content. However, the amplified region of the transposon used by Gallagher et al. had a much higher GC content. In this work, the reads from the library amplified with KAPA showed marginal improvement of the GC content of the reads and did not improve recovery of insertion sites in GC rich regions (Figures 3.2 and 3.3). The GC content of the nearly 4000 bp transposon sequence inserted into the genome is low at 51.3% GC overall, with 46.7% GC at 120 bases at the IR at 5' end with the trimethoprim cassette and 59.2% in the last 120 bases at the IR at the 3' end with the eGFP sequence (Figure 3.3). We suspect that the lower CG content of the transposon insertion sequence likely reduced the efficiency of PCR amplification of transposon insertion junctions. In order to reduce the biased amplification of A/T rich amplicons using KAPA, a GC rich tag should be added to the transposon sequence.

The reason for the correlation of A/T rich regions with high insert and read coverage are currently unknown. Like other *Burkholderia* species, the genome of *B. cenocepacia* is mostly GC rich, however there are regions corresponding to genomic islands that have a high A/T content (Holden et al., 2009b). The Tn5 transposon is not known for insertion bias into A/T rich regions, however, a bias into highly transcribed regions has been demonstrated (Lodge and Berg, 1990). It is notable that although the highest insertion density and reads correlated to A/T-rich regions, the Tn5 transposon was preferentially recovered from GC at the insertion site. Although a similar trend of high insertion events in A/T-rich regions of *B. pseudomallei* using the Tn5 transposon was seen in a genome saturation study of (Moule et al., 2014a), it is unclear whether this is a true biological

occurrence or an artifact of library preparation and sequencing bias. The Tn*5*-mini transposon used to create the HDTM library has a degenerate consensus insertion sequence with a preference for G/C at the insertion site (Shevchenko *et al*., 2002), but has also been shown to insert preferentially into highly transcribed negatively supercoiled regions of DNA (Lodge & Berg., 1990). The increased recovery of reads from insertion sites at A/T–rich regions was confounding because of the preference of theTn5-mini transposon for high GC regions (Green et al., 2012; Lodge et al., 1988). However, loss of coverage of GC rich regions has been demonstrated in Illumina sequenced libraries. Amplicon libraries created using transposon-based 'tagmentation' protocols (eg. Nextera XT) of genomic DNA have been shown to be biased for A/T-rich regions (Lan et al., 2015). PCR amplification of the tagmented DNA has been demonstrated to underrepresent GC content (Aird et al., 2011; Oyola et al., 2012), and could be exacerbated during the bridge PCR to generate clusters on the Illumina flowcell (Stein et al., 2010). Considering this, it is likely that at least some of the GC bias seen in the insertion sites and reads count is due to the Illumina sequencing platform.

Many of the regions of dense insertion sites with high reads counts correspond to genomic islands (Figure 3.7). Genomic islands can account for as much as 10% of the genome in *B. cenocepacia* (Holden et al., 2009b). Genes contained within genomic islands can encode for functions that provide a growth advantage for the cell (Schmidt and Hensel, 2004). It is possible that insertions within such genomic islands could exacerbate this growth advantage due to expression by the P*rhaB*. P*rhaB* has a dynamic range of expression levels that is tightly regulated (Cardona and Valvano, 2005b), and capable of providing a level of expression consistent with that of essential genes, which are more highly expressed than nonessential genes (Bloodworth et al., 2013a). Since the HDTM library was grown in the presence of rhamnose at every stage of its production, it is possible that the mutants with insertions within genomic islands could have a

growth advantage over other mutants in the population. This could be partly responsible for the increased recovery of reads from insertion sites within the high A/T regions of genomic islands.

Amplification bias of A/T rich sequences could also account for the increased read count at regions with high A/T, as well as increased recovery of insertion sites from these areas. Although there was marginal improvement of the GC content of the reads in the sequencing library prepared with KAPA, the low coverage of the sequencing run prevented its use to determine gene essentiality. Since regions close to the origin of replication can be in a merodiploid state compared to the rest of the genome during DNA replication, we investigated whether the insertion/read count hotspots correspond to the origins of replication of the replicons. One of the difficulties with using a draft genome for a reference is normalizing the number of reads corresponding to the origins of replication. This is also computationally difficult in multireplicon organisms like *B. cenocepacia* K56-2. However, after aligning the 17 contigs to *B. cenocepacia* J2315, it was evident that the regions of highest insertion bias are not correlated with the origins of replication predicted based on the origins of replication identified in J2315 and the GC skew (Figure 3.7). The regions with higher than average coverage in the HDTM library and the Illumina whole genome sequencing of K56-2 correspond to regions of high GC content (Figure 3.7). Although the insertion bias appeared to be correlated with the Illumina sequencing (Figure 3.7), normalizing the reads to the regions with high read coverage from the shotgun Illumina shotgun reads did not account for the bias seen in the HDTM libraries. Since the highest read counts were correlated with the GC content and the read density mapping to each contig varied, we normalized the reads to each contig (opposed to the proximity to the origin of replication) and to GC content. Regardless of the source of the insertion bias, we were able to minimize these biases by normalizing the reads by contig and GC content (Figure 3.8).

Based on the number of essential genes in 14 bacteria with diverse genome sizes, we previously estimated the number of essential genes in *B. cenocepacia* to be 300-700 (Bloodworth et al., 2013b). Putative essential genomes of other *Burkholderia* species have since been identified by high-density transposon mutagenesis including 406 in *B. thailandensis* E264 (Baugh et al., 2013), 505 in *B. pseudomallei* K96243 (Moule et al., 2014b) and recently, 383 essential genes were identified in a member of the epidemic ET12 lineage, *B. cenocepacia* J2315, which is closely related to *B. cenocepacia* K56-2 (Wong et al., 2016b). From sequencing a library of 1 million transposon mutants amplified using iTaq we identified 293,568 unique insertion sites and 508 putative essential genes. The HDTM library had high genome coverage at an average of one insertion site for every 27 bp. The identification of 508 essential genes is in agreement with the essential genes predicted for other the other *Burkholderia* species (Baugh et al., 2013; Moule et al., 2014a; Wong et al., 2016a). 410 of the genes identified as essential in K56-2 have homologs in the DEG, and 291 and 211 have homologs to essential genes found in *B. thailandensis* and *B. pseudomallei*, respectively. Two hundred and ninety-six have homologs to 294 essential genes identified in J2315, due to the K56-2 genome containing two identical copies of each of the essential J2315 homologs, pBCA001 and pBCA002. This duplication could be an artifact of the genome assembly since duplicated genes are not essential. However, one copy of pBCA001/pBCA002 contains 3 deletions upstream of the locus (data not shown). Whether these deletions affect the expression of this locus is not known, therefore, both copies were included in the total count of essential genes for K56-2.

Previous studies of the functional processes represented by the essential gene sets in different bacteria have identified that information storage and processing and metabolism as commonly enriched and underrepresented, respectively, when compared to the non-essential gene

sets (Zhang and Zhang, 2007). The enrichment of genes involved in information and storage represented by essential and non-essential genes of K56-2 is consistent with the functional analysis of experimentally determined essential genes from *B. subtilis*, *H. influenzae* and *M. gentalium, E.coli and B. cenocepacia* J2315 (Baba et al., 2006; Wong et al., 2016a; Zhang and Zhang, 2007). While there were discrepancies between K56-2 essential genes and the essential gene sets of *B. subtilis*, *H. influenzae* and *M. gentalium and E.coli* in the metabolism category, the distribution of K56-2 essential genes in the metabolism subcategories is consistent with the essential genes of J2315 (Figure 3.11). The differential abundance of essential genes involved in energy production and conservation in *B. cenocepacia* and *E. coli* may be due to the differences in fermentation abilities between the two bacteria, as *B. cenocepacia* is not capable of fermentation. Overall, the high correlation with the functions represented by the *E. coli* and *B. cenocepacia* J2315 essential gene sets when grown in similar conditions as *B. cenocepacia* K56-2, support to the validity of the essentiality analysis in *B. cenocepacia* K56-2.

From comparing the *B. cenocepacia* essential gene sets, we identified 212 and 89 genes that were uniquely essential in K56-2 and J2315, respectively. To get a better insight on the reasons of the apparent differences in the number of essential genes between K56-2 and J2315, we compared the methods used to generate the HDTM libraries and the assignment of genes as essential by the two studies. *B. cenocepacia* K56-2 and J2315 were both mutagenized with a Tn5 transposon, however the J2315 HDTM libraries were constructed by transforming electrocompetent *B. cenocepacia* J2315 with an *in vitro* transposition system (Wong et al., 2016a). This is in contrast to the triparental mating used in our work. While both methods involve a 2 h incubation of cells at 37°C before selecting for transposon mutants by plating on selective media, competition among replicating cells is more likely to occur during the triparental mating than

during electroporation, as the electroporated cells are very fragile and are not expected to replicate. Competition among the transposon mutants created during the conjugation incubation period could deplete transposon mutants with serious growth disadvantages. Depletion of transposon mutants with poor fitness would cause the disrupted genes in those mutants to be identified as essential. By considering the relative abundance of each clone in the library in our analysis, we are likely identifying genes that are not strictly essential, but involved in the fitness of the strain. This is evidenced by fact that we identified 87 genes as essential in K56-2 that were only required for survival in LB or M9 in J2315.

Previous studies using HDTM libraries of *Burkholderia* have observed a higher density of transposon insertions into chromosome 1 compared with the smaller replicons, which could lead to overestimating the essential genes on chromosomes 2 and 3 (Moule et al., 2014a; Wong et al., 2016a). Wong et al. accounted for this bias by applying a more stringent cutoff for the determining essential genes in chromosome 2 and 3 (Wong et al., 2016a). While we did not modify our stringency for identifying essential genes on the smaller replicons, the raw read counts were normalized across contigs to minimize this effect (Figure 3.8). Of the 508 essential genes were identified, 381 are in chromosome 1, while 99 and 22 were identified for chromosome 2 and 3, respectively, and 6 were identified in the plasmid. The identification of essential genes on the smaller replicons in this work is consistent with the essential genes identified by Wong et al., who identified 12 and 2 essential genes on chromosome 3 and the plasmid, respectively, in J2315 (Wong et al., 2016a). As in our essential analysis for K56-2, Wong et al. found that both the *par* systems of the smallest replicons were essential for J2315 (Wong et al., 2016a). Previous work has demonstrated that chromosome 3 is dispensable for growth in other *B. cenocepacia* strains (Agnoli et al., 2012). However, Agnoli et al. found that chromosome 3 could not be cured from K56-2.

Although the lack of the ability to cure K56-2 of chromosome 3 was linked to the presence of toxin-antitoxin systems on this replicon, rather than an essential gene (Agnoli et al., 2012), a recent study found that deletion of the *par* system from chromosome 3 resulted in a reduced growth rate in J2315 (Du et al., 2016).

The other main difference between our HDTM libraries and Wong *et al*.'s is that conjugation and selection of the K56-2 transposon mutants was performed in the presence of rhamnose, to ensure expression of downstream genes by the transposon-delivered, outward facing rhamnose-inducible promoter. The presence of essential genes downstream and in the same operon of a non-essential gene interrupted by a transposon insertion could erroneously identify the interrupted gene as essential due to polar effects of the insertion. We considered that this could be responsible for the J2315 genes classified as essential by Wong et al., that we did not identify in K56-2, as their transposon did not contain an outward facing promoter. However, although we did identify essential operons with different essential genes between J2315 and K56-2, these differences were not correlated with the gene order (See Figure 3.13E), indicating that polar effects of the transposons used in this work and by Wong et al., are not responsible for the differences with respect to genes within operons. Identification of essential genes using negative selection methods like high density transposon mutagenesis can result in discrepancies of calling an essential gene as nonessential. Non-lethal insertions can occur in essential genes if the insertion site is located near the 3' or 5' ends, resulting in a truncated, but functional protein (Hutchison et al., 1999). In this work, we identified a gene as essential if there is not a significant number of reads mapped to the the inner 10%-90% of a gene. However, some essential genes could have been mistakenly identified as nonessential due to recovery of non-disruptive insertions within the functional part of a gene. Tolerance of insertions within the essential region of a gene could be

achieved due to a transient merodiploid state during replication. It is also possible that insertions into the central portion of essential genes encoding multidomain proteins could be non-lethal if the insertion site is in the region associated with the boundary of the domain (Gerdes et al., 2003), as could be the case in BCAL2054 (Figure 3.13C).

Overall, the differences in the methodology and data analysis used could account for discrepancy regarding the essentiality of genes common to J2315 and K56-2. In this work, the biggest influence on the discrepancies between the essential gene sets of J2315 and K56-2 seems to be due to calling K56-2 genes involved in growth as essential, and classifying genes with likely non-disruptive insertions as non-essential (Figure 3.13). However, genomic differences in the closely related isolates could account for some of the discrepancy in essential genes, due to the plasticity of the *B. cenocepacia* genomes (Holden et al., 2009b). While *B. cenocepacia* J2315 is closely related to *B. cenocepacia* K56-2, the essential genes of bacteria of the same species can be divergent (Turner et al., 2015) as gene essentiality is specific to the genomic context of the cell (D'Elia et al., 2009). Significant differences in the genomic content have even been seen between the same strain from different labs (Klockgether et al., 2010). This is a pattern seen in *B. cenocepacia* strains, where there are two large duplicated regions in *B. cenocepacia* J2315 that are present in only one copy in K56-2 (Bloodworth, 2013; Holden et al., 2009b). For example, the dense coverage of insertions disrupting the genes, BCAL0301-0302 that were identified as essential in J2315, indicate that these genes are not essential in K56-2 (Figure 3.13A) and 8 of the genes uniquely identified as essential in J2315 have no homologs in K56-2. Furthermore, a 57 kb region encoding 57 genes is duplicated in J2315 (BCAL0969 to BCAL1026 and BCAL2901 to BCAL2846) but not K56-2 (Holden et al., 2009b). While genes in this locus are not essential in J2315, our analysis predicts that 14 genes corresponding to this region are essential in K56-2, most

of which have homologs to essential genes identified in *B. thailandensis* and *B. pseudomallei*. While 23% of the J2315 essential genes (Wong et al., 2016a) were not identified as essential in K56-2, this is in line with the percent of essential genes that were uniquely essential in two closely related strains of *P. aeruginosa* (Turner et al., 2015). The genomes of *P. aeruginosa* PAO1 (6.26 Mb) and PA14 (6.54 Mb) are highly similar with strain specific regions comprising 4.2% and 8.3% of each genome, respectively (Lee et al., 2006). Turner et al. found strain specific differences in the genes of *P. aeruginosa* PAO1 and PA14 that are essential for growth in CF sputum media (Turner et al., 2015). While many of the essential genes were overlapping between PA14 and PAO1, approximately 17% and 26% of the PAO1 and PA14 essential genes, respectively, were uniquely essential to each strain.

While the functional category representation of the K56-2 gene set is representative of previous findings and identification of experimentally validated essential genes support the accuracy of our essential gene prediction in *B. cenocepacia* K56-2, we cannot discount that we could be including genes that may not be strictly essential, but have a severe growth defect when disrupted with the transposon insertion. Whether the distinct essential genes in *B. cenocepacia* K56-2 and J2315 are actually uniquely essential in each strain remains to be confirmed by further experimental evidence.

By comparing the essential gene set of K56-2 with the essential genes in *B. pseudomallei*, *B. thailandensis* and *B. cenocepacia* J2315, we identified 158 essential genes that are shared amongst the four *Burkholderia* strains. The core essential genome between these four strains consists of 131 genes that have been predicted in silico to be a part of the core genome of the *Burkholderiales* by Juhas et al. (Juhas et al., 2012b). The genes and metabolic capabilities can be disparate in different *Burkholderia* species. *B. cenocepacia* belongs to the Bcc, which are distinct

from *B. thailandensis* and *B. pseudomallei*. *B. thailandensis* does not cause disease in humans, but can replicate in cultured mammalian cells and resists predation by amoeba (Harley et al., 1998; Hasselbring et al., 2011). *B. thailandensis* and *B. pseudomallei* are genetically similar species that have different lifestyles and diverged from a common ancestor over 40 million years ago (Yu et al., 2006). While *B. cenocepacia* and other Bcc bacteria have found a niche within CF patients and immunocompromised individuals, *B. pseudomallei* is an intracellular pathogen that infects humans and animals, causing fatal meliodosis, and is classified as a category B biothreat agent by the Centre for Disease Control (Centers for Disease Control and Prevention (CDC), Department of Health and Human Services (HHS), 2017). Horizontal gene transfer has been predicted to be a major driver in the adaptive evolution of *Burkholderia*, with as much as 60% of the gene families undergoing horizontal gene transfer at least once and contributing to the pathogenicity of *Burkholderia* strains (Zhu et al., 2011). Zhu et al. also predict that the acquired genes account for much of the diversity seen between the different species and that rearrangements with the genome and gene loss has caused the differences seen between newly diverged, closely related strains of *Burkholderia* (Zhu et al., 2011). The finding of 158 shared genes between these divergent strains highlights the importance of some essential processes in *Burkholderia*. The 158 common essential genes set was most significantly enriched in processes involved in nucleotide transport and metabolism, translation, ribosomal structure and biogenesis, and cell wall/membrane/envelope biogenesis (Figure 3.14). We identified three pathways that were enriched in the common essential genes that are involved in maintaining the impermeability of the cell (Figure 3.15), which is one of the most common (Mahenthiralingam and Coenye, 2014) and effective mechanisms of antibiotic resistance in *Burkholderia* species (Moore and Hancock, 1986; Parr et al., 1987). The fact that the essentiality of genes encoding proteins involved in maintaining the integrity of the

cell envelope have been conserved through divergent evolution of the *Burkholderia* species indicates their importance for survival within diverse environments. From the 158 conserved essential genes, we identified two genes involved in maintaining the integrity of the membrane that are uniquely essential in the four *Burkholderia* strains.

The first is a gene of unknown function that is transcribed with genes involved in L-Ara4N modified lipid A, which has been previously identified as an essential process in *B. cenocepacia* (Ortega et al., 2007b). In Gram-negative bacteria, the LPS in the outer membrane is made of lipid A, a core oligosaccharide and an polysaccharide or O-antigen (Raetz and Whitfield, 2002). Following transport across the inner membrane, the lipid A and O-antigen are ligated together by WaaL (Valvano, 2011), where the LPS is exported to the surface of the outer membrane via the lipopolysaccharide transport system (Ruiz et al., 2009; Sperandeo et al., 2009). Acetylation is achieved through the replacement of phosphate reducing the negative charge of the outer membrane. BCAL1935 is included in a transcriptional unit that encodes the polysaccharide deacetylase and BCAL1936, which are predicted to synthesize UDP-Ara4N (Ortega et al., 2007b), however, the function of BCAL1935 is not known. While L-Ara4N-modified lipid A is required for resistance to antimicrobial peptides, it is not essential in most Gram-negative bacteria (Raetz et al., 2007). In most bacteria, L-Ara4N is added to lipid A, in *Burkholderia* strains, L-Ara4N is added to the lipid A at an oligosaccharide residue in the inner core (X. Ortega et al., 2009). Recently it was discovered that in addition to L-Ara4N providing resistance to antimicrobial peptides, the presence of the L-Ara4N modification is required in order for LPS to be exported (Hamad, Di Lorenzo, Molinaro, & Valvano, 2012), indicating how this modification is essential in *B. cenocepacia*. In addition to providing resistance to antimicrobial peptides, L-Ara4N modified LPS are important for pathogenicity (Needham & Trent, 2013).

The second essential gene identified as uniquely essential in *Burkholderia* is LplT, a lysophospholipid transporter that transfers membrane-disrupting lysophospholipids across the inner membrane where they can be re-acylated by Aas (Harvat et al., 2005). Aas proteins contain at least one of two domains: PlsC, belonging to the lysophospholipid acyltransferase protein family, and ACS, an acyl-CoA synthetase. There is no ortholog for the *E. coli* K-12 substr. MG1655 Aas in *B. cenocepacia*, K56-2, J2315, *B. pseudomallei* or *B. thailandensis* (bidirectional best BLAST hit, BioCyc database (Caspi et al., 2016)). However, it is possible that other protein containing PlsC and ACS domains could provide the function of the Aas protein. LplT is not essential for growth in *E.coli* (Baba et al., 2006; Lin et al., 2016) and the reason LplT is essential for growth in *Burkholderia* is unknown. However, conservation of the *lplT* would provide an advantage for surviving within a microbial community as well as within the host, which both employ phospholipases as a defensive mechanism.

We also identified a porin, Omp38 (OpcP), that is uniquely essential in three of the four *Burkholderia* strains. While OpcP is not essential in *B. pseudomallei*, four other essential porins, BPSL1655, BPSL1674, BPSL1728 and BPSS0252, were identified as essential. There are no predicted orthologs of BPSL1655 and BPSL1674 in J2315. However, BCAM1549 is the predicted ortholog for BPSL1728 and BCAM1398 and BCAM2446 are the predicted orthologs for BPSS0252 (Winsor et al., 2008). Although none of the orthologs of the porins that are essential in *B. pseudomallei* were predicted to be essential in J2315 (Wong et al., 2016a) or K56-2, it is possible that these porins provide a similar function to Omp38 (OpcP). The reason for the essentiality of the Omp38 (OpcP) porin is unknown, however trimeric porins like Omp38 (OpcP) contain binding sites that stabilize the LPS in the outer membrane in Gram negative bacteria (Arunmanee et al., 2016). Whether the essentiality of Omp38 (OpcP) is a function of maintaining

the impermeability of the outer membrane or because it is required for the diffusion of an essential nutrient into the cell is unknown. It is interesting that the outer membrane of *Burkholderia* species has been shown to be 89% less permeable than *E.coli* (Hancock, 1998) and the impermeability of the membrane in Gram negative bacteria has been attributed to the functional characteristics of porins and lipopolysaccharide (Pagès et al., 2008; Raetz et al., 2007). The presence of the uniquely essential porin in *Burkholderia* strains indicates the importance for its conservation and a role in survival that is specific to *Burkholderia* strains.

In summary, the intrinsic antimicrobial resistance and cell envelope impermeability that characterizes the *Burkholderia* genus may represent the Achilles heel of *Burkholderia* species and attractive targets for genus-specific antimicrobial developments.

Chapter 4: Enrichment of conditional growth mutants from the 1 million high density transposon mutant library

4.1 Introduction

The *Burkholderia cepacia* complex (Bcc) is a group of at least 20 different species of closely related Gram-negative bacteria infecting cystic fibrosis patients (Mahenthiralingam et al., 2005a; Peeters et al., 2013; Smet et al., 2015; Vanlaere et al., 2008, 2009). *Burkholderia cenocepacia* is an epidemic strain of the Bcc responsible for the most severe infections in cystic fibrosis patients that can lead to cepacia syndrome, a fatal necrotizing pneumonia followed by septicemia (Mahenthiralingam et al., 2005a). *B. cenocepacia* infections are difficult to treat due to the intrinsic multidrug resistance. Infections with antibiotic resistant bacteria are becoming more difficult to treat due to the lack of development of novel antibiotics (Boucher et al., 2009; Brown and Wright, 2016). One bottle neck in the antibiotic development pipeline is the lack of knowledge of the mechanism of action and novel antibiotics (Burdine and Kodadek, 2004).

In vitro target based approaches have been unsuccessful in identifying antibiotics capable of *in vivo* activity (Payne et al., 2007). Whole cell screens are necessary for identifying compounds with good permeability, as there are no guidelines established for identifying compounds that will penetrate the cell envelope. High density transposon mutant libraries have been used to find conditionally essential or resistant genes in response to antibiotic treatment (Gallagher et al., 2011a). The limitation of these assays is that the essential genome cannot be interrogated using these libraries, since disruption of an essential gene would render the strain unviable. Essential gene libraries are achieved by creating conditional growth (CG) mutants, where the essential gene product can be expressed in permissive conditions and depleted in non-permissive conditions. This has been accomplished through inducible antisense RNA systems (Donald et al., 2009a; Forsyth et al., 2002b; Huber et al., 2009), CRISPR interference (Larson et al., 2013b; Peters et al., 2016b),

and replacement of the native promoter with an inducible promoter (Cardona et al., 2006b; Carroll et al., 2005; Ehrt et al., 2005c; Judson and Mekalanos, 2000b). While the use of these systems have been successful in identifying the targets of novel antibiotics, there are limitations. Nonspecific binding of antisense RNA to off targets can confound results, while the sequence of the targeted essential gene is required to design probes for CRISPR interference, which is not always known in non-model strains. Furthermore, most chemogenomic assays measure the sensitivity of a strain to an antibiotic as the growth defect of clonally grown strains. Employing assays like this can be a daunting task, where specialized robotic equipment and statistical assessment to account for plate to plate variances are required (Blomberg, 2011). In addition to the vast amount of disposables required for these assays, the amount of novel antibiotic required to perform a screen can be significant impediment if the compound is available in limited amounts.

Advances in sequencing technology have allowed for the quantification of individual mutants in a mixed population by sequencing the transposon-genome junctions, where the proportion of reads corresponding to unique insertion sites are representative of the relative abundance of the mutants in the population. In an attempt to create a CG mutant library that represents the essential operons of *B. cenocepacia* K56-2, we previously used random transposon mutagenesis to insert a rhamnose inducible promoter (P*rhaB*) (Cardona and Valvano, 2005a) into the genome of *B. cenocepacia* K56-2. CG mutants are generated when the transposon inserts so P*rhaB* is oriented to control the expression of an essential gene (Cardona et al., 2006b). After screening 200,000 transposon mutants for a conditional growth phenotype in response to rhamnose, approximately 106 CG mutants from 54 unique operons were obtained (Bloodworth et al., 2013a). We have demonstrated that limiting the amount of rhamnose available to induce expression, the CG mutants become sensitized to antibiotics that target the essential gene product

that is under-expressed in an enhanced sensitivity assay (ESA) (Bloodworth et al., 2013a). In an attempt to increase the throughput of the ESA, we then used next generation sequencing to measure the relative abundance of CG mutants after growth within a pool in a competitive ESA. As a result, we identified an essential two-component regulatory system, *esaSR*, that can be targeted to reduce antibiotic resistance in *B. cenocepacia* after a pilot library of 25 CG mutants was screened against eight antibiotics with known MOAs. In addition, we found that competitive growth increased the enhanced sensitivity of a CG mutant under-expressing GyrB to novobiocin (Gislason et al., 2016). However, in order to screen more CG mutants in the ESA, there were two bottlenecks that needed to be addressed. First, the frequency of isolating CG mutants was a low, at 1 CG mutant isolated for every 1500 mutants screened and the process was time-consuming and costly (Bloodworth et al., 2013a). Second, the use of multiplex PCR to amplify the transposon-genome interface limited number of mutants that could be assayed.

To increase the frequency of isolating CG mutants, we enriched for CG mutants from a high density transposon mutant library prior to screening for the conditional growth phenotype. The enrichment process is based on a method developed to isolate auxotrophic mutants (Davis, 1948; Lederberg and Zinder, 1948). Using the same transposon to randomly insert the rhamnose inducible promoter into the genome, we created a high-density transposon mutant (HDTM) library. The colonies of the HDTM were grown in the presence of rhamnose so that mutants with P*rhaB* controlling the expression of essential genes can be recovered. In our previous work we found that in the absence of rhamnose, all the CG mutants either do not grow or have a reduced growth rate, but remain viable for at least 24 hours and can be rescued by the addition of rhamnose to the media (Bloodworth et al., 2015). We exploited this to enrich for CG mutants from a high density mutant library. By growing the HDTM without rhamnose, selective killing of transposon mutants with

P*rhaB* controlling the expression of a non-essential gene was achieved by the addition of meropenem, which inhibits cell wall synthesis (Wishart et al. 2006) and kills only actively growing cells. The non-growing, but viable CG mutants were then collected and screened for the conditional growth phenotype.

In this work we used meropenem enrichment to increase the frequency of isolating CG mutants from a HDTM library of 1 million mutants. From one enrichment of the HDTM, we increased the frequency of isolating CG mutants 500-fold and added 830 CG mutants to our collection.

4.2 Materials and Methods

4.2.1 Bacterial strains and growth conditions

The bacterial strains and plasmids used in this study are listed in Table 4.1. *B. cenocepacia* K56-2, a clonal strain of J2315 isolated from a cystic fibrosis patient (Darling et al. 1998), was the strain used in this study. All bacteria grown in this study were grown in Luria-Bertani (LB) media (BD, Franklin Lakes, NJ) at 37°C with shaking at 220 rpm in a New Brunswick Scientific E24 shaking incubator (Edison, NJ) for broth cultures unless otherwise indicated. *E. coli* strains were grown in 40 μg/mL of kanamycin (KAN40) or 50 μg/mL of trimethoprim (TMP50) when appropriate. *B. cenocepacia* transposon mutants were selected for in 100 μg/mL of TMP (TMP100), 50 μg/mL of gentamicin (Gm50), and 0.2% rhamnose (0.2% rha). Additionally, the transposon mutants were grown in TMP100 with or without 0.2% rha when appropriate. Growth was estimated by measuring OD_{600nm} using a Biotek Synergy 2 plate reader (Winooski, VT). All chemicals were purchased from Sigma Chemical Co. (St. Louis, MO) unless otherwise indicated.

Table 4.1 Bacterial strains and plasmids used in this study

	Features[a]	Source
Strains		
Burkholderia cenocepacia K56-2	ET12 lineage, CF isolate	Darling et al. (1998)
Escherichia coli SY327	*araD* Δ(*lac pro*) *argE* (Am) *recA56* Rif^r *nalA λ pir*	Miller and Mekalanos (1988)
E. coli MM290	F$^-$, φ 80 lacZΔM15 *endA1 recA1 hsdR17* ($r_H^- m_K^+$) *supE*44 *thi*-1 Δ*gyrA96* (*ΔlacZYA-arg*F) U169 *relA*1	Bloodworth et al. (2013)
Plasmids		
pRK2013	ori_{colE1}, RK2 derivative, Km^r *mob*$^+$ *tra*$^+$	Figurski and Helinski (1979)
pRBrhaBoutgfp	pSCrhaBoutgfp derivative (Cardona et al. 2006), ori_{R6K}, *rhaR rhaS PrhaB* e-*gfp*	Bloodworth et al. (2013)

[a]CF = cystic fibrosis, Km = kanamycin, Rif = rifampicin

4.2.2 Enrichment of CG mutants from the HDTM library

The CG mutant enrichment is based on a method for isolating auxotrophic mutants in the absence of amino acids (Davis, 1948; Lederberg and Zinder, 1948). The 1M HDTM library was inoculated at 10^9 CFU (final OD_{600nm} of 0.025) into a 250 mL Erlenmeyer flask containing 50mL of LB supplemented with TMP100 and 0.2% rha and incubated for 3 h at 37°C until the culture reached early exponential phase (OD_{600nm} of approximately 0.13-0.18). 25 mL aliquots from the 50 mL suspension were then transferred to two 50 mL centrifuge tubes (Fisher Scientific, Waltham, MA) and centrifuged for 10 min at 4,000 rpm in a Sorvall RC-5B Refrigerated Superspeed Centrifuge (GMI, Ramsey, MN). After removing the supernatant, the pellet from each tube was resuspended in 25 mL of LB. This was followed by another centrifugation for 10min at 4,000 rpm. The supernatant was removed and the pellets were resuspended in LB at a total volume of 1 mL. After this wash step, the OD_{600nm} of the suspension was measured. The suspension was inoculated into a 250 mL Erlenmeyer flask containing 50 mL of LB to a final OD_{600nm} of 0.01. This was grown for 3-4 h to an OD_{600nm} of 0.18. The culture was then treated with 800 µL of 10 mg/mL meropenem to a final meropenem concentration of 160 µg/mL (10x the MIC of meropenem for *B. cenocepacia*). The culture was then incubated for another 3 h at 37°C. The culture was washed with LB and the pellet was resuspended in 10mL LB then transferred to a 250 mL Erlenmeyer flask containing 40 mL of LB. The suspension was incubated for 30 min, after which a second dose, 800 µL of 10 mg/mL meropenem, was added. The culture was incubated for a further 3 h at 37°C. Lysed cells were filtered from the media using a Filtropur V25 0.2 250 mL vacuum filter (Sarstedt). The cells remaining on the filter were then washed with 100 mL of LB. The cells form the filter were resuspended in LB then plated out in four or five 500 cm^2 QTrays

with LB agar supplemented with TMP100 and 0.2% rha. The QTrays were incubated for 48 h at 37°C, after which the resulting colonies were robotically picked by a Genetix QPix2 XT colony picker into 96- or 384-well plates containing LB supplemented with TMP100 and 0.2% rha. These plates were incubated for 48 h without shaking and used as master plates for the primary screen.

4.2.3 Screening for the conditional growth phenotype

The master plates were robotically replica plated using the colony picker into well plates containing LB supplemented with TMP100 and with or without 0.2% rha. The plates were incubated for 16 h at 37°C without shaking, after which the OD_{600nm} of the two conditions were compared. The CG phenotype was defined as 50% or less growth in the lack of rhamnose (Bloodworth et al. 2013). Mutants that exhibited the conditional growth phenotype were classified as putative CG mutants, and were placed through a secondary screen to confirm the CG phenotype. The putative CG mutants from the primary screen master plates were diluted by 10-fold into 96-well plates containing LB+TMP100. These 96-well plates were replica plated using 96-pin replicators (Genetix, Hampshire, UK) onto three LB well plates; two were supplemented with 0.2% rha, and one was not. The replica plates were incubated for 16 h at 37°C without shaking. The OD_{600nm} were compared between one of the 0.2% rha-supplemented plates and the plate lacking 0.2% rha. Putative CG mutants that exhibited the CG phenotype were confirmed as CG mutants. An equal volume of LB with 40% glycerol was added to the wells of the 0.2% rha-supplemented well plates that were not used for screening. These were stored as glycerol stocks at -80°C.

4.2.4 Production of CG mutant subpools and the meropenem enriched CG mutant library

Each of the glycerol stock 96-well plates containing the confirmed CG mutants were replicated using 96-pin replicators into a 96-well plate containing 200 µL of LB supplemented with TMP100 and 0.2% rha, with the inner surface of the lid treated with Triton X solution (0.05% Triton X-100, 20% ethanol) to prevent condensation. The plates were incubated for 16-18hr at 37°C, after which the OD_{600nm} was measured. Each individual CG mutant in the plate was standardized to the CG mutant with the lowest growth as follows. For each CG mutant, the OD_{600nm} is divided by the OD_{600nm} corresponding to the CG mutant least amount of growth in the well plate to obtain a ratio. The CG mutant with the least growth would have a ratio of 1. This ratio was multiplied by 160 µL to obtain the volume from each CG mutant in the well plate required for equal representation of all the CG mutants from that plate. These volumes were mixed together to create a subpool of CG mutants containing equal representation of the CG mutants from the well plate. The resulting suspension was washed twice in LB to remove rhamnose. An OD-adjusted glycerol stock of pooled mutants was created at a final OD_{600nm} of 0.5. 110 µL aliquots from the glycerol stock were transferred into PCR tubes to be stored at -80°C**.** This process was repeated to produce subpools from all the CG mutant well plate stocks. For sequencing the mutant libraries, the glycerol stocks from each subpool from the enrichments were combined together to create a pool that contains equal representation of each CG mutant from the library. The genomic DNA was then isolated and sequencing ready libraries were prepared by Tn-seq circle.

4.2.5 Genomic DNA isolation

0.5-1 mL cell suspensions were washed twice, first in 500 µL 0.85% saline followed by 500 µL TES. Afterwards, the pellet was resuspended in 250 µL T10E25. 50µL of 2 mg/mL

lysozyme solution and 1 µL of 1 mg/mL RNase (QIAgen) were added, then incubated for 15 min at 37°C. 60 µL of sarcosyl-protease solution was added, followed by incubation for 16-18 h at 37°C. After incubation, the suspension was mixed with 361 µL P:C:I (50% buffer-saturated phenol, 48% chloroform, 2% isoamyl alcohol), then gently inverted for 10min until the mixture was homogenous. The suspension was transferred to a 1.5 mL phase-lock gel tube (Five Prime, San Francisco, CA) and centrifuged for 5min at 13,000 rpm. The upper aqueous phase was then transferred to a low DNA-binding microcentrifuge tube. To precipitate the DNA, 0.10 volumes of 10 mM sodium acetate was added, followed by 0.54 volumes of isopropanol. The suspension was allowed to sit at room temperature for at least 30 min then centrifuged for 30 min in a table top centrifuge at 13,000 rpm at 4°C. After removal of the supernatant, 1 mL of ice-cold 70% ethanol was added. The suspension was centrifuged for 10 min at 13,000 rpm at 4°C. After removal of the ethanol, the DNA pellet was allowed to air dry for five minutes to allow evaporation of excess ethanol. The DNA was resuspended in TE (Tris, EDTA) buffer and stored at 4°C. More TE buffer was added as necessary until the DNA was fully solubilized. Agarose gel electrophoresis was carried out to assess the quality of the DNA before quantifying by Qubit.

4.2.6 Molecular biology techniques

The DNA concentration of the samples was measured using the Qubit dsDNA BR Assay kit (Invitrogen, Carlsbad, CA). 1-2 µL of DNA was added to Qubit dsDNA BR working solution such that the total volume was 200 µL. The mixture was vortexed for 2-3 sec, ensuring that no bubbles formed. The mixture was then incubated for 2-5 min at room temperature prior to the measurement of DNA concentration with a Qubit 2.0 fluorometer (Invitrogen).

DNA purification of amplicons was carried out using the Agencourt AMPure XP system (Beckman Coulter, Brea, CA). Room temperature AMPure XP beads were mixed with DNA samples in low DNA-binding microcentrifuge tubes (Eppendorf, Hamburg, Germany), after which the mixtures were incubated for 5min at room temperature. The tubes were then placed next to the magnets on the magnet rack to sit until all the beads were pulled towards the magnet. The supernatant was then removed, after which the beads were washed twice with 1 mL of 80% Ethanol while the tubes were still on the rack. After the supernatant was removed, the beads were allowed to air dry for 5 min on the magnet to allow evaporation of excess Ethanol. The tubes were removed from the magnets, and DNA was eluted with EB buffer (QIAgen, Hilden, Germany) The DNA samples were quantified after purification.

4.2.7 Tn-seq Circle

The Tn-seq circle method (Gallagher et al., 2011c) was used to enrich for the transposon-genome junction from the genomic DNA of transposon mutant libraries for subsequent sequencing to identify the transposon insertion sites. The oligonucleotides used are listed in Table 3.2. 130 µL of approximately 38 ng/ µLof genomic DNA was fragmented to an average size of 300 bp via ultrasonication using a Covaris S220 (duty factor of 10%, a peak incident power of 140, 200 cycles per burst, and a treatment time of 4 cycles at 20 sec each). The 130 µL aliquots of fragmented DNA were transferred to new low DNA-binding PCR tubes (Eppendorf). The fragmented DNA was end repaired using a NEBNext End Repair kit (NEB). In each tube, 15.5 µL of 10x NEBNext buffer, 1.75 µL nuclease-free H_2O (Ambion, Austin, TX), and 7.75 µL enzyme were mixed for a total volume of 153 µL. The reaction mix was incubated for 30 min at 20°C in an Eppendorf Mastercycler ep gradient S thermal cycler. Afterwards, the end-repaired DNA samples were

purified using 1:1.8 sample:AMPure XP beads, eluted in a final volume of 50 μL EB buffer (Qiagen) and quantified by Qubit.

A-tailing was carried out on the purified end-repaired DNA in 50 μL reaction mixtures composed of 25 μL end-repaired DNA, nuclease-free H_2O, 5 μL QIAgen 10x buffer, 10 μL (1 mM) dATP, and 0.2 μL of Taq (QIAgen). The reaction mixtures were incubated for 20 min at 72°C in the thermal cycler. Afterwards, the A-tailed DNA samples were purified using 1:1.8 sample:AMPure XP beads eluted in 30 μL EB buffer and quantified by Qubit. Adapters were prepared by annealing the single stranded oligos 683 and 684 (Table 3.2). The annealing reaction consisted of 90 μL of each oligo at 100 μM in 10 mM Tris, 20 μL (100 mM) NaCl, and 10 mM EDTA as follows: 2 min for 97°C, 72 cycles of 1 min at 97°C (-1°C per cycle), followed by 5 min at 25°C. The adapters were then stored at -20°C. 683 and 684 were ligated to the purified A-tailed DNA using a Quick Ligation kit (NEB). The molar quantity of the DNA was first calculated to determine the appropriate volumes for the reaction mixture. Using approximately 3 μg of DNA, the ligation was carried out in 80 μL reactions composed of A-tailed DNA, 20x molar excess of adapter relative to the A-tailed DNA, 40 μL of 2x Quick Ligation Buffer, 0.3 μL nuclease-free H_2O, and 2.96 μL Quick Ligase. Reaction mixtures were incubated for exactly 15 min at room temperature. Adapters were removed by mixing the reaction mixture with an equal volume of AMPure XP beads (1:1). The DNA was quantified by Qubit. Size-selected DNA with ligated adaptors were then digested with PacI (NEB) in 50 μL reaction mixtures containing DNA, nuclease-free H_2O, 5 μL Cutsmart buffer, and 1 μL PacI for 16-18 h at 37°C. Size selection for 200-400 bp fragments was repeated, followed by DNA quantification.

Circularization of the digested DNA was carried out in 30 μL reaction mixtures in 0.2 mL thin-walled PCR tubes (Axygen) containing 1-4 pmol DNA, 10x molar excess of collector probe

(682), 3 µL of 10x Ampligase buffer, 0.5 µL Ampligase, and nuclease-free H_2O. Two controls, no Ampligase and no probe were prepared simultaneously. The reaction mixtures were cycled as follows: 30 sec at 95°C, 25 cycles of 30 sec at 95°C and 3 min at 67°C, followed by 3 min at 72°C, 2 min at 95°C, and holding at 4°C. Afterwards, 2 µL of exonuclease mixture composed of 0.50 µL Exonuclease I (NEB, 20 U/µL), 0.75 µL Lambda Exonuclease (NEB, 5 U/µL), and 0.75 µL T7 Gene 6 Exonuclease (USB (Cleveland, OH), 50 U/µL) was added to the Ampligase reaction mixtures except for the no exonuclease control. The reaction mixtures were incubated for 16 h at 37°C followed by 20 min at 85°C in the thermal cycler. The DNA was then purified and quantified. Prior to PCR amplification, the optimal number of cycles was first tested via real-time PCR using a Bio-Rad CFX Connect thermocycler (Mississauga, ON). The enrichment of the transposon-genome junctions was confirmed by comparing the amplification of the HDTM library with K56-2 wild type prepared simulateously via real-time PCR using a Bio-Rad CFX Connect thermocycler (Mississauga, ON). 10 µL reaction mixtures composed of template DNA, nuclease-free H_2O, 0.2 µM of each primer, 690 and 681 (Table 3.2), and 5 µL iTaq SYBRgreen Supermix (Bio-Rad) were cycled as follows: 3 min at 95°C, 35 cycles of 30 sec at 95°C, 30 sec at 63.5°C, and 30 sec at 72°C. The optimal number of cycles is where there is at least 25% of maximum fluorescence, but there is still exponential amplification of the DNA. The optimal number of cycles was 20-25 cycles. PCR was repeated using new reaction mixtures similarly prepared as before. The reaction was carried out until the determined optimal number of cycles was reached. The PCR products were purified using 1:0.8 sample:AMPure XP beads, resuspended in EB buffer and quantified using a qubit. The removal of primers containing the MiSeq adapter sequences from the amplicons was verified by running the sample on a bioanalyzer. The purified samples were sequenced using the

Illumina MiSeq standard kit v2 with 150 bp single reads at the Children's Hospital Research Institute of Manitoba (Winnipeg, Canada) following the manufacturer's instructions.

Table 4.2 Oligonucleotides used in this study

Name	Sequence (5' - 3')[a]	Description
683	CCGTAGTGAGTTCTTCGTCCGAGCCACTCGGAGATGTGTATAAGAGACAGT	Top strand adaptor (has 3' T overhang) for Tn-seq circle
684	CTGTCTCTTATACACATCTCCGAGTGGCTCGGACGAAGAACTCACTACGG	Bottom strand adaptor for Tn-seq circle
682	CACAAGTGCGGCCGCACTAGTCTAGATTTAAATTACCGTAGTGAGTTCTTCGTCCGAGCCAC	Collector probe for Tn-seq circle
690	AATGATACGGCGACCACCGAGATCTACACTAGATCGCTCGTCGGCAGCGTCAGATGTGTATAAGAGACAGNNNNAATCTAGACTAGTGCGGCC	Nextera index N501 Tn-seq circle forward primer
681	CAAGCAGAAGACGGCATACGAGATTCGCCTTAGTCTCGTGGGCTCGGAGATGTGTATAAGAGACAG	Nexteria index N701 Tn-seq circle reverse primer

[a]N is any nucleotide.

4.2.8 Bioinformatics

A custom python script, written by Dr. Ruhi Bloodworth and modified by Dr. Mike Domaratski, was used the identify reads containing the transposon sequence, trim the transposon sequence and map the remaining read against the *B. cenocepacia* K56-2 genbank file (GenBank Accession LAUA00000000) using Bowtie2 (Langmead and Salzberg, 2012). The position of each insertion and the number of reads mapping to it were collected. Another custom python script, written by Dr. Mike Domaratski, was used to identify the genes under the control of the rhamnose inducible promoter in each mutant. Briefly, a tabular file with the insertion sites was created using the annotations and gene position from the *B. cenocepacia* K56-2 genbank file (GenBank Accession LAUA00000000). A gene was considered to be under the control of P*rhaB* if the insertion co-oriented it with a downstream gene. Transposon insertions within 1000 bps upstream, or within 20% of the 5' end of a gene were considered to control the expression of that gene. Genes predicted to be within the same transcriptional unit and located downstream of the gene initially identified to be under the control of *Prha*B, were called based on predictions for the J2315 genome from DOOR (Mao et al., 2014b).

The protein sequences encoded by the genes predicted to be under the under the control of P*rhaB* were extracted from the draft genome *B. cenocepacia* K56-2 (GenBank Accession LAUA00000000) and searched against all the bacterial essential genes in the Database of Essential Genes (DEG 10, version 14.7, updated Oct. 24, 2016) (Luo et al., 2014a) by BLASTP using the default parameters provided in DEG and an E-value cutoff of 10^{-10}. *B. cenocepacia* K56-2 homologs in *B. cenocepacia* J2315 (Wong et al., 2016a), *B. thailandensis* E264 (Baugh et al., 2013), and *B. pseudomallei* K96243 (Moule et al., 2014a) were identified as the best hit from

performing BLASTP using Geneious software with an E-value cutoff of 10^{-10}, minimum 30% sequence identity and 45% coverage. Operon predictions and clusters of orthologous category (COG) (Tatusov et al., 2000) were assigned to genes of *B. cenocepacia* K56-2 from the corresponding homologous gene in *B. cenocepacia* J2315 listed in the Database of Prokaryotic Operons DOOR (Mao et al., 2014b).

4.2.9 Statistical analysis of the growth phenotype distribution obtained from the primary screen

To analyze the growth phenotype of the mutants that survive the meropenem treatment two statistical methods, the Bhattacharya (Bhattacharya, 1967) and the Modified Gregor (Soriano, 1990) methods were retroactively carried out to determine a method that accurately separates the two populations.

The Bhattacharya method separates a multimodal distribution into separate normal distributions, its Gaussian components, by converting the distribution into a plot of logarithmic differences against class midpoints, from which the mean and standard deviation of each Gaussian component is calculated (Bhattacharya, 1967). After the removal of outliers in the distributions the logarithmic differences (Δln) of each class were calculated from the frequency data:

$$\Delta \ln Y_n = \ln Y_{n+1} - \ln Y_n$$

Where:

- Y_n is the frequency of class n
- Y_{n+1} is the frequency of the class above class n

The resulting logarithmic differences were plotted on the Y-axis against the class mid-points to produce a scatter plot. In the resulting plot, each line of negative slope corresponded to a Gaussian component. The points corresponding to each line were manually selected. Because the

distribution is bimodal, there were two lines of negative slope. The mean and standard deviation were calculated from each line of negative slope:

$$\mu = -\frac{a}{b} \qquad \sigma = -\frac{1}{b}$$

Where:

- a is the y-intercept of the line
- b is the slope of the line

After the mean and standard deviation of each Gaussian component were determined; they were used to plot two normal distributions to find the intercept of the two curves at the X-axis. This value indicates the growth ratio cut-off value for the conditional growth phenotype.

The Modified Gregor method separates a multimodal distribution into its Gaussian components by using the region within the two classes of the modal class of each Gaussian component to calculate the mean and variance of the corresponding Gaussian component (Soriano, 1990). The mean of each Gaussian component was determined by calculating the weighted average of the frequency data within two classes of the corresponding modal class. The area of the region within two classes of the modal class was required to calculate the variance of the corresponding Gaussian component. The area was calculated by first normalizing the frequency data to a probability by dividing the frequency of each class by the sample size. Afterwards, the midpoints of the 5 classes that made up the region was plotted against the normalized frequency data to fit a cubic equation using MATLAB R2015a. To calculate the area, the integral of the equation was calculated using Simpson's approximation.

$$\int_a^b f(x)dx \sim \frac{b-a}{3n}[f(x_0) + 4f(x_1) + 2f(x_2) + 4f(x_3) + 2f(x_4) \ldots + f(x_n)]$$

Where:

- a and b is the interval where the area is approximated
- n is an arbitrarily selected number of intervals between a and b
- x_0 to x_n are n + 1 equally spaced intervals between a and b

After calculating the area, the variance (σ^2) is calculated using the following expression described by Soriano (1990).

$$\sigma^2 = \frac{7(Y_{n+2} + Y_{n-2})}{12(Y_{n+2} + Y_{n-2})} + \frac{26(Y_{n+1} + Y_{n-1}) + 6(Y_n)}{24(Y_{n+1} + Y_{n-1}) - 72(Y_n)} * -A^2$$

Where:

- Y_n is the mode
- Y_{n-2} to Y_{n+2} are the frequencies of the 2 classes before the modal class to 2 classes after the modal class
- A is the area of the region within 2 classes of the modal class

The mean and variance were then used to plot two normal distributions to find the intercept of the two curves at the X-axis.

4.3 Results

4.3.1 Meropenem enrichment increases the frequency of obtaining CG mutants

To isolate CG mutants, a HDTM library of 1,000,000 mutants was subjected to an enrichment protocol (Figure 4.1), which is based on the method used to isolate auxotrophic mutants (Davis, 1948; Lederberg and Zinder, 1948). To revive the glycerol stocked transposon mutants of both essential and nonessential genes, the HDTM library was grown in the presence of rhamnose to early exponential phase. The mutant population was then cultured in the absence of

rhamnose to prevent the growth of CG mutants while allowing the other transposon mutants to replicate. Two subcultures in meropenem are 10x the MIC were performed to selectively kill the population of mutants of nonessential genes that are actively growing, but not the CG mutants. The transposon mutants recovered from the enrichment were then screened for rhamnose dependent growth.

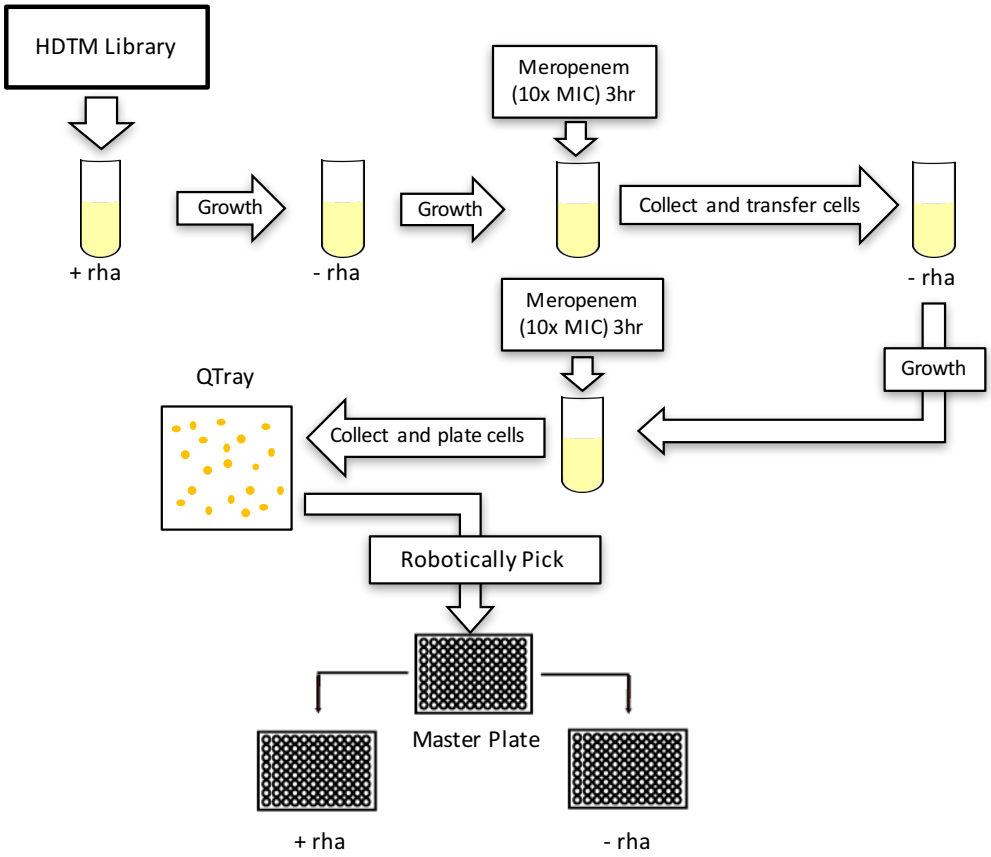

Figure 4.1 Construction of a meropenem enriched conditional growth mutant library.

Conditional growth (CG) mutants were enriched from the HDTM library by first growing the HDTM library in the presence of rhamnose to allow growth to early exponential phase. The HDTM library was then subcultured and grown in the absence of rhamnose, followed by meropenem treatment at 10x the MIC. After incubating for 3 h, the culture was pelleted and transferred to fresh media lacking rhamnose. A second dose of meropenem was subsequently added and the culture incubated for 3 h. Cells were then collected by filtering the culture, and the cells on the filter were plated on a QTray. The resulting colonies were robotically picked into 384-well master plates to be screened for the CG phenotype by comparing the growth in the presence and absence of rhamnose.

4.3.2 CG mutant library enriched from the 1M HDTM library

CG mutants were collected after performing one enrichment on an HDTM library of 1,000,000 (1M HDTM) mutants, created from 2 h triparental matings. 100-fold coverage of the 1M HDTM library was achieved by using approximately 10^9 CFU in the initial inoculum. From the meropenem enrichment, 2,304 mutants were collected. The original cut-off for screening for a growth defect in the absence of rhamnose was arbitrarily set for mutants with a growth ratio less than 0.5 and an OD_{600nm} greater than 0.1 in the presence of rhamnose to exclude CG mutants with a general growth defect (Bloodworth et al., 2013b). In theory, CG mutants where the rhamnose-inducible promoter is controlling an essential gene should not grow in the absence of rhamnose. The growth ratio cut-off of 0.5 was set to allow for residual growth due to low turnover of the essential protein, or the presence of an essential protein required a very low levels, compatible with transcription from the rhamnose promoter in the uninduced state (Bloodworth et al., 2013b). To explore the rational of choosing this cut-off value, we analyzed the growth phenotypes of the mutants that survived the meropenem-enrichment treatment. A scatter plot of growth in the absence vs. growth in the presence of rhamnose shows that the mutants consist of two populations (Figure 4.2). One population of mutants exhibited a growth defect in the absence of rhamnose while the other population did not. The mutants in these two populations could be approximately divided by a growth ratio of 0.8 (Figure 4.2B). This suggested that the growth ratio cut-off of 0.5 may be too stringent and that CG mutants may be being missed. Over 900 mutants had a growth ratio of less than 0.8, a much higher proportion than the 361 mutants with a growth ratio cut-off of 0.5 (Figure 4.2B).

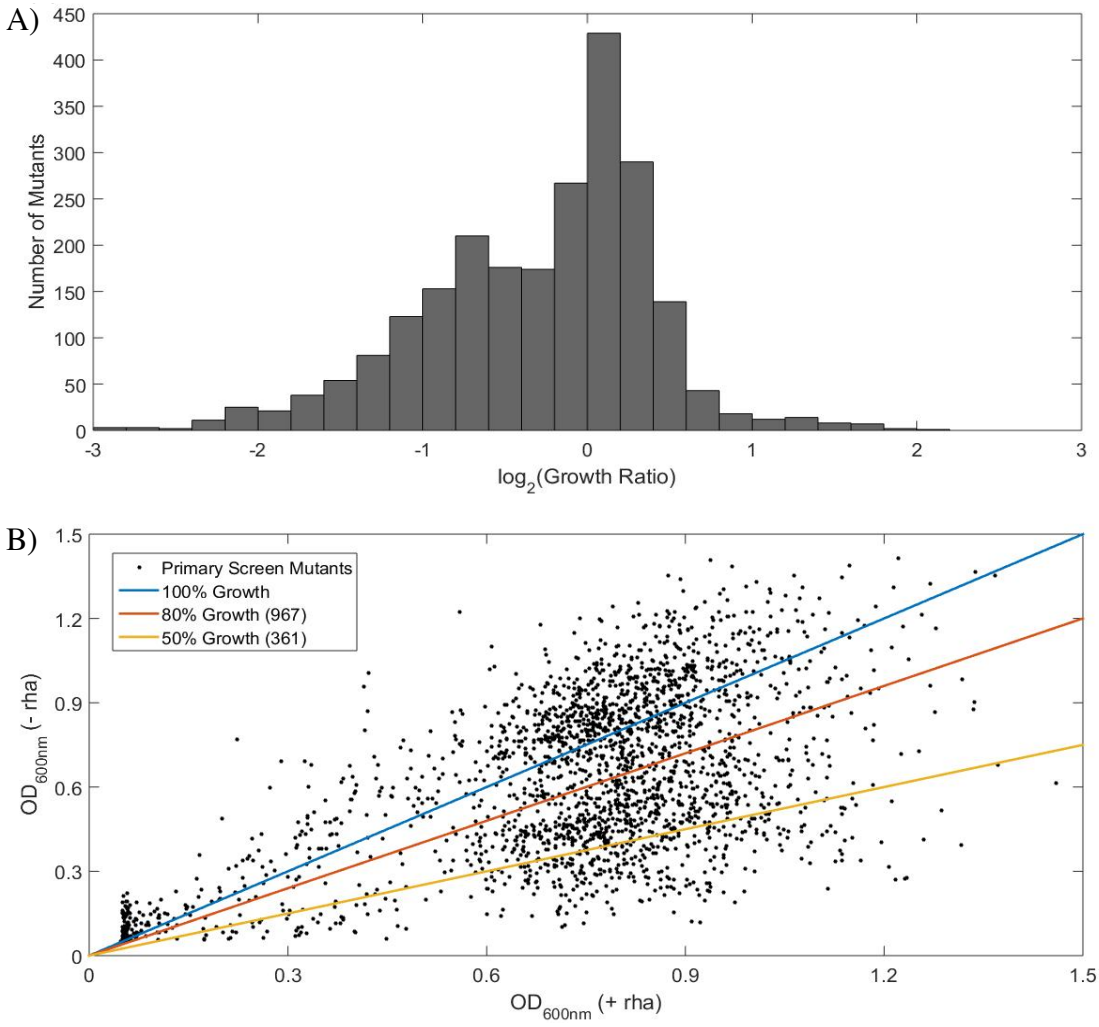

Figure 4.2 Primary screen of 2,304 mutants for the conditional growth phenotype.

Colonies from the meropenem enrichment were robotically picked into 384-well master plates containing LB medium with TMP100 and 0.2% rhamnose. Mutants were then replica plated after 48 h of growth at 37°C into 384-well plates containing LB TMP100 with or without 0.2% rhamnose. OD_{600nm} readings were taken after 18 h of growth at 37°C. A) The mutants exhibited a bimodal distribution between mutants with a growth defect in the absence of rhamnose and mutants without a growth defect. B) A growth ratio cut-off of 0.8 was selected to define the CG phenotype because it appeared to divide the two populations.

To determine the cut-off value that would more accurately differentiate the two populations for future screens, two statistical methods were used to analyze the bimodal distribution of mutants, the Modified Gregor method (Soriano, 1990) and the Bhattacharya method (Bhattacharya, 1967). The mean and variance of the two distributions was estimated using the Bhattacharya and Modified Gregor methods to determine the intercept point in the X-axis. The Bhattacharya and Modified Gregor methods identified intercepts of 0.737 and 0.868, respectively, as the growth ratio cut-off value that separates the two populations of mutants. (Figure 4.3). To allow for the inclusion of mutants of genes that may not be essential but important for growth, mutants were selected for a secondary screening if they had a growth ratio of 0.8 or less. Using a growth ratio cut-off of 0.8, 967 putative CG mutants were identified from the primary screen, which is close to the average number of mutants that would have been selected by both methods (Table 4.3).

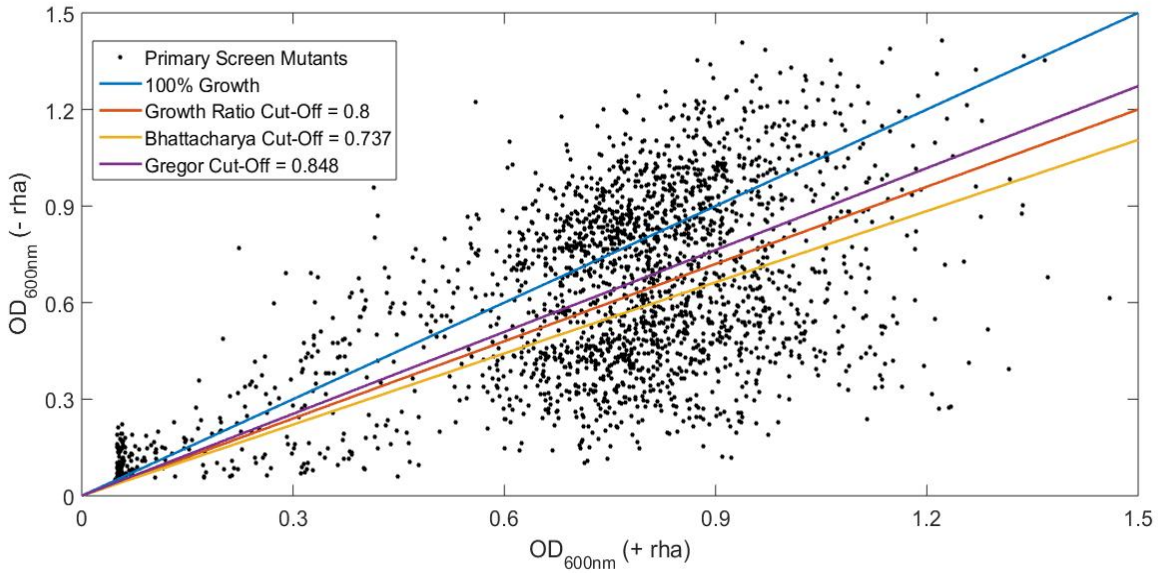

Figure 4.3. Separation of the distribution of CG mutants from the distribution of non CG mutants.

Colonies were robotically picked into 384-well master plates in LB medium containing 0.2% rhamnose, then replica plated after 48hr of growth at 37°C into 384-well plates containing LB with or without rhamnose. Optical density (OD_{600nm}) readings were taken after 18 h of growth at 37°C. The Bhattacharya (Bhattacharya, 1967) and Modified Gregor methods (Soriano, 1990) were used to determine a growth ratio cut-off value. Both methods set the cut-off values at approximately 0.8.

Table 4.3 Number of putative CG mutants identified from the Bhattacharya and Modified Gregor methods.

Method	Growth Ratio Cut-Off	Number of Putative CG Mutants
Actual	0.800	967
Bhattacharya	0.737	872
Modified Gregor	0.868	1,046

After a secondary screen for the rhamnose dependent growth phenotype, 852 CG mutants enriched from the 1M HDTM library had a growth ratio less than 0.8 and were individually collected and stored at -80ºC as glycerol stocks. In order to sequence the CG mutant library, equal amounts of each mutant (based on the OD_{600nm} of each mutant) were aliquoted together and sequencing ready libraries were prepared by Tn-seq circle (Gallagher et al., 2011c). From the 852 glycerol stocked CG mutants, the transposon insertion site was not identified for 14 as they had a slow growth phenotype in the presence of rhamnose. Eight hundred and thirty-eight of CG mutants were sequenced to determine the genes under the control of Pr*haB* (Table 4.4). More than 1500-fold read coverage of the library was achieved with 830 unique insertion sites identified (Table 4.4).

Table 4.4 CG mutants isolated after enrichment of the 1M HDTM library

No. of transposon mutants	1,000,000	200,000[1]
Treatment	(Enrichment[2])	(No enrichment)
Primary screen (No. of mutants)	2,304	200,000
No. of confirmed CG mutants	852	134
Hit frequency[3]	1 in 3	1 in 1500
No. of mutants sequenced	838	106
No. of unique mutants	830	106
No. of unique transcriptional units[5]	264	54

[1]Mutant library screened previously (Bloodworth et al., 2013a)
[2]The initial inoculation contained 10^9 cells from the 1M HDTM library.
[3]Number of confirmed CG mutant per mutants screened
[4]Putative transcriptional units under the control of P*rhaB*

Custom scripts were designed to find the location of the rhamnose-inducible promoter and call downstream genes based on the operons computationally predicted by DOOR (Mao et al., 2014b), in the clonally related isolate, *B. cenocepacia* J2315 (Holden et al., 2009b). Since insertion of the rhamnose-inducible promoter has a polar effect, it will control all the downstream genes in a transcriptional unit. In 50% of the 830 CG mutants identified, the P*rha* promoter is inserted either in the first 20% of the 5', within 20% of the 3', or within 1000 bps upstream of a gene and is oriented such that it is controlling the expression of an annotated open reading frame (orf). In these mutants, P*rhaB* is predicted to be controlling the expression of the gene it is located in, if inserted in the 5' end, or the downstream gene(s) predicted to be in the same transcription unit, if inserted in the 3' end of a gene. In 14 CG mutants, P*rhaB* inserted in an intergenic region within 1000 bases of a downstream gene. In 30% of the CG mutants, P*rhaB* is inserted within the interior 60% of a coding sequence and is predicted to be controlling the expression of downstream gene(s) predicted to be in the same transcriptional unit.

Less than 20% of the mutants from the meropenem enriched CG mutant library contain insertions where the P*rhaB* promoter is not located within 1000 bps upstream of an annotated gene. One has the transposon inserted in the center of WQ49_RS05110 (BCAM1883), which encodes a hypothetical protein. In this mutant, P*rhaB* is oriented in the opposite direction of both the gene it is inserted into, as well as the gene encoding a hypothetical protein located 800 bases downstream of P*rhaB*, WQ49_RS05115 (BCAM1884). However, two genes at the loci WQ_RS05105 and WQ_RS05100, encoding hypothetical proteins, are located 90 bases downstream of WQ_RS05115. These proteins are predicted to be in an operon and WQ_RS05100 is predicted to be essential. A second counter-oriented P*rhaB* insertion is located approximately 500 bases from the 5' end of a large gene, WQ49_RS06370 (BCAM2143), encoding a calcium-binding protein

that is not predicted to be essential in K56-2. The next gene downstream of the promoter is located approximately 9,300 bases away, WQ49_RS06375 (BCAM2144) encoding a hypothetical protein. No proteins within the vicinity are predicted to be essential by our essentiality analysis. Since the mutants in the CG mutant library were collected with a less stringent growth ratio cut-off of 0.8, it is possible that these mutants represent the 24% percent of the mutants with a growth ratio greater than 0.5. However, it is unknown whether mutants where P*rhaB* is not controlling the expression of an orf have a weaker growth defect in the absence of rhamnose.

4.3.3 P*rhaB* controls essential genes in the meropenem enriched CG mutants

The 830 unique CG mutants enriched from the 1M HDTM library represent 264 unique predicted transcriptional units (Table 4.5). Genes encoding core functions are located on chromosome 1 in *Burkholderia* species (Holden et al., 2009b; Juhas et al., 2012a). Consistent with this, 60% (159/264) of the transcriptional units identified in the meropenem-enriched CG mutants are located on this replicon. Approximately 29% (78/264), 8% (21/264) and 0.4% (1/264) of the unique transcriptional units are located on chromosomes 2, 3, and the plasmid, respectively. From the 264 unique operons identified in the meropenem enriched CG mutant library, 66% (175/264), contain genes that have homologs with essential genes in the DEG (Luo et al., 2014a). Sixty-two of the 264 (23.5%) putative operons identified, where P*rhaB* is oriented to control the expression of downstream genes, contain at least one gene that we predict to be essential in K56-2 (Table 4.5). The majority (87%) of the putative operons that contain at least one essential gene are located on chromosome 1, while 8% and 4% are located on chromosomes 2 and 3, respectively. All except 2 of the 62 predicted essential operons identified have homologs with essential genes in the DEG (Luo et al., 2014a). In these two operons, P*rhaB* is controlling the expression of WQ49_RS07605

located on chromosomes 2, and WQ49_RS08560, WQ49_RS08555 and WQ49_RS08550, located on chromosome 3. WQ49_RS07605 encodes a rifampin ADP-ribosyl transferase that is only predicted to be essential in K56-2, while WQ49_RS08555 encodes a hypothetical protein that is predicted to be essential in K56-2 and J2315 (Wong et al., 2016a).

Table 4.5. Summary of meropenem enriched CG mutant library

No. of unique CG mutants identified	830
No. of unique transcriptional units identified[1]	264
No. of unique transcriptional units containing at least one essential gene[1]	62
Percent of the essential operons represented[2]	17.3%
Percent of CG mutants with the P*rhaB* located upstream of genes identified as essential in *B. cenocepacia* K56-2[3]	47.4%
Percent of CG mutants with the P*rhaB* not located upstream of an orf	19.8%

[1] P*rhaB* predicted to be controlling the expression of an orf
[2] *B. cenocepacia* K56-2 putative essential operons
[3] *B. cenocepacia* K56-2 putative essential genes

4.3.4 Functional categories represented by the meropenem enriched CG mutant library

The four main functional COG categories are represented by 667 genes that are predicted to be controlled by P*rhaB* in the 830 unique mutants. CG mutants of genes involved in metabolism are the most overrepresented functional categories compared to the essential and non-essential genes of *B. cenocepacia* K56-2 (Figure 4.4). Of the unique mutants in the meropenem-enriched library, the category with the most significantly enriched genes over the non-enriched CG mutant library and the predicted essential gene set are involved in amino acid transport and metabolism (p-value <0.05, Fisher's exact test) and underrepresented in the cell wall/membrane/envelope biogenesis and the cell cycle control/cell division/chromosome partitioning categories (p-value <0.05, Fisher's exact test). In contrast to the non-enriched CG mutant library (Bloodworth et al., 2013a) and the predicted essential gene set, only one mutant of the genes involved in the cell cycle control/cell division/chromosome partitioning functional category was identified in the meropenem enriched CG mutant library.

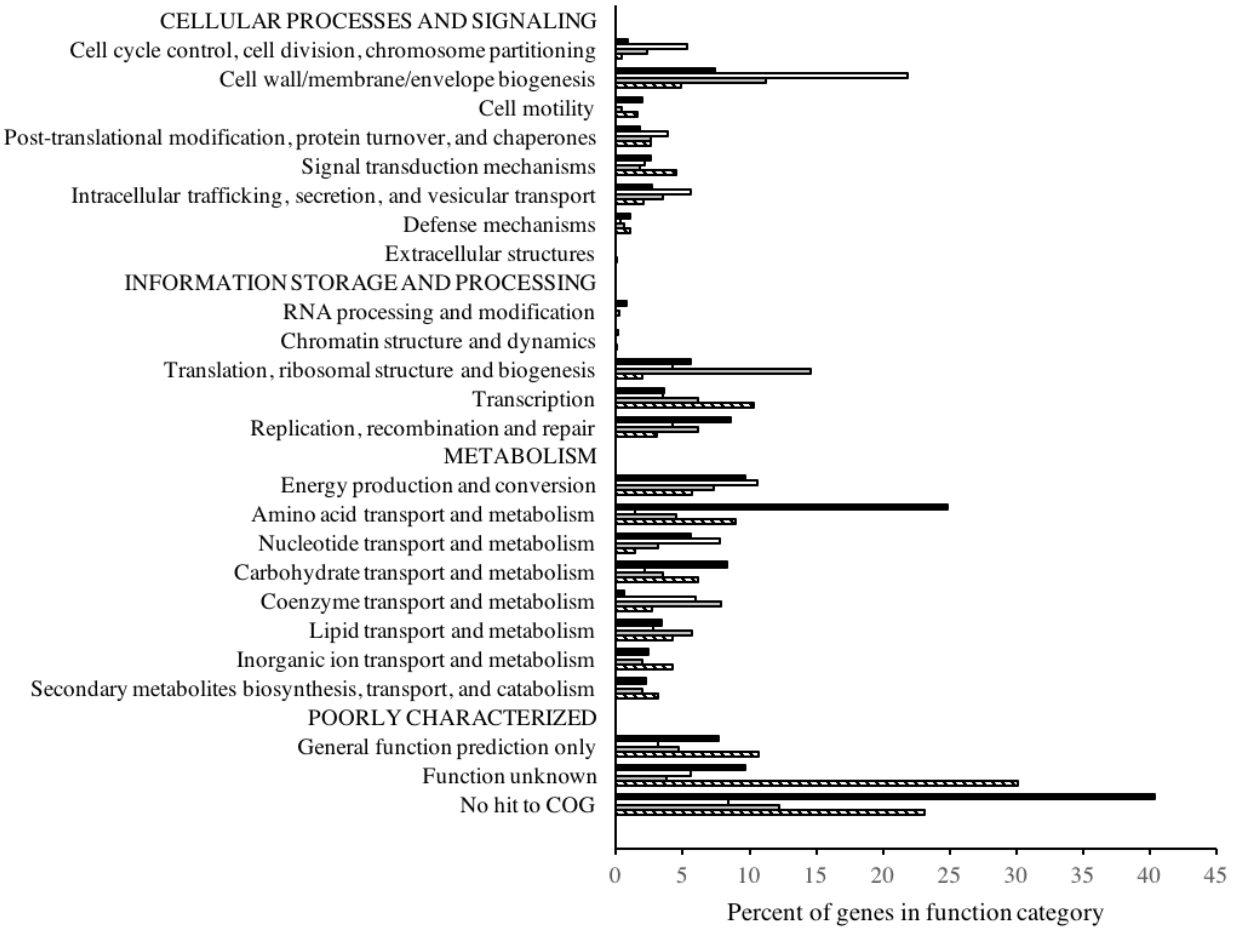

Figure 4.4 Distribution of the functional categories from the meropenem enriched CG mutants, non-enriched CG mutant library, and the essential and non-essential gene sets of *B. cenocepacia* K56-2.

The percent of genes in functional categories (X-axis) from genes under the control of P*rhaB* in CG mutants that were isolated after enrichment with meropenem (black bars) and without enrichment (white bars). The functional categories represented by the genes predicted to be essential (gray bars) and non-essential (hatched bars) in *B. cenocepacia* K56-2 are also shown.

The meropenem enrichment of the HDTM libraries improved the frequency of CG mutants obtained from 1 in 1500 to an average of 1 in 3 (Table 4.4). The mutants that did not show a CG phenotype were not investigated but likely survived the meropenem treatment by entering into a persister state (Lewis, 2010). The enrichment of gene functions of the CG mutants was consistent with those enriched in the essential genome of *B. cenocepacia* K56-2. In the majority of CG mutants identified, P*rhaB* is predicted to control the expression of at least one gene that is essential in *B. cenocepacia* K56-2 or has a homolog in the database of the essential genes. Overall, these results suggest that using the enrichment, we are isolating mutants of essential genes and the less stringent growth ratio cut-off of 0.8 in the secondary screen did not significantly increase the proportion of mutants with P*rhaB* controlling the expression of genes not predicted to be essential for growth. Combined with the original CG mutant library (Bloodworth et al., 2013a), we now have 296 unique transcriptional units containing 23% (83/358) of the prediction essential operons in *B. cenocepacia* K56-2. In addition, 58 of the 158 essential genes shared between *B. cenocepacia* K56-2, *B. cenocepacia* J2315 (Wong et al., 2016a), *B. thailandensis* E264 (Baugh et al., 2013) and *B. pseudomallei* K96243 (Moule et al., 2014a)., which represent common essential antibiotic targets in the *Burkholderia* genus identified thus far, are represented in the CG library.

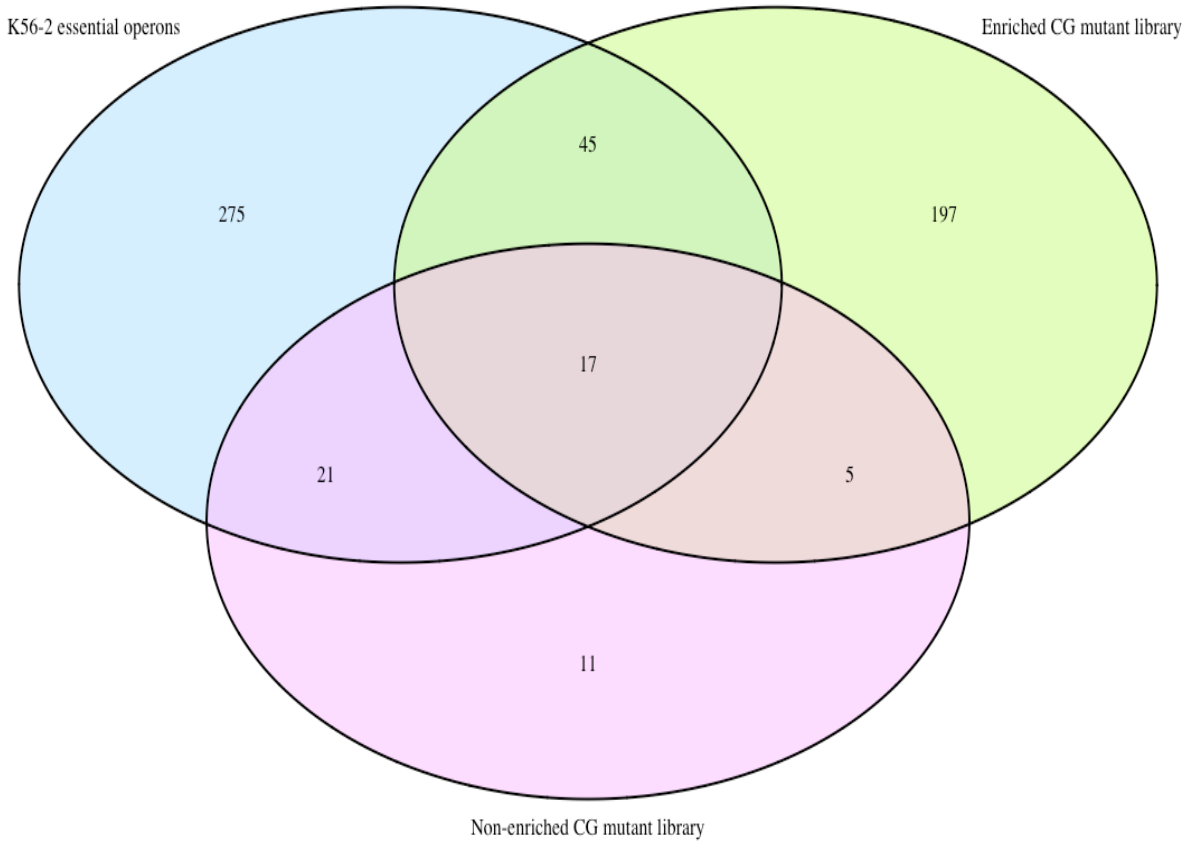

Figure 4.5 Proportion of essential operons identified in *B. cenocepacia* K56-2 represented by the non-enriched, and enriched CG mutants.

The common and unique genes between *B. cenocepacia* K56-2 essential gene set, and the genes from unique transcriptional units from the meropenem-enriched CG mutants (Enriched CG mutant library) and the previously created CG mutant library (Non-enriched CG mutant library) (Bloodworth et al., 2013a).

4.4 Discussion

Using high-density transposon mutangenesis, we previously identified 508 genes to be essential in K56-2. While saturated transposon mutagenesis allows for the identification identifying novel antibiotic targets, it does not produce essential gene mutants to assay in chemogenetic screens to identify the targets of novel antibiotics. Since essential gene deletion mutants are not viable, either controlled depletion or increased expression of the essential gene is required to investigate their functions.

We previously used random transposon mutagenesis to deliver P*rhaB* into the genome of *B. cenocepacia* K56-2 to recover CG mutants. However, we were unable to achieve genomic coverage of the essential genes. The reason for the bottleneck in isolating CG mutants is unknown, but our analysis showed that this was not likely due to the expression range of the P*rhaB* promoter, or a bias of the Tn5 transposon (Bloodworth et al., 2013a). In this work we exploited the fact that CG mutants remain viable for 24 h in the absence of rhamnose (Bloodworth et al., 2015) to enrich for CG mutants from a HDTM library of non-essential and essential gene mutants. We used Tn-seq circle (Gallagher et al., 2011c) to identify the insertion sites in the CG mutants and quantify the relative abundance of mutants in the library. Using this method, we isolated a diverse population of CG mutants and increased the frequency of identifying CG mutants 500-fold (Table 4.4).

Eight hundred and thrirty CG mutants were identified from screening 2,304 transposon mutants that were collected after meropenem enrichment of the HDTM library. CG mutants representing 264 unique putative transcriptional units were recovered from screening a fraction of the 200,000 transposon mutants that was required previously to recover 106 CG mutants

representing 54 transcriptional units (Bloodworth et al., 2013a). Eighty-nine percent of the 62 operons containing genes that are predicted to be essential in *B. cenocepacia* K56-2, are also predicted to essential in at least one of *B. cenocepacia* J2315 (Wong et al., 2016a), *B. cenocepacia* E264 (Baugh et al., 2013) or *B. pseudomallei* K96243 (Moule et al., 2014a). Of the 9 genes that were not, 5 have essential homologs in the DEG (Luo et al., 2014a). From the 62 unique operons in the meropenem enriched CG mutant library that contain an essential gene, 23.5% have more than one essential gene. Even considering that the meropenem enriched CG mutant library contains mutants representing redundant operons, the rate of identifying new operons was improved to 1 in 9, over 400-fold higher than was achieved without the enrichment protocol. In addition, having CG mutants that represent different regions of an operon is useful since essential genes tend to cluster in operons (Luo et al., 2014a). Because of the potential polar effect of P*rhaB*, the inclusion of mutants with insertion into different regions in the operon will allow for more precise target identification in chemogenetic screens. Approximately 66% of the 264 operons are represented by CG mutants with insertions into multiple regions in the operon. Among the 264 unique putative operons identified, we recovered CG mutants where P*rhaB* is controlling the expression of transcripts containing genes that have been experimentally determined as essential in *Burkholderia* species, including two involved in coenzyme transport and metabolism (*dxs, hemE*) and translation (*infB*, *valS*), replication (*gyrB*), ubiquinone biosynthesis (*ubiB)* and a hypothetical protein homologous to BCAL3369 in *B. cenocepacia* J2315 (Cardona et al., 2006b; Juhas et al., 2012b; Mohamed and Valvano, 2014; Ortega et al., 2007a).

There were CG mutants identified where an essential gene homolog could not be placed within 1000 bp downstream of P*rhaB*. These mutants comprise less than 20% of the unique CG mutants identified. The reason why these mutants, where P*rhaB* is inserted into genes in the

opposite orientation from their transcription or in an intergenic region more than 1000 bp upstream of a orf, have a conditional growth phenotype is unclear. It is possible that these mutants have a weak conditional growth phenotype, since they were identified as part of the CG library that was collected using the less stringent growth ratio cut-off of 0.8. Alternatively, recent studies have highlighted the involvement of non-coding RNA in regulating essential functions (van Wolfswinkel and Ketting, 2010). It is possible that in these mutants, the placement of P*rhaB* is preventing the expression of non-coding RNA that is acting as a regulator of an essential process.

Limitations for meropenem-enrichment of CG libraries

It is notable that only two CG mutants were isolated where P*rhaB* is controlling genes involved in cell division, considering that is was an enriched functional category in the essential genes identified for *B. cenocepacia* K56-2. We believe this bias was introduced because of the use of the cell wall synthesis inhibitor, meropenem, to enrich for CG mutants. It is expected that CG mutants depleted in proteins involved in cell division would be hypersensitive to meropenem treatment. It is apparent that the mechanism of action of the antibiotic used to enrich for CG mutants can bias the functions represented by the mutants. Therefore, in order to recover mutants of all the essential functional groups, future enrichments should be performed using other bactericidal antibiotics with different mechanisms of action, such as ciprofloxacin.

The mutants from the enriched HDTM libraries that did not show a CG phenotype were not analyzed, but could have survived the meropenem treatment by entering into a persister state (Lewis, 2010). The enrichment of genes involved in metabolism and transport indicates a bias of the CG mutant enrichment. The enrichment method used was originally designed to enrich cultures for rare auxotrophic mutants from a wildtype prototrophic population (Davis, 1948; Lederberg and

Zinder, 1948). It is interesting that CG mutants where P*rhaB* is controlling genes involved in metabolism and transport were enriched more so than those from the essential gene prediction and the original conditional growth mutant library. A situation could arise where the combined effect of mutation plus depletion of a non-essential gene creates an auxotroph that requires a metabolite that is limited or not present in LB. Regardless, when used in the competitive enhanced sensitivity assay, any hits identified would need to be confirmed in a newly generated mutant, as done previously (Bloodworth et al., 2013a; Gislason et al., 2017).

Combined with the original CG mutant library, and CG mutants isolated previously, we currently have a CG mutant library representing 297 unique transcriptional units that contain 23% of the 358 putative essential operons identified in *B. cenocepacia* K56-2 (Figure 4.5). Forty-five new operons containing at least one essential gene, were added to our collection of CG mutants (Bloodworth et al., 2013a) by screening a meropenem-enriched HDTM library for a conditional growth phenotype. Combined with the previously isolated CG mutants, our CG mutant library represents 58 of the 158 essential genes that are common to different *Burkholderia* species. It is notable that using the enrichment successfully increased the frequency of recovering unique essential operons over 400-fold in a single enrichment of the 1M HDTM library. To recover a more diverse library of CG mutants, the incubation times and inoculum size should be varied in addition to modifying the drug used to select against transposon mutants of non-essential genes. Three different growth phenotypes are exhibited by CG mutants in the absence of rhamnose: slow growth rate, no growth, and early onset of stationary phase. By varying the incubation time used to recover the glycerol stocked HDTM library and performing multiple enrichments using a smaller inoculum size, we predict that genomic coverage of the essential genome is attainable using the enrichment method.

Applications of the CG mutant library

The detectability of each CG mutant in the library will depend on the growth phenotypes of the individual CG mutants. Sensitization of CG mutants is achieved when the CG mutants are growth in rhamnose concentrations that induce 30-60% of wildtype growth (Bloodworth et al., 2013a; Gislason et al., 2017). In the previous competitive ESA, CG mutants were grouped for pooled growth if they had a similar rhamnose-dependent growth phenotype. For the current CG mutant library, instead of previous characterization of the response to rhamnose for each mutant, all the CG mutants can be grown together at different rhamnose concentrations. This would result in a certain population of the mutants be sensitized, that would vary with the rhamnose concentration the library is exposed to.

Since the HDTM library was grown in the presence of rhamnose, it would be theoretically possible to screen the HDTM in different concentrations of rhamnose in the presence and absence of antibiotic. Assaying the HDTM in this way would allow for the identification of non-essential accessory genes required to buffer the effect of the antibiotic treatment. However, because of the growth defect needed to induce sensitization of the CG mutants, they could be outcompeted by other mutants that do not have a growth defect. This would be confounded by their underrepresentation in the library with respect to mutants with insertion in nonessential genes, which would also require high sequencing depth of the library. By assaying just the CG mutants, the likelihood of recovering all the CG mutants increases at a much lower sequencing depth.

Using this array of CG mutants in a competitive ESA will provide a tool to expedite matching novel antibiotics to bacterial targets, as well aid in chemical optimization during the antibiotic development process. For any drug to be implemented as an antibiotic therapy,

successive rounds of chemical optimization processes are typically employed. At each stage of the optimization process, the compound is altered, which can affect its specificity for the target positively or negatively. In general, mutants representing the target of the antibiotic have the strongest signal in chemogenetic screens (Pathania et al., 2009). Therefore, a deviation from the original signal could indicate a change the specificity of the compound. In addition, during the optimization stage, each modification can be assessed for its activity using phenotypic screens such as transcriptomic profiling (Murima et al., 2013). Similar to the gene expression signatures from these phenotypic screens, the enhanced sensitivity profile of an array of CG mutants can provide a signature for the mechanism of action (Donald et al., 2009a; Xu et al., 2010b).

Chapter 5: Conclusions

Burkholderia cenocepacia is a multidrug resistant Gram-negative bacterium that causes fatal lung infections in immunocompromised and cystic fibrosis (CF) patients (Mahenthiralingam et al., 2005a). In order to develop therapeutics to treat *B. cenocepacia* infections and infections caused by other antibiotic resistant bacteria, novel antibiotics need to be developed (Forum, 2014; Organization, 2014; Spellberg et al., 2008). The successful antibiotics currently in use target only a few essential genes involved in protein synthesis, DNA replication and cell wall synthesis. Therefore, it is likely that the identification of new essential genes will provide suitable targets for novel antibiotics (Murima et al., 2013). Furthermore, since resistance mechanism have developed to combat the action of antibiotics currently in use, novel essential processes need to be targeted in order to bypass theses resistance mechanisms. A previous attempt to make a CG mutant library using random transposon mutagenesis had a low recovery rate of CG mutants and did not reach genomic coverage (Bloodworth et al., 2013a).

The objectives of this thesis were to enrich a HDTM library for CG mutants to increase the frequency of recovering CG mutants in order to reach genomic coverage of the essential genes of *B. cenocepacia* K56-2. The HDTM library was also sequenced to determine the essential genome of *B. cenocepacia* K56-2. In order to use an essential gene library in a chemogenomic screen against novel antibiotics, the throughput of the ESA needed to be increased. In a proof of principle experiment, we demonstrated that CG mutants could be grown together competitively in the ESA, and that their relative abundance can be measured by next generation sequencing.

For the competitive ESA, a pilot library of 25 CG mutants was screened against 8 antibiotics with known MOAs. The purpose of this work was to show that the enhanced sensitivity of the CG*gyrB* mutant to its cognate antibiotic, novobiocin, could be detected by NGS after competitive growth within the pool of mutants. Using this method, the enhanced sensitivity of

CG*gyrB* to novobiocin, was successfully measured and the level of enhanced sensitivity was increased due to competitive growth. In addition, the competitive ESA revealed an essential TCS, EsaSR, that can be targeted to reduce antibiotic resistance in *B. cenocepacia*. This was a significant finding since TCSs are considered valuable drug targets because they are not present in humans and targeting them could reduce virulence (Gotoh et al., 2010). Finding an inhibitor of a TCS involved in antibiotic resistance could provide adjuvant therapies for effective treatment of multidrug resistant infections in combination with current antibiotics.

While these results suggest that EsaSR is regulating processes involved in maintaining the cell envelope, the mechanism by which it is achieving this is unknown. Another student has based his Master's thesis on characterizing EsaSR and identifying the genes it regulates. Since sensitized CG*esaR* is more susceptible to multiple antibiotics distinguishing inhibitors that target EsaR or EsaR-related processes directly in the competitive ESA is not possible. Identification of the genes regulated by EsaSR would allow for the creation of a reporter system that could be used for further characterization and to identify EsaSR inhibitors.

The next objective for this thesis was to create a HDTM library to determine the essential genome as well as develop a method to enrich for mutants that have the P*rhaB* controlling the expression of an essential gene to add to the CG mutant library.

By creating and sequencing a HDTM library of 1,000,000 mutants, 508 essential genes were identified in *B. cenocepacia* K56-2. From comparing the essential gene set with other strains of *Burkholderia*, 158 genes were identified that are also essential in *B. cenocepacia* J2315, *B. thailandensis* and *B. pseudomallei*. Three genes within this common essential gene set encode proteins that contribute to the integrity of the cell envelope and were identified as uniquely essential in *Burkholderia*. This finding indicates that the intrinsic antimicrobial resistance and cell

envelope impermeability that characterizes the *Burkholderia* genus has evolved under strong selective pressure, turning these non-essential functions into mechanisms tied to survival.

Twenty-two and 6 of the predicted essential genes are located on chromosome 3 and the plasmid, respectively, which have been shown to be dispensable for growth in *B. cenocepacia* (Agnoli et al., 2012). It is possible that we are overestimating the number of genes that are strictly essential for growth, and including genes that may not be essential, but are important for growth. It is also not known if the set of essential genes identified in J2315, but not K56-2 are truly strain-specific essential genes. Since the HDTM library was grown in the presence of rhamnose to allow for the expression of downstream genes, we classified insertions within the first 10% of the 5' end of a gene as non-disruptive and did not consider them in the essentiality analysis. However, it is possible that insertions within this region could result in a non-functional protein and that by not considering them in the analysis, these essential genes were not recognized as essential.

A limitation of this work was the insertion and read bias of the HDTM at A/T rich regions. The Tn5 transposon is not known to have insertion bias into A/T rich regions, however, a similar trend of high insertion events in A/T-rich regions of *B. pseudomallei* using the Tn5 transposon has been seen (Moule et al., 2014a). It is not known if this bias in the recovery of insertion in A/T rich regions is a biological occurrence or due to a bias from library preparation and sequencing. However, in two independent essential gene studies of *P. aeruginosa* PAO1 (Jacobs et al., 2003) and PA14 (Liberati et al., 2006), using a Tn5 transposon and a mariner transposon, approximately half of the orthologs identified using the mariner Tn were not hit by Tn5 (Liberati et al., 2007). For a more accurate estimation of the essential genome, biological replicates of HDTM libraries made with different transposons should be sequenced.

Approximately 2,300 transposon mutants were recovered from one meropenem enrichment of the HDTM library. Over one third of these mutants had a conditional growth phenotype and using the enrichment increased the frequency of recovery 500-fold. While only two CG mutants were identified where P*rhaB* is controlling genes involved in cell division was isolated, it is likely because these mutants are hypersensitive to meropenem. We believe that CG mutants representative of all the essential functional categories are recoverable by varying the type of antibiotic used in the enrichment. The CG mutants we have identified so far have three general growth phenotypes in the absence of rhamnose - slow growth rate, no growth, and early onset of stationary phase. Therefore, for future enrichments, varying the incubation times and inoculum size should help to recover CG mutants with more diverse phenotypes.

In total, 830 unique conditional growth mutants were isolated from one enrichment, adding 45 new operons to the existing CG mutant library that was created previously (Bloodworth et al., 2013a). We now have a CG mutant library representing unique essential operons that contain 23.2% of the 508 essential operons in K56-2 and 36.7% of the essential genes that are common among *B. cenocepacia* K56-2, *B. cenocepacia* J2315, *B. thailandensis* E264 and *B. pseudomallei*.

The limitation of the competitive ESA was that the use of multiplex primers limited the number of strains that could be assayed using the multiplex PCR. Future competitive enhanced sensitivity assays would benefit from the use of a method that does not require the use of multiplexed primers. To sequence the HDTM and CG mutant libraries, an adapted Tn-seq circle method developed by Gallagher et al. was used that does not require multiplex primers to amplify the transposon genome junctions (Gallagher et al., 2011a). In order to include all the CG mutants in the competitive ESA, this method could be used to create the sequencing libraries.

Future HDTM libraries would benefit from the use of a barcoded transposon as with RBTn-Seq (Smith et al., 2009). After creation of the HDTM using the barcoded transposon, one sequencing run using Tn-seq circle would be required to associate the barcode with the insertion site. Once the insertion sites have been barcoded, CG mutants could be tracked by sequencing the amplified barcodes. This would limit any bias seen from amplicons with differing sizes and GC content.

The HDCG library created in this work will provide a powerful tool in the high-throughput competitive ESA to expedite matching new antibiotics to bacterial targets and aid in chemical optimization during the antibiotic development process.

Literature cited

Agnoli, K., Schwager, S., Uehlinger, S., Vergunst, A., Viteri, D.F., Nguyen, D.T., Sokol, P.A., Carlier, A., and Eberl, L. (2012). Exposing the third chromosome of *Burkholderia cepacia* complex strains as a virulence plasmid. Mol. Microbiol. *83*, 362–378.

Ahn, Y., Kim, J.M., Kweon, O., Kim, S.J., Jones, R.C., Woodling, K., Costa, G.G. da, LiPuma, J.J., Hussong, D., Marasa, B.S., et al. (2016). Intrinsic Resistance of *Burkholderia cepacia* Complex to Benzalkonium Chloride. mBio *7*, 10.1128/mBio.01716-16.

Aird, D., Ross, M.G., Chen, W.-S., Danielsson, M., Fennell, T., Russ, C., Jaffe, D.B., Nusbaum, C., and Gnirke, A. (2011). Analyzing and minimizing PCR amplification bias in Illumina sequencing libraries. Genome Biol. *12*, R18.

Altschul, S.F., Gish, W., Miller, W., Myers, E.W., and Lipman, D.J. (1990). Basic local alignment search tool. J. Mol. Biol. *215*, 403–410.

Amaral, M.D., and Kunzelmann, K. (2007). Molecular targeting of CFTR as a therapeutic approach to cystic fibrosis. Trends Pharmacol. Sci. *28*, 334–341.

Amato, S.M., Fazen, C.H., Henry, T.C., Mok, W.W.K., Orman, M.A., Sandvik, E.L., Volzing, K.G., and Brynildsen, M.P. (2014). The role of metabolism in bacterial persistence. Front. Microbiol. *5*, 70.

Anders, S., McCarthy, D.J., Chen, Y., Okoniewski, M., Smyth, G.K., Huber, W., and Robinson, M.D. (2013). Count-based differential expression analysis of RNA sequencing data using R and Bioconductor. Nat. Protoc. *8*, 1765–1786.

Andries, K., Verhasselt, P., Guillemont, J., Gohlmann, H.W., Neefs, J.M., Winkler, H., Gestel, J.V., Timmerman, P., Zhu, M., Lee, E., et al. (2005). A diarylquinoline drug active on the ATP synthase of *Mycobacterium tuberculosis*. Science *307*, 223–227.

Antony, B., Cherian, E.V., Boloor, R., and Shenoy, K.V. (2016). A sporadic outbreak of *Burkholderia cepacia* complex bacteremia in pediatric intensive care unit of a tertiary care hospital in coastal Karnataka, South India. Indian J. Pathol. Microbiol. *59*, 197–199.

Aris, R.M., Routh, J.C., LiPuma, J.J., Heath, D.G., and Gilligan, P.H. (2001). Lung transplantation for cystic fibrosis patients with *Burkholderia cepacia* complex. Survival linked to genomovar type. AmJRespirCritCare Med *164*, 2102–2106.

Aronoff, S.C. (1988). Outer membrane permeability in *Pseudomonas cepacia*: diminished porin content in a beta-lactam-resistant mutant and in resistant cystic fibrosis isolates. Antimicrob. Agents Chemother. *32*, 1636–1639.

Arunmanee, W., Pathania, M., Solovyova, A.S., Le Brun, A.P., Ridley, H., Baslé, A., van den Berg, B., and Lakey, J.H. (2016). Gram-negative trimeric porins have specific LPS binding sites that are essential for porin biogenesis. Proc. Natl. Acad. Sci. U. S. A. *113*, E5034-5043.

Aubel-Sadron, G., and Londos-Gagliardi, D. (1984). Daunorubicin and doxorubicin, anthracycline antibiotics, a physicochemical and biological review. Biochimie *66*, 333–352.

Aubert, D.F., Hu, S., and Valvano, M.A. (2015). Quantification of type VI secretion system activity in macrophages infected with *Burkholderia cenocepacia*. Microbiol. Read. Engl. *161*, 2161–2173.

Azad, M.A., and Wright, G.D. (2012). Determining the mode of action of bioactive compounds. Bioorg. Med. Chem. *20*, 1929–1939.

Baba, T., Ara, T., Hasegawa, M., Takai, Y., Okumura, Y., Baba, M., Datsenko, K.A., Tomita, M., Wanner, B.L., and Mori, H. (2006). Construction of *Escherichia coli* K-12 in-frame, single-gene knockout mutants: the Keio collection. Mol. Syst. Biol. *2*, 2006.0008.

Badarinarayana, V., 3rd, P.W.E., Shendure, J., Edwards, J., Tavazoie, S., Lam, F., and Church, G.M. (2001). Selection analyses of insertional mutants using subgenic-resolution arrays. Nat. Biotechnol. *19*, 1060–1065.

Baell, J., and Walters, M.A. (2014). Chemistry: Chemical con artists foil drug discovery. Nature *513*, 481–483.

Baell, J.B., and Holloway, G.A. (2010). New substructure filters for removal of pan assay interference compounds (PAINS) from screening libraries and for their exclusion in bioassays. J. Med. Chem. *53*, 2719–2740.

Baldwin, A., Sokol, P.A., Parkhill, J., and Mahenthiralingam, E. (2004). The *Burkholderia cepacia* epidemic strain marker is part of a novel genomic island encoding both virulence and metabolism-associated genes in *Burkholderia cenocepacia*. Infect.Immun. *72*, 1537–1547.

Baldwin, A., Mahenthiralingam, E., Drevinek, P., Vandamme, P., Govan, J.R., Waine, D.J., LiPuma, J.J., Chiarini, L., Dalmastri, C., Henry, D.A., et al. (2007). Environmental *Burkholderia cepacia* complex isolates in human infections. Emerg. Infect. Dis. *13*, 458–461.

Balkhy, H.H., Cunningham, G., Francis, C., Almuneef, M.A., Stevens, G., Akkad, N., Elgammal, A., Alassiri, A., Furukawa, E., Chew, F.K., et al. (2005). A National Guard outbreak of *Burkholderia cepacia* infection and colonization secondary to intrinsic contamination of albuterol nebulization solution. Am. J. Infect. Control *33*, 182–188.

Baranova, N., and Nikaido, H. (2002). The *baeSR* two-component regulatory system activates transcription of the *yegMNOB* (*mdtABCD*) transporter gene cluster in *Escherichia coli* and increases its resistance to novobiocin and deoxycholate. J. Bacteriol. *184*, 4168–4176.

Barquist, L., Langridge, G.C., Turner, D.J., Phan, M.-D., Turner, A.K., Bateman, A., Parkhill, J., Wain, J., and Gardner, P.P. (2013). A comparison of dense transposon insertion libraries in the *Salmonella serovars Typhi* and *Typhimurium*. Nucleic Acids Res. *41*, 4549–4564.

Baugh, L., Gallagher, L.A., Patrapuvich, R., Clifton, M.C., Gardberg, A.S., Edwards, T.E., Armour, B., Begley, D.W., Dieterich, S.H., Dranow, D.M., et al. (2013). Combining functional and structural genomics to sample the essential *Burkholderia* structome. PloS One *8*, e53851.

Bazzini, S., Udine, C., Sass, A., Pasca, M.R., Longo, F., Emiliani, G., Fondi, M., Perrin, E., Decorosi, F., Viti, C., et al. (2011). Deciphering the Role of RND Efflux Transporters in *Burkholderia cenocepacia*. PloS One *6*, e18902.

Beckman, W., and Lessie, T.G. (1979a). Response of *Pseudomonas cepacia* to beta-Lactam antibiotics: utilization of penicillin G as the carbon source. J. Bacteriol. *140*, 1126–1128.

Beckman, W., and Lessie, T.G. (1979b). Response of *Pseudomonas cepacia* to beta-Lactam antibiotics: utilization of penicillin G as the carbon source. J. Bacteriol. *140*, 1126–1128.

Bell, S.C., Boeck, K.D., and Amaral, M.D. (2015). New pharmacological approaches for cystic fibrosis: Promises, progress, pitfalls. Pharmacol. Ther. *145*, 19–34.

Benjamini, Y., and Hochberg, Y. (1995). Controlling the False Discovery Rate: A Practical and Powerful Approach to Multiple Testing. J. R. Stat. Soc. Ser. B Methodol. *57*, 289–300.

Bentley, D.R., Balasubramanian, S., Swerdlow, H.P., Smith, G.P., Milton, J., Brown, C.G., Hall, K.P., Evers, D.J., Barnes, C.L., Bignell, H.R., et al. (2008). Accurate whole human genome sequencing using reversible terminator chemistry. Nature *456*, 53–59.

Berg, D.E., Davies, J., Allet, B., and Rochaix, J.D. (1975). Transposition of R factor genes to bacteriophage lambda. Proc. Natl. Acad. Sci. U. S. A. *72*, 3628–3632.

Bernhardt, S.A., Spilker, T., Coffey, T., and LiPuma, J.J. (2003). *Burkholderia cepacia* complex in cystic fibrosis: frequency of strain replacement during chronic infection. Clin. Infect. Dis. Off. Publ. Infect. Dis. Soc. Am. *37*, 780–785.

Bhattacharya, C.G. (1967). A Simple Method of Resolution of a Distribution into Gaussian Components. Biometrics *23*, 115–135.

Blomberg, A. (2011). Measuring growth rate in high-throughput growth phenotyping. Curr. Opin. Biotechnol. *22*, 94–102.

Bloodworth, R. (2013). Essential genes and genomes of the *Burkholderia cepacia* complex.

Bloodworth, R.A., Gislason, A.S., and Cardona, S.T. (2013a). *Burkholderia cenocepacia* conditional growth mutant library created by random promoter replacement of essential genes. MicrobiologyOpen *2*, 243–258.

Bloodworth, R.A., Gislason, A.S., and Cardona, S.T. (2013b). *Burkholderia cenocepacia* conditional growth mutant library created by random promoter replacement of essential genes. MicrobiologyOpen *2*, 243–258.

Bloodworth, R.A., Zlitni, S., Brown, E.D., and Cardona, S.T. (2015). An electron transfer flavoprotein (ETF) is essential for viability and its depletion causes a rod-to-sphere change in *Burkholderia cenocepacia*. Microbiol. Read. Engl. *161*, 1909–1920.

Bohacek, R.S., McMartin, C., and Guida, W.C. (1996). The art and practice of structure-based drug design: a molecular modeling perspective. Med. Res. Rev. *16*, 3–50.

Boucher, H.W., Talbot, G.H., Bradley, J.S., Edwards, J.E., Gilbert, D., Rice, L.B., Scheld, M., Spellberg, B., and Bartlett, J. (2009). Bad bugs, no drugs: no ESKAPE! An update from the Infectious Diseases Society of America. Clin. Infect. Dis. Off. Publ. Infect. Dis. Soc. Am. *48*, 1–12.

Breithaupt, H. (1999). The new antibiotics. Nat. Biotechnol. *17*, 1165–1169.

Bressler, A.M., Kaye, K.S., LiPuma, J.J., Alexander, B.D., Moore, C.M., Reller, L.B., and Woods, C.W. (2007). Risk factors for *Burkholderia cepacia* complex bacteremia among intensive care unit patients without cystic fibrosis: a case-control study. Infect. Control Hosp. Epidemiol. *28*, 951–958.

Brochet, M., Da Cunha, V., Couvé, E., Rusniok, C., Trieu-Cuot, P., and Glaser, P. (2009). Atypical association of DDE transposition with conjugation specifies a new family of mobile elements. Mol. Microbiol. *71*, 948–959.

Brown, E.D., and Wright, G.D. (2005). New targets and screening approaches in antimicrobial drug discovery. Chem Rev *105*, 759–774.

Brown, E.D., and Wright, G.D. (2016). Antibacterial drug discovery in the resistance era. Nature *529*, 336–343.

Brown, J.R., Douady, C.J., Italia, M.J., Marshall, W.E., and Stanhope, M.J. (2001). Universal trees based on large combined protein sequence data sets. Nat. Genet. *28*, 281–285.

Buchrieser, C., Prentice, M., and Carniel, E. (1998). The 102-kilobase unstable region of *Yersinia pestis* comprises a high-pathogenicity island linked to a pigmentation segment which undergoes internal rearrangement. J. Bacteriol. *180*, 2321–2329.

Buck, M.A., and Cooperman, B.S. (1990). Single protein omission reconstitution studies of tetracycline binding to the 30S subunit of *Escherichia coli* ribosomes. Biochemistry (Mosc.) *29*, 5374–5379.

Burdine, L., and Kodadek, T. (2004). Target identification in chemical genetics: the (often) missing link. Chem. Biol. *11*, 593–597.

Burns, J.L. (2007). Antibiotic resistance of *Burkholderia spp*. T. Coenye, and P. Vandamme, eds. (Norfolk: Horizon Bioscience), pp. 81–91.

Burns, J.L., Hedin, L.A., and Lien, D.M. (1989). Chloramphenicol resistance in *Pseudomonas cepacia* because of decreased permeability. Antimicrob Agents Chemother *33*, 136–141.

Burns, J.L., Wadsworth, C.D., Barry, J.J., and Goodall, C.P. (1996). Nucleotide sequence analysis of a gene from *Burkholderia (Pseudomonas) cepacia* encoding an outer membrane lipoprotein involved in multiple antibiotic resistance. Antimicrob Agents Chemother *40*, 307–313.

Buroni, S., Pasca, M.R., Flannagan, R.S., Bazzini, S., Milano, A., Bertani, I., Venturi, V., Valvano, M.A., and Riccardi, G. (2009). Assessment of three Resistance-Nodulation-Cell Division drug efflux transporters of *Burkholderia cenocepacia* in intrinsic antibiotic resistance. BMC Microbiol. *9*, 200.

Buroni, S., Matthijs, N., Spadaro, F., Van Acker, H., Scoffone, V.C., Pasca, M.R., Riccardi, G., and Coenye, T. (2014). Differential roles of RND efflux pumps in antimicrobial drug resistance of sessile and planktonic *Burkholderia cenocepacia* cells. Antimicrob. Agents Chemother. *58*, 7424–7429.

Bush, K., Courvalin, P., Dantas, G., Davies, J., Eisenstein, B., Huovinen, P., Jacoby, G.A., Kishony, R., Kreiswirth, B.N., Kutter, E., et al. (2011). Tackling antibiotic resistance. Nat. Rev. *9*, 894–896.

Bylund, J., Campsall, P.A., Ma, R.C., Conway, B.A., and Speert, D.P. (2005). *Burkholderia cenocepacia* induces neutrophil necrosis in chronic granulomatous disease. J. Immunol. Baltim. Md 1950 *174*, 3562–3569.

Cardona, S.T., and Valvano, M.A. (2005a). An expression vector containing a rhamnose-inducible promoter provides tightly regulated gene expression in *Burkholderia cenocepacia.* Plasmid *54*, 219–228.

Cardona, S.T., and Valvano, M.A. (2005b). An expression vector containing a rhamnose-inducible promoter provides tightly regulated gene expression in *Burkholderia cenocepacia*. Plasmid *54*, 219–228.

Cardona, S.T., Wopperer, J., Eberl, L., and Valvano, M.A. (2005). Diverse pathogenicity of *Burkholderia cepacia* complex strains in the *Caenorhabditis elegans* host model. FEMS MicrobiolLett *250*, 97–104.

Cardona, S.T., Mueller, C., and Valvano, M.A. (2006a). Identification of essential operons in *Burkholderia cenocepacia* with a rhamnose inducible promoter. Appl. Environ. Microbiol. *72*, 2547–2555.

Cardona, S.T., Mueller, C., and Valvano, M.A. (2006b). Identification of essential operons in *Burkholderia cenocepacia* with a rhamnose inducible promoter. Appl. Environ. Microbiol. *72*, 2547–2555.

Cardona, S.T., Selin, C., and Gislason, A.S. (2015a). Genomic tools to profile antibiotic mode of action. Crit. Rev. Microbiol. *4*, 465–472.

Cardona, S.T., Selin, C., and Gislason, A.S. (2015b). Genomic tools to profile antibiotic mode of action. Crit. Rev. Microbiol. *4*, 465–472.

Carroll, P., Muttucumaru, D.G., and Parish, T. (2005). Use of a tetracycline-inducible system for conditional expression in *Mycobacterium tuberculosis* and *Mycobacterium smegmatis*. Appl Env. Microbiol *71*, 3077–3084.

Caspi, R., Billington, R., Ferrer, L., Foerster, H., Fulcher, C.A., Keseler, I.M., Kothari, A., Krummenacker, M., Latendresse, M., Mueller, L.A., et al. (2016). The MetaCyc database of metabolic pathways and enzymes and the BioCyc collection of pathway/genome databases. Nucleic Acids Res. *44*, D471-80.

Caverly, L.J., Zhao, J., and LiPuma, J.J. (2015). Cystic fibrosis lung microbiome: opportunities to reconsider management of airway infection. Pediatr. Pulmonol. *50 Suppl 40*, S31-38.

Centers for Disease Control and Prevention (CDC), Department of Health and Human Services (HHS) (2017). Possession, Use, and Transfer of Select Agents and Toxins; Biennial Review of the List of Select Agents and Toxins and Enhanced Biosafety Requirements. Final rule. Fed. Regist. *82*, 6278–6294.

Chan, P.F., Holmes, D.J., and Payne, D.J. (2004). Finding the gems using genomic discovery: antibacterial drug discovery strategies – the successes and the challenges. Drug Discov. Today Ther. Strateg. *1*, 519–527.

Charlebois, R.L., and Doolittle, W.F. (2004). Computing prokaryotic gene ubiquity: rescuing the core from extinction. Genome Res. *14*, 2469–2477.

Chen, J.S., Witzmann, K.A., Spilker, T., Fink, R.J., and LiPuma, J.J. (2001). Endemicity and inter-city spread of *Burkholderia cepacia* genomovar III in cystic fibrosis. J. Pediatr. *139*, 643–649.

Christen, B., Abeliuk, E., Collier, J.M., Kalogeraki, V.S., Passarelli, B., Coller, J.A., Fero, M.J., McAdams, H.H., and Shapiro, L. (2011a). The essential genome of a bacterium. Mol. Syst. Biol. *7*, 528–535.

Christen, B., Abeliuk, E., Collier, J.M., Kalogeraki, V.S., Passarelli, B., Coller, J.A., Fero, M.J., McAdams, H.H., and Shapiro, L. (2011b). The essential genome of a bacterium. Mol. Syst. Biol. *7*, 528–535.

Clewell, D.B., and Gawron-Burke, C. (1986). Conjugative transposons and the dissemination of antibiotic resistance in *streptococci*. Annu. Rev. Microbiol. *40*, 635–659.

Coenye, T., and Vandamme, P. (2003). Diversity and significance of *Burkholderia* species occupying diverse ecological niches. Environ.Microbiol. *5*, 719–729.

Coenye, T., Acker, H.V., Peeters, E., Sass, A., Buroni, S., Riccardi, G., and Mahenthiralingam, E. (2011). Molecular mechanisms of chlorhexidine tolerance in *Burkholderia cenocepacia* biofilms. Antimicrob. Agents Chemother. *55*, 1912–1919.

Comenge, Y., Jr, R.Q., Li, L., Dubost, L., Brouard, J.P., Hugonnet, J.E., and Arthur, M. (2003). The CroRS two-component regulatory system is required for intrinsic beta-lactam resistance in *Enterococcus faecalis*. J. Bacteriol. *185*, 7184–7192.

Compant, S., Nowak, J., Coenye, T., Clément, C., and Barka, E.A. (2008). Diversity and occurrence of *Burkholderia spp*. in the natural environment. FEMS Microbiol Rev *4*, 607–626.

Conway, B.A., Venu, V., and Speert, D.P. (2002). Biofilm formation and acyl homoserine lactone production in the *Burkholderia cepacia* complex. J. Bacteriol. *184*, 5678–5685.

Cox, A.D., and Wilkinson, S.G. (1991). Ionizing groups in lipopolysaccharides of *Pseudomonas cepacia* in relation to antibiotic resistance. Mol. Microbiol. *5*, 641–646.

Craig, F.F., Coote, J.G., Parton, R., Freer, J.H., and Gilmour, N.J. (1989). A plasmid which can be transferred between *Escherichia coli* and *Pasteurella haemolytica* by electroporation and conjugation. J. Gen. Microbiol. *135*, 2885–2890.

Cunha, M.V., Pinto-de-Oliveira, A., Meirinhos-Soares, L., Salgado, M.J., Melo-Cristino, J., Correia, S., Barreto, C., and Sá-Correia, I. (2007). Exceptionally high representation of *Burkholderia cepacia* among *B. cepacia complex i*solates recovered from the major Portuguese cystic fibrosis center. J. Clin. Microbiol. *45*, 1628–1633.

Daddi Oubekka, S., Briandet, R., Fontaine-Aupart, M.-P., and Steenkeste, K. (2012). Correlative time-resolved fluorescence microscopy to assess antibiotic diffusion-reaction in biofilms. Antimicrob. Agents Chemother. *56*, 3349–3358.

Darling, A.E., Mau, B., and Perna, N.T. (2010). progressiveMauve: multiple genome alignment with gene gain, loss and rearrangement. PloS One *5*, e11147.

Darling, P., Chan, M., Cox, A.D., and Sokol, P.A. (1998). Siderophore production by cystic fibrosis isolates of *Burkholderia cepacia*. Infect. Immun. *66*, 874–877.

Davis, B.D. (1948). Isolation of biochemically deficient mutants of bacteria by penicillin. J. Am. Chem. Soc. *70*, 4267.

Davis, B.D. (1987). Mechanism of bactericidal action of aminoglycosides. Microbiol. Rev. *51*, 341–350.

Delcour, A.H. (2009). Outer membrane permeability and antibiotic resistance. Biochim. Biophys. Acta *1794*, 808–816.

D'Elia, M.A., Pereira, M.P., and Brown, E.D. (2009). Are essential genes really essential? Trends Microbiol. *17*, 433–438.

Deng, Z., Shan, Y., Pan, Q., Gao, X., and Yan, A. (2013). Anaerobic expression of the *gadE-mdtEF* multidrug efflux operon is primarily regulated by the two-component system ArcBA through antagonizing the H-NS mediated repression. Front. Microbiol. *4*, 194.

Dennis, J.J. (2016). *Burkholderia cenocepacia* virulence microevolution in the CF lung: Variations on a theme. Virulence 1–3.

Desai, M., Bühler, T., Weller, P.H., and Brown, M.R. (1998). Increasing resistance of planktonic and biofilm cultures of *Burkholderia cepacia* to ciprofloxacin and ceftazidime during exponential growth. J Antimicrob Chemother *42*, 153–160.

Dhillon, B.K., Laird, M.R., Shay, J.A., Winsor, G.L., Lo, R., Nizam, F., Pereira, S.K., Waglechner, N., McArthur, A.G., Langille, M.G., et al. (2015). IslandViewer 3: more flexible, interactive genomic island discovery, visualization and analysis. Nucleic Acids Res. *43*, W104–W108.

Dickson, R.P., Erb-Downward, J.R., and Huffnagle, G.B. (2013). The role of the bacterial microbiome in lung disease. Expert Rev. Respir. Med. *7*, 245–257.

Dobrindt, U., Hochhut, B., Hentschel, U., and Hacker, J. (2004). Genomic islands in pathogenic and environmental microorganisms. Nat. Rev. Microbiol. *2*, 414–424.

Dolan, S.A., Dowell, E., LiPuma, J.J., Valdez, S., Chan, K., and James, J.F. (2011). An outbreak of *Burkholderia cepacia* complex associated with intrinsically contaminated nasal spray. Infect. Control Hosp. Epidemiol. Off. J. Soc. Hosp. Epidemiol. Am. *32*, 804–810.

Donald, R.G.K., Skwish, S., Forsyth, R.A., Anderson, J.W., Zhong, T., Burns, C., Lee, S., Meng, X., LoCastro, L., Jarantow, L.W., et al. (2009a). A *Staphylococcus aureus* Fitness Test Platform for Mechanism-Based Profiling of Antibacterial Compounds. Chem. Biol. *16*, 826–836.

Donald, R.G.K., Skwish, S., Forsyth, R.A., Anderson, J.W., Zhong, T., Burns, C., Lee, S., Meng, X., LoCastro, L., Jarantow, L.W., et al. (2009b). A *Staphylococcus aureus* Fitness Test Platform for Mechanism-Based Profiling of Antibacterial Compounds. Chem. Biol. *16*, 826–836.

Drevinek, P., and Mahenthiralingam, E. (2010). *Burkholderia cenocepacia* in cystic fibrosis: epidemiology and molecular mechanisms of virulence. Clin. Microbiol. Infect. Off. Publ. Eur. Soc. Clin. Microbiol. Infect. Dis. *16*, 821–830.

Du, W.-L., Dubarry, N., Passot, F.M., Kamgoué, A., Murray, H., Lane, D., and Pasta, F. (2016). Orderly Replication and Segregation of the Four Replicons of *Burkholderia cenocepacia* J2315. PLoS Genet. *12*, e1006172.

Eberl, L., and Vandamme, P. (2016). Members of the genus *Burkholderia*: good and bad guys. F1000Research *5*.

Ehrt, S., Guo, X.V., Hickey, C.M., Ryou, M., Monteleone, M., Riley, L.W., and Schnappinger, D. (2005a). Controlling gene expression in *mycobacteria* with anhydrotetracycline and Tet repressor. Nucleic Acids Res. *33*, e21.

Ehrt, S., Guo, X.V., Hickey, C.M., Ryou, M., Monteleone, M., Riley, L.W., and Schnappinger, D. (2005b). Controlling gene expression in mycobacteria with anhydrotetracycline and Tet repressor. Nucleic Acids Res *33*, e21.

Ehrt, S., Guo, X.V., Hickey, C.M., Ryou, M., Monteleone, M., Riley, L.W., and Schnappinger, D. (2005c). Controlling gene expression in *mycobacteria* with anhydrotetracycline and Tet repressor. Nucleic Acids Res *33*, e21.

Elsbach, P., and Weiss, J. (1993). The bactericidal/permeability-increasing protein (BPI), a potent element in host-defense against gram-negative bacteria and lipopolysaccharide. Immunobiology *187*, 417–429.

Euzéby, J.P. (1997). List of Bacterial Names with Standing in Nomenclature: a folder available on the Internet. Int. J. Syst. Bacteriol. *47*, 590–592.

Falagas, M.E., Kasiakou, S.K., and Saravolatz, L.D. (2005a). Colistin: The Revival of Polymyxins for the Management of Multidrug-Resistant Gram-Negative Bacterial Infections. Clin. Infect. Dis. *40*, 1333–1341.

Falagas, M.E., Kasiakou, S.K., and Saravolatz, L.D. (2005b). Colistin: The Revival of Polymyxins for the Management of Multidrug-Resistant Gram-Negative Bacterial Infections. Clin. Infect. Dis. *40*, 1333–1341.

Falcão Pedrosa Costa, A., Castelo Branco Cavalcanti, F., and Modesto dos Santos, V. (2014). Endocarditis due to Burkholderia cepacia and an intracardiac foreign body in a renal transplant patient. Rev. Port. Cardiol. Orgao Of. Soc. Port. Cardiol. Port. J. Cardiol. Off. J. Port. Soc. Cardiol. *33*, 117.e1-4.

Fang, G., Rocha, E., and Danchin, A. (2005). How essential are nonessential genes? Mol. Biol. Evol. *22*, 2147–2156.

Ferrandiz, M.J., Martin-Galiano, A.J., Arnanz, C., Zimmerman, T., and de la Campa, A.G. (2015). Reactive Oxygen Species Contribute to the Bactericidal Effects of the Fluoroquinolone Moxifloxacin in *Streptococcus pneumoniae*. Antimicrob. Agents Chemother. *60*, 409–417.

Fetar, H., Gilmour, C., Klinoski, R., Daigle, D.M., Dean, C.R., and Poole, K. (2011). mexEF-oprN multidrug efflux operon of *Pseudomonas aeruginosa*: regulation by the MexT activator in response to nitrosative stress and chloramphenicol. Antimicrob. Agents Chemother. *55*, 508–514.

Fields, F.R., Lee, S.W., and McConnell, M.J. (2016). Using bacterial genomes and essential genes for the development of new antibiotics. Biochem. Pharmacol.

Figurski, D.H., and Helinski, D.R. (1979). Replication of an origin-containing derivative of plasmid RK2 dependent on a plasmid function provided in trans. Proc. Natl. Acad. Sci. U. S. A. *76*, 1648–1652.

Flannagan, R.S., Linn, T., and Valvano, M.A. (2008). A system for the construction of targeted unmarked gene deletions in the genus *Burkholderia*. Environ. Microbiol. *10*, 1652–1660.

Fleischmann, R.D., Adams, M.D., White, O., Clayton, R.A., Kirkness, E.F., Kerlavage, A.R., Bult, C.J., Tomb, J.F., Dougherty, B.A., and Merrick, J.M. (1995). Whole-genome random sequencing and assembly of *Haemophilus influenzae* Rd. Science *269*, 496–512.

Flemming, H.-C., Wingender, J., Szewzyk, U., Steinberg, P., Rice, S.A., and Kjelleberg, S. (2016). Biofilms: an emergent form of bacterial life. Nat. Rev. Microbiol. *14*, 563–575.

Forsyth, R.A., Haselbeck, R.J., Ohlsen, K.L., Yamamoto, R.T., Xu, H., Trawick, J.D., Wall, D., Wang, L., V, B.-D., Froelich, J.M., et al. (2002a). A genome-wide strategy for the identification of essential genes in *Staphylococcus aureus*. Mol Microbiol *43*, 1387–1400.

Forsyth, R.A., Haselbeck, R.J., Ohlsen, K.L., Yamamoto, R.T., Xu, H., Trawick, J.D., Wall, D., Wang, L., V, B.-D., Froelich, J.M., et al. (2002b). A genome-wide strategy for the identification of essential genes in *Staphylococcus aureus*. Mol Microbiol *43*, 1387–1400.

Forum, W.E. (2014). Global Risks Report 2014 http://www.weforum.org/reports/global-risks-2014-report.

Fox, S., Leitch, A.E., Duffin, R., Haslett, C., and Rossi, A.G. (2010). Neutrophil Apoptosis: Relevance to the Innate Immune Response and Inflammatory Disease. J. Innate Immun. *2*, 216–227.

Fraley, C., and Raftery, A.E. (1999). MCLUST: Software for Model-Based Cluster Analysis. J. Classif. *16*, 297–306.

Fraley, C., and Raftery, A.E. (2002). Model-Based Clustering, Discriminant Analysis, and Density Estimation. J. Am. Stat. Assoc. *97*, 611–631.

Fraser, C.M., Gocayne, J.D., White, O., Adams, M.D., Clayton, R.A., Fleischmann, R.D., Bult, C.J., Kerlavage, A.R., Sutton, G., Kelley, J.M., et al. (1995). The minimal gene complement of *Mycoplasma genitalium*. Science *270*, 397–403.

Fraud, S., and Poole, K. (2011). Oxidative stress induction of the MexXY multidrug efflux genes and promotion of aminoglycoside resistance development in *Pseudomonas aeruginosa*. Antimicrob. Agents Chemother. *55*, 1068–1074.

Fuller, N., and Rand, R.P. (2001). The influence of lysolipids on the spontaneous curvature and bending elasticity of phospholipid membranes. Biophys. J. *81*, 243–254.

Fung, S.K., Dick, H., Devlin, H., and Tullis, E. (1998). Transmissibility and infection control implications of *Burkholderia cepacia* in cystic fibrosis. Can. J. Infect. Dis. J. Can. Mal. Infect. *9*, 177–182.

Gallagher, L.A., Shendure, J., and Manoil, C. (2011a). Genome-scale identification of resistance functions in *Pseudomonas aeruginosa* using Tn-seq. mBio *2*, e00315-10.

Gallagher, L.A., Shendure, J., and Manoil, C. (2011b). Genome-scale identification of resistance functions in *Pseudomonas aeruginosa* using Tn-seq. mBio *2*, e00315-10.

Gallagher, L.A., Shendure, J., and Manoil, C. (2011c). Genome-scale identification of resistance functions in *Pseudomonas aeruginosa* using Tn-seq. mBio *2*, e00315-10.

Gallagher, L.A., Ramage, E., Patrapuvich, R., Weiss, E., Brittnacher, M., and Manoil, C. (2013). Sequence-defined transposon mutant library of *Burkholderia thailandensis*. mBio *4*, e00604-13.

Gautam, V., Shafiq, N., Singh, M., Ray, P., Singhal, L., Jaiswal, N.P., Prasad, A., Singh, S., and Agarwal, A. (2015). Clinical and in vitro evidence for the antimicrobial therapy in *Burkholderia cepacia* complex infections. Expert Rev. Anti Infect. Ther. *13*, 629–663.

Gawronski, J.D., Wong, S.M., Giannoukos, G., Ward, D.V., and Akerley, B.J. (2009). Tracking insertion mutants within libraries by deep sequencing and a genome-wide screen for *Haemophilus* genes required in the lung. Proc. Natl. Acad. Sci. U. S. A. *106*, 16422–16427.

Gellert, M., Mizuuchi, K., O'Dea, M.H., and Nash, H.A. (1976a). DNA gyrase: an enzyme that introduces superhelical turns into DNA. Proc. Natl. Acad. Sci. U. S. A. *73*, 3872–3876.

Gellert, M., O'Dea, M.H., Itoh, T., and Tomizawa, J. (1976b). Novobiocin and coumermycin inhibit DNA supercoiling catalyzed by DNA gyrase. Proc. Natl. Acad. Sci. U. S. A. *73*, 4474–4478.

Gerdes, S., Edwards, R., Kubal, M., Fonstein, M., Stevens, R., and Osterman, A. (2006). Essential genes on metabolic maps. Curr. Opin. Biotechnol. *17*, 448–456.

Gerdes, S.Y., Scholle, M.D., Campbell, J.W., Balazsi, G., Ravasz, E., Daugherty, M.D., Somera, A.L., Kyrpides, N.C., Anderson, I., Gelfand, M.S., et al. (2003). Experimental determination and system level analysis of essential genes in *Escherichia coli* MG1655. J Bacteriol *185*, 5673–5684.

Giaever, G., Shoemaker, D.D., Jones, T.W., Liang, H., Winzeler, E.A., Astromoff, A., and Davis, R.W. (1999). Genomic profiling of drug sensitivities via induced haploinsufficiency. Nat. Genet. *21*, 278–283.

Gibson, R.L., Burns, J.L., and Ramsey, B.W. (2003). Pathophysiology and management of pulmonary infections in cystic fibrosis. Am. J. Respir. Crit. Care Med. *168*, 918–951.

Gislason, A.S., Choy, M., Bloodworth, R.A., Qu, W., Stietz, M.S., Li, X., Zhang, C., and Cardona, S.T. (2016). Competitive Growth Enhances Conditional Growth Mutant Sensitivity to Antibiotics and Exposes a Two-Component System as an Emerging Antibacterial Target in *Burkholderia cenocepacia*. Antimicrob. Agents Chemother. *61*, 10.1128/AAC.00790-16. Print 2017 Jan.

Gislason, A.S., Choy, M., Bloodworth, R.A.M., Qu, W., Stietz, M.S., Li, X., Zhang, C., and Cardona, S.T. (2017). Competitive Growth Enhances Conditional Growth Mutant Sensitivity to Antibiotics and Exposes a Two-Component System as an Emerging Antibacterial Target in *Burkholderia cenocepacia*. Antimicrob. Agents Chemother. *61*.

Goodman, A.L., McNulty, N.P., Zhao, Y., Leip, D., Mitra, R.D., Lozupone, C.A., Knight, R., and Gordon, J.I. (2009). Identifying genetic determinants needed to establish a human gut symbiont in its habitat. Cell Host Microbe *6*, 279–289.

Gotoh, Y., Eguchi, Y., Watanabe, T., Okamoto, S., Doi, A., and Utsumi, R. (2010). Two-component signal transduction as potential drug targets in pathogenic bacteria. Curr. Opin. Microbiol. *13*, 232–239.

Govan, J.R., and Deretic, V. (1996). Microbial pathogenesis in cystic fibrosis: mucoid *Pseudomonas aeruginosa* and *Burkholderia cepacia*. Microbiol. Rev. *60*, 539–574.

Govan, J.R., Brown, P.H., Maddison, J., Doherty, C.J., Nelson, J.W., Dodd, M., Greening, A.P., and Webb, A.K. (1993). Evidence for transmission of *Pseudomonas cepacia* by social contact in cystic fibrosis. Lancet *342*, 15–19.

Govan, J.R., Hughes, J.E., and Vandamme, P. (1996). *Burkholderia cepacia*: medical, taxonomic and ecological issues. J. Med. Microbiol. *45*, 395–407.

Govan, J.R., Brown, A.R., and Jones, A.M. (2007). Evolving epidemiology of *Pseudomonas aeruginosa* and the *Burkholderia cepacia* complex in cystic fibrosis lung infection. Future Microbiol. *2*, 153–164.

Graindorge, A., Menard, A., Monnez, C., and Cournoyer, B. (2012). Insertion sequence evolutionary patterns highlight convergent genetic inactivations and recent genomic island acquisitions among epidemic *Burkholderia cenocepacia*. J. Med. Microbiol. *61*, 394–409.

Green, B., Bouchier, C., Fairhead, C., Craig, N.L., and Cormack, B.P. (2012). Insertion site preference of Mu, Tn5, and Tn7 transposons. Mob. DNA *3*, 3.

Greenberg, D.E., Goldberg, J.B., Stock, F., Murray, P.R., Holland, S.M., and Lipuma, J.J. (2009). Recurrent *Burkholderia* infection in patients with chronic granulomatous disease: 11-year experience at a large referral center. Clin. Infect. Dis. Off. Publ. Infect. Dis. Soc. Am. *48*, 1577–1579.

Grigoriev, A. (1998). Analyzing genomes with cumulative skew diagrams. Nucleic Acids Res. *26*, 2286–2290.

Guérillot, R., Da Cunha, V., Sauvage, E., Bouchier, C., and Glaser, P. (2013). Modular evolution of TnGBSs, a new family of integrative and conjugative elements associating insertion sequence transposition, plasmid replication, and conjugation for their spreading. J. Bacteriol. *195*, 1979–1990.

Guglierame, P., Pasca, M.R., Rossi, E.D., Buroni, S., Arrigo, P., Manina, G., and Riccardi, G. (2006). Efflux pump genes of the resistance-nodulation-division family in *Burkholderia cenocepacia* genome. BMC Microbiol. *6*, 66.

Gunn, J.S., and Miller, S.I. (1996). PhoP-PhoQ activates transcription of pmrAB, encoding a two-component regulatory system involved in *Salmonella typhimurium* antimicrobial peptide resistance. J. Bacteriol. *178*, 6857–6864.

Gutierrez, M.G. (2013). Functional role(s) of phagosomal Rab GTPases. Small GTPases *4*, 148–158.

Hacker, J., Bender, L., Ott, M., Wingender, J., Lund, B., Marre, R., and Goebel, W. (1990). Deletions of chromosomal regions coding for fimbriae and hemolysins occur in vitro and in vivo in various extraintestinal *Escherichia coli* isolates. Microb. Pathog. *8*, 213–225.

Hancock, R.E. (1998). Resistance mechanisms in *Pseudomonas aeruginosa* and other nonfermentative gram-negative bacteria. Clin. Infect. Dis. Off. Publ. Infect. Dis. Soc. Am. *27 Suppl 1*, S93-99.

Hanulik, V., Webber, M.A., Chroma, M., Uvizl, R., Holy, O., Whitehead, R.N., Baugh, S., Matouskova, I., and Kolar, M. (2013). An outbreak of *Burkholderia multivorans* beyond cystic fibrosis patients. J. Hosp. Infect. *84*, 248–251.

Harley, V.S., Dance, D.A., Drasar, B.S., and Tovey, G. (1998). Effects of *Burkholderia pseudomallei* and other *Burkholderia* species on eukaryotic cells in tissue culture. Microbios *96*, 71–93.

Harris, J.K., Kelley, S.T., Spiegelman, G.B., and Pace, N.R. (2003). The genetic core of the universal ancestor. Genome Res. *13*, 407–412.

Harvat, E.M., Zhang, Y.-M., Tran, C.V., Zhang, Z., Frank, M.W., Rock, C.O., and Saier, M.H. (2005). Lysophospholipid flipping across the *Escherichia coli* inner membrane catalyzed by a

transporter (LplT) belonging to the major facilitator superfamily. J. Biol. Chem. *280*, 12028–12034.

Hasselbring, B.M., Patel, M.K., and Schell, M.A. (2011). Dictyostelium discoideum as a model system for identification of *Burkholderia pseudomallei* virulence factors. Infect. Immun. *79*, 2079–2088.

Heijden, J. van der, Reynolds, L.A., Deng, W., Mills, A., Scholz, R., Imami, K., Foster, L.J., Duong, F., and Finlay, B.B. (2016). *Salmonella* Rapidly Regulates Membrane Permeability To Survive Oxidative Stress. mBio *7*, 10.1128/mBio.01238-16.

Heo, S.T., Kim, S.J., Jeong, Y.G., Bae, I.G., Jin, J.S., and Lee, J.C. (2008). Hospital outbreak of *Burkholderia stabilis* bacteraemia related to contaminated chlorhexidine in haematological malignancy patients with indwelling catheters. J. Hosp. Infect. *70*, 241–245.

Hirakawa, H., Nishino, K., Hirata, T., and Yamaguchi, A. (2003). Comprehensive studies of drug resistance mediated by overexpression of response regulators of two-component signal transduction systems in *Escherichia coli*. J. Bacteriol. *185*, 1851–1856.

Holden, M.T., Seth-Smith, H.M., Crossman, L.C., Sebaihia, M., Bentley, S.D., Cerdeno-Tarraga, A.M., Thomson, N.R., Bason, N., Quail, M.A., Sharp, S., et al. (2009a). The genome of *Burkholderia cenocepacia* J2315, an epidemic pathogen of cystic fibrosis patients. J. Bacteriol. *191*, 261–277.

Holden, M.T., Seth-Smith, H.M., Crossman, L.C., Sebaihia, M., Bentley, S.D., Cerdeno-Tarraga, A.M., Thomson, N.R., Bason, N., Quail, M.A., Sharp, S., et al. (2009b). The genome of *Burkholderia cenocepacia* J2315, an epidemic pathogen of cystic fibrosis patients. J. Bacteriol. *191*, 261–277.

Horvath, P., and Barrangou, R. (2010). CRISPR/Cas, the immune system of bacteria and archaea. Science *327*, 167–170.

Huber, B., Riedel, K., Hentzer, M., Heydorn, A., Gotschlich, A., Givskov, M., Molin, S., and Eberl, L. (2001). The cep quorum-sensing system of *Burkholderia cepacia* H111 controls biofilm formation and swarming motility. Microbiol. Read. Engl. *147*, 2517–2528.

Huber, J., Donald, R.G., Lee, S.H., Jarantow, L.W., Salvatore, M.J., Meng, X., Painter, R., Onishi, R.H., Occi, J., Dorso, K., et al. (2009). Chemical genetic identification of peptidoglycan inhibitors potentiating carbapenem activity against methicillin-resistant *Staphylococcus aureus*. Chem. Biol. *16*, 837–848.

Hutchison, C.A., Peterson, S.N., Gill, S.R., Cline, R.T., White, O., Fraser, C.M., Smith, H.O., and Venter, J.C. (1999). Global transposon mutagenesis and a minimal *Mycoplasma* genome. Science *286*, 2165–2169.

Huynh, K.K., Plumb, J.D., Downey, G.P., Valvano, M.A., and Grinstein, S. (2010). Inactivation of macrophage Rab7 by *Burkholderia cenocepacia*. J. Innate Immun. *2*, 522–533.

Hwang, S., Zhang, Q., Ryu, S., and Jeon, B. (2012). Transcriptional regulation of the CmeABC multidrug efflux pump and the KatA catalase by CosR in *Campylobacter jejuni*. J. Bacteriol. *194*, 6883–6891.

Irwin, J.J., and Shoichet, B.K. (2005). ZINC–a free database of commercially available compounds for virtual screening. J. Chem. Inf. Model. *45*, 177–182.

Isles, A., Maclusky, I., Corey, M., Gold, R., Prober, C., Fleming, P., and Levison, H. (1984). *Pseudomonas cepacia* infection in cystic fibrosis: an emerging problem. J. Pediatr. *104*, 206–210.

Isshiki, Y., Kawahara, K., and Zähringer, U. (1998). Isolation and characterisation of disodium (4-amino-4-deoxy-beta-L- arabinopyranosyl)-(1-->8)-(D-glycero-alpha-D-talo-oct-2-ulopyranosylona te)- (2-->4)-(methyl 3-deoxy-D-manno-oct-2-ulopyranosid)onate from the lipopolysaccharide of *Burkholderia cepacia*. Carbohydr. Res. *313*, 21–27.

Jackson, A.L., Bartz, S.R., Schelter, J., Kobayashi, S.V., Burchard, J., Mao, M., Li, B., Cavet, G., and Linsley, P.S. (2003). Expression profiling reveals off-target gene regulation by RNAi. Nat. Biotechnol. *21*, 635–637.

Jacobs, M.A., Alwood, A., Thaipisuttikul, I., Spencer, D., Haugen, E., Ernst, S., Will, O., Kaul, R., Raymond, C., Levy, R., et al. (2003). Comprehensive transposon mutant library of *Pseudomonas aeruginosa*. Proc Natl Acad Sci U A *100*, 14339–14344.

Ji, Q., Chen, P.J., Qin, G., Deng, X., Hao, Z., Wawrzak, Z., Yeo, W.S., Quang, J.W., Cho, H., Luo, G.Z., et al. (2016). Structure and mechanism of the essential two-component signal-transduction system WalKR in *Staphylococcus aureus*. Nat. Commun. *7*, 11000.

Ji, Y., Zhang, B., Van, S.F., Horn, Warren, P., Woodnutt, G., Burnham, M.K., and Rosenberg, M. (2001). Identification of critical staphylococcal genes using conditional phenotypes generated by antisense RNA. Science *293*, 2266–2269.

Jimenez, L. (2001). Molecular diagnosis of microbial contamination in cosmetic and pharmaceutical products: a review. J AOAC Int *84*, 671–675.

Johnson, W.M., Tyler, S.D., and Rozee, K.R. (1994). Linkage analysis of geographic and clinical clusters in *Pseudomonas cepacia* infections by multilocus enzyme electrophoresis and ribotyping. J. Clin. Microbiol. *32*, 924–930.

Judson, N., and Mekalanos, J.J. (2000a). Transposon-based approaches to identify essential bacterial genes. Trends Microbiol. *8*, 521–526.

Judson, N., and Mekalanos, J.J. (2000b). TnAraOut, a transposon-based approach to identify and characterize essential bacterial genes. Nat Biotechnol *18*, 740–745.

Juhas, M., Meer, J.R. van der, Gaillard, M., Harding, R.M., Hood, D.W., and Crook, D.W. (2009). Genomic islands: tools of bacterial horizontal gene transfer and evolution. FEMS Microbiol. Rev. *33*, 376–393.

Juhas, M., Eberl, L., and Glass, J.I. (2011). Essence of life: essential genes of minimal genomes. Trends Cell Biol. *21*, 562–568.

Juhas, M., Stark, M., Mering, C. von, Lumjiaktase, P., Crook, D.W., Valvano, M.A., and Eberl, L. (2012a). High confidence prediction of essential genes in *Burkholderia cenocepacia*. PloS One *7*, e40064.

Juhas, M., Stark, M., Mering, C. von, Lumjiaktase, P., Crook, D.W., Valvano, M.A., and Eberl, L. (2012b). High confidence prediction of essential genes in *Burkholderia cenocepacia*. PloS One *7*, e40064.

Katsu, T. (1991). New agents to increase the permeability of the outer membrane of *Escherichia coli*. Biochem. Int. *23*, 413–417.

Keith, K.E., Hynes, D.W., Sholdice, J.E., and Valvano, M.A. (2009). Delayed association of the NADPH oxidase complex with macrophage vacuoles containing the opportunistic pathogen *Burkholderia cenocepacia*. Microbiol. Read. Engl. *155*, 1004–1015.

Kerem, B., Rommens, J.M., Buchanan, J.A., Markiewicz, D., Cox, T.K., Chakravarti, A., Buchwald, M., and Tsui, L.C. (1989). Identification of the cystic fibrosis gene: genetic analysis. Science *245*, 1073–1080.

Khan, M.A., and Musarrat, J. (2003). Interactions of tetracycline and its derivatives with DNA in vitro in presence of metal ions. Int. J. Biol. Macromol. *33*, 49–56.

Khan, M.A., Mustafa, J., and Musarrat, J. (2003). Mechanism of DNA strand breakage induced by photosensitized tetracycline–Cu(II) complex. Mutat. Res. Mol. Mech. Mutagen. *525*, 109–119.

Klockgether, J., Munder, A., Neugebauer, J., Davenport, C.F., Stanke, F., Larbig, K.D., Heeb, S., Schock, U., Pohl, T.M., Wiehlmann, L., et al. (2010). Genome diversity of *Pseudomonas aeruginosa* PAO1 laboratory strains. J. Bacteriol. *192*, 1113–1121.

Kobayashi, K., Ehrlich, S.D., Albertini, A., Amati, G., Andersen, K.K., Arnaud, M., Asai, K., Ashikaga, S., Aymerich, S., Bessieres, P., et al. (2003). Essential *Bacillus subtilis* genes. Proc Natl Acad Sci U A *100*, 4678–4683.

Koebnik, R., Locher, K.P., and Van Gelder, P. (2000). Structure and function of bacterial outer membrane proteins: barrels in a nutshell. Mol. Microbiol. *37*, 239–253.

Koenig, D.W., and Pierson, D.L. (1997). Microbiology of the Space Shuttle water system. Water Sci. Technol. J. Int. Assoc. Water Pollut. Res. *35*, 59–64.

Koller, D., and Lohner, K. (2014). The role of spontaneous lipid curvature in the interaction of interfacially active peptides with membranes. Biochim. Biophys. Acta *1838*, 2250–2259.

Koonin, E.V. (2000). How many genes can make a cell: the minimal-gene-set concept. Annu. Rev. Genomics Hum. Genet. *1*, 99–116.

Koonin, E.V. (2003). Comparative genomics, minimal gene-sets and the last universal common ancestor. Nat. Rev. *1*, 127–136.

Kotloff, R.M., and Thabut, G. (2011). Lung transplantation. Am. J. Respir. Crit. Care Med. *184*, 159–171.

Kutty, P.K., Moody, B., Gullion, J.S., Zervos, M., Ajluni, M., Washburn, R., Sanderson, R., Kainer, M.A., Powell, T.A., Clarke, C.F., et al. (2007). Multistate outbreak of *Burkholderia cenocepacia* colonization and infection associated with the use of intrinsically contaminated alcohol-free mouthwash. Chest *132*, 1825–1831.

Lamothe, J., and Valvano, M.A. (2008). *Burkholderia cenocepacia*-induced delay of acidification and phagolysosomal fusion in cystic fibrosis transmembrane conductance regulator (CFTR)-defective macrophages. Microbiol. Read. Engl. *154*, 3825–3834.

Lan, J.H., Yin, Y., Reed, E.F., Moua, K., Thomas, K., and Zhang, Q. (2015). Impact of three Illumina library construction methods on GC bias and HLA genotype calling. Hum. Immunol. *76*, 166–175.

Landers, P., Kerr, K.G., Rowbotham, T.J., Tipper, J.L., Keig, P.M., Ingham, E., and Denton, M. (2000). Survival and growth of Burkholderia cepacia within the free-living amoeba *Acanthamoeba polyphaga.* Eur. J. Clin. Microbiol. Infect. Dis. Off. Publ. Eur. Soc. Clin. Microbiol. *19*, 121–123.

Langmead, B., and Salzberg, S.L. (2012). Fast gapped-read alignment with Bowtie 2. Nat. Methods *9*, 357–359.

Langmead, B., Trapnell, C., Pop, M., and Salzberg, S.L. (2009). Ultrafast and memory-efficient alignment of short DNA sequences to the human genome. Genome Biol. *10*, R25–2009–10–3–r25. Epub 2009 Mar 4.

Langridge, G.C., Phan, M.D., Turner, D.J., Perkins, T.T., Parts, L., Haase, J., Charles, I., Maskell, D.J., Peters, S.E., Dougan, G., et al. (2009). Simultaneous assay of every *Salmonella Typhi* gene using one million transposon mutants. Genome Res. *19*, 2308–2316.

Larson, M.H., Gilbert, L.A., Wang, X., Lim, W.A., Weissman, J.S., and Qi, L.S. (2013a). CRISPR interference (CRISPRi) for sequence-specific control of gene expression. Nat. Protoc. *8*, 2180–2196.

Larson, M.H., Gilbert, L.A., Wang, X., Lim, W.A., Weissman, J.S., and Qi, L.S. (2013b). CRISPR interference (CRISPRi) for sequence-specific control of gene expression. Nat. Protoc. *8*, 2180–2196.

Lederberg, J., and Zinder, N. (1948). Concentration of biochemical mutants of bacteria with penicillin. J. Am. Chem. Soc. *70*, 4267.

Lee, D.G., Urbach, J.M., Wu, G., Liberati, N.T., Feinbaum, R.L., Miyata, S., Diggins, L.T., He, J., Saucier, M., Déziel, E., et al. (2006). Genomic analysis reveals that *Pseudomonas aeruginosa* virulence is combinatorial. Genome Biol. *7*, R90.

Lee, S., Han, S.W., Kim, G., Song, D.Y., Lee, J.C., and Kwon, K.T. (2013). An outbreak of *Burkholderia cenocepacia* associated with contaminated chlorhexidine solutions prepared in the hospital. Am. J. Infect. Control.

Lee, S.A., Gallagher, L.A., Thongdee, M., Staudinger, B.J., Lippman, S., Singh, P.K., and Manoil, C. (2015). General and condition-specific essential functions of *Pseudomonas aeruginosa*. Proc. Natl. Acad. Sci. U. S. A. *112*, 5189–5194.

Lemon, K.P., and Grossman, A.D. (1998). Localization of bacterial DNA polymerase: evidence for a factory model of replication. Science *282*, 1516–1519.

Lessie, T.G., Hendrickson, W., Manning, B.D., and Devereux, R. (1996). Genomic complexity and plasticity of *Burkholderia cepacia.* FEMS Microbiol. Lett. *144*, 117–128.

Lewis, K. (2010). Persister Cells. Annu. Rev. Microbiol. *64*, 357–362.

Lewis, K. (2013). Platforms for antibiotic discovery. Nat. Rev. Discov. *12*, 371–387.

Lewis, R.J., Tsai, F.T., and Wigley, D.B. (1996). Molecular mechanisms of drug inhibition of DNA gyrase. BioEssays News Rev. Mol. Cell. Dev. Biol. *18*, 661–671.

Li, F.K., Chan, K.W., Chan, T.M., and Lai, K.N. (2003). Burkholderia urinary tract infection after renal transplantation. Transpl. Infect. Dis. Off. J. Transplant. Soc. *5*, 59–61.

Liberati, N.T., Urbach, J.M., Miyata, S., Lee, D.G., Drenkard, E., Wu, G., Villanueva, J., Wei, T., and Ausubel, F.M. (2006). An ordered, nonredundant library of *Pseudomonas aeruginosa* strain PA14 transposon insertion mutants. Proc Natl Acad Sci U A *103*, 2833–2838.

Liberati, N.T., Urbach, J.M., Thurber, T.K., Wu, G., and Ausubel, F.M. (2007). Comparing Insertion Libraries in Two *Pseudomonas aeruginosa* Strains to Assess Gene Essentiality. Methods Mol. Biol. Clifton NJ *416*, 153–170.

Lin, Y., Bogdanov, M., Tong, S., Guan, Z., and Zheng, L. (2016). Substrate Selectivity of Lysophospholipid Transporter LplT Involved in Membrane Phospholipid Remodeling in *Escherichia coli*. J. Biol. Chem. *291*, 2136–2149.

Lipinski, C.A. (2000). Drug-like properties and the causes of poor solubility and poor permeability. J. Pharmacol. Toxicol. Methods *44*, 235–249.

Lipuma, J.J. (2010). The changing microbial epidemiology in cystic fibrosis. Clin. Microbiol. Rev. *23*, 299–323.

LiPuma, J.J., and Mahenthiralingam, E. (1999). Commercial use of *Burkholderia cepacia*. Emerg. Infect. Dis. *5*, 305.

LiPuma, J.J., Spilker, T., Gill, L.H., 3rd, P.W.C., Liu, L., and Mahenthiralingam, E. (2001). Disproportionate distribution of *Burkholderia cepacia* complex species and transmissibility markers in cystic fibrosis. Am. J. Respir. Crit. Care Med. *164*, 92–96.

LiPuma, J.J., Currie, B.J., Peacock, S.J., and Vandamme, P.A.R. (2011). *Burkholderia, Stenotrophomonas, Ralstonia, Cupriavidus, Pandoraea, Brevundimonas, Comamonas, Delftia,* and *Acidovorax**. 692–713.

Lodge, J.K., and Berg, D.E. (1990). Mutations that affect Tn5 insertion into pBR322: importance of local DNA supercoiling. J. Bacteriol. *172*, 5956–5960.

Lodge, J.K., Weston-Hafer, K., and Berg, D.E. (1988). Transposon Tn5 Target Specificity: Preference for Insertion at G/C Pairs. Genetics *120*, 645–650.

Lomovskaya, O., Warren, M.S., Lee, A., Galazzo, J., Fronko, R., Lee, M., Blais, J., Cho, D., Chamberland, S., Renau, T., et al. (2001). Identification and characterization of inhibitors of multidrug resistance efflux pumps in *Pseudomonas aeruginosa*: novel agents for combination therapy. Antimicrob. Agents Chemother. *45*, 105–116.

Loutet, S.A., and Valvano, M.A. (2011). Extreme antimicrobial peptide and polymyxin B resistance in the genus *Burkholderia*. Front. Cell. Infect. Microbiol. *1*, 6.

Lucero, C.A., Cohen, A.L., Trevino, I., Rupp, A.H., Harris, M., Forkan-Kelly, S., Noble-Wang, J., Jensen, B., Shams, A., Arduino, M.J., et al. (2011). Outbreak of *Burkholderia cepacia* complex among ventilated pediatric patients linked to hospital sinks. Am. J. Infect. Control *39*, 775–778.

Luo, H., Lin, Y., Gao, F., Zhang, C.T., and Zhang, R. (2014a). DEG 10, an update of the database of essential genes that includes both protein-coding genes and noncoding genomic elements. Nucleic Acids Res. *42*, D574-80.

Luo, H., Lin, Y., Gao, F., Zhang, C.T., and Zhang, R. (2014b). DEG 10, an update of the database of essential genes that includes both protein-coding genes and noncoding genomic elements. Nucleic Acids Res. *42*, D574-80.

Madsen, J.S., Burmølle, M., Hansen, L.H., and Sørensen, S.J. (2012). The interconnection between biofilm formation and horizontal gene transfer. FEMS Immunol. Med. Microbiol. *65*, 183–195.

Mahenthiralingam, E., and Coenye, T. (2014). *Burkholderia*: From Genomes to Function (Norfolk, United Kingdom: Caister Academic Press).

Mahenthiralingam, E., and Vandamme, P. (2005). Taxonomy and pathogenesis of the *Burkholderia cepacia* complex. Chron Respir Dis *2*, 209–217.

Mahenthiralingam, E., Campbell, M.E., Henry, D.A., and Speert, D.P. (1996). Epidemiology of *Burkholderia cepacia* infection in patients with cystic fibrosis: analysis by randomly amplified polymorphic DNA fingerprinting. J. Clin. Microbiol. *34*, 2914–2920.

Mahenthiralingam, E., Simpson, D.A., and Speert, D.P. (1997). Identification and characterization of a novel DNA marker associated with epidemic *Burkholderia cepacia* strains recovered from patients with cystic fibrosis. J. Clin. Microbiol. *35*, 808–816.

Mahenthiralingam, E., Coenye, T., Chung, J.W., Speert, D.P., Govan, J.R., Taylor, P., and Vandamme, P. (2000a). Diagnostically and experimentally useful panel of strains from the *Burkholderia cepacia* complex. J. Clin. Microbiol. *38*, 910–913.

Mahenthiralingam, E., Bischof, J., Byrne, S.K., Radomski, C., Davies, J.E., Av-Gay, Y., and Vandamme, P. (2000b). DNA-Based diagnostic approaches for identification of *Burkholderia cepacia* complex, *Burkholderia vietnamiensi*s, *Burkholderia multivorans*, *Burkholderia stabilis*, and *Burkholderia cepaci*a genomovars I and III. J. Clin. Microbiol. *38*, 3165–3173.

Mahenthiralingam, E., Vandamme, P., Campbell, M.E., Henry, D.A., Gravelle, A.M., Wong, L.T., Davidson, A.G., Wilcox, P.G., Nakielna, B., and Speert, D.P. (2001). Infection with *Burkholderia cepacia* complex genomovars in patients with cystic fibrosis: virulent transmissible strains of genomovar III can replace *Burkholderia multivorans*. Clin. Infect. Dis. Off. Publ. Infect. Dis. Soc. Am. *33*, 1469–1475.

Mahenthiralingam, E., Urban, T.A., and Goldberg, J.B. (2005a). The multifarious, multireplicon *Burkholderia cepacia* complex. Nat. Rev. *3*, 144–156.

Mahenthiralingam, E., Urban, T.A., and Goldberg, J.B. (2005b). The multifarious, multireplicon *Burkholderia cepacia* complex. Nat. Rev. *3*, 144–156.

Mahenthiralingam, E., Baldwin, A., and Dowson, C.G. (2008). *Burkholderia cepacia* complex bacteria: opportunistic pathogens with important natural biology. J. Appl. Microbiol. *104*, 1539.

Mann, T., Ben-David, D., Zlotkin, A., Shachar, D., Keller, N., Toren, A., Nagler, A., Smollan, G., Barzilai, A., and Rahav, G. (2010). An outbreak of *Burkholderia cenocepacia* bacteremia in immunocompromised oncology patients. Infection *38*, 187–194.

Manniello, J.M., Heymann, H., and Adair, F.W. (1979). Isolation of atypical lipopolysaccharides from purified cell walls of *Pseudomonas cepacia*. J. Gen. Microbiol. *112*, 397–400.

Mao, X., Ma, Q., Zhou, C., Chen, X., Zhang, H., Yang, J., Mao, F., Lai, W., and Xu, Y. (2014a). DOOR 2.0: presenting operons and their functions through dynamic and integrated views. Nucleic Acids Res. *42*, D654-9.

Mao, X., Ma, Q., Zhou, C., Chen, X., Zhang, H., Yang, J., Mao, F., Lai, W., and Xu, Y. (2014b). DOOR 2.0: presenting operons and their functions through dynamic and integrated views. Nucleic Acids Res. *42*, D654-9.

Marchand, I., Damier-Piolle, L., Courvalin, P., and Lambert, T. (2004). Expression of the RND-type efflux pump AdeABC in *Acinetobacter baumannii* is regulated by the AdeRS two-component system. Antimicrob. Agents Chemother. *48*, 3298–3304.

Marciano, B.E., Spalding, C., Fitzgerald, A., Mann, D., Brown, T., Osgood, S., Yockey, L., Darnell, D.N., Barnhart, L., Daub, J., et al. (2015). Common severe infections in chronic granulomatous disease. Clin. Infect. Dis. Off. Publ. Infect. Dis. Soc. Am. *60*, 1176–1183.

Marraffini, L.A., and Sontheimer, E.J. (2010). CRISPR interference: RNA-directed adaptive immunity in bacteria and archaea. Nat. Rev. Genet. *11*, 181–190.

Martin, D.W., and Mohr, C.D. (2000). Invasion and intracellular survival of *Burkholderia cepacia*. Infect. Immun. *68*, 24–29.

Martin, P.K., Li, T., Sun, D., Biek, D.P., and Schmid, M.B. (1999). Role in cell permeability of an essential two-component system in *Staphylococcus aureus*. J. Bacteriol. *181*, 3666–3673.

Matteelli, A., Carvalho, A.C., Dooley, K.E., and Kritski, A. (2010). TMC207: the first compound of a new class of potent anti-tuberculosis drugs. Future Microbiol. *5*, 849–858.

Maxson, T., and Mitchell, D.A. (2016). Targeted Treatment for Bacterial Infections: Prospects for Pathogen-Specific Antibiotics Coupled with Rapid Diagnostics. Tetrahedron *72*, 3609–3624.

Memish, Z.A., Stephens, G., Balkhy, H.H., Cunningham, G., Francis, C., Poff, G., Prevention, S.N.G.I., and Group, C. (2009). Outbreak of *Burkholderia cepacia* bacteremia in immunocompetent children caused by contaminated nebulized sulbutamol in Saudi Arabia. Am. J. Infect. Control *37*, 431–432.

Metzker, M.L. (2010). Sequencing technologies - the next generation. Nat. Rev. *11*, 31–46.

Miki, R.A., Rubin, L.E., Kirk, J., and Dodds, S.D. (2006). Spontaneous septic arthritis caused by *Burkholderia cepacia*. Iowa Orthop. J. *26*, 147–150.

Miller, V.L., and Mekalanos, J.J. (1988). A novel suicide vector and its use in construction of insertion mutations: osmoregulation of outer membrane proteins and virulence determinants in *Vibrio cholerae* requires *toxR*. J. Bacteriol. *170*, 2575–2583.

Moehring, R.W., Lewis, S.S., Isaacs, P.J., Schell, W.A., Thomann, W.R., Althaus, M.M., Hazen, K.C., Dicks, K.V., Lipuma, J.J., Chen, L.F., et al. (2014). Outbreak of Bacteremia Due to *Burkholderia contaminans* Linked to Intravenous Fentanyl From an Institutional Compounding Pharmacy. JAMA Intern. Med.

Mohamed, Y.F., and Valvano, M.A. (2014). A *Burkholderia cenocepacia* MurJ (MviN) homolog is essential for cell wall peptidoglycan synthesis and bacterial viability. Glycobiology *24*, 564–576.

Moore, R.A., and Hancock, R.E. (1986). Involvement of outer membrane of P*seudomonas cepacia in* aminoglycoside and polymyxin resistance. Antimicrob. Agents Chemother. *30*, 923–926.

Mori, H., Isono, K., Horiuchi, T., and Miki, T. (2000). Functional genomics of *Escherichia coli* in Japan. Res. Microbiol. *151*, 121–128.

Moskowitz, S.M., Ernst, R.K., and Miller, S.I. (2004). PmrAB, a two-component regulatory system of *Pseudomonas aeruginosa* that modulates resistance to cationic antimicrobial peptides and addition of aminoarabinose to lipid A. J. Bacteriol. *186*, 575–579.

Moule, M.G., Hemsley, C.M., Seet, Q., Guerra-Assuncao, J.A., Lim, J., Sarkar-Tyson, M., Clark, T.G., Tan, P.B., Titball, R.W., Cuccui, J., et al. (2014a). Genome-wide saturation mutagenesis of *Burkholderia pseudomallei* K96243 predicts essential genes and novel targets for antimicrobial development. mBio *5*, e00926-13.

Moule, M.G., Hemsley, C.M., Seet, Q., Guerra-Assuncao, J.A., Lim, J., Sarkar-Tyson, M., Clark, T.G., Tan, P.B., Titball, R.W., Cuccui, J., et al. (2014b). Genome-wide saturation mutagenesis of *Burkholderia pseudomallei* K96243 predicts essential genes and novel targets for antimicrobial development. mBio *5*, e00926-13.

Muller, C., Plesiat, P., and Jeannot, K. (2011). A two-component regulatory system interconnects resistance to polymyxins, aminoglycosides, fluoroquinolones, and ß-lactams in *Pseudomonas aeruginosa.* - PubMed - NCBI. *55*, 1211–1221.

Murima, P., Sessions, P.F. de, Lim, V., Naim, A.N.M., Bifani, P., Boshoff, H.I.M., Sambandamurthy, V.K., Dick, T., Hibberd, M.L., Schreiber, M., et al. (2013). Exploring the Mode of Action of Bioactive Compounds by Microfluidic Transcriptional Profiling in Mycobacteria. PLOS ONE *8*, e69191.

Mushegian, A.R., and Koonin, E.V. (1996). A minimal gene set for cellular life derived by comparison of complete bacterial genomes. Proc. Natl. Acad. Sci. U. S. A. *93*, 10268–10273.

Nair, B.M., Jr, K.J.C., Griffith, A., and Burns, J.L. (2004). Salicylate induces an antibiotic efflux pump in *Burkholderia cepacia* complex genomovar III (B. cenocepacia). J. Clin. Invest. *113*, 464–473.

Nakae, T. (1976). Identification of the outer membrane protein of *E. coli* that produces transmembrane channels in reconstituted vesicle membranes. Biochem. Biophys. Res. Commun. *71*, 877–884.

Nannini, E.C., Ponessa, A., Muratori, R., Marchiaro, P., Ballerini, V., Flynn, L., and Limansky, A.S. (2015). Polyclonal outbreak of bacteremia caused by *Burkholderia cepacia* complex and the presumptive role of ultrasound gel. Braz. J. Infect. Dis. Off. Publ. Braz. Soc. Infect. Dis. *19*, 543–545.

Nikaido, H. (2003). Molecular basis of bacterial outer membrane permeability revisited. Microbiol. Mol. Biol. Rev. MMBR *67*, 593–656.

Nishino, K., and Yamaguchi, A. (2002). EvgA of the two-component signal transduction system modulates production of the yhiUV multidrug transporter in *Escherichia coli*. J. Bacteriol. *184*, 2319–2323.

Nivedhana, S., Sulochana, P., and Shobana, R. (2016). Spontaneous septic arthritis due to *Burkholderia cepacia* in a 3-month-old pre-term infant. Indian J. Med. Microbiol. *34*, 394–395.

Noble, W.S. (2009). How does multiple testing correction work? Nat. Biotechnol. *27*, 1135–1137.

Oh, J., Fung, E., Price, M.N., Dehal, P.S., Davis, R.W., Giaever, G., Nislow, C., Arkin, A.P., and Deutschbauer, A. (2010). A universal TagModule collection for parallel genetic analysis of microorganisms. Nucleic Acids Res. *38*, e146.

Onishi, H.R., Pelak, B.A., Gerckens, L.S., Silver, L.L., Kahan, F.M., Chen, M.H., Patchett, A.A., Galloway, S.M., Hyland, S.A., Anderson, M.S., et al. (1996). Antibacterial agents that inhibit lipid A biosynthesis. Science *274*, 980–982.

Opijnen, T., and Camilli, A. (2010). Genome-wide fitness and genetic interactions determined by Tn-seq, a high-throughput massively parallel sequencing method for microorganisms. Curr. Protoc. Microbiol. *19*, 1E.3.1-1E.3.16.

Opijnen, T. van, and Camilli, A. (2012). A fine scale phenotype-genotype virulence map of a bacterial pathogen. Genome Res. *22*, 2541–2551.

Opijnen, T. van, Bodi, K.L., and Camilli, A. (2009). Tn-seq: high-throughput parallel sequencing for fitness and genetic interaction studies in microorganisms. Nat. Methods *6*, 767–772.

Organization, W.H. (2014). Antimicrobial Resistance: Global Report on Surveillance 2014 http://www.who.int/drugresistance/documents/surveillancereport/en/.

Ortega, X.P., Cardona, S.T., Brown, A.R., Loutet, S.A., Flannagan, R.S., Campopiano, D.J., Govan, J.R., and Valvano, M.A. (2007a). A putative gene cluster for aminoarabinose biosynthesis is essential for *Burkholderia cenocepacia* viability. J. Bacteriol. *189*, 3639–3644.

Ortega, X.P., Cardona, S.T., Brown, A.R., Loutet, S.A., Flannagan, R.S., Campopiano, D.J., Govan, J.R., and Valvano, M.A. (2007b). A putative gene cluster for aminoarabinose biosynthesis is essential for *Burkholderia cenocepacia* viability. J. Bacteriol. *189*, 3639–3644.

O'Sullivan, L.A., and Mahenthiralingam, E. (2005). Biotechnological potential within the genus *Burkholderia*. Lett. Appl. Microbiol. *41*, 8–11.

Oyola, S.O., Otto, T.D., Gu, Y., Maslen, G., Manske, M., Campino, S., Turner, D.J., Macinnis, B., Kwiatkowski, D.P., Swerdlow, H.P., et al. (2012). Optimizing Illumina next-generation sequencing library preparation for extremely AT-biased genomes. BMC Genomics *13*, 1.

Pagès, J.-M., James, C.E., and Winterhalter, M. (2008). The porin and the permeating antibiotic: a selective diffusion barrier in Gram-negative bacteria. Nat. Rev. Microbiol. *6*, 893–903.

Pankhurst, C.L., and Philpott-Howard, J. (1996). The environmental risk factors associated with medical and dental equipment in the transmission of *Burkholderia (Pseudomonas) cepacia* in cystic fibrosis patients. J. Hosp. Infect. *32*, 249–255.

Parke, J.L., and Gurian-Sherman, D. (2001). Diversity of the *Burkholderia cepacia* complex and implications for risk assessment of biological control strains. Annu Rev Phytopathol *39*, 225–258.

Parr, T.R., Moore, R.A., Moore, L.V., and Hancock, R.E. (1987). Role of porins in intrinsic antibiotic resistance of *Pseudomonas cepacia*. Antimicrob. Agents Chemother. *31*, 121–123.

Pathania, R., Zlitni, S., Barker, C., Das, R., Gerritsma, D.A., Lebert, J., Awuah, E., Melacini, G., Capretta, F.A., and Brown, E.D. (2009). Chemical genomics in *Escherichia coli* identifies an inhibitor of bacterial lipoprotein targeting. Nat. Chem. Biol. *5*, 849–856.

Payne, D.J., Gwynn, M.N., Holmes, D.J., and Pompliano, D.L. (2007). Drugs for bad bugs: confronting the challenges of antibacterial discovery. Nat. Rev. Discov. *6*, 29–40.

Payne, G.W., Ramette, A., Rose, H.L., Weightman, A.J., Jones, T.H., Tiedje, J.M., and Mahenthiralingam, E. (2006). Application of a recA gene-based identification approach to the maize rhizosphere reveals novel diversity in *Burkholderia* species. FEMS Microbiol. Lett. *259*, 126–132.

Peeters, C., Zlosnik, J.E., Spilker, T., Hird, T.J., LiPuma, J.J., and Vandamme, P. (2013). *Burkholderia pseudomultivorans sp. nov*., a novel *Burkholderia cepacia* complex species from human respiratory samples and the rhizosphere. Syst. Appl. Microbiol. *36*, 483–489.

Peters, J.M., Colavin, A., Shi, H., Czarny, T.L., Larson, M.H., Wong, S., Hawkins, J.S., Lu, C.H., Koo, B.M., Marta, E., et al. (2016a). A Comprehensive, CRISPR-based Functional Analysis of Essential Genes in Bacteria. Cell *165*, 1493–1506.

Peters, J.M., Colavin, A., Shi, H., Czarny, T.L., Larson, M.H., Wong, S., Hawkins, J.S., Lu, C.H., Koo, B.M., Marta, E., et al. (2016b). A Comprehensive, CRISPR-based Functional Analysis of Essential Genes in Bacteria. Cell *165*, 1493–1506.

Phillips, J.W., Goetz, M.A., Smith, S.K., Zink, D.L., Polishook, J., Onishi, R., Salowe, S., Wiltsie, J., Allocco, J., Sigmund, J., et al. (2011). Discovery of kibdelomycin, a potent new class of bacterial type II topoisomerase inhibitor by chemical-genetic profiling in *Staphylococcus aureus.* Chem. Biol. *18*, 955–965.

Pickering, B.S., and Oresnik, I.J. (2010). The twin arginine transport system appears to be essential for viability in *Sinorhizobium meliloti*. J. Bacteriol. *192*, 5173–5180.

Porter, L.A., and Goldberg, J.B. (2011). Influence of neutrophil defects on *Burkholderia cepacia* complex pathogenesis. Front. Cell. Infect. Microbiol. *1*, 9.

Projan, S.J., and Youngman, P.J. (2002). Antimicrobials: new solutions badly needed. Curr. Opin. Microbiol. *5*, 463–465.

Pujol, M., Corbella, X., Carratala, J., and Gudiol, F. (1992). Community-acquired bacteremic *Pseudomonas cepacia* pneumonia in an immunocompetent host. Clin. Infect. Dis. Off. Publ. Infect. Dis. Soc. Am. *15*, 887–888.

Qi, L.S., Larson, M.H., Gilbert, L.A., Doudna, J.A., Weissman, J.S., Arkin, A.P., and Lim, W.A. (2013). Repurposing CRISPR as an RNA-guided platform for sequence-specific control of gene expression. Cell *152*, 1173–1183.

Quail, M.A., Otto, T.D., Gu, Y., Harris, S.R., Skelly, T.F., McQuillan, J.A., Swerdlow, H.P., and Oyola, S.O. (2011). Optimal enzymes for amplifying sequencing libraries. Nat. Methods *9*, 10–11.

Raetz, C.R.H., and Whitfield, C. (2002). Lipopolysaccharide Endotoxins. Annu. Rev. Biochem. *71*, 635–700.

Raetz, C.R.H., Reynolds, C.M., Trent, M.S., and Bishop, R.E. (2007). Lipid A modification systems in gram-negative bacteria. Annu. Rev. Biochem. *76*, 295–329.

Rajendran, R., Quinn, R.F., Murray, C., McCulloch, E., Williams, C., and Ramage, G. (2010). Efflux pumps may play a role in tigecycline resistance in *Burkholderia* species. Int. J. Antimicrob. Agents *36*, 151–154.

Ramette, A., LiPuma, J.J., and Tiedje, J.M. (2005). Species abundance and diversity of *Burkholderia cepacia* complex in the environment. Appl. Environ. Microbiol. *71*, 1193–1201.

Rao, S., and Grigg, J. (2006). New insights into pulmonary inflammation in cystic fibrosis. Arch. Dis. Child. *91*, 786–788.

Ratjen, F., and Doring, G. (2003). Cystic fibrosis. Lancet *361*, 681–689.

Regan, K.H., and Bhatt, J. (2016). Eradication therapy for *Burkholderia cepacia* complex in people with cystic fibrosis. Cochrane Database Syst. Rev. *11*, CD009876.

Reich, K.A. (2000). The search for essential genes. Res Microbiol *151*, 319–324.

Reik, R., Spilker, T., and Lipuma, J.J. (2005). Distribution of *Burkholderia cepacia* complex species among isolates recovered from persons with or without cystic fibrosis. J. Clin. Microbiol. *43*, 2926–2928.

Riedel, K., Hentzer, M., Geisenberger, O., Huber, B., Steidle, A., Wu, H., Hoiby, N., Givskov, M., Molin, S., and Eberl, L. (2001). N-acylhomoserine-lactone-mediated communication between *Pseudomonas aeruginosa* and *Burkholderia cepacia* in mixed biofilms. Microbiol. Read. Engl. *147*, 3249–3262.

Riordan, J.R., Rommens, J.M., Kerem, B., Alon, N., Rozmahel, R., Grzelczak, Z., Zielenski, J., Lok, S., Plavsic, N., and Chou, J.L. (1989). Identification of the cystic fibrosis gene: cloning and characterization of complementary DNA. Science *245*, 1066–1073.

Robinson, M.D., McCarthy, D.J., and Smyth, G.K. (2010). edgeR: a Bioconductor package for differential expression analysis of digital gene expression data. Bioinforma. Oxf. Engl. *26*, 139–140.

Rommens, J.M., Iannuzzi, M.C., Kerem, B., Drumm, M.L., Melmer, G., Dean, M., Rozmahel, R., Cole, J.L., Kennedy, D., and Hidaka, N. (1989). Identification of the cystic fibrosis gene: chromosome walking and jumping. Science *245*, 1059–1065.

Ruiz, N., Kahne, D., and Silhavy, T.J. (2009). Transport of lipopolysaccharide across the cell envelope: the long road of discovery. Nat. Rev. Microbiol. *7*, 677–683.

Russell, A.B., LeRoux, M., Hathazi, K., Agnello, D.M., Ishikawa, T., Wiggins, P.A., Wai, S.N., and Mougous, J.D. (2013). Diverse type VI secretion phospholipases are functionally plastic antibacterial effectors. Nature *496*, 508–512.

Saiman, L., Siegel, J.D., LiPuma, J.J., Brown, R.F., Bryson, E.A., Chambers, M.J., Downer, V.S., Fliege, J., Hazle, L.A., Jain, M., et al. (2014). Infection prevention and control guideline for cystic fibrosis: 2013 update. Infect. Control Hosp. Epidemiol. *35 Suppl 1*, S1–S67.

Saldias, M.S., and Valvano, M.A. (2009). Interactions of *Burkholderia cenocepacia* and other *Burkholderia cepacia* complex bacteria with epithelial and phagocytic cells. Microbiol. Read. Engl. *155*, 2809–2817.

Sampson, T.R., Liu, X., Schroeder, M.R., Kraft, C.S., Burd, E.M., and Weiss, D.S. (2012). Rapid killing of *Acinetobacter baumannii* by polymyxins is mediated by a hydroxyl radical death pathway. Antimicrob. Agents Chemother. *56*, 5642–5649.

Sangodkar, U.M., Chapman, P.J., and Chakrabarty, A.M. (1988). Cloning, physical mapping and expression of chromosomal genes specifying degradation of the herbicide 2,4,5-T by *Pseudomonas cepacia* AC1100. Gene *71*, 267–277.

Satpute, M.G., Telang, N.V., Dhakephalkar, P.K., Niphadkar, K.B., and Joshi, S.G. (2011). Isolation of *Burkholderia cenocepacia* J 2315 from non-cystic fibrosis pediatric patients in India. Am. J. Infect. Control *39*, e21-23.

Schaffer, K. (2015). Epidemiology of infection and current guidelines for infection prevention in cystic fibrosis patients. J. Hosp. Infect. *89*, 309–313.

Schmidt, H., and Hensel, M. (2004). Pathogenicity islands in bacterial pathogenesis. Clin. Microbiol. Rev. *17*, 14–56.

Schmieder, R., and Edwards, R. (2011). Quality control and preprocessing of metagenomic datasets. Bioinforma. Oxf. Engl. *27*, 863–864.

Schwab, U., Abdullah, L.H., Perlmutt, O.S., Albert, D., Davis, C.W., Arnold, R.R., Yankaskas, J.R., Gilligan, P., Neubauer, H., Randell, S.H., et al. (2014). Localization of *Burkholderia cepacia* complex bacteria in cystic fibrosis lungs and interactions with *Pseudomonas aeruginosa* in hypoxic mucus. Infect. Immun. *82*, 4729–4745.

Scoffone, V.C., Ryabova, O., Makarov, V., Iadarola, P., Fumagalli, M., Fondi, M., Fani, R., Rossi, E.D., Riccardi, G., and Buroni, S. (2015). Efflux-mediated resistance to a benzothiadiazol derivative effective against *Burkholderia cenocepacia*. Front. Microbiol. *6*, 815.

Shen, Z., Qu, W., Wang, W., Lu, Y., Wu, Y., Li, Z., Hang, X., Wang, X., Zhao, D., and Zhang, C. (2010). MPprimer: a program for reliable multiplex PCR primer design. BMC Bioinformatics *11*, 143.

Shendure, J., and Ji, H. (2008). Next-generation DNA sequencing. Nat. Biotechnol. *26*, 1135–1145.

Shi, L., Gunther, S., Hubschmann, T., Wick, L.Y., Harms, H., and Muller, S. (2007). Limits of propidium iodide as a cell viability indicator for environmental bacteria. Cytom. J. Int. Soc. Anal. Cytol. *71*, 592–598.

Shoemaker, D.D., Lashkari, D.A., Morris, D., Mittmann, M., and Davis, R.W. (1996). Quantitative phenotypic analysis of yeast deletion mutants using a highly parallel molecular bar-coding strategy. Nat. Genet. *14*, 450–456.

Shrivastava, B., Sriram, A., Shetty, S., Doshi, R., and Varior, R. (2016). An unusual source of *Burkholderia cepacia* outbreak in a neonatal intensive care unit. J. Hosp. Infect.

Siddiqui, A.H., Mulligan, M.E., Mahenthiralingam, E., Hebden, J., Brewrink, J., Qaiyumi, S., Johnson, J.A., and LiPuma, J.J. (2001). An episodic outbreak of genetically related *Burkholderia cepacia* among non-cystic fibrosis patients at a university hospital. Infect. Control Hosp. Epidemiol. *22*, 419–422.

Silver, L.L. (2011). Challenges of antibacterial discovery. Clin. Microbiol. Rev. *24*, 71–109.

Singh, S.B., Jayasuriya, H., Ondeyka, J.G., Herath, K.B., Zhang, C., Zink, D.L., Tsou, N.N., Ball, R.G., Basilio, A., Genilloud, O., et al. (2006). Isolation, structure, and absolute stereochemistry of platensimycin, a broad spectrum antibiotic discovered using an antisense differential sensitivity strategy. J. Am. Chem. Soc. *128*, 11916–11920.

Siritapetawee, J., Prinz, H., Samosornsuk, W., Ashley, R.H., and Suginta, W. (2004a). Functional reconstitution, gene isolation and topology modelling of porins from *Burkholderia pseudomallei* and *Burkholderia thailandensis*. Biochem. J. *377*, 579–587.

Siritapetawee, J., Prinz, H., Krittanai, C., and Suginta, W. (2004b). Expression and refolding of Omp38 from *Burkholderia pseudomallei* and *Burkholderia thailandensis*, and its function as a diffusion porin. Biochem. J. *384*, 609–617.

Smet, B.D., Mayo, M., Peeters, C., Zlosnik, J.E., Spilker, T., Hird, T.J., LiPuma, J.J., Kidd, T.J., Kaestli, M., Ginther, J.L., et al. (2015). *Burkholderia stagnalis sp. nov*. and *Burkholderia territorii sp. nov*., two novel *Burkholderia cepacia* complex species from environmental and human sources. Int. J. Syst. Evol. Microbiol. *65*, 2265–2271.

Smith, A.M., Heisler, L.E., Mellor, J., Kaper, F., Thompson, M.J., Chee, M., Roth, F.P., Giaever, G., and Nislow, C. (2009). Quantitative phenotyping via deep barcode sequencing. Genome Res. *19*, 1836–1842.

Smith, A.M., Heisler, L.E., Onge, R.P.S., Farias-Hesson, E., Wallace, I.M., Bodeau, J., Harris, A.N., Perry, K.M., Giaever, G., Pourmand, N., et al. (2010). Highly-multiplexed barcode sequencing: an efficient method for parallel analysis of pooled samples. Nucleic Acids Res. *38*, e142.

Soriano, M.L. (1990). Separation of a mixture distribution into its Gaussian component. Fishbyte *8*, 35–40.

Souza Dias, M.B., Cavassin, L.G.T., Stempliuk, V., Xavier, L.S., Lobo, R.D., Sampaio, J.L.M., Pignatari, A.C., Borrasca, V.L., Bierrenbach, A.L., and Toscano, C.M. (2013). Multi-institutional outbreak of *Burkholderia cepacia* complex associated with contaminated mannitol solution prepared in compounding pharmacy. Am. J. Infect. Control *41*, 1038–1042.

Speert, D.P., Bond, M., Woodman, R.C., and Curnutte, J.T. (1994). Infection with *Pseudomonas cepacia* in chronic granulomatous disease: role of nonoxidative killing by neutrophils in host defense. J. Infect. Dis. *170*, 1524–1531.

Speert, D.P., Henry, D., Vandamme, P., Corey, M., and Mahenthiralingam, E. (2002). Epidemiology of *Burkholderia cepacia* complex in patients with cystic fibrosis, Canada. Emerg. Infect. Dis. *8*, 181–187.

Spellberg, B., Guidos, R., Gilbert, D., Bradley, J., Boucher, H.W., Scheld, W.M., Bartlett, J.G., Jr, J.E., and America, I.D.S. of (2008). The epidemic of antibiotic-resistant infections: a call to action for the medical community from the Infectious Diseases Society of America. Clin. Infect. Dis. Off. Publ. Infect. Dis. Soc. Am. *46*, 155–164.

Sperandeo, P., Dehò, G., and Polissi, A. (2009). The lipopolysaccharide transport system of Gram-negative bacteria. Biochim. Biophys. Acta *1791*, 594–602.

Stein, A., Takasuka, T.E., and Collings, C.K. (2010). Are nucleosome positions in vivo primarily determined by histone-DNA sequence preferences? Nucleic Acids Res. *38*, 709–719.

Stephenson, K., and Hoch, J.A. (2002). Virulence- and antibiotic resistance-associated two-component signal transduction systems of Gram-positive pathogenic bacteria as targets for antimicrobial therapy. Pharmacol. Ther. *93*, 293–305.

Stephenson, A.L., Sykes, J., Berthiaume, Y., Singer, L.G., Aaron, S.D., Whitmore, G.A., and Stanojevic, S. (2015). Clinical and demographic factors associated with post-lung transplantation survival in individuals with cystic fibrosis. J. Heart Lung Transplant. Off. Publ. Int. Soc. Heart Transplant. *34*, 1139–1145.

Stock, A.M., Robinson, V.L., and Goudreau, P.N. (2000). Two-component signal transduction. Annu. Rev. Biochem. *69*, 183–215.

Suginta, W., Mahendran, K.R., Chumjan, W., Hajjar, E., Schulte, A., Winterhalter, M., and Weingart, H. (2011). Molecular analysis of antimicrobial agent translocation through the membrane porin BpsOmp38 from an ultraresistant *Burkholderia pseudomallei* strain. Biochim. Biophys. Acta *1808*, 1552–1559.

Sun, L., Jiang, R.Z., Steinbach, S., Holmes, A., Campanelli, C., Forstner, J., Sajjan, U., Tan, Y., Riley, M., and Goldstein, R. (1995). The emergence of a highly transmissible lineage of cbl+ *Pseudomonas* (*Burkholderia*) *cepacia* causing CF centre epidemics in North America and Britain. Nat. Med. *1*, 661–666.

Svensson, S.L., Davis, L.M., MacKichan, J.K., Allan, B.J., Pajaniappan, M., Thompson, S.A., and Gaynor, E.C. (2009). The CprS sensor kinase of the zoonotic pathogen *Campylobacter jejuni* influences biofilm formation and is required for optimal chick colonization. Mol. Microbiol. *71*, 253–272.

Svensson, S.L., Hyunh, S., Parker, C.T., and Gaynor, E.C. (2015). The *Campylobacter jejuni* CprRS two-component regulatory system regulates aspects of the cell envelope. Mol. Microbiol. *96*, 189–209.

Tatusov, R.L., Galperin, M.Y., Natale, D.A., and Koonin, E.V. (2000). The COG database: a tool for genome-scale analysis of protein functions and evolution. Nucleic Acids Res *28*, 33–36.

Taylor, B.L., and Zhulin, I.B. (1999). PAS domains: internal sensors of oxygen, redox potential, and light. Microbiol. Mol. Biol. Rev. MMBR *63*, 479–506.

Tomasz, A. (1979). The mechanism of the irreversible antimicrobial effects of penicillins: how the beta-lactam antibiotics kill and lyse bacteria. Annu. Rev. Microbiol. *33*, 113–137.

Torbeck, L., Raccasi, D., Guilfoyle, D.E., Friedman, R.L., and Hussong, D. (2011). *Burkholderia cepacia*: This Decision Is Overdue. PDA J. Pharm. Sci. Technol. PDA *65*, 535–543.

Tseng, S.P., Tsai, W.C., Liang, C.Y., Lin, Y.S., Huang, J.W., Chang, C.Y., Tyan, Y.C., and Lu, P.L. (2014). The contribution of antibiotic resistance mechanisms in clinical *Burkholderia cepacia* complex isolates: an emphasis on efflux pump activity. PloS One *9*, e104986.

Turner, K.H., Wessel, A.K., Palmer, G.C., Murray, J.L., and Whiteley, M. (2015). Essential genome of *Pseudomonas aeruginosa* in cystic fibrosis sputum. Proc. Natl. Acad. Sci. U. S. A. *112*, 4110–4115.

Ussery, D.W., Kiil, K., Lagesen, K., Sicheritz-Ponten, T., Bohlin, J., and Wassenaar, T.M. (2009). The genus *burkholderia*: analysis of 56 genomic sequences. Genome Dyn. *6*, 140–157.

Vaara, M. (1992). Agents that increase the permeability of the outer membrane. Microbiol. Rev. *56*, 395–411.

Valvano, M.A. (2011). Common themes in glycoconjugate assembly using the biogenesis of O-antigen lipopolysaccharide as a model system. Biochem. Biokhimiia *76*, 729–735.

Vandamme, P., Holmes, B., Coenye, T., Goris, J., Mahenthiralingam, E., LiPuma, J.J., and Govan, J.R. (2003). *Burkholderia cenocepacia* sp. nov.–a new twist to an old story. Res.Microbiol. *154*, 91–96.

Vanlaere, E., Lipuma, J.J., Baldwin, A., Henry, D., Brandt, E.D., Mahenthiralingam, E., Speert, D., Dowson, C., and Vandamme, P. (2008). B*urkholderia latens sp. nov., Burkholderia diffusa sp. nov., Burkholderia arboris sp. nov., Burkholderia seminalis sp. nov. and Burkholderia metallica sp. nov*., novel species within the *Burkholderia cepacia* complex. Int. J. Syst. Evol. Microbiol. *58*, 1580–1590.

Vanlaere, E., Baldwin, A., Gevers, D., Henry, D., Brandt, E.D., LiPuma, J.J., Mahenthiralingam, E., Speert, D.P., Dowson, C., and Vandamme, P. (2009). Taxon K, a complex within the

Burkholderia cepacia complex, comprises at least two novel species, *Burkholderia contaminans sp. nov*. and *Burkholderia lata sp. nov*. Int. J. Syst. Evol. Microbiol. *59*, 102–111.

Vardi, A., Sirigou, A., Lalayanni, C., Kachrimanidou, M., Kaloyannidis, P., Saloum, R., Anagnostopoulos, A., and Sotiropoulos, D. (2013). An outbreak of *Burkholderia cepacia* bacteremia in hospitalized hematology patients selectively affecting those with acute myeloid leukemia. Am. J. Infect. Control *41*, 312–316.

Varga, J.J., Losada, L., Zelazny, A.M., Kim, M., McCorrison, J., Brinkac, L., Sampaio, E.P., Greenberg, D.E., Singh, I., Heiner, C., et al. (2013). Draft Genome Sequences of *Burkholderia cenocepacia* ET12 Lineage Strains K56-2 and BC7. Genome Announc. *1*, 10.1128/genomeA.00841-13.

Vergunst, A.C., Meijer, A.H., Renshaw, S.A., and O'Callaghan, D. (2010). *Burkholderia cenocepacia* creates an intramacrophage replication niche in zebrafish embryos, followed by bacterial dissemination and establishment of systemic infection. Infect. Immun. *78*, 1495–1508.

Vogt, S.L., and Raivio, T.L. (2012). Just scratching the surface: an expanding view of the Cpx envelope stress response. FEMS Microbiol. Lett. *326*, 2–11.

Walsh, C.T., and Wencewicz, T.A. (2014). Prospects for new antibiotics: a molecule-centered perspective. J. Antibiot. (Tokyo) *67*, 7–22.

Wang, X., and Quinn, P.J. (2010). Endotoxins: lipopolysaccharides of gram-negative bacteria. Subcell. Biochem. *53*, 3–25.

Wang, H., Claveau, D., Vaillancourt, J.P., Roemer, T., and Meredith, T.C. (2011). High-frequency transposition for determining antibacterial mode of action. Nat. Chem. Biol. *7*, 720–729.

Wang, J., Soisson, S.M., Young, K., Shoop, W., Kodali, S., Galgoci, A., Painter, R., Parthasarathy, G., Tang, Y.S., Cummings, R., et al. (2006). Platensimycin is a selective FabF inhibitor with potent antibiotic properties. Nature *441*, 358–361.

Wang, J., Kodali, S., Lee, S.H., Galgoci, A., Painter, R., Dorso, K., Racine, F., Motyl, M., Hernandez, L., Tinney, E., et al. (2007). Discovery of platencin, a dual FabF and FabH inhibitor with in vivo antibiotic properties. Proc. Natl. Acad. Sci. U. S. A. *104*, 7612–7616.

Weber, D.J., Rutala, W.A., and Sickbert-Bennett, E.E. (2007). Outbreaks associated with contaminated antiseptics and disinfectants. Antimicrob. Agents Chemother. *51*, 4217–4224.

Weerdenburg, E.M., Abdallah, A.M., Rangkuti, F., Abd El Ghany, M., Otto, T.D., Adroub, S.A., Molenaar, D., Ummels, R., Ter Veen, K., van Stempvoort, G., et al. (2015). Genome-wide transposon mutagenesis indicates that *Mycobacterium marinum* customizes its virulence mechanisms for survival and replication in different hosts. Infect. Immun. *83*, 1778–1788.

Wetmore, K.M., Price, M.N., Waters, R.J., Lamson, J.S., He, J., Hoover, C.A., Blow, M.J., Bristow, J., Butland, G., Arkin, A.P., et al. (2015). Rapid quantification of mutant fitness in diverse bacteria by sequencing randomly bar-coded transposons. mBio *6*, e00306-15.

White, D.G., Goldman, J.D., Demple, B., and Levy, S.B. (1997). Role of the *acrAB* locus in organic solvent tolerance mediated by expression of *marA*, *soxS*, or *robA* in *Escherichia coli*. J. Bacteriol. *179*, 6122–6126.

Whitfield, C., and Trent, M.S. (2014). Biosynthesis and export of bacterial lipopolysaccharides. Annu. Rev. Biochem. *83*, 99–128.

Wiersinga, W.J., van der Poll, T., White, N.J., Day, N.P., and Peacock, S.J. (2006). Melioidosis: insights into the pathogenicity of *Burkholderia pseudomallei*. Nat. Rev. Microbiol. *4*, 272–282.

Williamson, D.A., and McBride, S.J. (2011). A case of tricuspid valve endocarditis due to *Burkholderia cepacia* complex. N. Z. Med. J. *124*, 84–86.

Winkelstein, J.A., Marino, M.C., Jr, R.B.J., Boyle, J., Curnutte, J., Gallin, J.I., Malech, H.L., Holland, S.M., Ochs, H., Quie, P., et al. (2000). Chronic granulomatous disease. Report on a national registry of 368 patients. Medicine (Baltimore) *79*, 155–169.

Winsor, G.L., Khaira, B., Rossum, T.V., Lo, R., Whiteside, M.D., and Brinkman, F.S. (2008). The *Burkholderia* Genome Database: facilitating flexible queries and comparative analyses. Bioinforma. Oxf. Engl. *24*, 2803–2804.

van Wolfswinkel, J.C., and Ketting, R.F. (2010). The role of small non-coding RNAs in genome stability and chromatin organization. J. Cell Sci. *123*, 1825–1839.

Wong, S.M., and Akerley, B.J. (2007). Identification and Analysis of Essential Genes in *Haemophilus influenzae*. Methods Mol. Biol. Clifton NJ *416*, 27–44.

Wong, Y.C., Ghany, M.A.E., Naeem, R., Lee, K.W., Tan, Y.G., Pain, A., and Nathan, S. (2016a). Candidate Essential Genes in *Burkholderia cenocepacia* J2315 Identified by Genome-Wide TraDIS. Front. Microbiol. *7*, 1288.

Wong, Y.C., Ghany, M.A.E., Naeem, R., Lee, K.W., Tan, Y.G., Pain, A., and Nathan, S. (2016b). Candidate Essential Genes in *Burkholderia cenocepacia* J2315 Identified by Genome-Wide TraDIS. Front. Microbiol. *7*, 1288.

Worthington, R.J., Blackledge, M.S., and Melander, C. (2013). Small-molecule inhibition of bacterial two-component systems to combat antibiotic resistance and virulence. Future Med. Chem. *5*, 1265–1284.

Wright, G.C., Weiss, J., Kim, K.S., Verheij, H., and Elsbach, P. (1990). Bacterial phospholipid hydrolysis enhances the destruction of *Escherichia coli* ingested by rabbit neutrophils. Role of cellular and extracellular phospholipases. J. Clin. Invest. *85*, 1925–1935.

Xu, H.H., Trawick, J.D., Haselbeck, R.J., Forsyth, R.A., Yamamoto, R.T., Archer, R., Patterson, J., Allen, M., Froelich, J.M., Taylor, I., et al. (2010a). *Staphylococcus aureus* TargetArray: comprehensive differential essential gene expression as a mechanistic tool to profile antibacterials. Antimicrob. Agents Chemother. *54*, 3659–3670.

Xu, H.H., Trawick, J.D., Haselbeck, R.J., Forsyth, R.A., Yamamoto, R.T., Archer, R., Patterson, J., Allen, M., Froelich, J.M., Taylor, I., et al. (2010b). *Staphylococcus aureus* TargetArray: comprehensive differential essential gene expression as a mechanistic tool to profile antibacterials. Antimicrob. Agents Chemother. *54*, 3659–3670.

Yabuuchi, E., Kosako, Y., Oyaizu, H., Yano, I., Hotta, H., Hashimoto, Y., Ezaki, T., and Arakawa, M. (1992). Proposal of *Burkholderia gen. nov*. and transfer of seven species of the genus *Pseudomonas* homology group II to the new genus, with the type species *Burkholderia cepacia* (Palleroni and Holmes 1981) comb. nov. Microbiol. Immunol. *36*, 1251–1275.

Yang, H., Krumholz, E.W., Brutinel, E.D., Palani, N.P., Sadowsky, M.J., Odlyzko, A.M., Gralnick, J.A., and Libourel, I.G.L. (2014). Genome-Scale Metabolic Network Validation of *Shewanella oneidensis* Using Transposon Insertion Frequency Analysis. PLoS Comput. Biol. *10*.

Yu, Y., Kim, H.S., Chua, H.H., Lin, C.H., Sim, S.H., Lin, D., Derr, A., Engels, R., DeShazer, D., Birren, B., et al. (2006). Genomic patterns of pathogen evolution revealed by comparison of *Burkholderia pseudomallei*, the causative agent of melioidosis, to avirulent *Burkholderia thailandensis*. BMC Microbiol. *6*, 46.

Zgurskaya, H.I., Lopez, C.A., and Gnanakaran, S. (2015). Permeability Barrier of Gram-Negative Cell Envelopes and Approaches To Bypass It. ACS Infect. Dis. *1*, 512–522.

Zhang, C.T., and Zhang, R. (2007). Gene Essentiality Analysis Based on DEG, a Database of Essential Genes. Methods Mol. Biol. Clifton NJ *416*, 391–400.

Zhang, Y.-M., and Rock, C.O. (2008). Membrane lipid homeostasis in bacteria. Nat. Rev. Microbiol. *6*, 222–233.

Zhang, L., Li, X.Z., and Poole, K. (2001). Fluoroquinolone susceptibilities of efflux-mediated multidrug-resistant *Pseudomonas aeruginosa*, *Stenotrophomonas maltophilia* and *Burkholderia cepacia*. J. Antimicrob. Chemother. *48*, 549–552.

Zhou, X., Kini, R.M., and Sivaraman, J. (2011). Application of isothermal titration calorimetry and column chromatography for identification of biomolecular targets. Nat. Protoc. *6*, 158–165.

Zhou, Z., Ribeiro, A.A., Lin, S., Cotter, R.J., Miller, S.I., and Raetz, C.R. (2001). Lipid A modifications in polymyxin-resistant *Salmonella typhimurium*: PMRA-dependent 4-amino-4-deoxy-L-arabinose, and phosphoethanolamine incorporation. J. Biol. Chem. *276*, 43111–43121.

Zhu, B., Zhou, S., Lou, M., Zhu, J., Li, B., Xie, G., Jin, G., and De Mot, R. (2011). Characterization and inference of gene gain/loss along *Burkholderia* evolutionary history. Evol. Bioinforma. Online *7*, 191–200.

Zlosnik, J.E., Zhou, G., Brant, R., Henry, D.A., Hird, T.J., Mahenthiralingam, E., Chilvers, M.A., Wilcox, P., and Speert, D.P. (2015). *Burkholderia* species infections in patients with cystic fibrosis in British Columbia, Canada. 30 years' experience. Ann. Am. Thorac. Soc. *12*, 70–78.

Zomer, A., Burghout, P., Bootsma, H.J., Hermans, P.W., and Hijum, S.A. van (2012). ESSENTIALS: software for rapid analysis of high throughput transposon insertion sequencing data. PloS One *7*, e43012.